LIBRARY Michigan State University

PLACE IN RETURN BOX to remove this checkout from your record. TO AVOID FINES return on or before date due.

DATE DUE	DATE DUE	DATE DUE
		-

MSU is An Affirmative Action/Equal Opportunity Institution

FTIR STUDIES OF WATER AND ARENE SORPTION MECHANISMS ON TMA- AND TMPA- MONTMORILLONITES

Ву

Jeffrey Jay Stevens

A DISSERTATION

Submitted to
Michigan State University
in partial fulfillment of the requirements
for the degree of

DOCTOR OF PHILOSOPHY

Department of Crop and Soil Science

1994

ABSTRACT

FTIR STUDIES OF WATER AND ARENE SORPTION MECHANISMS ON TMA- AND TMPA- MONTMORILLONITES

Bv

Jeffrey Jay Stevens

This research evaluated properties of normal- and reduced-charge Wyoming montmorillonites saturated with tetramethylammonium (TMA) and trimethylphenylammonium (TMPA) ions. Infrared spectroscopy was used to determine mechanisms of arene and water sorption on these clays and other properties. For normal-charge TMPA-montmorillonite, infrared spectroscopy showed that the C-N bond axis of TMPA was neither perpendicular nor parallel to the surface, yet X-ray data suggested that the TMPA phenyl ring was perpendicular to the siloxane surface. Reduced-charge montmorillonite was a randomly interstratified mixture of 25% collapsed layers with no adsorbed cations and 75% expanded layers that were propped open by TMPA's methyl groups, not the aromatic ring. Water vapor sorption isotherms showed water sorption was greater for normal-charge clays than reduced-charge clays, though the N₂ surface area of the reduced-charge clays was larger. This suggested that water sorbed preferentially on cations, not the siloxane surface. TMA-saturated clays sorbed more water vapor than did TMPA-saturated clays, indicating that the phenyl group of TMPA may sterically hinder sorption of water vapor. The infrared spectra of TMA and TMPA cations saturating

normal- and reduced-charge montmorillonite were perturbed by water vapor at 7.5% RH, providing further evidence that water interacted preferentially with adsorbed TMA and TMPA, not with uncharged siloxane surfaces, at low relative humidity. Arene sorption perturbed vibrational frequencies of adsorbed TMA and TMPA differently than did water sorption, allowing spectroscopic differentiation between water and arene interaction with TMA and TMPA. The infrared data showed that benzene and ethylbenzene interact directly with adsorbed TMA and TMPA ions on dry clay, but do not preclude sorption on the siloxane surface. The cation vibrational frequencies of clay films exposed to both water vapor and saturated benzene vapor remained at the frequencies characteristic of benzene alone for all relative humidity treatments. The cation vibrational frequencies of films exposed to ethylbenzene and water vapor shifted from those characteristic of ethylbenzene vapor alone toward frequencies characteristic of water vapor alone as relative humidity increased. Thus, water sorption drove ethylbenzene, but not benzene, from cation sites. Water vapor sorption and higher clay charge density both inhibited sorption of larger arenes more than smaller arenes.

ACKNOWLEDGEMENTS

I would like to thank my advisor, Dr. Sharon Anderson for her encouragement, training, advice, and hard work in obtaining financial assistance for my Doctoral program and in editing the manuscript for this dissertation. I would also like to thank her for motivating me when I fell short of my potential. Special thanks also go to my committee members, Dr. Steve Boyd, Dr. Boyd Ellis, and Dr. Dave Long, for helping me during my comprehensive exam, and in their suggestions for my dissertation. Thanks also go to Drs. Max Mortland and George Leroi for their comments. I would also like to thank the Clay Minerals Society and DOW for providing financial support for this research.

Thanks also go to my friends and fellow graduate students in the Crop and Soil Sciences Department for their technical assistance and camaraderie, especially my office mates Sven Böem and Inez Toro-Suarez.

Special thanks go to my wife and friend Donna for providing understanding, love and support, and also for asking the question "So what's this good for?" Finally, I would like to thank the rest of my family (mom, dad, brother and sister) for their support and understanding.

TABLE OF CONTENTS

List of Tables	ix
List of Figures	хi
Chapter I. Introduction and Review of Literature	1
Introduction	1
Review of Literature	2
TMPA orientation	2
Water adsorption on clays	6
Competitive sorption of arenes and water	8
References	12
Chapter II. Orientation of the Phenyl Group of Trimethylphenylammonium on Normal- and Reduced-charge Wyoming Montmorillonite	15
Abstract	15
Introduction	16
Materials and Methods	18
Preparation of reduced- and normal-charge TMPA montmorillonite	18
Infrared dichroism	19
Preparation of methyl-deuterated TMPA	19
Clay film preparation	22
Spectral collection	23
X-ray diffraction and Fourier analysis	24
Results	26

Infrared dichroism	26
X-ray diffraction analysis	28
Glycerol-solvated Na-montmorillonite	28
TMPA-montmorillonite	30
Discussion	32
TMPA orientation on normal-charge montmorillonite	32
TMPA orientation on reduced-charge montmorillonite	36
Conclusions	39
References	41
Chapter III. An FTIR study of water sorption on tetramethylammoni trimethylphenylammonium-saturated normal- and reduced-charge Wymontmorillonite	
Abstract	43
Introduction	44
Materials and Methods	46
Reduced- and normal-charge organoclay preparation	46
Water vapor sorption isotherms	48
Infrared spectroscopy	50
Clay film preparation	50
Water vapor sorption on clay films	50
Results and Discussion	53
Water sorption isotherms	53
Effect of sorbed water on cation vibrations	57
TMA-methyl vibrations	57
TMPA-methyl vibrations	63
TMPA ring vibrations	67
Conclusions	60

References	70
Chapter IV. An FTIR study of competitive water-arene sorption on tetramethylammonium- and trimethylphenylammonium-saturated normal-and reduced-charge Wyoming montmorillonite	72
Abstract	72
Introduction	73
Materials and Methods	75
Reduced- and normal-charged organoclay preparation	75
Infrared Spectroscopy	77
Clay film preparation	77
Competitive water and arene vapor sorption on clay films	77
Results	80
TMA-montmorillonite	80
Arene sorption on dry clay	80
Benzene sorption	80
Benzene-d ₆ sorption	83
Ethylbenzene sorption	83
Summary for arene sorption on dry TMA-clay	86
Arene-water competition on hydrated TMA-montmorillonite	86
Benzene-d ₆ sorption	86
Ethylbenzene sorption	87
Summary for arene sorption on hydrated TMA-clay	88
Effect of layer charge on arene sorption on TMA-clay	88
Effect of size on arene sorption on TMA-clay	88
TMPA-montmorillonite	89
Arene sorption on dry TMPA-clay	89
Benzene sorption	89

Ethylbenzene sorption	92
Summary for arene sorption on dry TMA-clay	94
Arene-water competition on hydrated TMA-montmorillonite	94
Benzene sorption	94
Ethylbenzene sorption	95
Summary for arene sorption on hydrated TMA-clay	95
Effect of layer charge on arene sorption on TMA-clay	95
Effect of solute size on arene sorption on TMA-clay	96
Discussion	97
References	100
Appendix A. Supplementary FTIR Dichroism and X-ray Diffraction Data	101
Materials and Methods	101
Clay film preparation	101
Spectral collection	101
Appendix B. Evaluation of ATR-FTIR for Determination of Benzene Sorption Mechanisms from Methanol on Clays	108
Materials and Methods	108
Clay film preparation	108
Spectral collection	108
Appendix C. Supplementary ATR-FTIR sorption spectra	115
Annendix D. Sunnlementary mixed benzene-water sorntion spectra	151

LIST OF TABLES

Chapter :	II		Page	
	Table 1	Selected physical and chemical properties of normal- and reduced-charge TMPA-montmorillonite	20	
	Table 2	Terms used for calculating the Fourier transforms of X-ray diffractograms of glycerol-solvated, normal- and reduced-charge Na+-saturated montmorillonite	24	
	Table 3	Terms used for calculating the Fourier transforms of X-ray diffractograms of normal- and reduced-charge TMPA montmorillonite	25	
Chapter 1	ш			
	Table 1	Selected physical and chemical properties of normal (Norm)- and reduced (Red)-charge TMA- and TMPA-montmorillonite.	47	
	Table 2	Solutions used to regulate the partial pressure of water vapor in the desiccator and in the controlled-atmosphere FTIR cell used to equilibrate TMA- and TMPA-saturated smectites with water vapor.	52	
	Table 3	Infrared band assignments for methyl symmetric and asymmetric deformation vibrations of chloride, bromide, and iodide salts of tetramethylammonium (TMA) in pressed KBr pellets, and observed peak positions of TMA-Cl 1)dispersed in KBr using diffuse reflectance (DRIFT) and 2)dissolved in methanol using attenuated total reflectance (ATR).	60	

Table 4	Infrared band assignments for the v_{19a} and v_{19b} C-C ring stretch of methyl-deuterated (d9) TMPA-iodide and for	
	the v_{19a} , v_{19b} , and methyl asymmetric and symmetric deformation vibrations for TMPA-Br in 1)KBr using	
	diffuse reflectance (DRIFT) and 2)in methanol using	
	attenuated total reflectance (ATR)	64
Chapter IV		
Table 1	Selected physical and chemical properties of normal	
	(Norm)- and reduced (Red)-charge TMA- and TMPA-	
	montmorillonite.	76
Table 2	Solutions used to regulate the partial pressure of water	
	vapor in desiccator and in the controlled-atmosphere	
	FTIR cell.	78
Table 3	Infrared band assignments for methyl symmetric and	
	asymmetric deformation vibrations of chloride, bromide,	
	and iodide salts of tetramethylammonium (TMA) in	
	pressed KBr pellets, and observed peak positions of	
	TMA-Cl 1)dispersed in KBr using diffuse reflectance	
	(DRIFT) and 2)dissolved in methanol using attenuated	
	total reflectance (ATR).	81
Table 4	Infrared band assignments for neat liquid benzene,	
	ethylbenzene, and benzene-d ₆ ·	81
Table 5	Infrared band assignments for the v_{19a} and v_{19b} C-C	
	ring stretch and the methyl asymmetric and symmetric	
	deformation vibrations for TMPA-Br in KBr using diffuse	
	reflectance (DRIFT) and in methanol using attenuated total	
	reflectance (ATR).	90

LIST OF FIGURES

Chapter II		Page
Figure	2-1 Selected infrared vibrations of TMPA adsorbed on normal-charge and reduced-charge Wyoming montmorillonite for 90° and 45° angles of incidence and for TMPA-d ₉ iodide pressed in a KBr pellet (bottom spectrum). Inset at right shows the orientations of the symmetry axes of TMPA and the band assignments for TMPA-d ₉ vibrations along these axes.	27
Figure	2-2 Fourier transforms of X-ray diffraction data for glycerol-solvated Na-montmorillonites. Peaks due to combinations of expanded (E) and collapsed (C) layers are labeled for reduced-charge montmorillonite.	29
Figure	2-3 Fourier transforms of X-ray diffraction data for TMPA-montmorillonites. Peaks due to combinations of expanded (E) and collapsed (C) layers are labeled for reduced-charge montmorillonite.	31
Figure	2-4 Schematic representation of proposed TMPA orientation on normal-charge montmorillonite, with phenyl ring perpendicular to the siloxane surface. Interlayer electron probabilities from one-dimensional Fourier analysis are shown at the right. Both aromatic and methyl protons key into the siloxane surface.	33
Figure	2-5 Schematic representation of TMPA orientation on expanded layers of reduced-charge Wyoming montmorillonite. Layers are propped open by methyl groups, with some methyl protons keying into siloxane surface. Phenyl ring is not parallel to the surface, but exact orientation is not known.	37

Chapter III

Figure 3-1	Diagram of the McBain balance used to collect water vapor sorption isotherms on TMA- and TMPA-saturated smectites. Water vapor pressure is controlled by releasing water vapor from the sorbate reservoir into vacuum. Quantity of water on the clay is determined by measuring the displacement of the quartz springs attached to the sample holders.	49
Figure 3-2	Diagram of the controlled-atmosphere FTIR cell used to equilibrate TMA- and TMPA-saturated smectites with water vapor and collect spectra of clay-water complexes	51
Figure 3-3	Example of the procedure used to normalize all spectra to the same film thickness by normalizing the absorbance of the lattice O-H stretch. A) Original spectrum. B) Original spectrum with the lattice O-H stretching vibration removed. C) difference spectrum of A - B, giving the lattice O-H stretching vibration only and the multiplication factor necessary to bring the absorbance of this band to 0.700A. D) Original spectrum (A) after multiplying it by the factor calculated in (C).	54
Figure 3-4	Water vapor sorption isotherms on normal- (squares) and reduced-(circles) charge clay saturated with TMA (left) and TMPA (right). Graph also shows number of water molecules sorbed per cation at different values of x/m	55
Figure 3-5	Infrared spectra of reduced-charge (top) and normal-charge (bottom) TMA-saturated Wyoming montmorillonite at six different relative humidities. The left side (3600 - 2800 cm ⁻¹) shows the changes in intensity of the sorbed water O-H stretching vibration (3400 cm ⁻¹) with changes in relative humidity. The right side (1800 - 1500 cm ⁻¹) shows the changes in intensity of the sorbed water O-H bending (1630 cm ⁻¹) vibration	
	with changes in relative humidity.	58

Figure 3-6	Infrared spectra of reduced-charge (top) and normal-charge (bottom) TMPA-saturated Wyoming montmorillonite at six different relative humidities. The left side (3600 - 2800 cm ⁻¹) shows the changes in intensity of the sorbed water O-H stretching vibration (3400 cm ⁻¹) with changes in relative humidity. The right side (1800 - 1500 cm ⁻¹) shows the changes in intensity of the sorbed water O-H bending (1630 cm ⁻¹) vibration with changes in relative humidity.	59
Figure 3-7	Effect of relative humidity on the center-of-mass frequency of the methyl asymmetric (top) and methyl symmetric (bottom) deformation vibrations of TMA saturating normal-charge (left) and reduced-charge (right) Wyoming montmorillonite.	61
Figure 3-8	Infrared spectra of normal-charge (left) and reduced-charge (right) TMA-saturated Wyoming montmorillonite showing the changes in frequency of the methyl asymmetric and symmetric deformation vibrations with changes in relative humidity.	62
Figure 3-9	Effect of relative humidity on peak maximum frequencies of the methyl symmetric (top), methyl asymmetric (middle) deformations and low-frequency branch of the v_{19a} ring stretch, (bottom) of TMA saturating normal-charge (left) and reduced-charge (right) Wyoming montmorillonite.	65
Figure 3-10	Infrared spectra of normal-charge (left) and reduced-charge (right) TMPA-saturated Wyoming montmorillonite showing changes in frequency and intensity of the v_{19a} ring stretch and the methyl asymmetric and symmetric deformation vibrations with changes in relative humidity.	66
Figure 3-11	Infrared spectra of normal-charge (left) and reduced- charge (right) TMPA-saturated Wyoming montmorillonite showing changes in intensity of the methyl asymmetric deformation vibration with changes in relative humidity.	68

Chapter IV

V	water -arene complexes.	79
ir r c f g	Effect of mixed benzene-water sorption on the infrared spectrum of normal-charge (left) and reduced-charge (right) TMA-saturated clay. The clay spectra are drawn at the same scale, but stacked for comparison. Band assignments for TMA are given in Table 3 and benzene in Table 4. Peak positions were estimated from peak maxima	82
i c a E b	Effect of mixed deuterobenzene-water sorption on the infrared spectrum of normal-charge (left) and reduced-charge (right) TMA-saturated clay. The clay spectra are drawn at the same scale, but stacked for comparison. Band assignments for TMA are given in Table 3 and benzene-d6 in Table 4. Peak positions were estimated from peak center-of-mass	84
ir C W C ir	Effect of mixed ethylbenzene-water sorption on the infrared spectrum of normal-charge (left) and reduced-charge (right) TMA-saturated clay. The clay spectra were drawn at the same scale, but stacked for comparsion. Band assignments for TMA are given in Table 3 and ethylbenzene in Table 4. Peak cositions were estimated from peak maxima.	85
s _j (1 d B	Effect of mixed benzene-water sorption on the infrared pectrum of normal-charge (left) and reduced-charge right) TMPA-saturated clay. The clay spectra are trawn to the same scale, but stacked for comparison. Band assignments for TMPA are given in Table 5. Peak positions were estimated from peak maxima.	91

	the infraredspectrum of normal-charge (left) and reduced-charge (right) TMPA-saturated clay. The clay spectra are drawn to the same scale, but stacked for comparison. Band assignments for TMPA are given in Table 5. Peak positions were estimated from peak maxima	93
Appendix A		
Figure A1	Clay O-H stretching region of self-supporting normal- and reduced-charge TMPA-d9-saturated clay films oriented at 90° and 45° with respect to the IR beam. Normal-charge clay spectra were normalized to a clay O-H stretch absorbance of 1.000 and the reduced-charge clay spectra were normalized to a clay O-H stretch absorbance of 0.800.	103
Figure A2	O-H stretching region of normal-charge and reduced-charge TMPA-d9 montmorillonite films supported on AgCl disks. The overlaid spectra show the films perpendicular to the IR beam and tilted 30° from perpendicular. No normalization factor was applied.	104
Figure A3	C-C ring-stretching region of the TMPA-d9-iodide salt in a pressed KBr pellet (bottom spectra) and normal-charge and reduced-charge TMPA-d9-montmorillonite films supported on AgCl disks. The overlaid spectra show the film perpendicular to and tilted 30° from perp. with respect to the IR	
	beam.	105

Figure 4-6 Effect of mixed ethylbenzene-water sorption on

Figure A4	iodide salt in a pressed KBr pellet (bottom spectra) and normal-charge and reduced-charge TMPA-d9-montmorillonite films supported on AgCl disks. The overlaid spectra show the film perpendicular to and tilted 30° from perpendicular, with respect to the IR beam.	106
Figure A5	C-C ring stretching region of normal-charge (top) and reduced-charge (bottom) TMPA-montmorillonite films supported on AgCl disks.	107
Figure A6	X-ray diffractogrms of glycerol-solvated, Na+-saturated,normal-charge (left) and reduced-charge (right) Wyoming montmorillonite. Inset numbers indicate d(001)-d(0014).	108
Figure A7	X-ray diffractograms of normal- (left) and reduced- (right) charge TMPA-montmorillonite.	109
Appendix B		
Figure B1	Effect of benzene and methanol sorption on the infrared spectra of reduced-charge hexadecyltrimethylammonium (HDTMA) montmorillonite. Spectra labeled A are clay only in methanol, B 3% benzene in methanol, and C 3% benzene in methanol on HDTMA-saturated clay.	112
Figure B2	Effect of benzene and methanol sorption on the infrared spectra of reduced-charge tetramethylammonium (TMA) montmorillonite. Spectra labeled A are clay only in methanol, B 3% benzene in methanol, and C 3% benzene in methanol on TMA-saturated clay.	113
Figure B3	Effect of benzene and methanol sorption on the infrared spectra of reduced-charge trimethylphenylammonium (TMPA) montmorillonite. Spectra labeled A are clay only in methanol, B 3% benzene in methanol, and C 3% benzene in methanol on TMPA-saturated clay.	114

Figure B4	Effect of benzene and methanol sorption on the infrared spectra of reduced-charge Cs- montmorillonite. Spectra labeled A are clay only in methanol, B 3% benzene in methanol, and C 3% benzene in methanol on Cs-saturated clay.	115
Figure B5	Effect of benzene and methanol sorption on the infrared spectra of reduced-charge Mg- montmorillonite. Spectra labeled A are clay only in methanol, B 3% benzene in methanol, and C 3% benzene in methanol on Mg-saturated clay.	116
Appendix C		
Figure C1	ATR difference spectrum of 3% toluene in methanol.	117
Figure C2	ATR difference spectrum of 3% ethylbenzene in methanol.	118
Figure C3	ATR difference spectrum of 3% chlorobenzene in methanol.	119
Figure C4	ATR difference spectrum of 3% nitrobenzene in methanol.	120
Figure C5	ATR difference spectrum of 3% aniline in methanol.	121
Figure C6	ATR difference spectrum of 3% phenol in methanol.	122
Figure C7	ATR difference spectrum (methanol subtracted) of 3% toluene in methanol on reduced-charge TMA-saturated Wyoming montmorillonite.	123
Figure C8	ATR difference spectrum (methanol subtracted) of 3% toluene in methanol on reduced-charge TMPA-saturated Wyoming montmorillonite.	124
Figure C9	ATR difference spectrum (methanol subtracted) of 3% toluene in methanol on reduced-charge HDTMA-saturated Wyoming montmorillonite.	125

Figure C10	ATR difference spectrum (methanol subtracted) of 3% toluene in methanol on reduced-charge Cs ⁺ -saturated	
	Wyoming montmorillonite.	126
Figure C11	ATR difference spectrum (methanol subtracted) of 3%	
	toluene in methanol on reduced-charge Mg ²⁺ -saturated	
	Wyoming montmorillonite.	127
Figure C12	ATR difference spectrum (methanol subtracted) of 3%	
	ethylbenzene in methanol on reduced-charge TMA-	
	saturated Wyoming montmorillonite.	128
Figure C13	ATR difference spectrum (methanol subtracted) of 3%	
	ethylbenzene in methanol on reduced-charge TMPA-	
	saturated Wyoming montmorillonite.	129
Figure C14	ATR difference spectrum (methanol subtracted) of 3%	
	ethylbenzene in methanol on reduced-charge HDTMA-	
	saturated Wyoming montmorillonite.	130
Figure C15	ATR difference spectrum (methanol subtracted) of 3%	
	ethylbenzene in methanol on reduced-charge Cs+-	
	saturated Wyoming montmorillonite.	131
Figure C16	ATR difference spectrum (methanol subtracted) of 3%	
	ethylbenzene in methanol on reduced-charge Mg ²⁺ -	4.00
	saturated Wyoming montmorillonite.	132
Figure C17	ATR difference spectrum (methanol subtracted) of 3%	
	chlorobenzene in methanol on reduced-charge TMA-	
	saturated Wyoming montmorillonite.	133
Figure C18	ATR difference spectrum (methanol subtracted) of 3%	
	chlorobenzene in methanol on reduced-charge TMPA-	
	saturated Wyoming montmorillonite.	134
Figure C19	ATR difference spectrum (methanol subtracted) of 3%	
	chlorobenzene in methanol on reduced-charge HDTMA-	
	saturated Wyoming montmorillonite.	135

Figure C20	ATR difference spectrum (methanol subtracted) of 3%	
	chlorobenzene in methanol on reduced-charge Cs+- saturated Wyoming montmorillonite.	136
Figure C21	ATR difference spectrum (methanol subtracted) of 3%	
	chlorobenzene in methanol on reduced-charge Mg ²⁺ -	127
	saturated Wyoming montmorillonite.	137
Figure C22	ATR difference spectrum (methanol subtracted) of 3%	
	nitrobenzene in methanol on reduced-charge TMA-	
	saturated Wyoming montmorillonite.	138
Figure C23	ATR difference spectrum (methanol subtracted) of 3%	
	nitrobenzene in methanol on reduced-charge TMPA-	
	saturated Wyoming montmorillonite.	139
Figure C24	ATR difference spectrum (methanol subtracted) of 3%	
	nitrobenzene in methanol on reduced-charge HDTMA-	
	saturated Wyoming montmorillonite.	140
Figure C25	ATR difference spectrum (methanol subtracted) of 3%	
	nitrobenzene in methanol on reduced-charge Cs+-	
	saturated Wyoming montmorillonite.	141
Figure C26	ATR difference spectrum (methanol subtracted) of 3%	
	nitrobenzene in methanol on reduced-charge Mg ²⁺ -	
	saturated Wyoming montmorillonite.	142
Figure C27	ATR difference spectrum (methanol subtracted) of 3%	
	aniline in methanol on reduced-charge TMA-	
	saturated Wyoming montmorillonite.	143
Figure C28	ATR difference spectrum (methanol subtracted) of 3%	
	aniline in methanol on reduced-charge TMPA-	
	saturated Wyoming montmorillonite.	144
Figure C29	ATR difference spectrum (methanol subtracted) of 3%	
	aniline in methanol on reduced-charge HDTMA-	
	saturated Wyoming montmorillonite.	145

	Figure C30	ATR difference spectrum (methanol subtracted) of 3% aniline in methanol on reduced-charge Cs ⁺ -saturated	
		Wyoming montmorillonite.	146
	Figure C31	ATR difference spectrum (methanol subtracted) of 3% aniline in methanol on reduced-charge Mg ²⁺ -saturated	1.45
		Wyoming montmorillonite.	147
	Figure C32	ATR difference spectrum (methanol subtracted) of 3% phenol in methanol on reduced-charge TMA-saturated	
		Wyoming montmorillonite.	148
	Figure C33	ATR difference spectrum (methanol subtracted) of 3% phenol in methanol on reduced-charge TMPA-saturated	
		Wyoming montmorillonite.	149
	Figure C34	ATR difference spectrum (methanol subtracted) of 3% phenol in methanol on reduced-charge HDTMA-saturated	
		Wyoming montmorillonite.	150
	Figure C35	ATR difference spectrum (methanol subtracted) of 3% phenol in methanol on reduced-charge Cs+-saturated	
		Wyoming montmorillonite.	151
	Figure C36	ATR difference spectrum (methanol subtracted) of 3%	
		phenol in methanol on reduced-charge Mg ²⁺ -saturated Wyoming montmorillonite.	152
Appendi	x D		
	Figure D1	Effect of water sorption on the intensity and position of the C-H out-of-plane deformation vibration of	
		sorbed benzene on normal-charge (left) and reduced-	
		charge (right) TMA-saturated clay. Spectra are drawn to the same scale, but stacked for comparison.	153

Figure D2	of the C-H out-of-plane deformation vibration of sorbed benzene on normal-charge (left) and reduced-charge (right) TMPA-saturated clay. Spectra are drawn to the same scale, but stacked for comparison.	154
Figure D3	Effect of vacuum treatment and exposure to saturated water vapor on the intensity of the C-H out-of-plane deformation vibration of sorbed benzene on normal-charge (left) and reduced-charge (right) TMA-saturated clay. Spectra shown are drawn at same scale, but stacked for comparison.	155
Figure D4	Effect of vacuum treatment and exposure to saturated water vapor on the intensity of the C-H out-of-plane deformation vibration of sorbed benzene on normal-charge (left) and reduced-charge (right) TMPA-saturated clay. Spectra shown are drawn at same scale, but stacked for comparison.	156
	stacked for comparison.	130

CHAPTER I

INTRODUCTION AND REVIEW OF LITERATURE

INTRODUCTION

The topic of this research is evaluation of properties of clay minerals saturated with organic cations and mechanisms of arene and water sorption on these clays by spectroscopic methods. These materials have shown promise as sorbents for arenes and other pollutant compounds (Boyd et. al, 1991). Three major topics of research will be studied: 1. Changes in cation orientation due to variations in clay charge density. 2. Determining whether water preferentially sorbs on organic cation sites or on siloxane surface sites of the clay mineral. 3. Evaluating competition between water and arene sorbates on sorption sites of the modified clay. Understanding interaction mechanisms of arenes with modified clay mineral surfaces will help us understand interaction mechanisms between arenes and mineral surfaces in the environment.

REVIEW OF LITERATURE

TMPA orientation

Expanding 2:1 clay minerals saturated with organic cations like trimethylphenylammonium (TMPA) have been proposed for remediating solvent waste streams and contaminated soils (Boyd et al., 1991). Determining orientation of TMPA phenyl groups in the interlamellar region of expanding 2:1 clay minerals may provide clues to how solutes diffuse and sorb in the interlamellar space. Phenyl group orientation may change depending on the charge density of the clay.

Jaynes and Boyd (1991) showed that sorption of nonpolar arenes from water onto TMPA-saturated smectites increased as clay surface-charge density and the quantity of adsorbed TMPA decreased. As average separation between TMPA ions increased, the area of accessible siloxane surface increased. Thus, arene sorption increased as accessible siloxane surface area increased. This suggested that aromatic compounds are adsorbed on uncharged siloxane surfaces and that these surfaces are hydrophobic (Jaynes and Boyd, 1991).

An alternative to Jaynes and Boyd's (1991) hypothesis is suggested by the carbon content of their fully-charged Arizona montmorillonite which showed there were 1050 mmols TMPA per kilogram of clay while the CEC was 1300 mmols kg⁻¹. Since they added a 5- to 10- fold excess of TMPA, it may not be possible to fully saturate this clay with TMPA because of the clay charge density and the cation size. Perhaps, there was insufficient siloxane surface area to completely saturate the clay with TMPA cations. If it is not possible to fully saturate this clay with TMPA, it might suggest that the sorption of nonpolar arenes may also be restricted. Reducing the charge density might cause the phenyl rings of the cations to reside farther apart without interaction with other TMPA

cations. This could permit greater sorption of arenes on the these clays regardless of whether arenes sorb on the siloxane surface or on the cation.

Determining TMPA cation arrangement in the interlayer of clays with different charge densities would help determine the mechanism for the increase in arene sorption due to charge reduction. Tighter cation packing of higher-charge clay cations might sterically hinder diffusion of arenes into the interlayer and provide fewer available sorption sites for arenes on normal-charge clays (Lee et al., 1989, 1990; Jaynes and Boyd, 1991). Less competition for space on the siloxane surface of lower-charge smectites could allow TMPA phenyl groups to lie in a flatter orientation rather than being forced upright as might occur on higher-charge smectites. A flat orientation may indicate greater spacing between cations, which may favor diffusion and sorption in the interlayer.

The d(001) spacings observed by Jaynes and Boyd (1991) for normal-and reduced-charge (~40% reduced) TMPA-smectite were 15.3 Å and 14.4 Å respectively. The shift to 14.4 Å may be the result of random interstratification of different d(001) spacings (Reynolds 1980). For example, in the higher-charge clay, phenyl groups may lie perpendicular to the siloxane surface. Some phenyl groups in reduced-charge clay may be oriented parallel to the siloxane surface in some of the interstratified layers, giving the reduced spacing.

Further X-ray diffraction analysis can provide a clue to the orientation of TMPA cations on expanding clays. Greene-Kelly (1955) collected X-ray powder photographs of 70 different montmorillonite-aromatic complexes. Through Fourier transforms of diffraction patterns and d-spacing measurements, Greene-Kelly (1955) proposed that 15 Å d(001) spacings of mononuclear aromatics were due to phenyl rings of the sorbates lying perpendicular to the siloxane surface of the clay. Spacings of 12.5 Å to 13 Å were due to all aromatic rings lying flat on the siloxane surface of the clay. Randomly interstratified 13

Å and 15 Å spacings due to flat and parallel orientations of the TMPA phenyl group could give d(001) spacings between 14 and 15 Å like those observed by Boyd et al. (1991).

Possible interstratified spacings for a reduced-charge smectite saturated with TMPA

(Jaynes and Boyd, 1991) might be:

- 1. 9.5 Å for clay layers which completely collapsed with their charge reduction treatment and were not re-expanded before adsorbing TMPA.
- 2. 15.3 Å for clay layers where phenyl groups of the cations are oriented perpendicular to the siloxane surface of the clay, similar to what might be the case in normal-charge clay.
- 3. An intermediate spacing of 12 Å to 13 Å where the change in charge density allowed cation phenyl groups to shift to a parallel orientation with respect to the siloxane surface.

The Fourier transform method was outlined by MacEwan (1956) for determining components of the observed spacings of randomly interstratified mixtures of 2:1 clay minerals. This method estimates the "..probability of finding a given layer to layer distance in crystal space" (Reynolds (1980). For example, a randomly interstratified micamontmorillonite complex solvated with glycerol would likely give a single, broad X-ray diffractogram peak at 13 to 14 Å. Yet, such a material would have interlayer spacings of 10 Å due to mica layers and 17 Å due to smectite layers in the clay mineral structure (MacEwan 1956). Spacings due solely to mica would be visible on a Fourier transform in 10 Å increments beginning at 10 Å and continuing through the transform as far as it was calculated. Spacings due solely to the smectite would be visible in 17 Å, increments beginning at 17 Å and continuing through the transform. The Fourier transform can also give spacings due to mixtures of the two components. For example a peak at 27 Å would be observed for the combination of the first peak of mica and the first peak of smectite (10 Å+17 Å).

The Fourier transform can be used to verify various interlayer spacings of interstratified unknowns and even estimate relative proportions of different interlayer spacings (MacEwan, 1956). This method has also been used to determine orientation of organic sorbates in the interlayer of smectite (Greene-Kelly, 1955) and vermiculite (Serratosa, 1966) by estimating where regions of electron density due to sorbates in the interlayer occur.

Another tool used for determining orientation of adsorbed compounds on clays is infrared spectroscopy. Vibrational transitions responsible for absorption of infrared radiation occur along specific symmetry axes of molecules (Cotton, 1960). If sorbed molecules assume a preferred orientation on an oriented clay mineral specimen, it is possible that one of the vibrational symmetry axes of the sorbed molecules will be parallel to incident infrared radiation. The absorbance of that vibration would be minimized and tend to approach zero (Serratosa, 1966; Farmer and Mortland, 1966). If the clay mineral specimen with the sorbed molecules is then tilted with respect to the infrared radiation of the spectrometer, vibrations which were parallel to the incident radiation, now have a greater cross section to absorb the infrared radiation, and the intensity observed for that band will increase dramatically. This phenomenon, called infrared dichroism, has been used by Farmer and Mortland (1966) and Serratosa (1966) to determine the orientation of pyridine and pyridinium when adsorbed on clay minerals. Infrared band positions of TMPA can also be observed to determine if different interactions occur between the cation and the clay (or other cations) due to differences in charge density. For example, if $\pi - \pi$ interactions occur between TMPA phenyl groups with high charge density, then a decrease in charge density could cause band positions of TMPA phenyl groups to change because of less π - π interaction.

Water adsorption on clavs

Determining the preferred adsorption site for water on alkylammonium-saturated clays is necessary for determining the effect of hydration on arene sorption. There are two major sites of water adsorption on expanding 2:1 clay minerals. Water molecules can form coordination shells around the saturating cation or sorb on the siloxane surface (Sposito and Prost, 1982). Most spectroscopic data for water sorption on clays has focused on clays saturated with inorganic cations.

When clay is saturated with inorganic cations, the most important site for water adsorption on clays is around cations saturating the clay mineral (Farmer and Russel, 1971; Sposito and Prost, 1982; Sposito, 1984). Prost (1975) collected infrared spectra of water and deuterated water vapor sorbed on montmorillonite and hectorite films saturated with different inorganic cations. Prost (1975) concluded that at low water contents, water molecules were arranged in three-fold coordination around the saturating cation in a single plane parallel to the siloxane surfaces. Other studies cited by Sposito and Prost (1982) used nuclear magnetic resonance and electron spin resonance, in conjunction with X-ray diffraction to verify that the structure of water around the inorganic saturating cations of partially hydrated smectites was similar to that proposed by Prost (1975). Pinnavaia (1980) described changes in water structure around saturating cations of clays as water content changed from slightly hydrated to fully hydrated. When slightly hydrated, water was arranged in planer coordination around the cation as described by Prost (1975). As water content increased water formed a 3-layer coordination shell around the saturating cation with water molecules above and below the cation as well as in the plane of the cation parallel to the siloxane surface. With further increasing water content, the cation-water coordination complex developed a tumbling motion suggesting that the siloxane surface

was no longer restricting its motion. This meant the cation-water complex was behaving more like an ion in solution. This is important when considering the competitive sorption of solutes and water on smectites. At low water contents, a solute can sorb on sites unoccupied by hydrated cations. At high water contents, a solute must compete with a bulk water-like phase occupying the clay interlayer.

Another possible site of water sorption on expanding 2:1 clay minerals is the siloxane surface. Siloxane surface oxygens are weak, soft Lewis bases and could potentially form hydrogen bonds with water (Sposito, 1984). Lewis basicity of the surface oxygens increases with isomorphous substitution and is dependent on the location of the substitution. When isomorphous substitution occurs in the tetrahedral layer (Sposito, 1984; Bleam, 1990), the negative charge is effectively distributed among three surface oxygen atoms as opposed to ten surface oxygen atoms when substitution is in the octahedral layer (Sposito and Prost, 1982). Lewis basicity, and thus hydrogen bonding, is greatest when the substitution is in the tetrahedral layer. Cations balance the charge on these sites, so any water in the vicinity of an isomorphous substitution will also be affected by the cation.

The preferred site of water adsorption on clays saturated with quaternary ammonium cations has not been studied spectroscopically. Water vapor sorption isotherms collected by Gast and Mortland (1971) showed that TMA- saturated montmorillonite consistently sorbed more water vapor than NH₄⁺- saturated montmorillonite. Prost (1975) collected water vapor sorption isotherms on K⁺-and Cs⁺-saturated hectorite which showed similar amounts of water sorption to that observed by Gast and Mortland (1971) for NH₄⁺- and TMA-saturated montmorillonite. The shapes of these isotherms was also similar. Since the primary site of water sorption on K⁺-and Cs⁺-saturated clays has been shown to be coordinated around cations, this suggests that TMA cations are the primary sorption site,

rather than the siloxane surface. Sorption isotherms of arenes on TMA- and TMPAsaturated montmorillonites collected in the presence and absence of water have shown that water inhibits arene sorption on these clays (Lee et al., 1990; Jaynes and Boyd, 1991). The effect of charge density on the sorption of arenes from water provides indirect evidence for sites of water sorption on clays. Lee et al. (1990) stated that water sorption on either TMA cations or the siloxane surface might have caused the decrease in arene sorption from aqueous solution compared with arene sorption on dry TMA-montmorillonite. In addition, Lee et al. (1990) noted greater sorption of arenes from water on low-charge TMA-clay than higher-charge clay. In Jaynes and Boyd (1991) arene sorption from water was compared between reduced- and normal-charge Arizona montmorillonite saturated with TMPA to determine whether aromatic hydrocarbons preferentially sorbed on the siloxane surface or the cations. Sorption of arenes from water increased as the layer charge of the clay was reduced, implying that arene sorption was more favored than water adsorption on the siloxane surface and that the siloxane surface was more hydrophobic than the cations. This result was in agreement with the observations of Lee et al. (1990) noting the effect of charge on arene sorption. These results suggested that the cations are the preferred sorption site for water since the siloxane surface was more hydrophobic than the cations. Although circumstantial evidence is rather strong that quaternary ammonium cation sites are preferred for water sorption on TMA- and TMPA-saturated clay, spectroscopic evidence will help to verify whether water sorbs preferentially on the siloxane surface or around cations on these clays.

Competitive sorption of arenes and water

Sorption of arenes onto clays can be divided into two broad categories: simple physical sorption and sorption involving strong chemical interactions of the π -electrons of the aromatic ring with some substituent of the sorbent. An example of a strong interaction

was observed by Mortland and Pinnavaia (1971) where a red complex formed between benzene and Cu²⁺-saturated montmorillonite when the clay was dry. Using infrared spectroscopy, they determined that the red color formed because Cu²⁺ ions saturating the clay withdrew π -electrons from benzene. Similar complexes can form between Cu²⁺saturated montmorillonite and toluene, and ortho, meta, and para-xylene (Pinnavaia and Mortland, 1971; Johnston et al., 1992). Clementz and Mortland (1972) also observed formation of ligand complexes between Ag1+ saturated montmorillonite and benzene, toluene, and ortho-, meta-, and para-xylene. In all studies, physical sorption of nonpolar arenes occurred on clays when ligand or charge-transfer complexes formed. Johnston et al. (1992) found spectroscopic evidence for physical sorption, but no ligand complexes formed between p-xylene and Co²⁺- saturated montmorillonite. The Co²⁺ did not withdraw π -electron density from the p-xylene as did copper. This result could be predicted from the electronic structure of the ions. Cu²⁺ tends to withdraw electron density from the π -cloud of benzene because it only needs one electron to fill its d orbital, while Co²⁺ needs 3 electrons (Shriver, Atkins, and Langford, 1990).

The ligand and charge transfer complexes of benzene and alkylbenzenes on smectites saturated with transition metal ions studied by Mortland and Pinnavaia (1971), Pinnavaia and Mortland, (1971), Clementz and Mortland (1972) and Johnston et al. (1992) were destroyed by sorbed water. When clay films were exposed to water vapor, color created by ligand complexes immediately disappeared. Infrared spectroscopy revealed only physical sorption of benzene or alkylbenzene on the clays. In all of these studies, the cations on the clay surface were being hydrated by the water, destroying the complex formed between the π -cloud of the aromatic and the cation. The only sites remaining for benzene and alkylbenzenes to sorb on these clays were on the siloxane surface.

The competitive sorption of arenes and water on clays saturated with alkali and alkaline earth cations has been studied with vapor sorption isotherms. Rhue et al. (1989) collected ethylbenzene vapor sorption isotherms on a (Ca²⁺, Na¹⁺) saturated bentonite with partial water vapor pressures ranging from 0.00 to 0.56. The amount of ethylbenzene sorbed was the same at P/P_o of 0.00 as it was at 0.20. At 0.50, ethylbenzene sorption was substantially reduced. The shape of the sorption isotherms also changed at higher relative humidities. Isotherms at low relative humidities were S-shaped, while at higher relative humidities isotherms were linear. The authors suggested that a change in the sorption mechanism of ethylbenzene occurred as clay-water content increased, but the mechanism could not be deduced from the isotherms alone. Rhue et al. (1989) theorized about possible sorption mechanisms of the ethylbenzene on the hydrated surface of the bentonite, but did not state whether the water was hydrating cations or forming H-bonds with the siloxane surfaceRhue et al. (1989) felt that competition between water vapor and ethylbenzene at higher water vapor pressures caused the decrease in ethylbenzene sorption and changes in isotherm shape. Infrared spectroscopic data from Johnston et al. (1992) would suggest that Rhue et al. (1989) observed simple physical sorption of ethylbenzene on the siloxane surface of the clay which decreased as water hydrating the cations saturating the clay occupied more siloxane surface.

Clays saturated with quaternary ammonium cations may sorb arenes physically on the siloxane surface and/or at the cation when dehydrated. Barrer and Perry (1961) used X-ray diffraction to measure the d(001) spacings of a dry bentonite saturated with TMA after sorbing benzene vapors at P/P_0 between 0.05 and 0.8. The spacing increased from 13.6 Å to 14.6 Å at $P/P_0 = 0.05$ and remained at that spacing for all other treatments. Using estimated interlayer surface area, and the clay cation exchange capacity, Barrer and Perry (1961) concluded that the most likely orientation of the benzene in the interlayers was

restricted by TMA cations forcing benzene to sorb on cation sites in a tilted orientation between cations. Lee et al. (1990) noted that sorption of vapor-phase benzene was greater for dry TMA- saturated high-charge Arizona montmorillonite than it was for lower-charge TMA saturated Wyoming montmorillonite at partial pressures of benzene greater than 0.6. The Arizona clay may have had greater sorption because it had more cation sites.

Understanding the mechanism by which water reduces arene sorption on quaternary ammonium-saturated clays is important to understanding the sorptive properties of these clays. Lee et al. (1990) theorized that the decreased amount of aqueous benzene, toluene, and o-xylene sorption on TMA-saturated high-charge Arizona montmorillonite relative to low-charge Wyoming montmorillonite was because of a water-induced sieving effect in high-charge clay. They stated that hydration of mineral surfaces or saturating cations reduced accessibility of the interlayer to arenes. Lee et al. (1990) also observed that arene sorption on the clay from water decreased as the number of methyl groups on the arene were increased. This was attributed to steric hinderance to diffusion of larger arenes into the interlayer of clay. In further work, Jaynes and Boyd (1991) collected sorption isotherms of arenes from water on TMPA clays with varied charge densities and found that arene sorption increased as charge density decreased. This finding indicated that the siloxane surface of the clay was the probable sorption site for arenes and the cations probably functioned as a pillars to hold the clay layers open. Jaynes and Boyd (1991) further concluded that "...a large part of the siloxane surface in smectites has a hydrophobic nature. A conclusion that can be drawn from this work is that since the siloxane surface of the clay was hydrophobic, the TMPA cations were hydrophillic and were the probable site for water sorption on these clays.

The basic mechanisms of arene sorption and water inhibition of sorption on TMA-and TMPA-saturated clay of different charge densities may be investigated using spectroscopic techniques. Clay films with different charge densities saturated with TMA and TMPA can be prepared. These films can be treated with different combinations of arene and water vapor and probed using infrared spectroscopy to determine the effect of charge density, water sorption, and arene sorption on the position of cation and arene vibrational frequencies. From this information, the preferred sorption sites for water and arenes on TMA- and TMPA-saturated clay may be determined.

REFERENCES

- Barrer, R.M. and G.S. Perry. 1961. Sorption of mixtures and selectivity in alkylammonium montmorillonites. Part II. Tetramethylammonium bentonite. J. Chem. Soc. 57:849-859.
- Bleam, W.F. 1990. The nature of cation substitution sites in phyllosilicates. Clay and Clay Minerals 38:527-536.
- Boyd, S. A., W. F. Jaynes, and B. S. Ross. 1991. p. 181-372 (ed.) Organic substances and sediments in water vol. 1. CRC Press, Boca Raton, FL
- Clementz, D.M., and M.M. Mortland. 1972. Interlamellar metal complexes in layer silicates III Silver(I)-Arene complexes in smectites. Clays and Clay Minerals 20:181-187.
- Cotton, F.A., 1960. The infrared spectra of transitional metal complexes. pp. 305-315. In J. Lewis and R.G. Wilkins (ed.) Modern Coordination Chemistry. Interscience Publishers Inc. New York.
- Farmer, V. C., and M. M. Mortland. 1966. An Infrared Study of the Co-ordination of Pyridine and Water to Exchangeable Cations in Montmorillonite and Saponite. J. Chem Soc. 344-351.
- Farmer, V.C., and J.D. Russell. 1971. Interlayer complexes in layer silicates—The structure of water in lamellar ionic solutions. Trans Farad. Soc. 67:2737-2749.

- Gast, R.G., and M.M. Mortland. 1971. Self-diffusion of alkylammonium ions in montmorillonite. J. Coll. Int. Sci. 37:80-92.
- Greene-Kelly, R. 1955. Sorption of Aromatic Organic Compounds by Montmorillonite Pt. 1.—Orientation Studies. Trans. Faraday Soc. 51:412-424.
- Jaynes, W.F., and S.A. Boyd. 1991. Hydrophobicity of siloxane surfaces in smectites as revealed by aromatic hydrocarbon adsorption from water. Clays and Clay Minerals 39:428-436.
- Johnston C.T., T. Tiupton, S.L. Trabue, C. Erickson, and D.A. Stone. 1992. Vapor-Phase Sorption of p-Xylene on Co- and Cu-Exchanged SAz-1 Montmorillonite. Env. Sci. Tech. 26:382-390.
- Lee, J.-F., M.M. Mortland, S.A. Boyd and C.T. Chiou. 1989. Shape-selective adsorption of aromatic compounds from water by tetramethylammonium-smectite: J. Chem Soc Faraday Trans. I 85: 2953-2962.
- Lee, J.-F., M.M. Mortland, C.T. Chiou, D.E. Kile, and S.A. Boyd. 1990. Adsorption of benzene, toluene, and xylene by two tetramethylammonium-smectites having different charge densities. Clays Clay Minerals. 38:113-120/
- MacEwan, D.M.C., 1956. Fourier Transform Methods for Studying Scattering from Lamellar Systems I. A Direct Method for Analysing Interstratified Mixtures. Kolloid Zeitschrift 149:96-108.
- Mortland, M.M. and T.J. Pinnavaia. 1971. Formation of copper (II) arene complexes on the interlamellar surfaces of montmorillonite. Nature Physical Science 229:75-77.
- Pinnavaia, T.J. 1980. Advanced Chemical methods for soil and Clay Minerals Research Ch. 8. J.W Stucki and W.F. Banwart (Ed.) D. Reidel: Boston.
- Pinnavaia, T.J., and M.M. Mortland. 1971. Interlamellar metal complexes on layer silicates. I. Copper(II)-arene complexes on montmorillonite. J. Phys Chem. 75:3957-3962.
- Prost, R. 1975. Étude de l'hydration des argiles: Interactions eau-minéral et mécanisme de la rétention de L'eau II. Étude d'une smectite (Hectorite). Ann. Agron 26:463.

- Reynolds, R.C. 1980. Interstratified Clay Minerals. in Mineralogical Society Monograph no. 5. Crystal Structures of Clay minerals and their X-ray identification. G.W. Brindley and G. Brown eds. Mineralogical Society 41 Queen's Gate London SW7 5HR.
- Rhue, R.D., K.D. Pennell, P.S.C. Rao, and W.H. Reve. 1989. Competitive adsorption of alkylbenzene and water vapors on predominantly mineral surfaces.

 Chemosphere 18:1971-1986.
- Serratosa, J.M. 1966. Infrared Analysis of the orientation of Pyridine molecules in clay minerals. Clays and Clay Minerals 14:385-391.
- Shriver, D.F., P.W. Atkins, and C.H. Langford. 1990. Inorganic Chemistry. W.H. Freeman and Co. New York.
- Sposito, G., and R. Prost. 1982. Structure of water adsorbed on smectites. Chemical Reviews 82:553-573.
- Sposito, G. 1984. The surface chemistry of soils. Oxford University Press. New York, 234pp.

CHAPTER II

Orientation of the Phenyl Group of Trimethylphenylammonium on Normal- and Reduced-charge Wyoming montmorillonite

ABSTRACT

The orientation of trimethylphenylammonium (TMPA) cations adsorbed on montmorillonite affects the adsorbate-accessible siloxane surface and determines whether the TMPA phenyl ring can interact with other aromatic adsorbates by π - π interactions. The purpose of this study was to determine the orientation of TMPA ions in the interlayer of normal-charge and reduced-charge Wyoming montmorillonite. The orientation of TMPA's phenyl group was investigated using infrared dichroism of selected aromatic ring vibrations. X-ray diffraction and one-dimensional Fourier analysis were used to determine interlayer spacings and the interlayer electron distribution of TMPA and to ascertain whether reduced-charge Wyoming montmorillonite is a randomly interstratified mixture of layers with two different d-spacings. For normal-charge montmorillonite, the infrared results showed that the C-N bond axis is neither perpendicular nor parallel to the surface, yet X-ray data suggested that the TMPA phenyl ring is perpendicular to the siloxane surface. In this orientation, the average adsorbate-accessible surface area is 50 Å²/cation, which is consistent with N₂ BET surface-area measurements. Reduced-charge montmorillonite is a randomly interstratified mixture of 25% collapsed layers with no adsorbed cations and 75% expanded layers that are propped open by TMPA's methyl groups, not the aromatic ring. The adsorbate-accessible surface area on expanded layers of reduced-charge montmorillonite is about twice that on normal-charge TMPA-clay. When

the phenyl ring of TMPA is perpendicular to the surface, it should be possible for polar compounds such as water to interact with the positively charged nitrogen atom while aromatic compounds interact with the phenyl ring by π - π interactions.

INTRODUCTION

Smectite and other expanding 2:1 clay minerals sorb aromatic hydrocarbons from water when small quaternary alkylammonium cations such as trimethylphenylammonium (TMPA) occupy the clay's cation exchange sites (Boyd et al., 1991 and references cited therein). Information about the orientation and distribution of organocations within clay interlayers will aid in developing suitable organoclay sorbents for a particular waste stream because these properties affect sorption capacity and sorption mechanisms. For example, the surface-charge density of a clay may affect the orientation of an adsorbed organic cation's aromatic ring (Serratosa, 1966), which in turn may affect the interlayer surface area accessible to uncharged organic sorbates such as aromatic pollutants. The orientation of TMPA phenyl rings may also determine whether TMPA's π -electrons can interact with other aromatic sorbates by π - π interactions.

Infrared dichroism experiments can be used to determine the orientation of the aromatic ring and the C-N bond axis of TMPA. When an infrared beam is parallel to an axis of molecular vibration, the absorption intensity of that vibration will be minimized. If the sample is rotated so that the infrared beam is no longer parallel to the infrared vibration, the absorption intensity will increase. Thus, any preferred orientation of molecules adsorbed on siloxane surfaces will cause the intensity of one or more vibrational bands to change when an oriented clay film is rotated in an infrared beam. For example, infrared dichroism experiments have shown that uncharged polar aromatic molecules like pyridine

(Farmer and Mortland, 1966; Serratosa, 1966) and benzonitrile (Serratosa, 1968) lie perpendicular to the siloxane surface of montmorillonite, with the polar group midway between opposing clay surfaces. This orientation allows the polar group to either solvate adsorbed inorganic cations directly or to interact with water molecules in the hydration shell of the inorganic cation. In contrast, when pyridinium ions satisfy a clay's negative charge, infrared dichroism experiments have shown that the pyridinium ring lies parallel to montmorillonite but perpendicular to vermiculite surfaces (Serratosa, 1966). The difference in orientation was attributed to the higher charge density of vermiculite: the surface area per negative charge on Wyoming montmorillonite can accommodate pyridinium ions lying flat on the clay surface, whereas pyridinium can only satisfy the structural charge of vermiculite in an upright position (Serratosa, 1966). In either case, the orientation of the pyridinium ring minimizes charge separation between the NH⁺ group of pyridinium and the structural charge of the clay. The orientation of adsorbed TMPA cations should also minimize charge separation within steric constraints imposed by the size of the TMPA ion and the clay's surface-charge density.

X-ray diffraction, particularly Fourier transform analysis of diffraction data, can provide complementary information about clay structure and adsorbate orientation. Fourier analysis of X-ray diffractograms can be used to verify the existence of random interstratification, to determine d-spacings of individual components in an interstratified mixture, and to estimate relative proportions of each component in an interstratified mixture (MacEwan, 1956; Reynolds, 1980). Fourier transforms of X-ray diffraction data can also be used to determine the orientation of organic adsorbates (e.g., Greene-Kelly, 1955; Bradley et al., 1963; Johns and Sen Gupta, 1967). One-dimensional Fourier analysis of nitrobenzene and pyridine complexes with montmorillonite (Greene-Kelly, 1955) gave

interlayer electron density distributions that are completely consistent with infrared dichroism results for polar aromatic compounds (Serratosa, 1966; 1968).

The objective of this research was to determine the orientation of TMPA cations on normal-charge and reduced-charge Wyoming montmorillonites. Specifically, infrared dichroism experiments were used to test the hypothesis that TMPA phenyl groups are perpendicular to the surface of normal-charge montmorillonite and parallel to the surface of reduced-charge montmorillonite. Infrared dichroism will not be observed if the principal vibration axes of TMPA are randomly oriented or if the preferred orientation is such that none of the principal vibration axes is perpendicular to the surface. Additionally, little or no dichroism will be observed if a clay comprises interstratified layers with different TMPA orientations. One-dimensional Fourier analysis of X-ray diffraction data was used to test the hypothesis that reduced-charge clay comprises a randomly interstratified mixture of layers with different TMPA orientations and hence with different d-spacings.

MATERIALS AND METHODS

Preparation of reduced- and normal-charge TMPA montmorillonite

Wyoming montmorillonite (SWy-1) was obtained from the Clay Minerals Society Source Clays Repository at the University of Missouri-Columbia. The <2-μm fraction was separated from the coarser material by sedimentation. Half of the <2-μm clay was saturated with Na⁺ and the other half with Li⁺ by shaking 4 g of clay with 200 ml of the appropriate 0.1 M chloride solution, centrifuging the suspensions, and decanting the supernatant solutions. This shaking-centrifugation-decantation process was repeated three times. Excess salts were removed from the homoionic clays by dialysis until an AgNO₃ test for chloride was negative. Part of the dialyzed Na⁺-saturated clay suspension ("normal-charge" clay) was freeze-dried and set aside.

The layer charge of the remaining clay was reduced by a method similar to that described by Brindley and Ertem (1971). Briefly, a suspension composed of 50% Li⁺-saturated and 50% Na⁺-saturated clay by mass was freeze-dried, then heated 18 h in quartz crucibles at 250 °C to dehydrate adsorbed Li and promote Li migration into vacant octahedral sites. The collapsed, reduced-charge clay was re-expanded by sonicating 2-g subsamples of clay in 200 ml of a 70% methanol-water mixture for 20 min in an ice-water bath (Greene-Kelly, 1953; Brindley and Ertem, 1971; Jaynes and Bigham, 1987). A Heat Systems, Ultrasonic Inc. model W-385 sonicator with a 7-mm diameter probe tip on a setting of 7 (out of 10) was used.

To prepare TMPA-saturated montmorillonites for the X-ray diffraction studies described below, TMPA-Br was added to both normal- and reduced-charge montmorillonites in 70% methanol-water suspensions (10 g clay l⁻¹) and stirred for 72 h. The amount of TMPA added was ten times the CEC. After the suspensions were stirred, clays were dialyzed until bromide-free and then were freeze-dried. Selected properties of normal- and reduced-charge TMPA-clays are reported in Table 2-1.

Infrared dichroism

Preparation of methyl-deuterated TMPA.

As will be discussed later, accurate assignment and identification of the v_{19a} and v_{19b} infrared bands of TMPA is essential for using infrared dichroism to determine the orientation of adsorbed TMPA. Methyl C-H deformation vibrations of TMPA overlap at least partially with the v_{19a} and v_{19b} ring stretching vibrations, but the ring vibrations are distinct in methyl-deuterated TMPA. Thus, methyl-deuterated TMPA (TMPA-d₉) was prepared, and montmorillonites saturated with TMPA-d₉ were used in the infrared dichroism experiments described below.

Table 2-1. Selected physical and chemical properties of normal- and reduced-charge TMPA- montmorillonite.

Treatment	d(001) ¹ (Å)	N ₂ Surface Area ² (m ² g ⁻¹)	Total C ³ (g kg ⁻¹)	_	A ⁴ CEC ⁵ (mmol kg ⁻¹)
Reduced	13.9	318±14	48.6±0.9	449±8	390±30
Normal	14.9	252±28	88.1±1.0	814±11	870±80

- 1 = Obtained from Fourier transform of XRD data.
- $2 = \text{Avg} \pm \text{SD}$ (N=2 or 3) from three-point BET N₂ adsorption isotherms using a Quantachrome Quantasorb Jr. surface area analyzer.
- 3 = Avg ± SD (N=2) of total C determined by combustion at 900 °C using a Dohrmann DC-190 high-temperature carbon analyzer.
- $4 = Avg \pm SD$ (N=2) calculated with the equation:

Adsorbed TMPA =
$$\frac{\text{Total g C}}{\text{kg Clay}} \times \frac{\text{mmol TMPA}}{\text{g C}}$$

5 = Avg ± SD (N=3 or 4) Determined by Na⁺ saturation and ammonium displacement of the parent normal- and reduced-charge clays. Statistically identical values were obtained with Mg²⁺ saturation and Ba²⁺ extration.

Methyl-deuterated TMPA (TMPA-d₉) was synthesized using a procedure modified from that of Cope et al. (1960). Aniline, NaHCO₃, and CD₃I in a mole ratio of 1:3:3 were refluxed in methanol [10:1 methanol:aniline (v:v)] with constant stirring for 75 h.

Deuterated methyl iodide was added after 24 and 48 h to give a final CD₃I:aniline mole ratio of 4.5:1. After the mixture was refluxed, it was evaporated to dryness in the reflux flask. The residual solid was extracted three times with boiling chloroform. The volume of chloroform for each extraction was equal to the volume of methanol used during reflux. The hot chloroform extracts, which contained the deuterated TMPA-iodide, were decanted from the solid material remaining in the flask and were filtered. Much of the deuterated TMPA-iodide crystallized on the filter because the boiling chloroform cooled rapidly at room temperature. Deuteration of the TMPA methyl groups was verified by obtaining the FTIR spectrum of the white crystalline product in a pressed KBr pellet.

Clay film preparation.

Oriented, self-supporting TMPA-d₉-saturated clay films were prepared by sedimenting Na⁺-saturated normal-charge and reduced-charge montmorillonite suspensions onto glass slides. The Na-montmorillonite films were air-dried at room temperature and then were reacted overnight at 60 °C with 20 ml of TMPA-d₉ in ethanol (5 mmol TMPA-d₉ kg⁻¹ solution) in covered Petri dishes. During this reaction, the clay films partially separated from the glass slides. Next, the ethanol was allowed to evaporate, and the dry films were removed from the slides and washed gently with 20 ml of ethanol to remove excess salts. The ethanol wash solutions were removed with a Pasteur pipette, and the clay was allowed to dry. The normal-charge film contained 4.6 mg clay cm⁻², and the reduced-charge film contained 2.2 mg clay cm⁻².

Spectral collection.

Self-supporting TMPA-do montmorillonite films were placed in the sample holder of a Perkin-Elmer 1710 FTIR that was purged with high-purity N₂. Single-beam background (empty, purged sample compartment) and clay spectra were collected with a DTGS detector using 2 cm⁻¹ resolution, no apodisation, and 100 scans. After spectra were collected with the montmorillonite films normal to the beam, a second spectrum of each film was collected with the film tilted approximately 45°. Spectra were stored on diskette and converted from single-beam spectra to absorbance using the MS-DOS program SpectraCalc (Galactic Software, Inc.). Baselines were leveled in spectral regions of interest and zeroed. To correct for small differences (<10%) in absorbance that might be caused by differences in the amount of clay probed by the infrared beam with the clay films 90° and 45° to the infrared beam, the spectra were normalized to make the absorbance of the clay lattice O-H stretching band (3628 cm⁻¹) equal at the two angles of incidence. To determine whether the TMPA phenyl group adopts a preferred orientation with respect to the siloxane surface in either the normal-charge or reduced-charge montmorillonite, the normalized 90° absorbance of each TMPA ring vibration was compared with the normalized absorbance at 45°.

X-ray diffraction and Fourier analysis

Fourier analysis of X-ray diffraction data for glycerol-solvated, normal-charge and reduced-charged Na-montmorillonites was used to determine whether some layers in the reduced-charge clay were collapsed and hence inaccessible to cations. Aqueous suspensions of Na-montmorillonite suspensions were sedimented on X-ray slides, allowed to dry overnight, then sprayed with a 10% aqueous glycerol solution. The slides then were placed in a desiccator over CaCl₂ to dry overnight. The slides were X-rayed from 3 to 90°

20 in 50-s, 0.05° steps with Cu-K_{α} radiation and a Ni filter at 10 mA and 25 kV using a Phillips APD3270 diffractometer equipped with a monochrometer and theta-compensating slit.

X-ray diffractograms were also collected for TMPA-saturated normal- and reduced-charged montmorillonite. Freeze-dried TMPA-saturated montmorillonites were resuspended in methanol, and the suspensions were sedimented onto glass slides. Slides of normal-charge clay were X-rayed at 20 mA and 35 kV from 3 to 60° 20 in 4-s, 0.05° steps and from 60 to 85° 20 in 10-s, 0.05° steps. Slides of reduced-charge montmorillonite were X-rayed in 50-s, 0.05° steps from 3 to 90° 20.

Fourier transforms of the X-ray diffraction peaks were calculated to determine the amount of interstratified, collapsed material in the Na⁺-saturated clays and to determine TMPA cation orientation in the interlayer of normal-charge and reduced-charge Wyoming montmorillonites. The procedure outlined by MacEwan (1956) was programmed into a computer spreadsheet. Form factors were taken from Figure 8-2 in MacEwan (1956). Some form factors approached zero, resulting in amplitude factors that approached infinity. As recommended by Reynolds (1980), X-ray peaks that caused the amplitude factor to approach infinity were not used to calculate the Fourier transform. The Lorentz factor was taken as a constant, since the diffractometer has a theta-compensating slit that causes the X-ray beam to irradiate a constant volume of sample. The polarization factors were calculated to account for use of the monochrometer as described by Azaroff (1955). The Fourier transforms were calculated every 0.05 Å from 0 to 45 Å. Terms used for calculating the Fourier transforms for Na⁺- and TMPA-saturated clays are shown in Tables 2 and 3 respectively.

Table 2-2. Terms used for calculating the Fourier transforms of X-ray diffractograms of glycolated, normal- and reduced-charged, Na+-montmorillonite.

Term	Intensity	spacing Å	form factor	¹ _A(r) ² _		
	Normal-Charge					
1	19848	17.84	100	1058		
2	2226	8.97	7	504		
3	926	5.96	12	405		
4	1947	4.48	10	689		
5	2160	3.58	13	828		
6	1655	2.99	32	808		
7	265	2.56	10	353		
8	428	2.23	1	474		
9	441	1.99	6	498		
10	156	1.79	4	303		
11	67	1.69	1	204		
12	376	1.45	7	514		
13	213	1.38	12	403		
14	97	1.29	10	283		
15	64	1.20	3	237		
		Reduced-Ch	narge			
1	14339	17.84	60	490		
2	10374	9.06	7	1226		
3	1282	5.88	20	257		
4	8131	4.54	3	1691		
5	4336	3.57	18	512		
6	6817	3.02	38	448		
7	366	2.58	15	168		
8	815	2.25	0.5	1387		
9	1091	1.98	5	512		
10	496	1.81	4	387		
12	199	1.50	9	160		
13	397	1.37	13	185		
14	126	1.29	9	123		
15	82	1.20	0.5	411		

¹ Estimated from Figure 8-2 of MacEwan (1956)

² Fourier amplitude terms as calculated by MacEwan (1956)

Table 2-3. Terms used for calculating the Fourier transforms of X-ray diffractograms of normal- and reduced-charged TMPA-montmorillonite.

Term	Intensity	spacing Å	form factor 1	A(r) ²	
Normal-Charge					
1	25619	14.84	38	823.29	
3	2401	4.99	20	354.39	
4	622	3.76	10	259.08	
5	2685	3.01	38	281.01	
6	75	2.54	0.5	416.42	
8	335	1.89	4	317.82	
9	76	1.67	0.4	477.48	
10	140	1.49	8	142.69	
11	130	1.37	15	98.39	
12	15	1.25	6	51.36	
13	42	1.15	0.4	297.56	
		Reduced-Cl	narge		
1	125400	13.57	42	267.48	
2	893	6.72	8	119.64	
3	8773	4.66	20	151.95	
4	9982	3.35	22	150.45	
5	212	2.75	37	13.27	
7	1536	1.93	6	226.71	
9	283	1.54	5	115.38	
10	100	1.35	15	22.15	
11	33	1.21	4	46.17	

¹ Estimated from Figure 8-2 of MacEwan (1956)

² Fourier amplitude terms as calculated by MacEwan (1956)

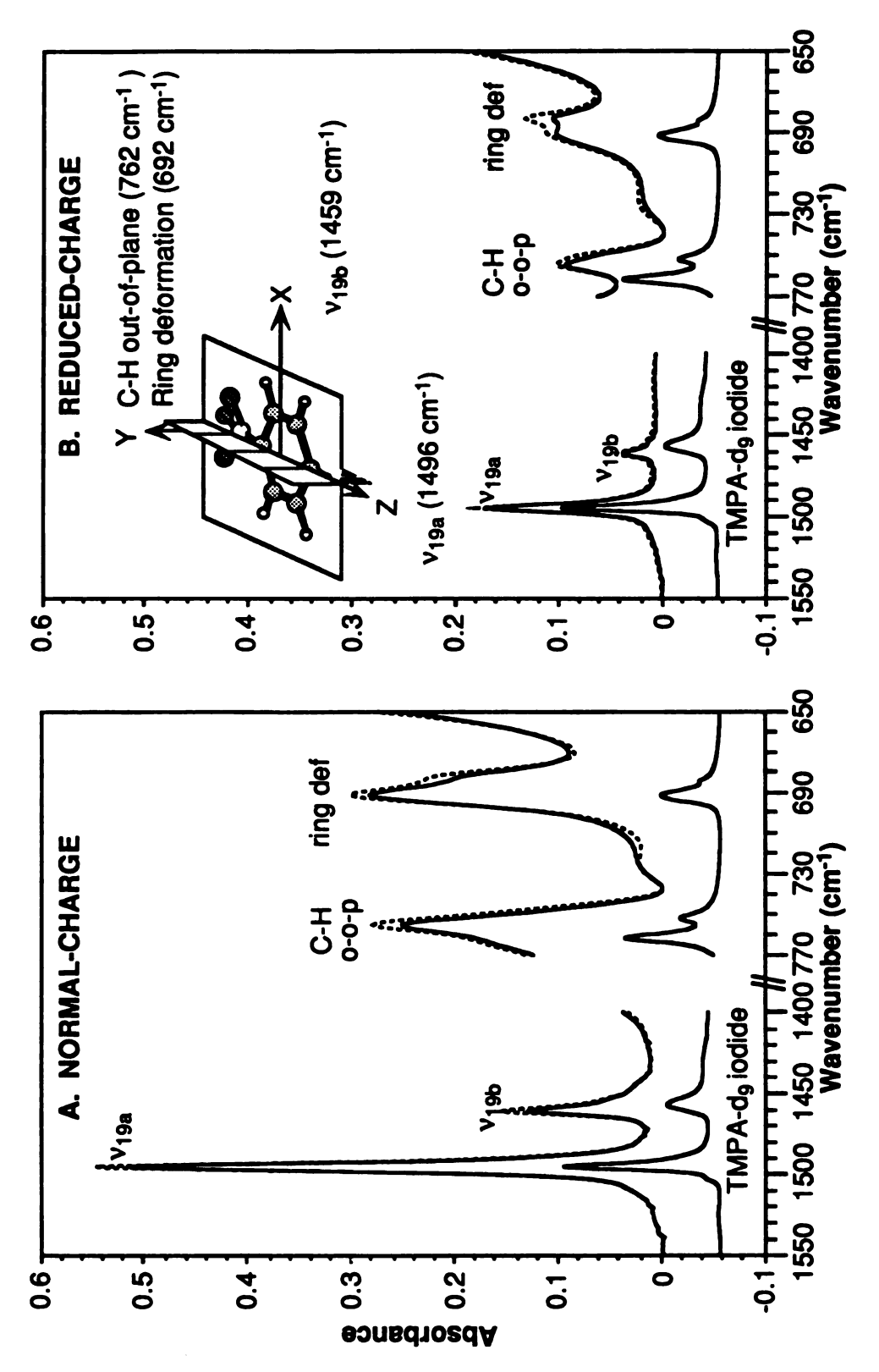
RESULTS

Infrared dichroism

To determine whether the TMPA phenyl ring is perpendicular or parallel to the siloxane surface, the normalized absorbances of the v_{19a} , v_{19b} , C-H out-of-plane, and ring deformation bands of TMPA-d₉ with a clay film perpendicular to the infrared beam can be compared to the normalized absorbances for the clay film tilted 45° with respect to the infrared beam. The vibration directions of the v_{19a} , v_{19b} , C-H out-of-plane, and ring deformation vibrations of the TMPA phenyl ring are shown in the inset of Figure 2-1. If the x-axis of the phenyl ring (v_{19b} vibration) is perpendicular to the siloxane surface, the absorbance of the v_{19b} vibration should increase by as much as a factor of two (Serratosa, 1966) when a TMPA-d₉-montmorillonite film perpendicular to the infrared beam is rotated 45°. The v_{19a} absorbance should exhibit dichroism if the phenyl ring and z-axis (C-N bond axis) are perpendicular to the infrared beam, whereas the C-H out-of-plane and ring deformation vibrations should be dichroic if the phenyl ring is parallel to the siloxane surface.

For TMPA-d₉ adsorbed on normal-charge montmorillonite, the normalized absorbance of all of the TMPA ring vibrations increased slightly when the clay film was rotated in the infrared beam, but none of the vibrations exhibited significant dichroism (Figure 2-1a). The phenyl ring itself may be perpendicular to the siloxane surface even though neither the x-axis nor z-axis is perpendicular, but infrared dichroism alone cannot show the orientation of the phenyl ring when neither the x-, y-, nor z-axis is perpendicular.

For reduced-charge montmorillonite, none of the TMPA ring vibrations showed significant dichroism. Thus, none of the axes is perpendicular to the clay surface, and the phenyl ring is not parallel to the siloxane surface. The original hypothesis that the phenyl



(bottom spectrum). Inset at right shows the orientations of the symmetry axes of TMPA and the band assignments for TMPA-d9 vibrations along these axes. montmorillonite for 90° (___) and 45° (- - -) angles of incidence and for TMPA-d9 iodide pressed in a KBr pellet Figure 2-1. Selected infrared vibrations of TMPA adsorbed on normal-charge and reduced-charge Wyoming

ring of TMPA is parallel to the surface of reduced-charge Wyoming montmorillonite is therefore false.

X-ray diffraction analysis

Glycerol-solvated Na-montmorillonite.

One-dimensional Fourier analysis of X-ray diffraction data for normal-charge, glycerol-solvated Na-montmorillonite (Table 2-2) showed that this clay contains only expanded layers with a d-spacing of about 18 Å (Figure 2-2a). In contrast, the reduced-charge montmorillonite (Figure 2-2b) comprises a randomly interstratified mixture of 18-Å expanded layers and 9.25-Å collapsed layers. Previous research (Clementz et al., 1974; Clementz and Mortland, 1974) has shown that reduced-charge montmorillonites with greater than 50% charge reduction are interstratified mixtures of layers with two different d-spacings. This conclusion was based on the irrationality of the X-ray diffraction peaks; these authors did not calculate Fourier transforms to determine the primary spacings of the collapsed and expanded layers (Clementz et al., 1974; Clementz and Mortland, 1974). Clementz and Mortland (1974) proposed that collapsed layers occur because their structural charge is reduced completely and no cations are adsorbed in these layers (which requires that the collapsed layers have no tetrahedral charge).

Fourier transform peaks caused by combinations of expanded and collapsed layers in glycerated reduced-charge Na-montmorillonite are labeled in Figure 2-2b. Based on the amplitudes of the 9.25 Å and 18 Å peaks, the reduced-charge montmorillonite contains about 2/3 expanded layers and about 1/3 collapsed layers, assuming that the 18-Å peak from expanded layers does not contain a significant contribution at about 18.5 Å from a collapsed-collapsed layer sequence. For comparison, the proportion of expanded layers also was estimated from the primary diffraction data (Table 2-2) using Mering's method

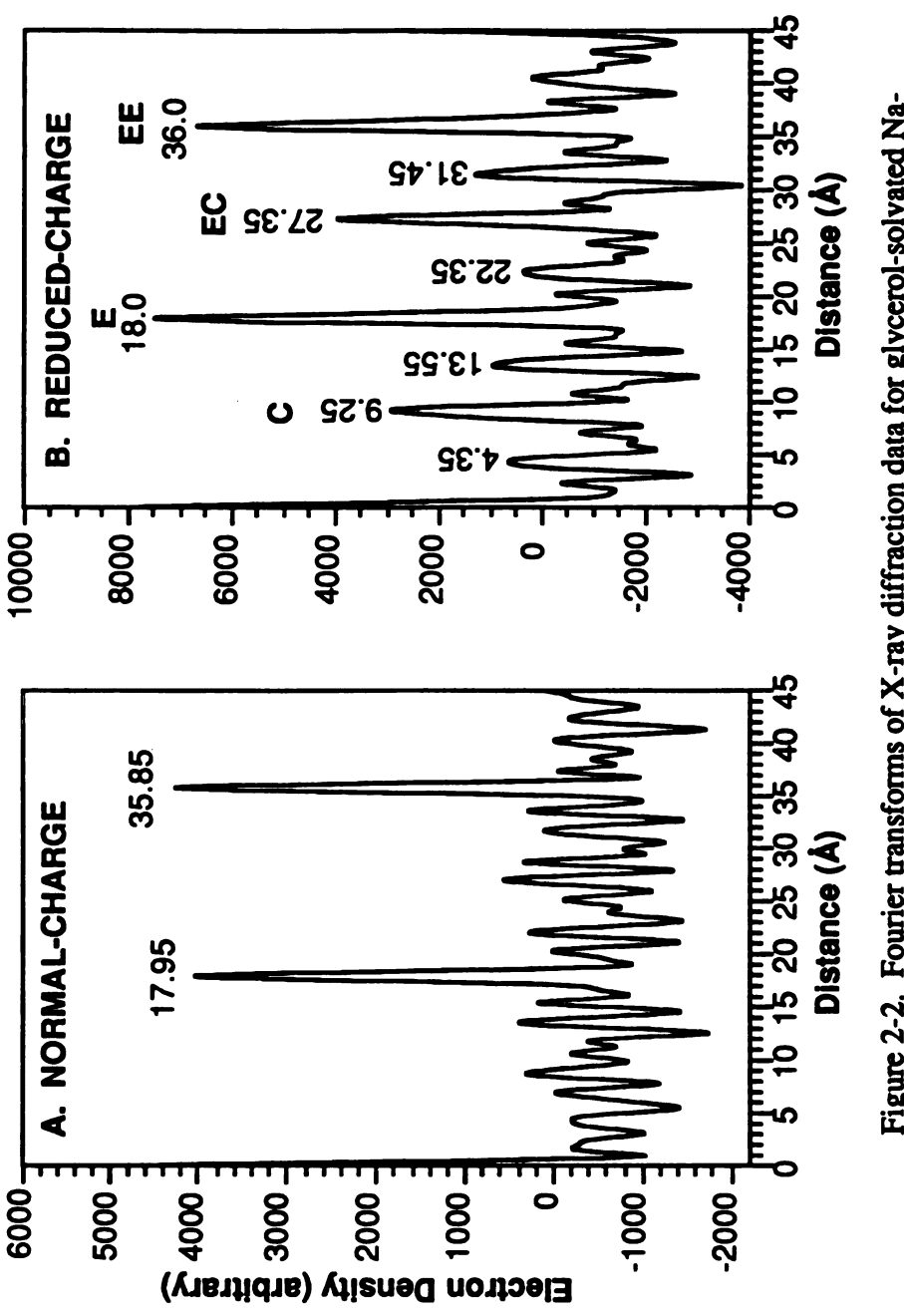


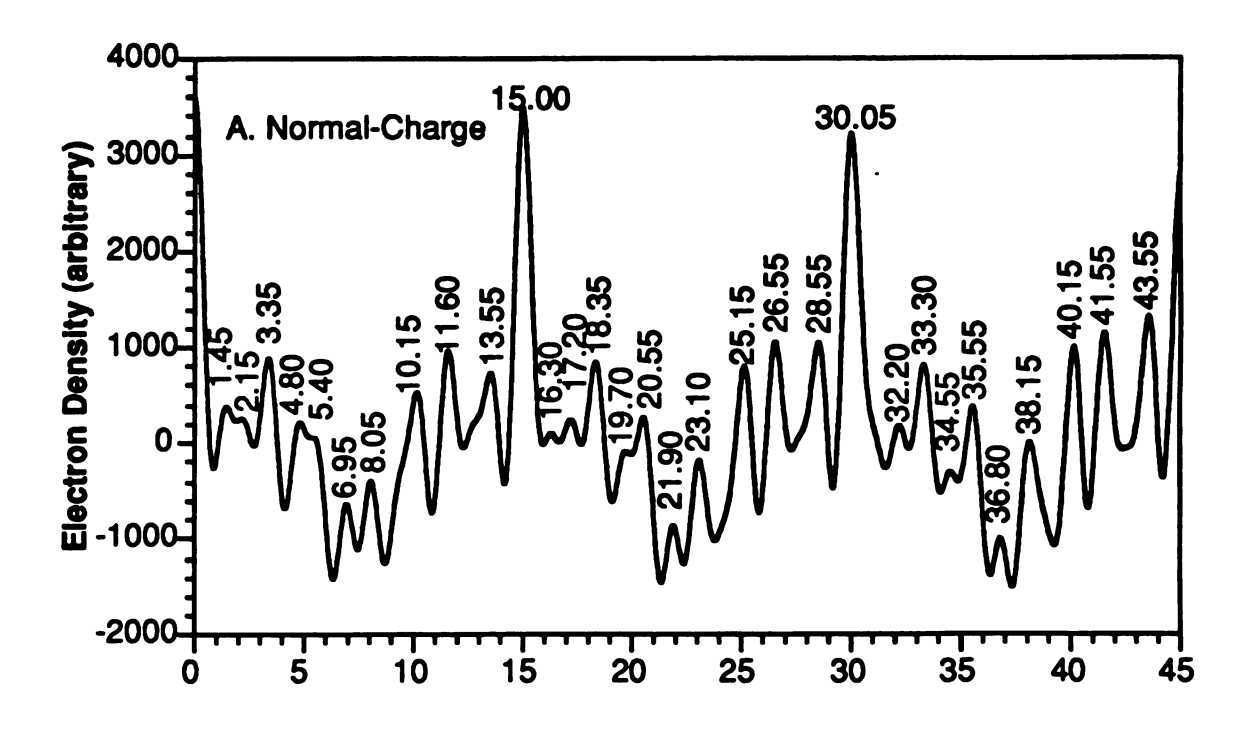
Figure 2-2. Fourier transforms of X-ray diffraction data for glycerol-solvated Namontmorillonites. Peaks due to combinations of expanded (E) and collapsed (C) layers are labeled for reduced-charge montmorillonite.

(Reynolds, 1980): diffraction peaks at 9.06, 4.54, and 3.03 Å are produced by a mixture that comprises 65-75% expanded (18 Å) layers and 25 to 35% collapsed (=9.3 Å) layers.

TMPA-montmorillonite

The Fourier transform for normal-charge TMPA-montmorillonite (Figure 2-3a) shows that the primary interlayer distance is 15.0 Å. The smaller peaks in the Fourier transform are periodic with respect to the octahedral cations at 0, 15, 30, and 45 Å. The peaks closest to the 0-Å and 15-Å peaks for the octahedral cations are caused by planes of 0, OH, and Si atoms (Bradley, 1963). The peaks from 4.8 to 10.5 Å and from 19.7 to 23.1 Å can be attributed to interlayer electron density of TMPA. The interlayer peaks are most periodic between 0 and 15 Å and slightly less periodic between 15 and 30 Å. At distances greater than 30 Å, resolution is limited by the poor crystallinity of montmorillonite and the number of diffraction orders that can be observed (Brindley and Hoffmann, 1962). The TMPA orientation consistent with the interlayer electron density peaks will be described in the Discussion section.

The Fourier transform for the reduced-charge montmorillonite (Figure 2-3b) is dominated by a peak at 13.6 Å from layers expanded by adsorbed TMPA. There also is a smaller peak at 9.5 Å from collapsed layers with no adsorbed TMPA ions, in addition to peaks at greater distances that correspond to various combinations of expanded and collapsed layers. Thus, reduced-charge TMPA-montmorillonite consists of randomly interstratified 13.6-Å and 9.5-Å collapsed layers. The 13.6-Å Fourier transform peak for expanded layers is evidence that the layer charge in the expanded, TMPA-saturated layers is partially reduced, allowing TMPA aromatic rings to assume a flatter orientation than in the normal-charge montmorillonite. If the layer charge of the expanded layers were not reduced at all, there would be a 15-Å peak in the Fourier transform, not a 13.6-Å peak.



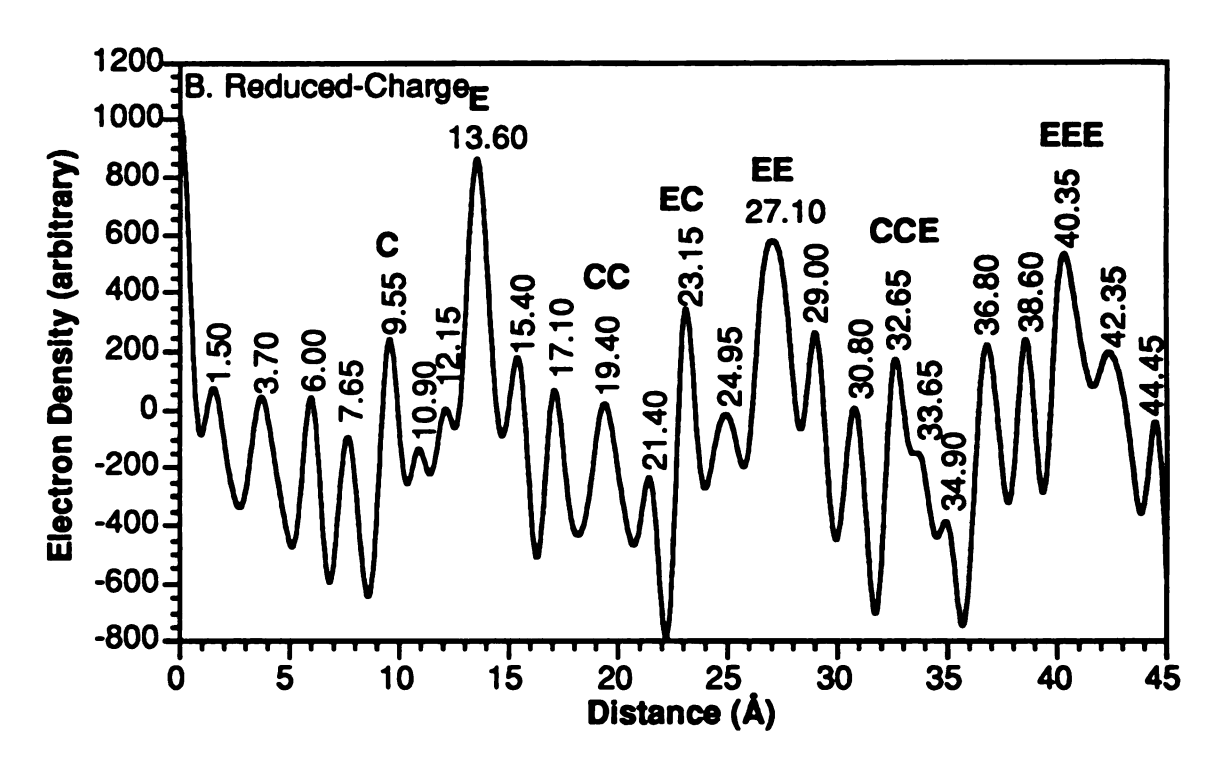


Figure 2-3. Fourier transforms of X-ray diffraction data for TMPA-montmorillonites. Peaks due to combinations of expanded (E) and collapsed (C) layers are labeled for reduced-charge montmorillonite.

The proportions of expanded and collapsed layers in reduced-charge TMPA-montmorillonite cannot be estimated directly from the amplitudes of the 13.6-Å and 9.5-Å peaks in the Fourier transform because the baseline for the 9.5-Å peak cannot be determined accurately. But the primary diffraction peaks at 4.46, 3.35, and 1.93 Å (Table 2-2) and Mering's method indicate that reduced-charge TMPA-montmorillonite comprises 70 to 80% TMPA-saturated, expanded layers, a result that is in good agreement with the estimate for the glycerol-solvated Na-montmorillonite. Random interstratification in the reduced-charge clay makes it impossible to interpret the Fourier transform in terms of the interlayer electron density of adsorbed TMPA.

DISCUSSION

TMPA orientation on normal-charge montmorillonite

Infrared dichroism experiments (Figure 2-1a) revealed that none of the symmetry axes of TMPA is perpendicular to the siloxane surface of normal-charge montmorillonite. The 15-Å d-spacing measured by X-ray diffraction, however, indicates that the aromatic ring may be perpendicular to the surface. Other researchers have measured 14.8-Å to 15.2-Å d-spacings for montmorillonite when polar aromatic compounds are adsorbed with their aromatic ring and x-axis perpendicular to the siloxane surface (Greene-Kelly, 1955; Serratosa, 1966). Therefore, a 15-Å d-spacing supports the contention that the TMPA phenyl ring is perpendicular to the siloxane surface. The x- and z-axes may be tilted in order to minimize the distance between the negative charge in the clay and the positively charged nitrogen atom of TMPA, as shown in Figure 2-4.

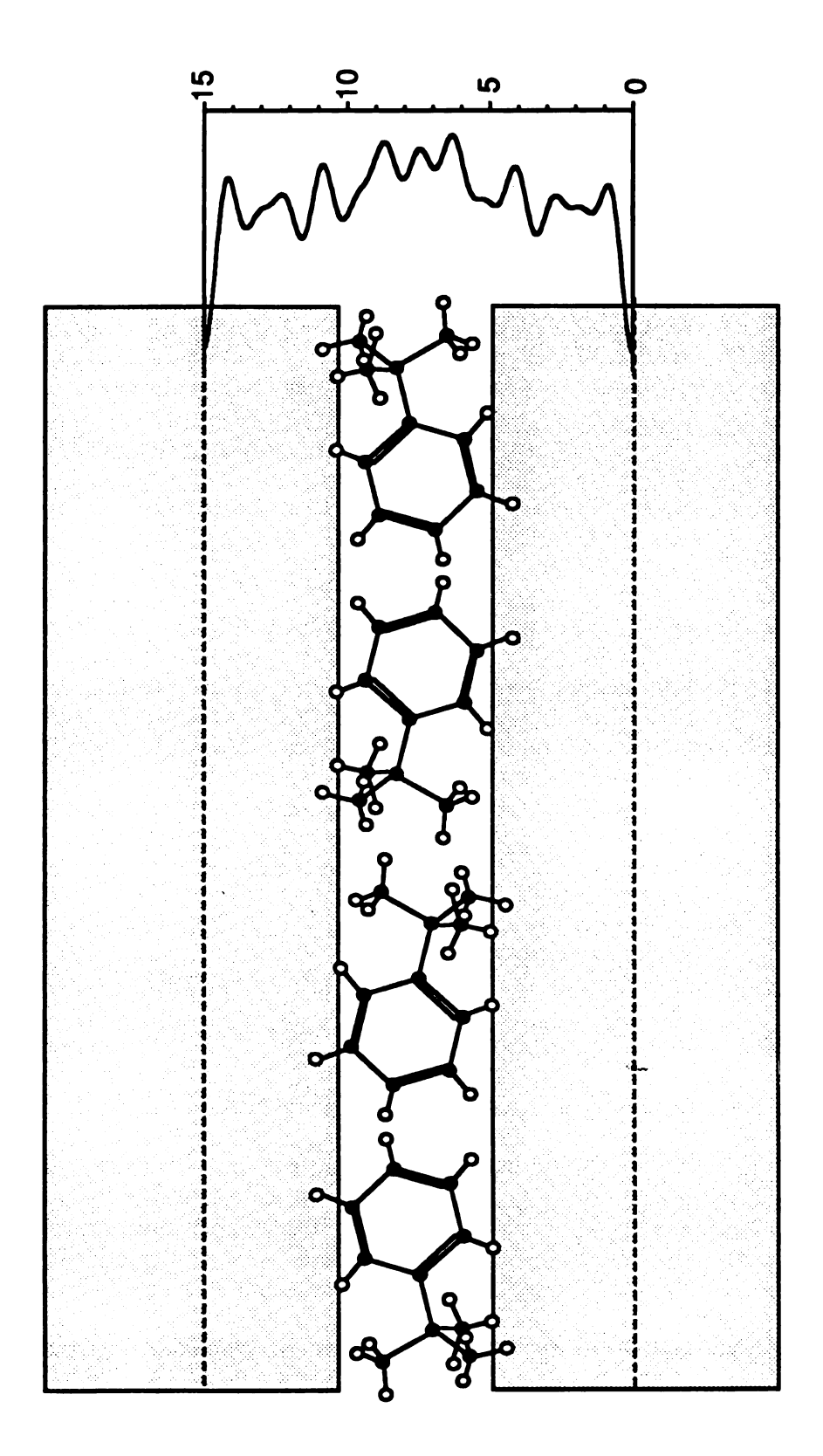


Figure 2-4. Schematic representation of proposed TMPA orientation on normal-charge montmorillonite, with phenyl ring perpendicular to the siloxane surface. Interlayer electron probabilities from one-dimensional Fourier analysis are shown at the right. Both aromatic and methyl protons key into the siloxane surface.

The 15-Å d-spacing is smaller than the combined dimensions of the aromatic ring (6.7 Å in the x-direction) and the clay layer (9.4 Å according to Brindley and Hoffmann, 1962). Consequently, a 15-Å d-spacing requires "keying" of aromatic protons into the siloxane surface when the TMPA phenyl ring is perpendicular to the surface of montmorillonite. The separation between adjacent protons in an aromatic ring is 2.5 Å, whereas the distance between adjacent siloxane ditrigonal cavities is 5.2 Å. Thus, one aromatic proton may key into a ditrigonal cavity and another may fit into a closest-packing arrangement with surface oxygen atoms. This type of keying is shown schematically for TMPA in Figure 2-4.

The orientation of adsorbed TMPA must minimize the separation between the negatively charged site in the clay and the positively charged nitrogen atom of TMPA. With the phenyl ring roughly perpendicular to the siloxane surface, charge separation will be minimized when one methyl proton from each of two methyl groups keys into the siloxane surface (Figure 2-4). The interlayer electron probabilities from the onedimensional Fourier analysis are superimposed on Figure 2-4 to show that the proposed orientation is consistent with the Fourier analysis results. The electron probability plot shows four main regions of interlayer electron density that are nearly symmetric with respect to the midpoint of the clay interlayer and to the upper and lower siloxane surfaces. Keying of methyl and aromatic protons is required to give the Fourier transform peaks at 4.80 and 10.15 Å (Figure 2-4), which are nearly coincident with the upper and lower siloxane surfaces. The peaks in the electron probability plot are symmetric with respect to the siloxane surfaces and the midpoint of the interlayer, even though individual adsorbed TMPA ions lack this symmetry, because some TMPA ions have their positively charged nitrogen atom close to the bottom clay surface and some TMPA nitrogen atoms are closer to the upper surface of each interlayer (Figure 2-4).

In the normal-charge montmorillonite, the surface area per negative charge is about 151 Å², based on unit-cell dimensions and the structural formula of Wyoming montmorillonite. In the TMPA orientation depicted in Figure 2-4 with the aromatic ring perpendicular to the surface, each interlayer TMPA ion occupies a total of $100\ \text{Å}^2$ on the upper and lower siloxane surfaces, which includes 25 Å² on each surfaces for the edge area of the aromatic ring and 25 Å² per surface for the projection of two methyl groups (Pauling, 1960). Thus, TMPA ions occupy about 2/3 of the available siloxane surface area per negative charge on normal-charge montmorillonite, which leaves 1/3 is accessible to other adsorbates. This molecular-level picture is consistent with macroscopic surface area measurements, provided that N₂ can form a bilayer in the interlayer of normal-charge TMPA-montmorillonite: the measured N₂-accessible surface area of 252 m² g⁻¹ (Table 2-1) is about 1/3 the theoretical surface area of 770 m² g⁻¹ calculated from the unit-cell dimensions and structural formula of Wyoming montmorillonite (Gast, 1977). Thus, surface area measurements support the X-ray Fourier analysis result that the aromatic ring of TMPA is perpendicular to the siloxane surface of normal-charge montmorillonite. In this orientation, it is possible that neighboring TMPA phenyl rings may interact with one another by π - π interactions, although the experiments reported here provide no direct evidence to either support or disprove this hypothesis.

If benzene were to adsorb perpendicular to the surface in order to interact with TMPA phenyl rings by π - π interactions, each benzene ring would require 50 Å² (25 Å² on both the upper and lower siloxane surfaces of an interlayer), which is exactly the accessible siloxane surface area on dry normal-charge TMPA-montmorillonite. The accessible surface would be even smaller in the presence of adsorbed water. Thus, no aromatic molecule larger than benzene could adsorb on normal-charge TMPA-montmorillonite if TMPA ions were uniformly distributed on the surface. The fact that small amounts of alkylbenzenes

and naphthalene are sorbed from aqueous solution by high-charge TMPA-montmorillonites (Jaynes and Boyd, 1991) is evidence that TMPA ions are not uniformly distributed on the surface.

The perpendicular orientation of TMPA on normal-charge montmorillonite (Figure 2-4) will allow other aromatic compounds to sorb in the interlayer with their phenyl rings perpendicular to the surface. Maximum sorption of aromatic compounds will occur when their phenyl rings are perpendicular to the surface because the interlayer space of 5.4 Å is not large enough to accommodate two or more aromatic rings stacked parallel to the surface, and sorption of a single ring parallel to the surface would be more sterically restricted and less energetically favorable than sorption with aromatic rings perpendicular to the surface. Because sorption parallel to the surface is less favorable, it is unlikely that p- π interactions between surface oxygen atoms and aromatic sorbates contribute to arene sorption by normal-charge TMPA-montmorillonite. A perpendicular orientation, however, would allow aromatic sorbates to interact with the phenyl ring and with one another by π - π interactions but at the same time permit polar sorbates such as water to interact with the positively charged nitrogen atom of TMPA.

TMPA orientation on reduced-charge montmorillonite

The 13.6-Å d-spacing for reduced-charge TMPA-montmorillonite, which is not large enough to accommodate the phenyl ring perpendicular to the surface, is the same as that reported for tetramethylammonium (TMA)-montmorillonite (Barrer and Reay, 1957; Barrer and Perry, 1961). Thus, a 13.6-Å d-spacing suggests that TMPA's three methyl groups prop open adjacent clay layers, with some methyl protons keying into the siloxane surface, as shown schematically in Figure 2-5. Infrared dichroism showed that the phenyl ring is not parallel to the surface of reduced-charge montmorillonite. Therefore, the ring

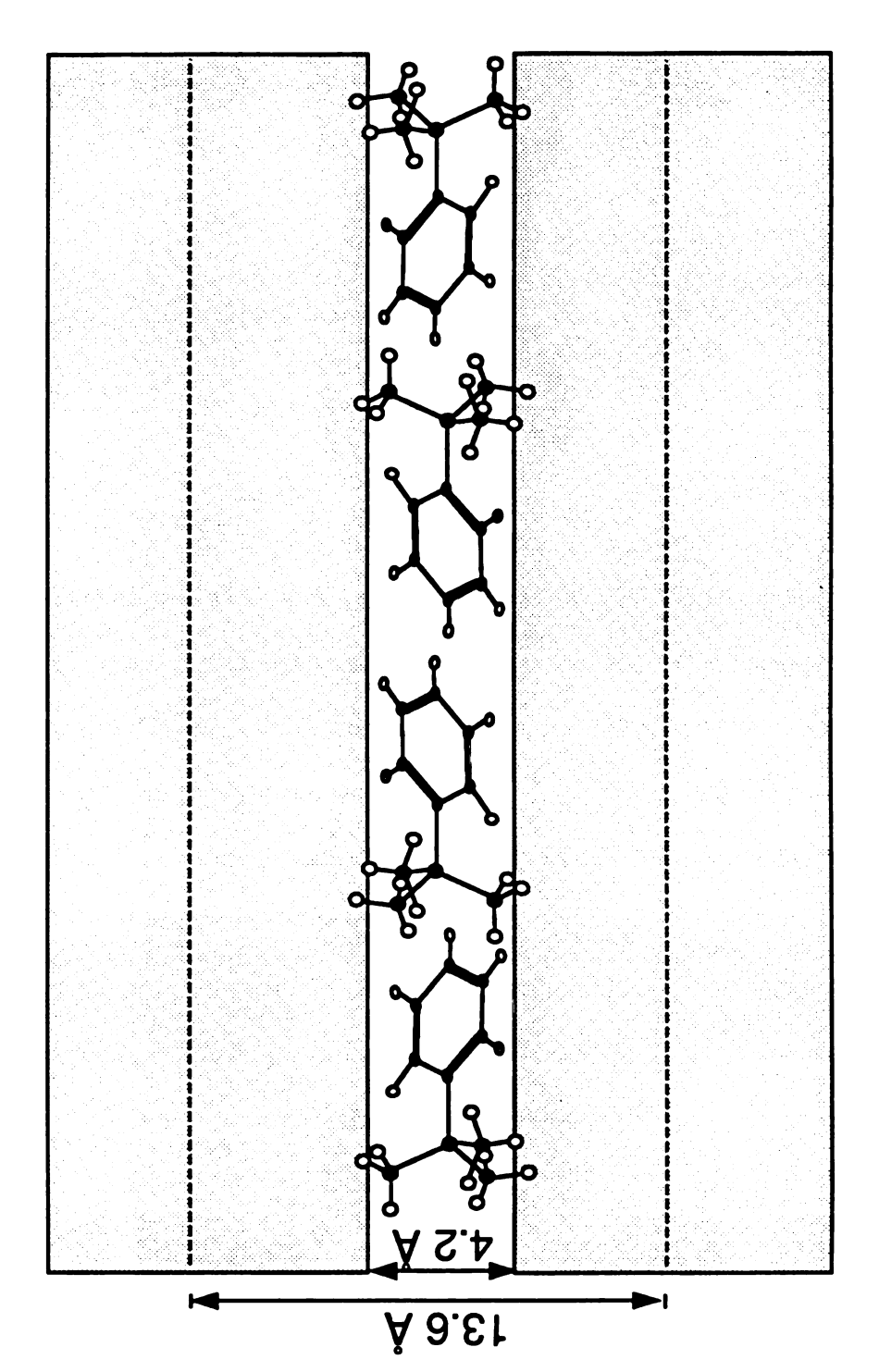


Figure 2-5. Schematic representation of TMPA orientation on expanded layers of reduced-charge Wyoming montmorillonite. Layers are propped open by methyl groups, with some methyl protons keying into siloxane surface. Phenyl ring is not parallel to the surface, but exact orientation is not known.

must be intermediate between parallel and perpendicular, or it may be free to rotate within the interlayer space. One-dimensional Fourier analysis provided no information about the orientation of interlayer TMPA cations because collapsed and TMPA-saturated (expanded) layers are randomly interstratified in the reduced-charge montmorillonite.

The surface area per negative charge on TMPA-containing expanded layers is 205 $Å^2$ per site when calculated with the following equation:

$$\frac{\left(\frac{814 \text{ mmol}_{c}}{\text{kg}}\right)_{NCM}}{\left(\frac{449 \text{ mmol}_{c}}{\text{kg}}\right)_{RCM} \times \frac{1 \text{ layer RCM}}{0.75 \text{ expanded layer RCM}} \times \left(\frac{151 \text{ A}^{2}}{\text{charge}}\right)_{NCM} = \left(\frac{205 \text{ A}^{2}}{\text{charge}}\right)_{expanded RCM}$$

where 449 and 814 mmol_c kg⁻¹ are the TMPA-exchange capacities of the reduced-charge (RCM) and normal-charge montmorillonites (NCM), 0.75 is the approximate proportion of expanded layers in the reduced-charge clay, and 151 Å² is the area per structural charge in normal-charge Wyoming montmorillonite. Each TMPA cation would occupy 130 Å² if the aromatic ring were parallel to the clay surface and 100 Å² if perpendicular. Because the TMPA orientation must be intermediate between perpendicular and parallel, each TMPA ion must occupy between 100 and 130 Å² on reduced-charge Wyoming montmorillonite. This leaves 75 to 105 Å² per cation available to other adsorbates, which is 1.5 to 2.1 times the accessible area on normal-charge montmorillonite. For comparison, the N₂ BET surface area calculated for expanded layers of reduced-charge TMPA-montmorillonite was 424 m² g⁻¹ (i.e., 318 m² g⁻¹ + 0.75 expanded layers), which is 1.68 times the N₂-accessible area on normal-charge montmorillonite.

Previous research has shown that benzene sorption causes TMA-montmorillonite to expand from 13.6 to 15.0 Å so that the benzene ring can adsorb perpendicular to the siloxane surface (Barrer and Reay, 1957; Barrer and Perry, 1961), and preliminary experiments in our laboratory confirm that TMPA montmorillonite also expands when benzene is sorbed. Presumably the favorable energetics of π - π interactions among aromatic rings promote layer expansion and the upright orientation of the aromatic ring. In the case of TMPA-montmorillonite, the driving force for benzene to sorb perpendicular to the surface would be even greater than for TMA montmorillonite because the phenyl ring of TMPA can interact with aromatic sorbates by π - π interactions. As was discussed above, the adsorbate-accessible surface area for the perpendicular orientation would be would be about twice that on normal-charge TMPA montmorillonite. The greater accessible surface area of reduced-charge TMPA-montmorillonite should allow more sorption, particularly of larger aromatic compounds (Jaynes and Boyd, 1991), and should permit faster diffusion into the interlayer.

CONCLUSIONS

In normal-charge montmorillonite, Fourier transform X-ray analysis showed that the phenyl ring of TMPA likely is perpendicular to the siloxane surface, though none of the ring vibrations is perpendicular to the surface. The perpendicular phenyl ring could serve as a "nucleating site" for aromatic sorbates to interact with TMPA and with one another by π - π interactions. At the same time, sorbed water and other polar compounds would tend to interact with the positively charged nitrogen atom of TMPA; water and aromatic sorbates may interact with different parts of the TMPA ion yet compete for siloxane surface area. The perpendicular orientation of TMPA maximizes the surface area available to other

sorbates, yet on normal-charge montmorillonite only 50 Å² per cation is not occupied by TMPA ions, which is exactly the area required for benzene to sorb with its aromatic ring perpendicular to the surface. The fact that small amounts of larger aromatic compounds are sorbed by high-charge TMPA-montmorillonites (Jaynes and Boyd, 1991) is evidence that TMPA ions are not uniformly distributed on the surface and that some of the interlayer pore spaces between adjacent TMPA ions are sufficiently large to accommodate alkylbenzenes and compounds such as naphthalene.

The reduced-charge TMPA-montmorillonite used in these experiments is a randomly interstratified mixture composed of about 25% collapsed layers with no interlayer cations and about 75% expanded layers with a 13.6-Å d-spacing. The 13.6-Å d-spacing indicates first that layers are propped open by the methyl groups of TMPA, not the phenyl ring, and second that the charge of expanded layers is reduced sufficiently that the aromatic ring need not be perpendicular to the surface, as it is in normal-charge montmorillonite. The phenyl ring is neither parallel nor perpendicular to the surface of reduced-charge TMPA-montmorillonite, though preliminary experiments suggest that the layers may expand in the presence of aromatic sorbates. This would allow the phenyl ring of TMPA to rotate into a perpendicular orientation and would allow π - π interactions between TMPA and the aromatic sorbates, as well as among aromatic sorbates. Rotation or TMPA's phenyl ring into a perpendicular orientation on reduced-charge montmorillonite would not only increase the d-spacing but also would increase both the arene-accessible surface area per cation and the interlayer pore dimensions to more than twice those in the normal-charge montmorillonite. Thus, macroscopic surface area measurements, in which the N2accessible surface area of reduced-charge montmorillonite was only 1.25 times that of normal-charge montmorillonite, give an incomplete picture of interlayer accessibility to aromatic sorbates. Measured surface areas do not reflect the fact that essentially all of the

accessible surface area on reduced-charge montmorillonite resides on the 75% of the layers that are expanded, and that the phenyl ring of TMPA likely rotates in the presence of aromatic sorbates (but not N_2) to create more adsorbate-accessible surface area on reduced-charge montmorillonite.

REFERENCES

- Azaroff, L.V. (1955) Polarization correction for crystal-monochromatized X-radiation: *Acta Crystallogr.* 8, 701-704.
- Barrer, R.M., and Reay, J.S.S. (1957) Sorption and intercalation by methylammonium montmorillonites: *Trans. Faraday Soc.* 53, 1253-1261.
- Barrer, R.M., and Perry, G.S. (1961) Sorption of mixtures, and selectivity in alkylammonium montmorillonites. Part II. Tetramethylammonium montmorillonite: *J. Chem. Soc.* 850-858.
- Boyd, S. A., Jaynes, W. F. and Ross, B. S. (1991) Immobilization of organic contaminants by organo-clays: Application to soil restoration and hazardous waste containment: in *Organic substances and sediments in water*, R.S. Baker, ed., vol. 1. CRC Press, Boca Raton, FL 181-372.
- Bradley, W.F., Weiss, E.J., and Rowland, R.A. (1963) A glycol-sodium vermiculite complex: Clays & Clay Minerals 10, 117-122.
- Brindley, G.W and Ertem, G. (1971) Preparation and solvation properties of some variable charge montmorillonites: Clays & Clay Minerals 19, 399-404.
- Brindley, G.W., and Hoffmann, R.W. (1962) Orientation and packing of aliphatic chain molecules on montmorillonite: Clays & Clay Minerals 9, 546-556.
- Clementz, D.M., and Mortland, M.M. (1974) Properties of reduced charge montmorillonites: Tetra-alkylammonium ion exchange forms: Clays & Clay Minerals 22, 223-229.
- Clementz, D.M., Mortland, M.M., and Pinnavaia, T.J. (1974) Properties of reduced charge montmorillonites: Hydrated Cu(II) ions as a spectroscopic probe: Clays & Clay Minerals 22, 49-57.

- Cope, A.C., Ciganer, E., Fleckenstein, L.J. and Meisinger, M.A.P. (1960) Tertiary amines from methiodides and lithium aluminum hydride: *J. Amer. Chem. Soc.* 82, 4651-4655.
- Farmer, V. C., and Mortland, M. M. (1966). An infrared study of the coordination of pyridine and water to exchangeable cations in montmorillonite and saponite: *J. Chem Soc.* 344-351.
- Gast, R.G. (1977) Surface and colloid chemistry. In Minerals in Soil Environments, J.B. Dixon and S.B. Weed, eds., American Society of Agronomy, Madison, WI, 27-73.
- Greene-Kelly, R. (1953) The identification of montmorillonoids in clays: J. Soil Sci. 4, 233-237.
- Greene-Kelly, R. (1955) Sorption of aromatic organic compounds by montmorillonite. Pt. 1. Orientation studies: *Trans. Faraday Soc.* 51, 412-424.
- Jaynes, W.J., and S.A. Boyd. (1991) Hydrophobicity of siloxane surfaces in smectites as revealed by aromatic hydrocarbon adsorption from water: *Clays & Clay Minerals* 39, 428-436.
- Jaynes, W.J., and Bigham, J.M. (1987) Charge reduction, octahedral charge, and lithium retention in heated, Li-saturated smectites: Clays & Clay Minerals 35, 440-448.
- Johns, W.D., and Sen Gupta, P.K. (1967) Vermiculite-alkylammonium complexes: Amer. Mineral. 52, 1706-1724.
- MacEwan, D.M.C. (1956) Fourier transform methods for studying scattering from lamellar systems I. A direct method for analysing interstratified mixtures: *Kolloid Zeitschrift* 14, 96-108.
- Pauling, L. (1960) The Nature of the Chemical Bond, Cornell University Press, Ithaca, New York, 3rd ed., 644 p.
- Reynolds, R.C. (1980) Interstratified Clay Minerals. In Crystal Structures of Clay Minerals and their X-ray Identification, G.W. Brindley and G. Brown eds., Mineralogical Society, London, 249-304.
- Serratosa, J.M. (1966) Infrared analysis of the orientation of pyridine molecules in clay minerals: Clays & Clay Minerals 14, 385-391.
- Serratosa, J.M. (1968) Infrared study of benzonitrile (C₆H₅-CN)-montmorillonite complexes: *Amer. Mineral.* 53, 1244-1251.

CHAPTER III

An FTIR study of water sorption on tetramethylammonium- and trimethylphenylammonium-saturated normal- and reduced-charge Wyoming montmorillonite

ABSTRACT

The presence of water inhibits sorption of solutes from water on clays saturated with organic cations. The purpose of this study was to determine whether water sorbs preferentially on the siloxane surface or on cation sites of montmorillonite saturated with tetramethylammonium (TMA) and trimethylphenylammonium (TMPA). Water vapor sorption isotherms were collected on TMA- and TMPA-saturated, normal- and reducedcharge montmorillonite to determine the effect of cation type and clay charge density on water sorption. Normal- and reduced-charge clay films saturated with TMA and TMPA were equilibrated at different water vapor pressures and probed by infrared spectroscopy to determine if water vapor sorbs on the cations and support conclusions drawn from the macroscopic data of the sorption isotherms. Water vapor sorption isotherms showed that sorption was greater for normal-charge clays than reduced-charge clays though the N₂ surface area of the reduced-charge clays was larger. This suggests that water sorbs preferentially on cations, not the siloxane surface. TMA-saturated clays sorbed more water vapor than did TMPA-saturated clays, indicating either that the phenyl group of TMPA may sterically hinder sorption of water vapor. The infrared spectra of both TMA and TMPA cations saturating normal- and reduced-charge montmorillonite were perturbed by water vapor at 7.5% RH, providing further evidence that water interacts preferentially with adsorbed TMA and TMPA, not with uncharged siloxane surfaces, at low relative humidity.

INTRODUCTION

Clays saturated with quaternary alkylammonium cations have been proposed as sorbents to remove organic pollutants from aqueous waste streams (Boyd, et al., 1991), an application in which water competes with organic solutes for sorption sites on the clays (Lee et al.,1990; Jaynes and Boyd, 1990, 1991). The sorption mechanism of water on clays saturated with inorganic cations has been studied extensively and reviewed elsewhere (Farmer and Russell, 1971; Sposito and Prost, 1982), but the sorption mechanism of water on clays saturated with quaternary ammonium cations is not well understood. The object of this study is to determine whether water sorbs preferentially at the cation or on the siloxane surface of clays saturated with tetramethylammonium (TMA) and trimethylphenylammonium (TMPA). This information is necessary to determine how pollutant sorption is inhibited by water and may aid selection of organoclays appropriate for waste cleanup applications.

The preferred site of water adsorption on clays saturated with quaternary ammonium cations has not been studied spectroscopically. When clays are saturated with inorganic cations, the most important site for water adsorption is around the cations (Farmer and Russell, 1971; Sposito and Prost, 1982). Infrared spectroscopic data indicates that at high water content, water may also form weak hydrogen bonds with siloxane surface oxygen atoms, but only after exchangeable cations have been hydrated (Sposito and Prost, 1982). It is probable that small alkylammonium ions like TMA and TMPA also are hydrated before water sorbs or condenses on siloxane surfaces. Like NH₄⁺ (Bernal and Fowler, 1933), TMA has a small but finite hydration energy (Nagano et al., 1988), and water sorption isotherms on TMA-montmorillonite are nearly identical to water sorption isotherms for NH₄⁺-montmorillonite (Gast and Mortland, 1971).

Sorption isotherms of arenes on TMA-saturated montmorillonites collected in the presence and absence of water have shown that water inhibits arene sorption on these clays (Lee et al., 1990). The effect of charge density on the sorption of arenes from water provides indirect evidence for sites of water sorption on clays (Jaynes and Boyd, 1991). Lee et al. (1990) stated that water sorption on either TMA cations or the siloxane surface might have caused the decrease in arene sorption from aqueous solution compared with arene sorption on dry TMA-montmorillonite. In addition, Lee et al. (1990) noted greater sorption of arenes from water on low-charge TMA-clay than higher-charge clay. In Jaynes and Boyd (1991) arene sorption from water was compared between reduced- and normalcharge Arizona montmorillonite saturated with TMPA to determine whether aromatic hydrocarbons preferentially sorbed on the siloxane surface or the cations. Sorption of arenes from water increased as the layer charge of the clay was reduced, implying that arene sorption was more favored than water adsorption on the siloxane surface and that the siloxane surface was more hydrophobic than the cations. This result was in agreement with the observations of Lee et al. (1990) noting the effect of charge on arene sorption. These results suggested that the cations are the preferred sorption site for water since the siloxane surface was more hydrophobic than the cations. Preferential water sorption on cations could be evaluated more directly by collecting water vapor sorption isotherms on normal- and reduced-charge TMA- and TMPA-saturated clay. This would provide stronger evidence that cation sites are preferred for water sorption on TMA- and TMPA-saturated clay over the siloxane surface.

This paper describes a combination of macroscopic and spectroscopic experiments used to test the hypothesis that water interacts preferentially with adsorbed TMA and TMPA ions, not with the siloxane surface. Water vapor adsorption isotherms on normal-and reduced-charge TMA- and TMPA-montmorillonite will provide macroscopic information about the site of water sorption. If water sorbs preferentially on adsorbed

cations, more water should be adsorbed on the normal-charge clay, which has a higher cation concentration. If, however, water interacts preferentially with siloxane surfaces, then water vapor sorption at low P/P_o should be greater on reduced-charge than normal-charge clay. In addition to the water sorption isotherms, infrared spectroscopy will be used to provide molecular-level evidence to test the hypothesis that water preferentially hydrates adsorbed TMA and TMPA, not the siloxane surface. Hydration of adsorbed TMA and TMPA should perturb the infrared spectra of these cations. Thus, displacement or splitting of cation vibrational bands at low water vapor pressure would support the hypothesis that water interacts preferentially with adsorbed TMA and TMPA.

MATERIALS AND METHODS

Reduced-and normal-charged organoclay preparation

Wyoming montmorillonite (SWy-1) was obtained from the Clay Minerals Society Source Clays Repository at the University of Missouri-Columbia. The <2-µm fraction was separated from the coarser material by sedimentation and the charge was reduced for half the clay as described in Chapter 2.

To prepare TMA- and TMPA-montmorillonites, TMA-chloride and TMPA bromide were added to normal-charge and reduced-charge montmorillonites in 70% methanol-water suspensions and stirred 72 h. Four times the CEC of TMA-chloride and ten times the CEC of TMPA-bromide were added to the clays. The clays were dialyzed until chloride-free and were freeze-dried. To improve the homogeneity of the clays, each clay (normal-or reduced-charge, TMA- and TMPA-saturated) was mixed gently in a mortar and pestle. Selected properties of the clays are reported in Table 3-1.

Table 3-1. Selected physical and chemical properties of normal (Norm)- and reduced (Red)-charge TMA- and TMPA-montmorillonite.

Treatment	d(001) (Å)	N ₂ Surface Area ² (m ² g ⁻¹)	Total C ³ (g kg ⁻¹)	Adsorbed cation ⁴ (mmol kg ⁻¹)	CEC ⁵ (mmol kg ⁻¹)
Red TMA	13.6	289±30	27.7±0.7	474±14	390±30
Norm TMA	13.6	202±26	40.7±0.3	847±6	870±80
Red TMPA	13.7 ¹	318±14	48.6±0.9	449±8	390±30
Norm TMPA	14.9 ¹	252±28	88.1±1.0	814±11	870±80

¹ Obtained from Fourier transform of XRD data (Chapter 2).

Adsorbed cation =
$$\frac{\text{Total g C}}{\text{kg clay}} \times \frac{\text{mmol cation}}{\text{g C}}$$

 $^{^2}$ Avg \pm SD (N=2 or 3) from three-point BET N₂ adsorption isotherms using a Quantachrome Quantasorb Jr. surface area analyzer.

 $^{^3}$ Avg \pm SD (N=2) of total C determined by combustion at 900 °C using a Dohrmann DC-190 high-temperature carbon analyzer.

 $^{^4}$ Avg \pm SD (N=2) calculated with the equation:

 $^{^5}$ Avg \pm SD (N=3 or 4) Determined by Na⁺ saturation and ammonium displacement of the parent normal - and reduced - charge clays (i.e. not treated with organic cations). Statistically identical values were obtained with Mg²⁺ saturation and Ba²⁺ extration.

Water vapor sorption isotherms

Figure 3-1 shows the device used to collect water vapor sorption isotherms (McBain and Bakr, 1926). The precision of the mass measurements was ± 0.25 mg. Vapor pressure was accurate to ± 0.01 torr. Between 200 and 500 mg of each of the four freeze-dried, homogenized clays (dried at 80 °C and stored in a P₂O₅ desiccator) was placed in the sample holders before the balance was sealed. Vacuum was applied to the balance and the sample chambers were heated to 80 °C for 72 h to remove any water which may have sorbed on the clay while transferring it from the desiccator to the balance. Gast and Mortland (1971) showed that the infrared spectrum of dry TMA-montmorillonite did not change when the clay was heated to 105 °C, a result that suggests that no decomposition occurs when TMA- and TMPA-montmorillonite is heated to 80 °C. After the heat and vacuum treatment, the four clay samples were allowed to return to room temperature and the sorption isotherms were collected. The clays were equilibrated with water vapor at absolute pressures ranging from 0.90 to 17.25 torr. Each isotherm point was collected by opening the sorbate reservoir to the vacuum or near-vacuum in the sample chambers, then closing the reservoir when the pressure rose sufficiently. After one hour of equilibration, the manometer reading, temperature, and spring displacements were noted. For example, one point was collected by opening the reservoir until the pressure rose to 2.00 torr, then equilibrating for one hour, at which time the pressure had dropped to 1.47 torr. After the spring displacements were measured, the water pressure was increased to 3.20 tort for the next point. Because it was important to collect water sorption data for each of the two charge treatments and two organic cations under identical conditions, it was necessary to have each of the four clays in the sample chamber simultaneously. Consequently, it was not possible to collect replicates of each data point because final

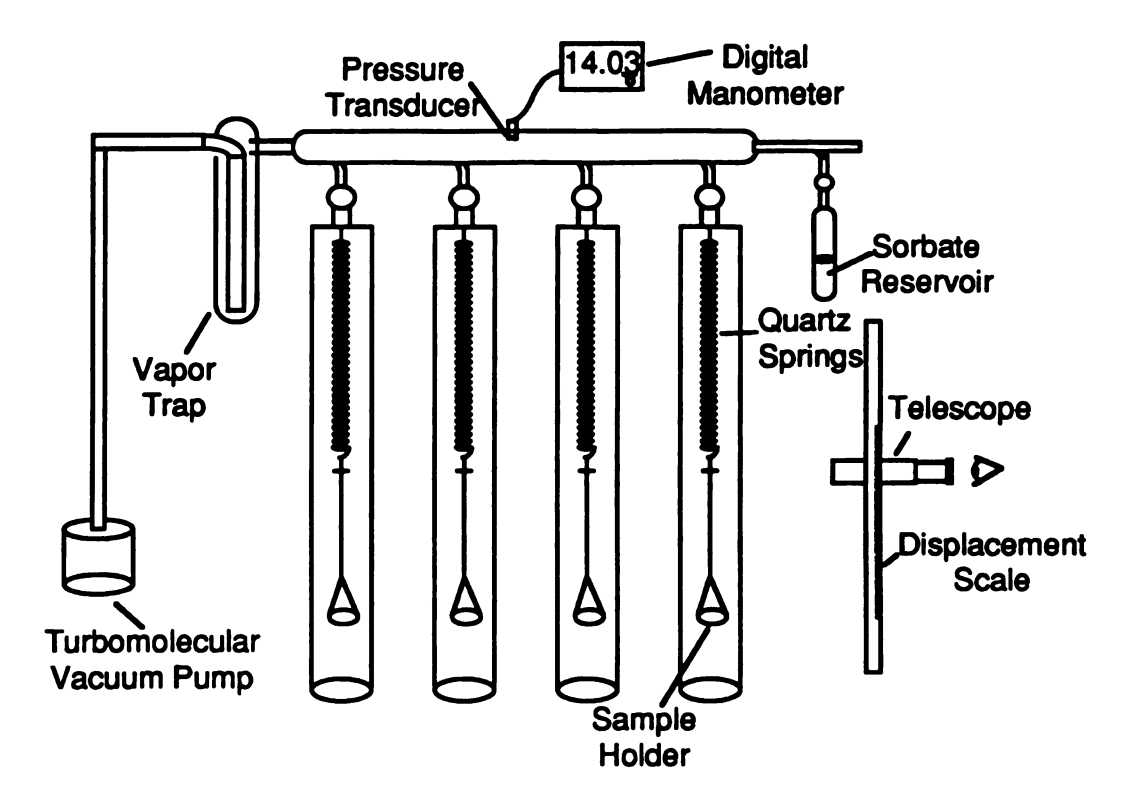


Figure 3-1. Diagram of the McBain balance used to collect water vapor sorption isotherms on TMA-and TMPA-saturated smectites. Water vapor pressure is controlled by releasing water vapor from the sorbate reservoir into vacuum. Quantity of water on the clay is determined by measuring the displacement of the quartz springs attached to the sample holders.

equilibrium water vapor pressures could not be accurately predicted from initial pressure, and it was nearly impossible to exactly replicate the final pressure from one experiment to the next.

Infrared spectroscopy

Clay film preparation:

Seventy mg each of normal-and reduced-charge TMA- and TMPA- clay were resuspended in 10 ml of methanol by sonicating for three 10-min intervals in an ice bath using a Heat Systems sonicator with 2.5-mm microprobe and a setting of 4.5. After the third sonication, coarse material was allowed to settle from the suspensions, 1-ml aliquots of the clay suspension were pipetted onto 13-mm diameter DelrinTM AgCl Disks (E.I. duPont de Nemours®), and the methanol was allowed to evaporate. It was necessary to repeat the pipetting several times to obtain a sufficiently thick film, defined as a film for which the clay O-H stretching vibration at 3650 cm⁻¹ was approximately 20% transmittance. The amount of clay on the disks was 0.8 ± 0.15 mg cm⁻².

Water vapor sorption on clay films:

TMA- and TMPA-saturated Wyoming montmorillonite clay films were equilibrated in a specially constructed IR cell (Figure 3-2) using the saturated salt solutions or concentrated H₂SO₄ solutions shown in Table 3-2 to regulate relative humidity. During this equilibration the O-H stretching region of sorbed water (3000 - 3600 cm⁻¹) was monitored until no change occurred (usually 1.5 h) Spectra were collected using a Perkin-Elmer 1600 FTIR spectrophotometer with a DTGS detector, 2 cm⁻¹ resolution, no apodisation, and 50 to 75 scans. The background spectrum was of the empty cell with a clean AgCl disk placed in the sample holder.

Single-beam spectra were stored on diskette, imported into the MS-DOS program SpectraCalc® (Galactic Software Inc.) then transformed into absorbance units. Spectra

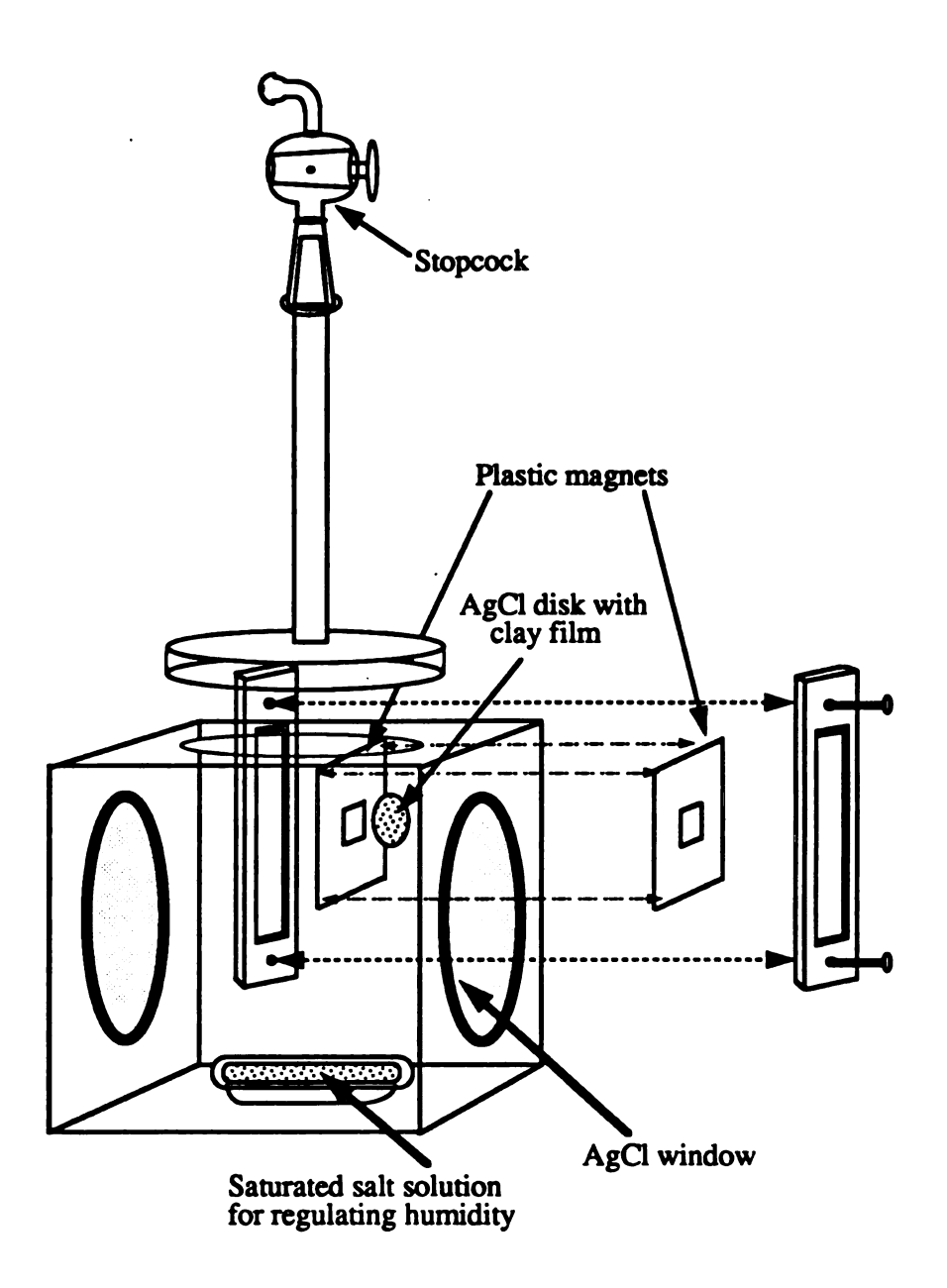


Figure 3-2. Diagram of the controlled atmosphere FTIR cell used to equilibrate TMA- and TMPA-saturated smectites with water vapor and collect spectra of clay-water complexes.

Table 3-2. Solutions used to regulate the partial pressure of water vapor in the desiccator and in the controlled-atmosphere FTIR cell used to equilibrate TMA and TMPA saturated smectites with water vapor¹.

P/Po	salt	
0	P_2O_5	
0.075	77% H ₂ SO ₄	
0.11	66.2% H ₂ SO ₄	
0.15	saturated LiCl	
0.17	61.5% H ₂ SO ₄	
0.20	saturated K-acetate	
0.25	56.5% H ₂ SO ₄	
0.33	saturated CaCl ₂	
0.43	saturated K ₂ CO ₃	
0.52	saturated NaHSO ₄	
0.58	saturated NaBr	
0.65	saturated Mg-acetate	
0.69	34.5% H ₂ SO ₄	
0.72	saturated NH ₄ Cl	
0.81	saturated (NH ₄) ₂ SO ₄	
0.92	saturated K ₂ HPO ₄	

¹ Weast, 1987.

were smoothed using an 11-point Savitsky-Golay procedure. The baseline was leveled along six or seven baseline points in the spectrum, then zeroed. Variance in the absorbance of the lattice O-H stretch suggested that the thickness of the clay film probed by the IR beam was not always the same. The following procedure was used to normalize all spectra to correct for differences in film thickness: A baseline-leveled, zeroed absorbance spectrum between 3800 and 2800 cm⁻¹ (Figure 3-3a) was displayed and the clay O-H stretching band removed by extrapolating a straight line between 3720 cm⁻¹ and 3560 cm⁻¹ in the spectrum, giving Figure 3-3b. This second spectrum was subtracted from the first, leaving the spectrum of the clay O-H band only (Figure 3-3c). The peak absorbance of this band was measured and the multiplication factor necessary to bring this peak to 0.700 A was calculated. The original (Figure 3-3a) spectrum was multiplied by this factor to give the normalized spectrum (Figure 3-3d).

RESULTS AND DISCUSSION

Water sorption isotherms

Figure 3-4 shows water vapor sorption isotherms on normal- and reduced-charge TMA- and TMPA-saturated montmorillonite. Isotherm shapes were consistent with water sorption isotherms collected by Gast and Mortland (1971) for TMA-saturated smectites, which were type II by Brunauer's (1945) classification, suggesting strong interaction between water and the sorbent. The amount of water sorbed by TMA-montmorillonite in this study was greater than Gast and Mortland (1971) observed, possibly because they used saturated salt solutions to control the partial pressure of water vapor in a system of one atm total pressure, whereas the present study was conducted at near-vacuum conditions.

The water vapor sorption isotherms (Figure 3-4) show that TMA-saturated clays sorb more water vapor than TMPA-clays. This result indicates that TMA-montmorillonites

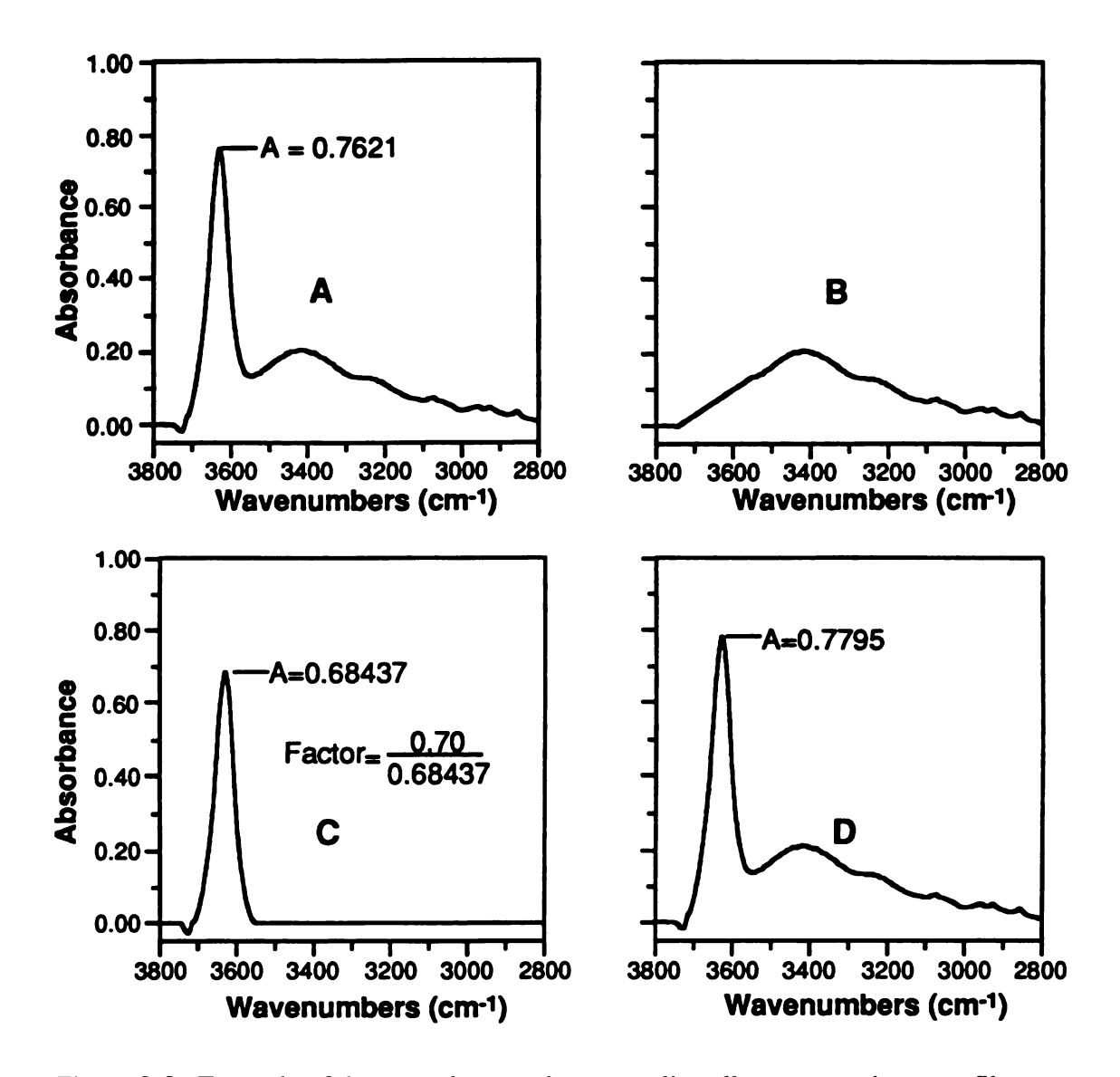


Figure 3-3. Example of the procedure used to normalize all spectra to the same film thickness by normalizing the absorbance of the lattice O-H stretch. A) Original spectrum. B) Original spectrum with the lattice O-H stretching vibration removed. C) difference spectrum of A - B, giving the lattice O-H stretching vibration only and the multiplication factor necessary to bring the absorbance of this band to 0.700A. D) Original spectrum (A) after multiplying it by the factor calculated in (C).

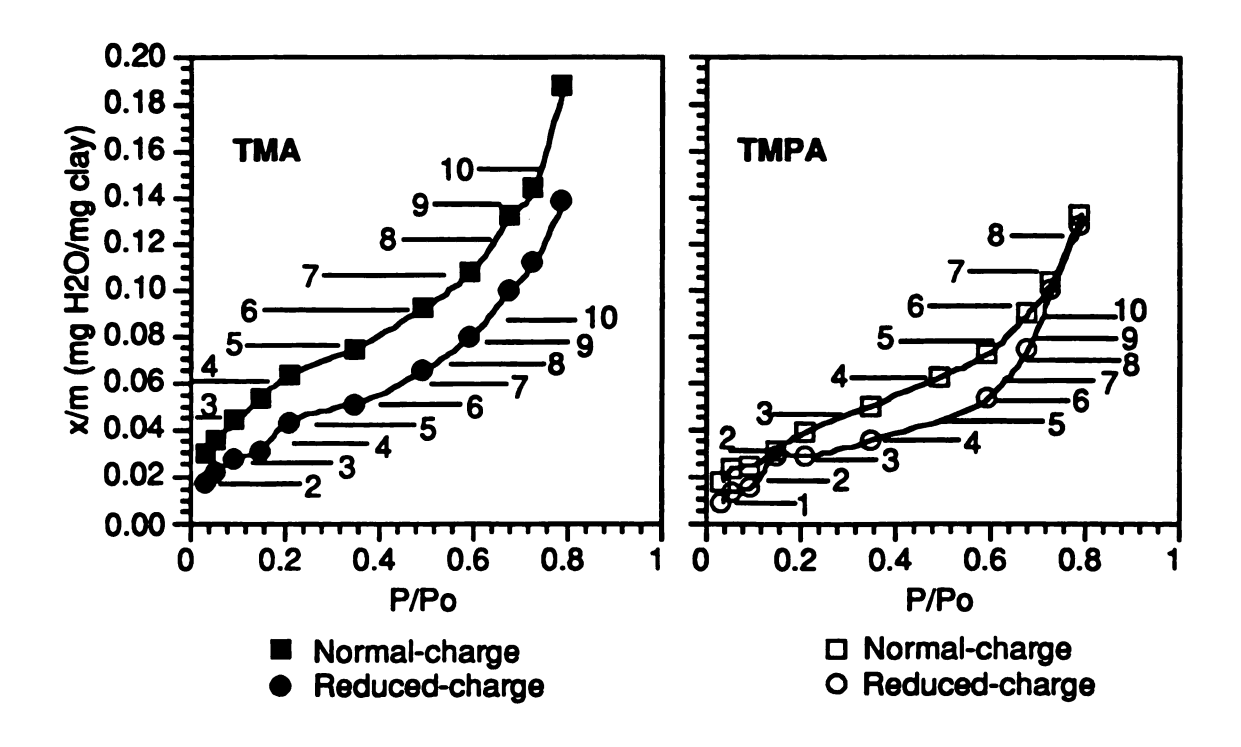


Figure 3-4. Water vapor sorption isotherms on normal-(squares) and reduced-(circles) charge clay saturated with TMA (left) and TMPA (right). Graph also shows number of water molecules sorbed per cation at different values of x/m.

are more hydrophillic than TMPA-montmorillonites. This behavior could either be because TMA likely has a greater hydration energy than TMPA (assuming that water interacts with the adsorbed cations) or because the phenyl groups of adsorbed TMPA sterically inhibit sorption of water vapor by TMPA-saturated clays as described below.

The most notable feature of the sorption isotherms in Figure 3-4 is that within each cation treatment, normal-charge clays sorb more water vapor than do reduced-charge clays, even though reduced-charge clays have greater N₂ surface area than do normal-charge clays (Table 3-1). If water preferred to sorb on the siloxane surface, greater sorption would have occurred on the reduced-charge clays. This is strong evidence that the cation, not the siloxane surface is the preferred sorption site for water on clays saturated with TMA and TMPA. This also supports the conclusion of Jaynes and Boyd (1991) that the siloxane surface of TMPA-saturated clays is more hydrophobic than the cations.

When the amount of water vapor sorbed is calculated on the basis of water molecules sorbed per cation (Figure 3-4), it appears that reduced-charge clays sorb at least one more water molecule per cation than do normal-charge clays for most values of P/P_o. On the TMA-saturated clay, this difference appears first at about P/Po=0.21, where there are five water molecules per cation on the reduced-charge clay, but four on the normal-charge clay. On the TMPA-saturated clay, at P/Po=0.21, there are three water molecules per cation on the reduced-charge clay but two on the normal-charge clay. A possible explanation for this behavior is that close proximity of adjacent cations on normal-charge clays may sterically restrict the number of water molecules in cation hydration shells of normal-charge clays. Steric restriction of hydration shell size may also explain why TMPA-montmorillonite has fewer molecules per cation at the same P/P_o than does TMA-montmorillonite: the bulky TMPA phenyl group may also restrict the number of water molecules in the TMPA hydration shell, especially on the normal-charge clay.

The trends in water vapor sorption shown in the sorption isotherms (Figure 3-4) can also be observed in the infrared spectra of adsorbed water on TMA- (Figure 3-5) and TMPA- (Figure 3-6) saturated montmorillonites. The sorbed water O-H stretching (3600 cm⁻¹) and deformation (1630 cm⁻¹) vibrations increase in intensity with increasing relative humidity (and amount of water sorbed). The IR spectra provide additional qualitative evidence that more water is sorbed on TMA- than TMPA-montmorillonites, though the effect of charge reduction is more difficult to discern. Because the molar absorptivities of sorbed water O-H vibrations decrease with increasing water content (Johnston et al, 1992) and may also depend on other factors such as layer charge, the intensities of the water O-H bands are only shown to provide a link between the water sorption isotherms and the infrared data described below.

Effect of sorbed water on cation vibrations

TMA-methyl vibrations

Infrared band assignments for methyl symmetric and asymmetric deformation vibrations of TMA are given in Table 3-3. The infrared band positions of TMA (estimated from the center-of mass, not peak maximum) on both normal- and reduced-charge clays are shown as a function of relative humidity in Figure 3-7, with selected infrared spectra shown in Figure 3-8. The increase in frequency of the methyl asymmetric deformation (Figure 3-7, top) and the slight decrease in frequency of the methyl symmetric deformation (Figure 3-7, bottom) with increases in relative humidity suggest that water vapor sorbs on the cations at low humidity. The methyl symmetric deformation vibrations are less intense (Figure 3-8) than the methyl asymmetric vibrations, which may have introduced some error into their estimated center-of-mass peak positions and contributed to the greater scatter in the methyl symmetric deformation data (Figure 3-7). The frequencies of both the methyl symmetric and asymmetric deformation vibrations shift most between 0% and 20% RH.

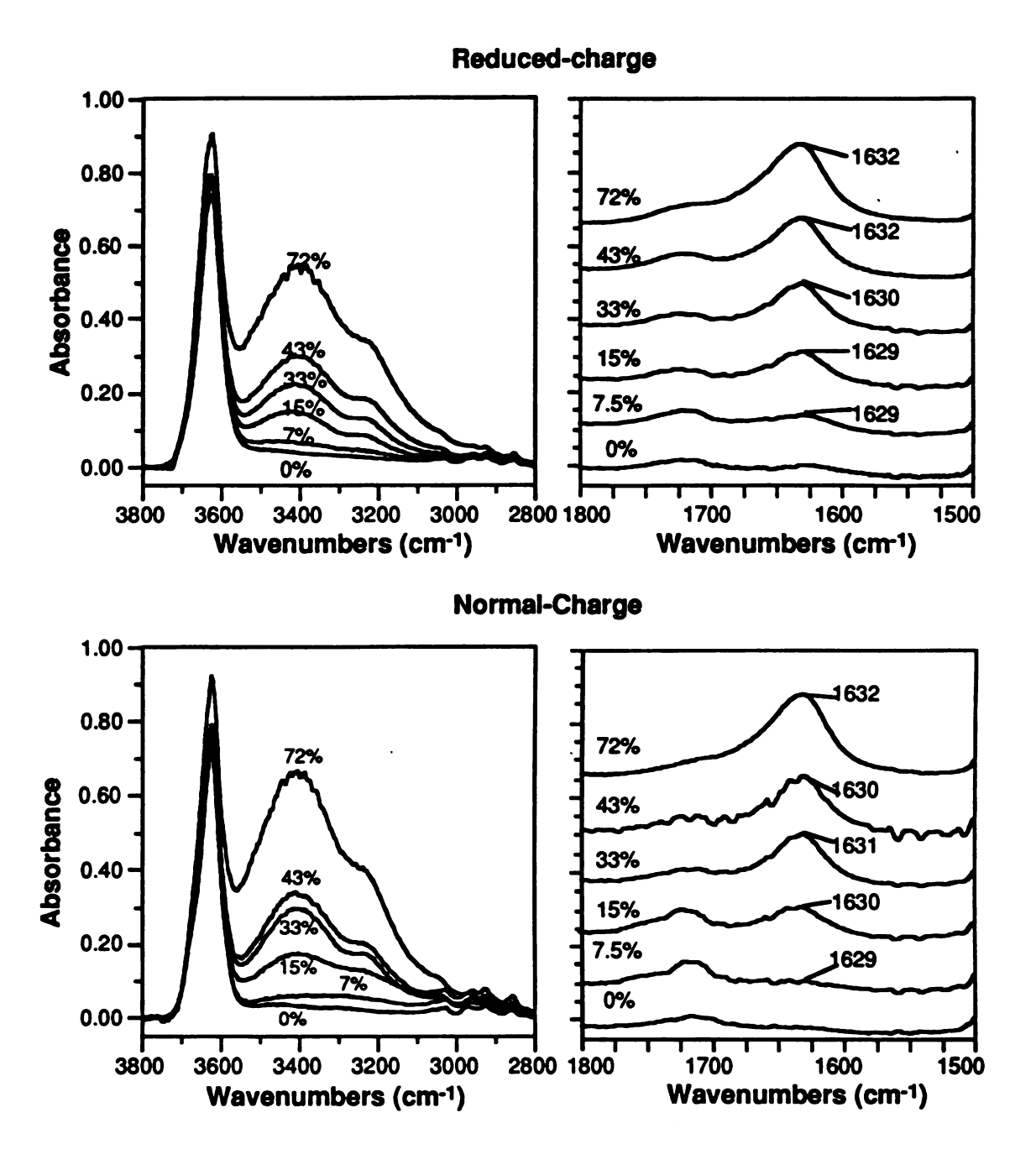


Figure 3-5. Infrared spectra of reduced-charge (top) and normal-charge (bottom) TMA- saturated Wyoming montmorillonite at six different relative humidities. The left side (3600 - 2800 cm⁻¹) shows the increase in intensity of the sorbed water O-H stretching vibration (3400 cm⁻¹) with changes in relative humidity. The right side (1800 - 1500 cm⁻¹) shows the increase in intensity of the sorbed water O-H bending (1630 cm⁻¹) vibration with changes in relative humidity.

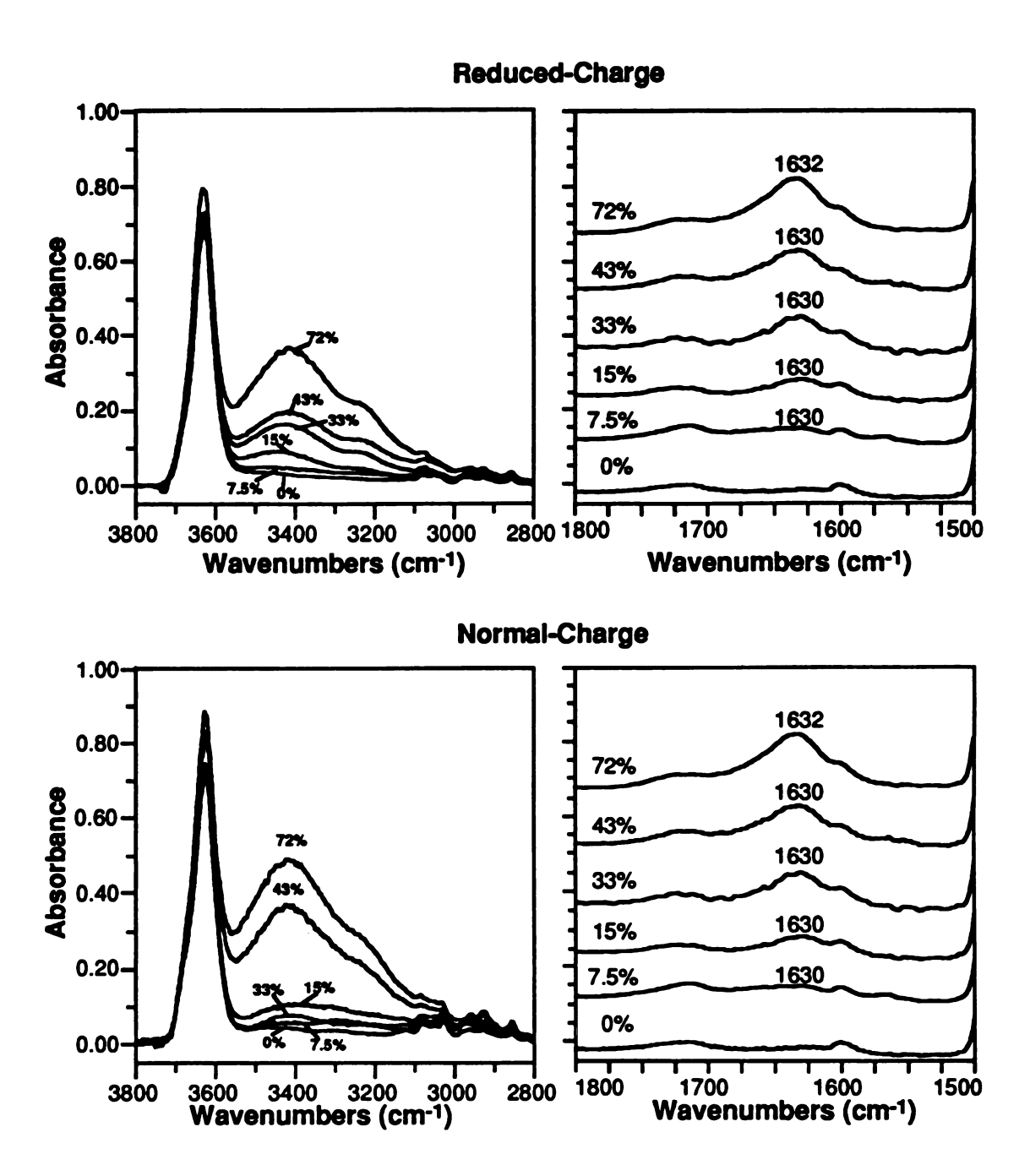


Figure 3-6. Infrared spectra of reduced-charge (top) and normal-charge (bottom) TMPA-saturated Wyoming montmorillonite at six different relative humidities. The left side (3600 - 2800 cm⁻¹) shows the changes in intensity of the sorbed water O-H stretching vibration (3400 cm⁻¹) with changes in relative humidity. The right side (1800 - 1500 cm⁻¹) shows the changes in intensity of the sorbed water O-H bending (1630 cm⁻¹) vibration with changes in relative humidity.

Table 3-3. Infrared band assignments for methyl symmetric and asymmetric deformation vibrations of chloride, bromide, and iodide salts of tetramethylammonium (TMA) in pressed KBr pellets, and observed peak positions of of TMA-Cl 1)dispersed in KBr using diffuse reflectance (DRIFT) and 2)dissolved in methanol using attenuated total reflectance (ATR).

	Methyl asym deformation	Methyl symm deformation	
TMA-Cl (pressed) ^a	1490	1405, 1398	
TMA-Br (pressed) ^a	1488	1405, 1397	
TMA-I (pressed) ^a	1483	1403, 1395	
TMA-Cl (DRIFT)b	1488	1404, 1398	
TMA-Cl Methanol (ATR) ^b	1491	1414	

^a Bottger and Geddes (1965)

b This study

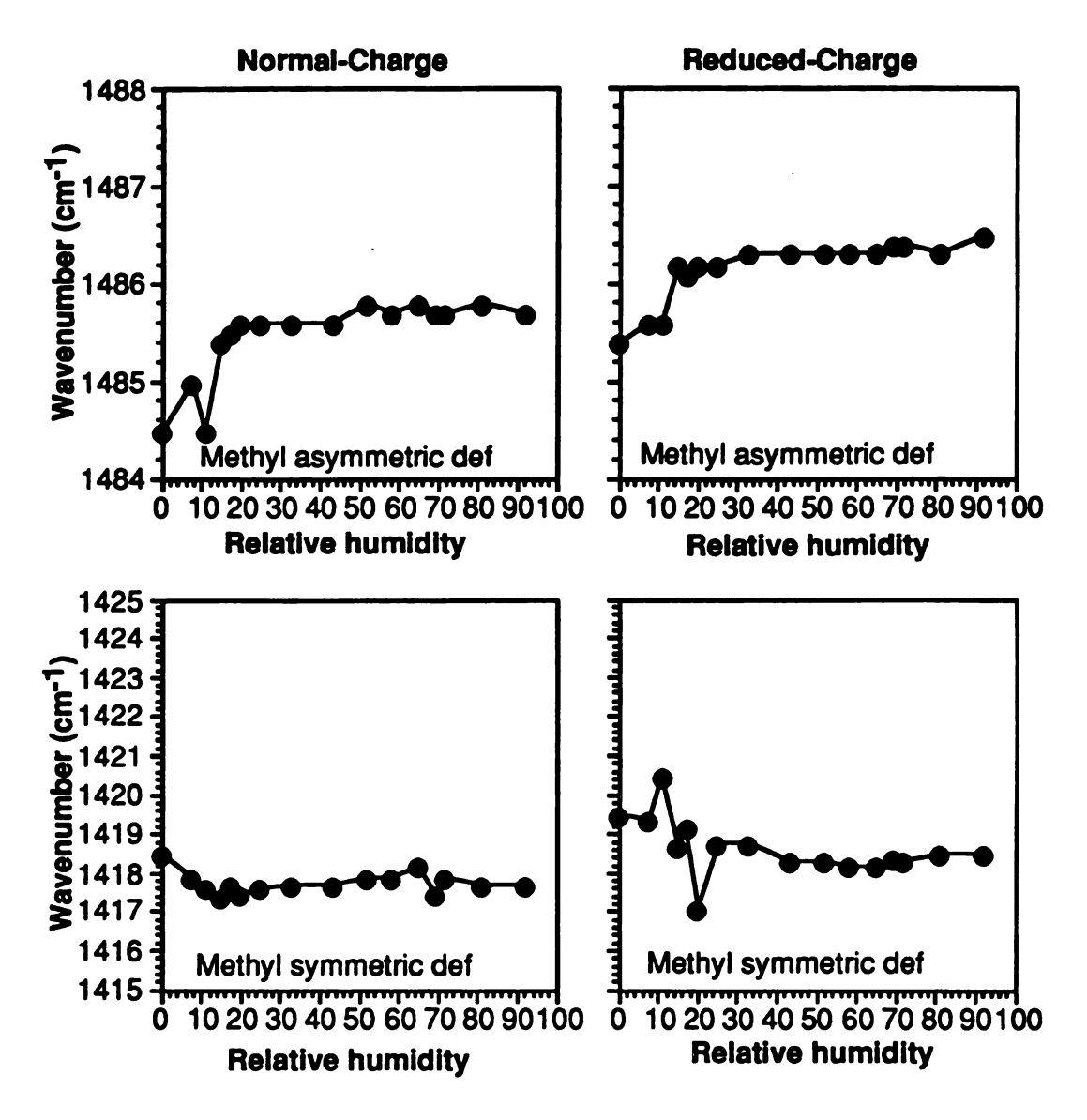


Figure 3-7. Effect of relative humidity on the center-of-mass frequency of the methyl asymmetric (top) and methyl symmetric (bottom) deformation vibrations of TMA saturating normal-charge (left) and reduced-charge (right) Wyoming montmorillonite.

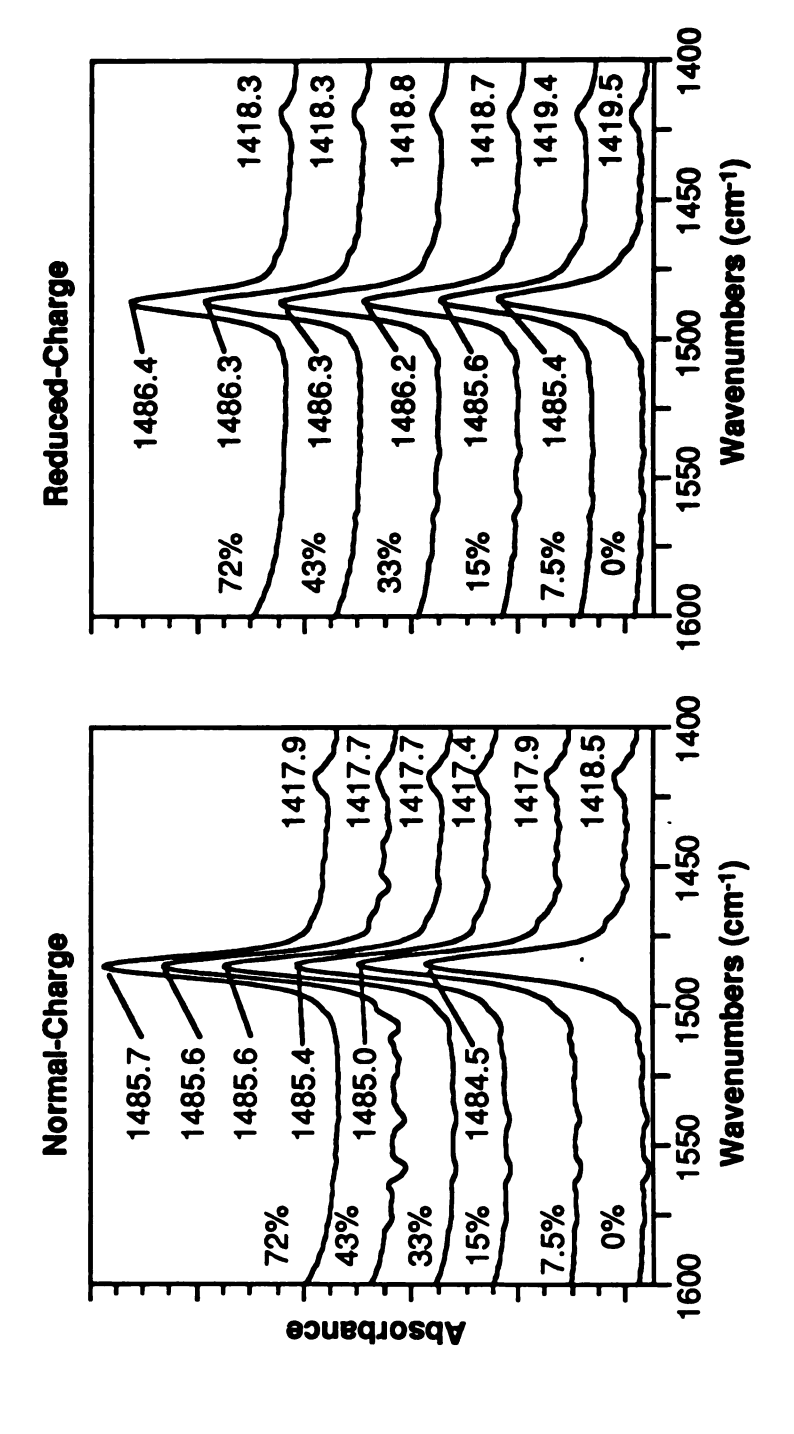


Figure 3-8. Infrared spectra of normal-charge (left) and reduced-charge (right) TMA-saturated Wyoming montmorillonite showing changes in frequency of the methyl asymmetric and symmetric deformation vibrations with changes in relative humidity. See Table 3 for band assignments.

after which there is little change. This suggests that beyond 20% RH, water molecules don't interact directly with the cation, but either form a second hydration shell around the cation or interact with the siloxane surface. It may also be possible that above 20% RH, water continues to interact directly with cations, but does not cause any additional shift in the methyl vibrations. However, at 20% and larger RH, there may already be at least 4 water molecules per cation on TMA-clay (Figure 3-4). Stearically, it seems unlikely that more than four water molecules can be coordinated directly to each cation.

TMPA-methyl vibrations

Infrared band assignments for some methyl vibrations of TMPA are given in Table 3-4. Infrared band positions on both normal- and reduced-charge clays for all relative humidity treatments are plotted in Figure 3-9, and selected infrared spectra shown in Figure 3-10. Peak maxima, not peak center-of-masses, are plotted in Figure 3-9 because the methyl asymmetric deformation vibration (\approx 1490 cm⁻¹) overlapped with the v_{19} , and v_{19h} ring stretch peaks, which made it impossible to estimate the center-of-mass for any of these peaks. The methyl symmetric deformation vibration of TMPA on normal-charge clay increased with increasing relative humidity, but no real trend is apparent in the reducedcharge clay (Figure 3-9, top). The methyl asymmetric deformation frequency of adsorbed TMPA definitely increased with increases in relative humidity on normal-charge clay (Figure 3-9, bottom). On the reduced-charge clay, the methyl asymmetric band was only a shoulder for many of the RH treatments, but appeared to exhibit the same trend as the normal-charge clay (Figure 3-9, bottom). Since the peak maxima positions could only be resolved to ± 1 cm⁻¹ on the TMPA spectra it was difficult to determine exactly at what relative humidity the slope changed on the RH vs. peak position plots (Figure 3-9). On normal-charge TMPA-montmorillonite it appears that above 15 to 25% RH, additional

Table 3-4. Infrared band assignments for the v_{19a} and v_{19b} C-C ring stretch of methyldeuterated (d₉) TMPA iodide and for the v_{19a} , v_{19b} , and methyl vibrations for TMPA-Br in 1)KBr using diffuse reflectance (DRIFT) and 2)in methanol using attenuated total reflectance (ATR).

	v19a C-C	v19b C-C	Methyl Asym	Methyl Symm	other
	ring stretch	ring stretch	deformation	deformation	Methyl
TMPA-I d ₉ ¹	1496	1459			
TMPA-Br (DRIFT)	1500	1461	1475, 1481	1416	1451
TMPA-Br (methano	l) 1498	1464	1475	1411	

¹ Chapter 2

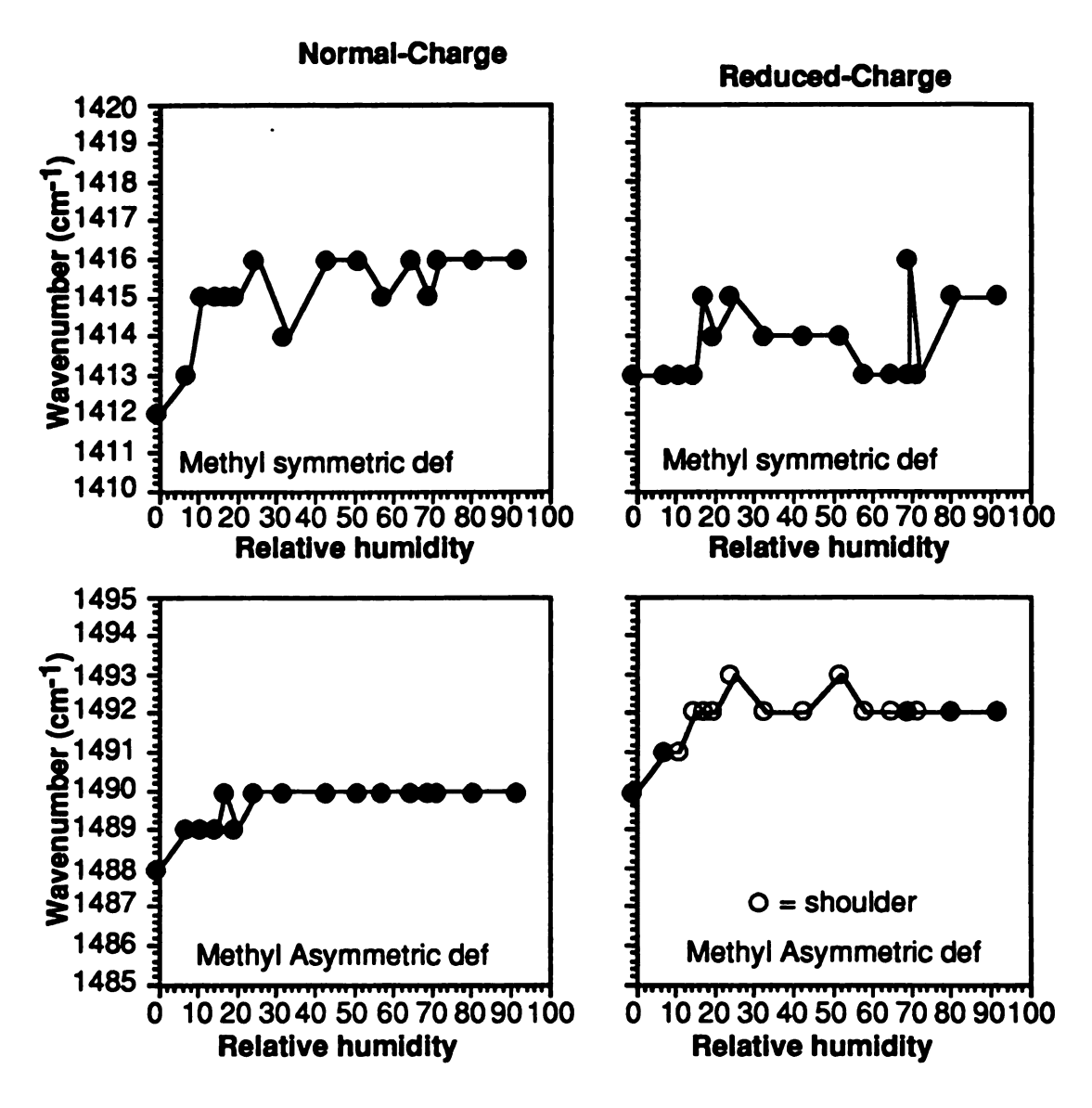


Figure 3-9. Effect of relative humidity on peak maximum frequencies of the methyl symmetric (top), and asymmetric (bottom) deformations of TMPA saturating normal-charge (left) and reduced-charge (right) Wyoming montmorillonite.

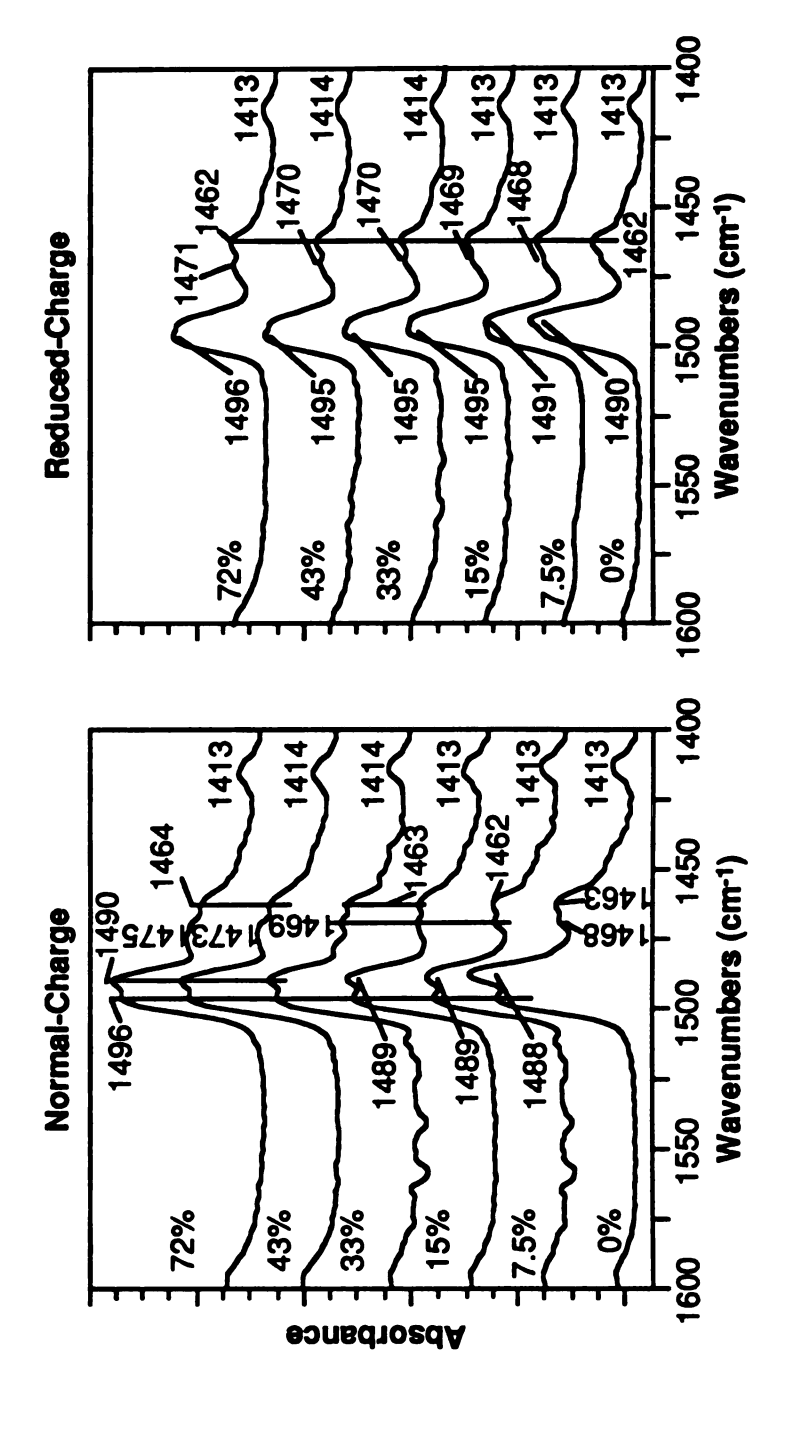


Figure 3-10. Infrared spectra of normal-charge (left) and reduced-charge (right) TMPA-saturated Wyoming montmorillonite showing changes in frequency and intensity of the ring stretching and methyl vibrations with changes in relative humidity. See Table 4 for band assignments.

water sorption had no effect on the band position, whereas the same was true above 15% RH on the reduced-charge TMPA clay (Figure 3-9, bottom).

Water sorption also affected the intensity of the methyl asymmetric deformation vibration at ~1490 cm $^{-1}$. Assuming the v_{19a} ring stretch vibration at 1496 cm $^{-1}$ remains at the same intensity with water sorption, the intensity of the methyl asymmetric deformation vibration decreases with water sorption. On normal-charge clay the methyl asymmetric deformation peak is resolved at all RH treatments, while on reduced-charge clay, the methyl asymmetric deformation vibration becomes a shoulder with water sorption.

TMPA ring vibrations

Infrared band assignments for some ring stretching vibrations of TMPA are given in Table 3-4. Peak maxima for the v_{19a} and the v_{19b} bands exhibited no trends with water sorption (Figure 3-10), so neither band was plotted as a function of relative humidity. On normal-charge clay, the v_{19a} band remained at 1496 cm⁻¹, while on reduced charge clay, the band appeared as a peak or shoulder at 1496 cm⁻¹ or 1495 cm⁻¹. The low-intensity v_{19b} band is obscured by an unassigned methyl vibration at \approx 1468cm⁻¹ (this methyl band was not present on methyl-deuterated TMPA-clay). The peak maximum of the v_{19b} remained at 1462 cm⁻¹ for all relative humidity treatments on reduced-charge clay while on normal-charge clay, this peak maximum shifted between 1462 cm⁻¹ and 1464 cm⁻¹, at least in part because of shifts in the unidentified methyl band (Figure 3-10).

When absorbances of the methyl asymmetric deformation at $1490 \, \mathrm{cm}^{-1}$ and the v_{19a} band at $1496 \, \mathrm{cm}^{-1}$ are compared between relative humidity treatments (Figure 3-11), it appears that the v_{19a} band remains at the same intensity while the methyl asymmetric deformation band decreases in intensity with water sorption. This decrease in intensity is

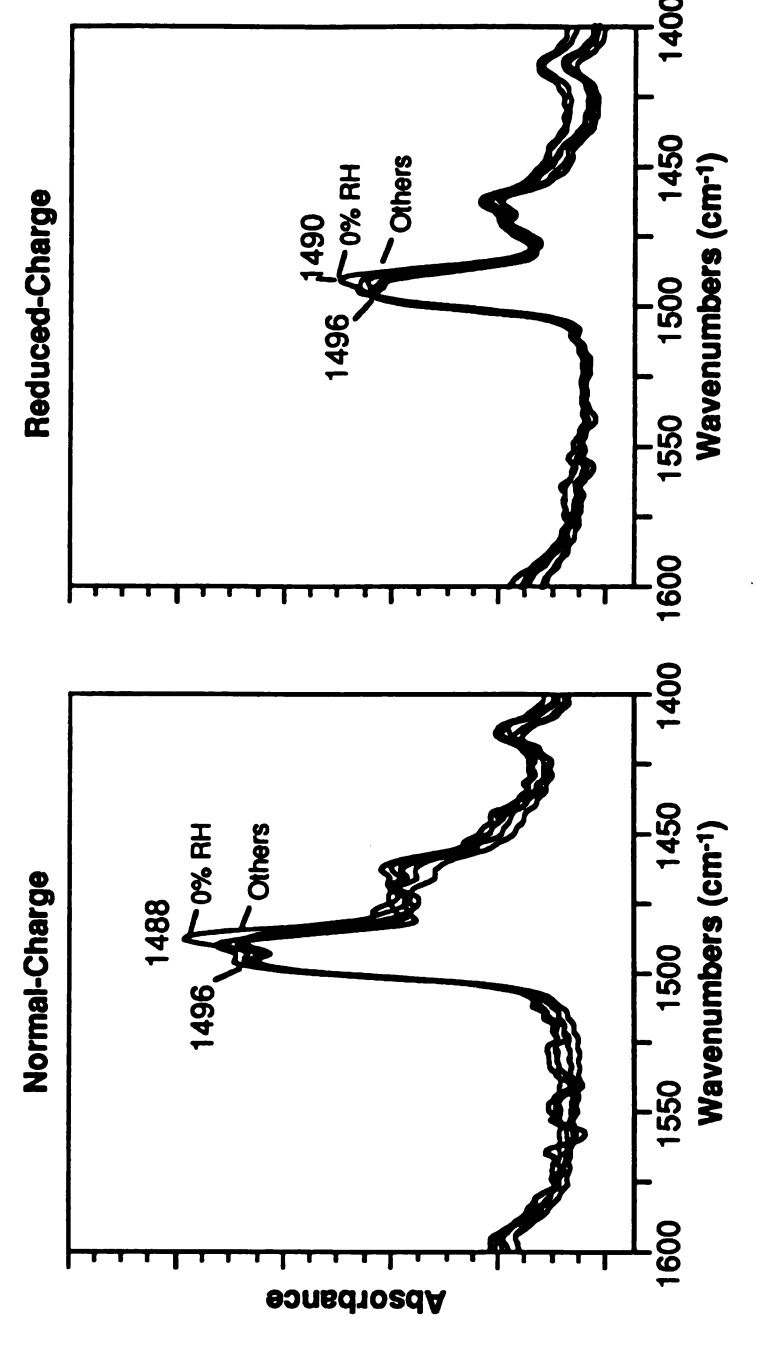


Figure 3-11. Infrared spectra of normal-charge (left) and reduced-charge (right) TMPA-saturated Wyoming montmorillonite showing changes in intensity of the methyl asymmetric deformation vibration with changes in relative humidity.

most evident between 0% and 7.5% RH (Figure 3-10), with less distinct changes in intensity with higher relative humidity.

The changes in intensity and position of the methyl asymmetric deformation vibrations of TMPA on normal- and reduced-charge clay show that, as with the TMA-montmorillonite, the infrared spectra of adsorbed TMPA are affected by water sorbed at low relative humidity, strongly suggesting that the preferred sorption site for water on TMPA-saturated clays is on the adsorbed TMPA cations. On TMPA, it further suggests that water preferentially interacts with the trimethyl portion of TMPA cations, since the ring stretching vibrations do not appear to be affected by water sorption. However, it is also possible that the ring stretching vibrations are not perturbed because their positions are more resistant to changes in the environment of the molecule.

CONCLUSIONS

Water vapor sorption isotherms showed more water sorption on the normal-charge clays than on reduced-charge clays, even though the N₂ surface area was greater for the reduced-charge clays. This indicated that the organic cations, not the siloxane surface were the preferred sorption sites for water vapor and that these cations are hydrophyllic. Water vapor sorption isotherms also showed that TMA-saturated clays sorb more water vapor than do TMPA-saturated clays, suggesting that TMA-saturated clays are more hydrophillic than TMPA-saturated clays. The lower sorption of water by the TMPA-saturated clays may be due to steric hinderance by the TMPA phenyl group, the lower hydration energy of TMPA or both. The calculated number of water molecules sorbed per cation on the reduced-charge clay was greater than on normal-charge clay, possibly because the closer cation spacing on the normal-charge clay restricts the number of water molecules within hydration shells around adjacent cations. The effect of water sorption on the infrared spectra of adsorbed TMA and TMPA provide additional evidence that the preferred site of

water sorption on these clays at low water content was the organic cations, not the siloxane surface.

The conclusion that the cations, and not the siloxane surface are the preferred site for water sorption on TMA- and TMPA-saturated clays will aid the design of organoclays for remediation of aqueous waste streams containing nonionic organic compounds. The sorptivity of organoclays for nonionic organic compounds can be increased by decreasing the number of cations on the clay, which will in turn reduce the amount of water competing for sorption sites on the clay.

REFERENCES

- Bernal, J.D., and Fowler, R.H. (1933) A theory of water and ionic solution with particular reference to hydrogen and hydroxyl ions. J. Chem. Phys. 1, 515-548.
- Bottger, G.L., and Geddes, A.L. (1965). The infrared spectra of the crystalline tetramethylammonium halides: *Spectrochim*. *Acta* 21,1701-1708.
- Boyd, S. A., Jaynes, W. F. and Ross, B. S. (1991) Immobilization of organic contaminants by organo-clays: Application to soil restoration and hazardous waste containment: in *Organic substances and sediments in water*, R.S. Baker, ed., vol. 1. CRC Press, Boca Raton, FL 181-372.
- Brindley, G.W, and Ertem, G. (1971) Preparation and solvation properties of some variable charge montmorillonites: Clays & Clay Minerals 19, 399-404.
- Farmer, V.C., and Russell, J.D. (1971). Interlayer complexes in layer silicates—The structure of water in lamellar ionic solutions: *J. Chem. Soc. Faraday Trans..* 67, 2737-2749.
- Gast, R.G., and Mortland, M.M. (1971) Self-diffusion of alkylammonium ions in montmorillonite: Journal of Colloid and Interface Science. 37, 80-92.
- Greene-Kelly, R. (1953) The identification of montmorillonoids in clays: J. Soil Sci. 4, 233-237.
- Jaynes, W.J., and Bigham, J.M. (1987) Charge reduction, octahedral charge, and lithium retention in heated, Li-saturated smectites: Clays & Clay Minerals 35, 440-448.

- Jaynes, W.J., and S.A. Boyd. (1991) Hydrophobicity of siloxane surfaces in smectites as revealed by aromatic hydrocarbon adsorption from water: *Clays & Clay Minerals* 39, 428-436.
- Jaynes, W.F., and. Boyd, S.A (1990) Trimethyphenylammonium-smectite as an effective adsorbent of water soluble aromatic hydrocarbons: *J. Air and Waste Management*. *Assoc.* 40, 1649-1653.
- Johnston, C.T., Sposito, G., and Erkckson, G. (1992) Vibrational probe studies of water interactions with montmorillonite: Clays &Clay Minerals 40, 722-730.
- Lee, J.F., Mortland, M.M, Chiou, C.T, Kile, D.E. and Boyd, S.A. (1990) Adsorption of benzene, toluene, and xylene by two tetramethylammonium-smectites having different charge densities: Clays & Clay Minerals 38, 113-120.
- McBain, J.W., and Bakr, A.M. (1926) A new sorption balance: J. Am. Chem. Soc. 48, 690-695.
- Nagano, Y., Sakiyama, M., Fujiwara, T., and Kondo, Y. (1988) Thermochemical study of tetramethyl- and tetraethylammonium halides: Nonionic cohesive energies in the crystals and hydration enthalpies of the cations. *J. Phys. Chem.* 92, 5823.
- Sposito, G., and R. Prost. 1982. Structure of water adsorbed on smectites: *Chemical Reviews* 82, 553-573.
- Weast, R.C. ed., (1986) CRC handbook of chemistry and physics 67th ed. CRC press, Inc. Boca Raton, Florida. E-42.

CHAPTER IV

An FTIR study of competitive water-arene sorption on tetramethylammonium- and trimethylphenylammonium-saturated normal-and reduced-charge Wyoming montmorillonite

ABSTRACT

Sorption of arenes by quaternary alkylammonium-saturated clays is enhanced by reducing the charge density of the clay, but inhibited by water sorption and increasing solute size. The objectives of this study are to determine: 1) whether arenes sorb on cation sites of dry tetramethylammonium- (TMA) and trimethylphenylammonium- (TMPA) saturated clays; 2) if water sorption inhibits arene sorption on these sites; 3) if higher clay charge density inhibits arene sorption on cation sites; 4) if water -arene competition and high clay charge density inhibit arene-cation interaction more for large arenes than for small arenes. TMA- and TMPA-saturated clay films with different charge densities were treated with different combinations of arene and water vapor and probed using infrared spectroscopy to determine the effect of charge density, water sorption, and arene sorption on the position of cation vibrational frequencies. Arene sorption perturbed vibrational frequencies of adsorbed TMA and TMPA differently than did water sorption, allowing spectroscopic differentiation between the water and arene interaction with TMA and TMPA. The infrared data show that benzene and ethylbenzene sorption occurs on cation sites on dry TMA-and TMPA-saturated clays. The closer cation spacing of higher charge TMA-

and TMPA-clays, apparently restricted arene sorption from a larger proportion of cation sites compared to reduced-charge clay. The cation vibrational frequencies of clay films exposed towater vapor and saturated benzene vapor remained at the frequencies characteristic of benzene alone for all relative humidity treatments. The cation vibrational frequencies of films exposed to ethylbenzene and water vapor shifted from those characteristic of ethylbenzene vapor alone toward frequencies characteristic of water vapor alone as relative humidity increased. Thus, water sorption drove ethylbenzene, but not benzene, from cation sites. Water vapor sorption and higher clay charge density both inhibited sorption of larger arenes more than smaller arenes.

INTRODUCTION

Clays saturated with quaternary alkylammonium cations have been proposed as sorbents to remove organic pollutants from aqueous industrial waste streams (Boyd et al., 1991). In this application, water and organic pollutants compete for sorption sites on the clay. Possible pollutant sorption sites include the siloxane surface and the organic cations (Lee et al., 1990; Jaynes and Boyd, 1990,1991).

Arene sorption on clays saturated with small organic cations such as
tetramethylammonium (TMA) and trimethylphenylammonium (TMPA) is affected by water
sorption, clay charge density and arene size. Vapor-phase arene sorption on dry TMAmontmorillonite is much greater than is arene sorption from aqueous solution (Lee et al.,
1990). The inhibition in aqueous sorption may be due to water hydrating the organic
cations on the clay (Chapter 3, Lee et al., 1990; Jaynes and Boyd, 1991). Lee et al.,
(1990) also observed that aqueous arene sorption on TMA-montmorillonite decreases with
increasing clay charge density and with increasing arene size. Jaynes and Boyd, 1991
observed decreased aqueous arene sorption with increased clay charge density on TMPA

clay, but they did not observe the arene size trend noted by Lee et al. (1990). With dry vapor-phase sorption, Lee et al. (1990) observed similar clay charge effects where more vapor phase sorption of toluene and o-xylene occurred on reduced-charge clay than on normal-charge clay at all values of P/P₀. At P/P₀ values less than 0.3, a similar reduction in sorption occurred for benzene vapor on dry clay. Jaynes and Boyd (1991) concluded that increases in arene sorption with decreasing charge density (and hence with increasing uncharged siloxane surface area) indicated that in the presence of water, arenes sorb preferentially onto uncharged siloxane surfaces. At P/P₀ values greater than 0.3, Lee et al. (1990) observed more benzene sorption on the normal-charge clay than on reduced-charge clay. This observation suggests that benzene may interact with cation sites at high P/P₀ as a secondary sorption site.

The mechanism by which water inhibits arene sorption is not well understood. Spectroscopic studies can be conducted to determine whether arenes interact with TMA and TMPA, with uncharged siloxane surfaces, or with both types of potential sorption sites. Two hypotheses are suggested in the literature and Chapter 3 for the mechanism for arene sorption inhibition on TMA- and TMPA-clay. The first hypothesis is that water inhibits arene sorption on TMA- and TMPA-clay by hydrating the adsorbed cations and displacing arenes that interact with the cations on dry TMA- and TMPA-montmorillonites. This hypothesis is consistent with infrared spectroscopic data reported in Chapter 3 which showed that water interacts with both TMA and TMPA cations even at P/P_0 corresponding to between one and two H_2O molecules per cation, depending on cation type and layer charge. The second theory (Lee et al., 1990) is that when water molecules hydrate cations in clay interlayers, they sterically restrict the diffusion of solutes such as benzene, toluene, and xylene into the interlayer region. On low-charge clay, hydrated cations are farther apart, leaving more space in which arenes can diffuse and sorb. The latter theory (Lee et al., 1990) is also consistent with published sorption data that show that the inhibitory effect

of water on arene sorption increases (i.e., arene sorption decreases) as the number of arene methyl substituents increases (Lee et al, 1990). Another reason for the greater inhibitory effect of water sorption of larger arenes, however, may be that water more readily displaces methyl-substituted benzenes from cation sorption sites. The two hypothesized mechanisms may act simultaneously to reduced arene sorption on TMA- and TMPA-clay.

Spectroscopic data are needed to test these hypotheses. This paper describes research in which the positions of TMA and TMPA vibrational frequencies in the infrared spectra of TMA- and TMPA-saturated normal-and reduced-charge montmorillonite clay films treated with different proportions of arene and water vapor were recorded and interpreted to answer the following questions: 1. do arenes sorb on cation sites of dry clays saturated with TMA and TMPA? 2. does water sorption cause arene desorption from cation sites? 3. does higher clay charge density inhibit arene sorption on cation sites? 4. is sorption of a larger arene (ethylbenzene) on cation sites more inhibited by water sorption and high charge density than is benzene sorption?

MATERIALS AND METHODS

Reduced-and normal-charged organoclay preparation

Wyoming montmorillonite (SWy-1) was obtained from the Clay Minerals Society Source Clays Repository at the University of Missouri-Columbia. The <2-µm fraction was separated from the coarser material by sedimentation and the charge was reduced for half the clay as described in Chapter 2. Normal- and reduced charge montmorillonite saturated with TMA- and TMPA-were prepared as described in Chapter 3. Selected properties of the clays are reported in Table 4-1.

Table 4-1. Selected physical and chemical properties of normal (Norm)- and reduced
(Red)-charge TMA- and TMPA-montmorillonite.

Treatment	d(001) (Å)	N ₂ Surface Area ² (m ² g ⁻¹)	Total C ³ (g kg ⁻¹)	Adsorbed cation ⁴ (mmol kg ⁻¹)	CEC ⁵ (mmol kg ⁻¹)
Red TMA	13.6	289±30	27.7±0.7	474±14	390±30
Norm TMA	13.6	202±26	40.7±0.3	847±6	870±80
Red TMPA	13.7 ¹	318±14	48.6±0.9	449±8	390±30
Norm TMPA	14.9 ¹	252±28	88.1±1.0	814±11	870±80

¹ Obtained from Fourier transform of XRD data (Chapter 2).

Adsorbed cation =
$$\frac{\text{Total g C}}{\text{kg clay}} \times \frac{\text{mmol cation}}{\text{g C}}$$

 $^{^2}$ Avg \pm SD (N=2 or 3) from three-point BET N₂ adsorption isotherms using a Quantachrome Quantasorb Jr. surface area analyzer.

 $^{^3}$ Avg \pm SD (N=2) of total C determined by combustion at 900 °C using a Dohrmann DC-190 high-temperature carbon analyzer.

 $^{^4}$ Avg \pm SD (N=2) calculated with the equation:

⁵ Avg \pm SD (N=3 or 4) Determined by Na⁺ saturation and ammonium displacement of the parent normal - and reduced - charge clays (i.e. not treated with organic cations). Statistically identical values were obtained with Mg²⁺ saturation and Ba²⁺ extration.

Infrared spectroscopy

Clay film preparation:

Seventy mg each of normal-and reduced-charge TMA- and TMPA- clay were resuspended in 10 ml of methanol by sonicating for three 10-min intervals in an ice bath using a Heat Systems sonicator with 2.5-mm microprobe and a setting of 4.5. After the third sonication, coarse material was allowed to settle from the suspensions, 1-ml aliquots of the clay suspension were pipetted onto 13-mm diameter DelrinTM AgCl Disks (E.I. duPont de Nemours[®]), and the methanol was allowed to evaporate. It was necessary to repeat the pipetting several times to obtain a sufficiently thick film, defined as a film for which the clay O-H stretching vibration at 3650 cm⁻¹ was approximately 20% transmittance. The amount of clay on the disks was 0.8 ± 0.15 mg cm⁻².

Competitive water and arene vapor sorption on clay films:

TMA- and TMPA-saturated Wyoming montmorillonite clay films were equilibrated overnight in a desiccator that contained a liquid reservoir of either benzene, benzene-d₆, or ethylbenzene, and either P₂O₅ or an aquous salt or H₂SO₄ solution. The free liquid benzene, benzene-d₆, and ethylbenzene provided an atmosphere that was saturated with respect to that arene, whereas the P₂O₅ and the aqueous salt and H₂SO₄ solutions controlled the partial pressure of water (Table 4-2). After overnight equilibration in the desiccator, the films were transferred rapidly from the desiccator into a gas-tight IR cell (Figure 4-1) with the same salt or acid solution found in the equilibration desiccator. No arenes were added in the IR cell. The films were equilibrated with water vapor in the IR cell for 75 min. Benzene and ethylbenzene sorption spectra were collected using a dry-air-purged Perkin-Elmer PE1600 FTIR spectrophotometer with a DTGS detector, 2 cm⁻¹ resolution, no apodisation, and 50 to 75 scans. Benzene-d₆ sorption spectra were collected

Table 4-2. Solutions used to regulate the partial pressure of water vapor in desiccator and in the controlled-atmosphere FTIR cell.

P/Po	<u>salt</u>
0	P_2O_5
0.11	66.2% H ₂ SO ₄
0.33	saturated CaCl ₂
0.43	saturated K ₂ CO ₃
0.58	saturated NaBr
0.72	saturated NH ₄ Cl
1.00	pure water

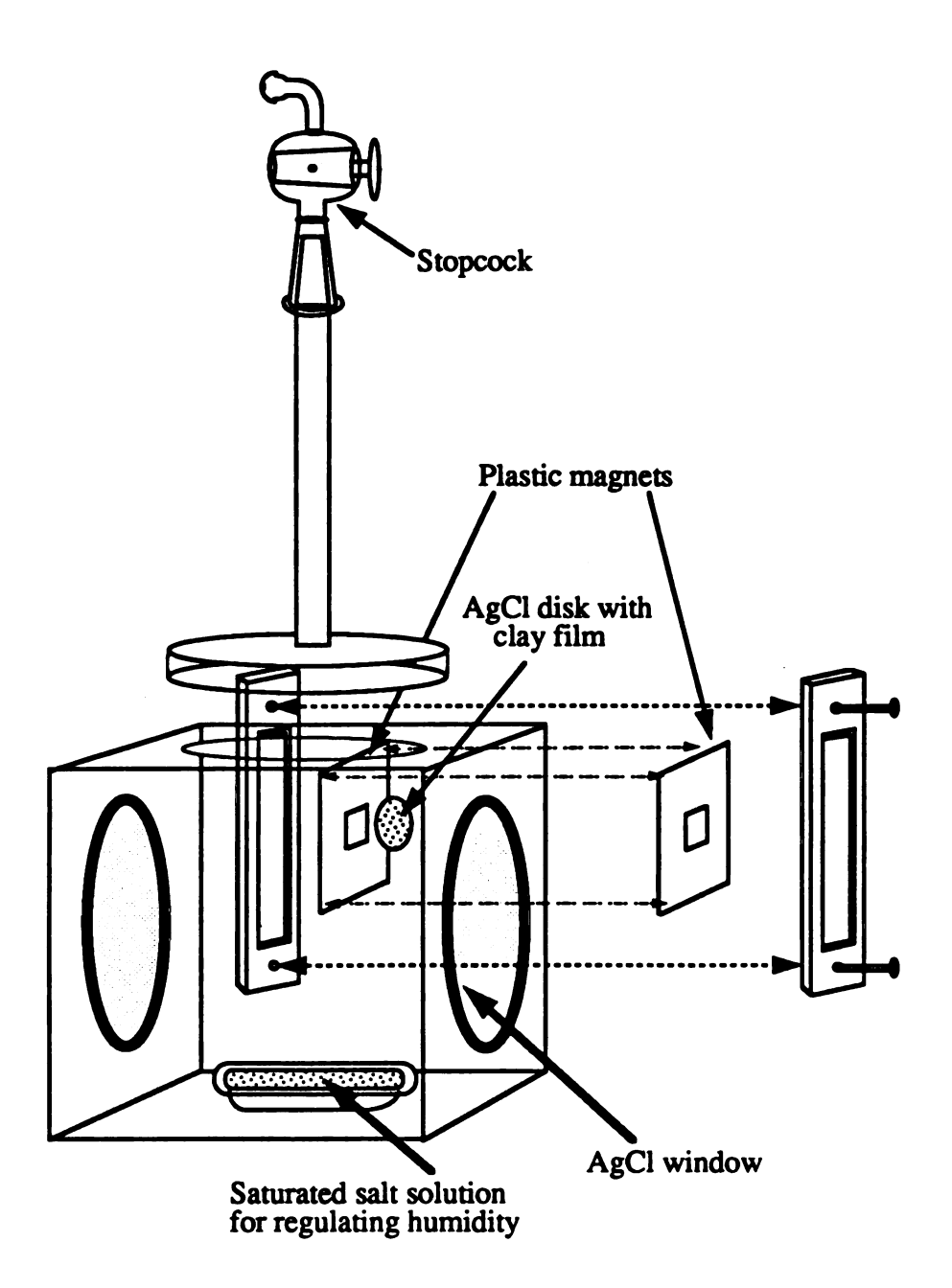


Figure 4-1. Diagram of the controlled atmosphere FTIR cell used to equilibrate arene-saturated TMA-and TMPA-saturated clay films with water vapor and collect spectra of clay-water -arene complexes

using an N_2 -purged Nicollet IR/42 FTIR with a DTGS detector, 2 cm⁻¹ resolution,.Happ-Genzel apodisation, and 100 scans. A background spectrum of the empty cell with a clean AgCl disk placed in the sample holder over the appropriate salt or acid solution was collected for each arene-water vapor treatment.

Single-beam spectra were stored on diskette and imported into the MS-DOS program SpectraCalc® (Galactic Software Inc.) then transformed into absorbance units. Spectra were smoothed using an 11-point Savitsky-Golay procedure. The baseline was leveled along six or seven baseline points in the spectrum, then zeroed. Variance in the absorbance of the lattice O-H stretch suggested that the thickness of the clay film probed by the IR beam may not always the same. The spectra were normalized for this variation to make the intensities of all clay O-H stretching vibrations at 3650 cm⁻¹ equal. (The details of this proceedure were described in Chapter 3.

RESULTS

TMA-montmorillonite

Arene sorption on dry clay

Benzene sorption

Band assignments for TMA and benzene are given in Tables 3 and 4, respectively. The 0% RH spectra in Figure 4-2 show the effect of benzene sorption on the infrared spectrum of dry normal- and reduced-charge TMA-saturated Wyoming montmorillonite. The intense v_{19} ring stretching vibration of sorbed benzene (1478 cm⁻¹) overlapped with the weaker methyl asymmetric deformation vibration of TMA on both normal-charge

Table 4-3. Infrared band assignments for methyl symmetric and asymmetric deformation vibrations of chloride, bromide, and iodide salts of tetramethylammonium (TMA) in pressed KBr pellets, and observed peak positions of TMA-Cl 1)dispersed in KBr using diffuse reflectance (DRIFT) and 2)dissolved in methanol using attenuated otal reflectance (ATR).

Demonand Codden	Methyl Asym	Methyl Symm	
Bottger and Geddes	deformation	deformation	
TMA-Cl (pressed)	1490	1405, 1398	
TMA-Br (pressed)	1488	1405, 1397	
TMA-I (pressed)	1483	1403, 1395	
This study	**************************************		
TMA-CI DRIFT	1488	1404, 1398	
TMA-Cl Methanol	1491	1414	

Table 4-4. Infrared band assignments for neat liquid benzene¹, ethylbenzene², and benzene- d_6^3 .

	ν ₁₉	CH ₃ /CH ₂ bend	
Arene	-	cy (cm ⁻¹)—	
Benzene	1478		
Ethylbenzene	$1495(v_{19a})$	1452	
Benzene-d ₆	1333		

¹ Duinker and Mills, 1968

² Green, 1962

³ Varsányi, 1969

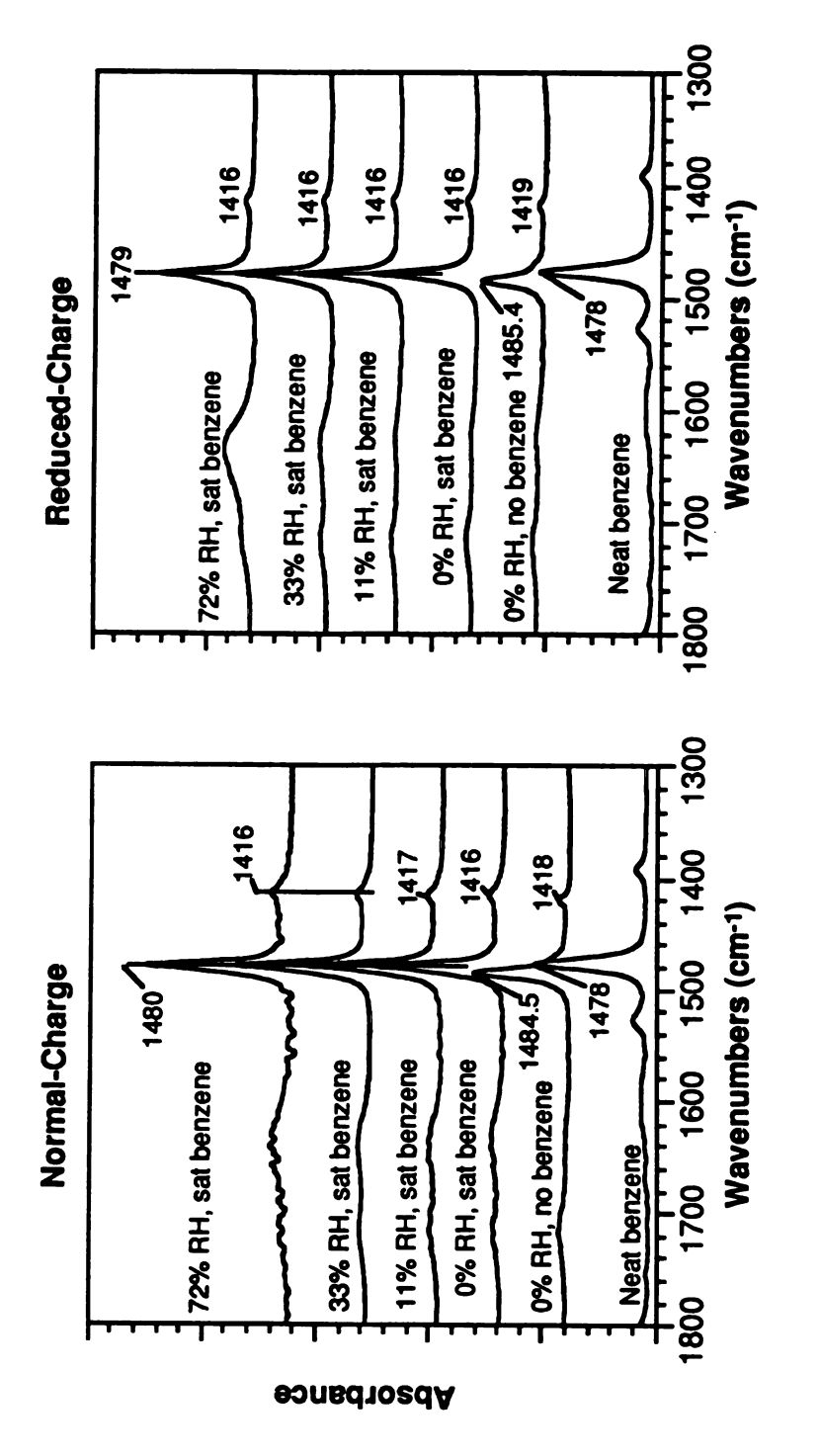


Figure 4-2. Effect of mixed benzene-water sorption on the infrared spectrum of normal-charge (left) and reduced-charge (right) TMA-saturated clay. The clay spectra are drawn at the same scale, but stacked for comparison. Band assignments for TMA are given in Table 3 and benzene in Table 4. Peak positions were estimated from peak maxima.

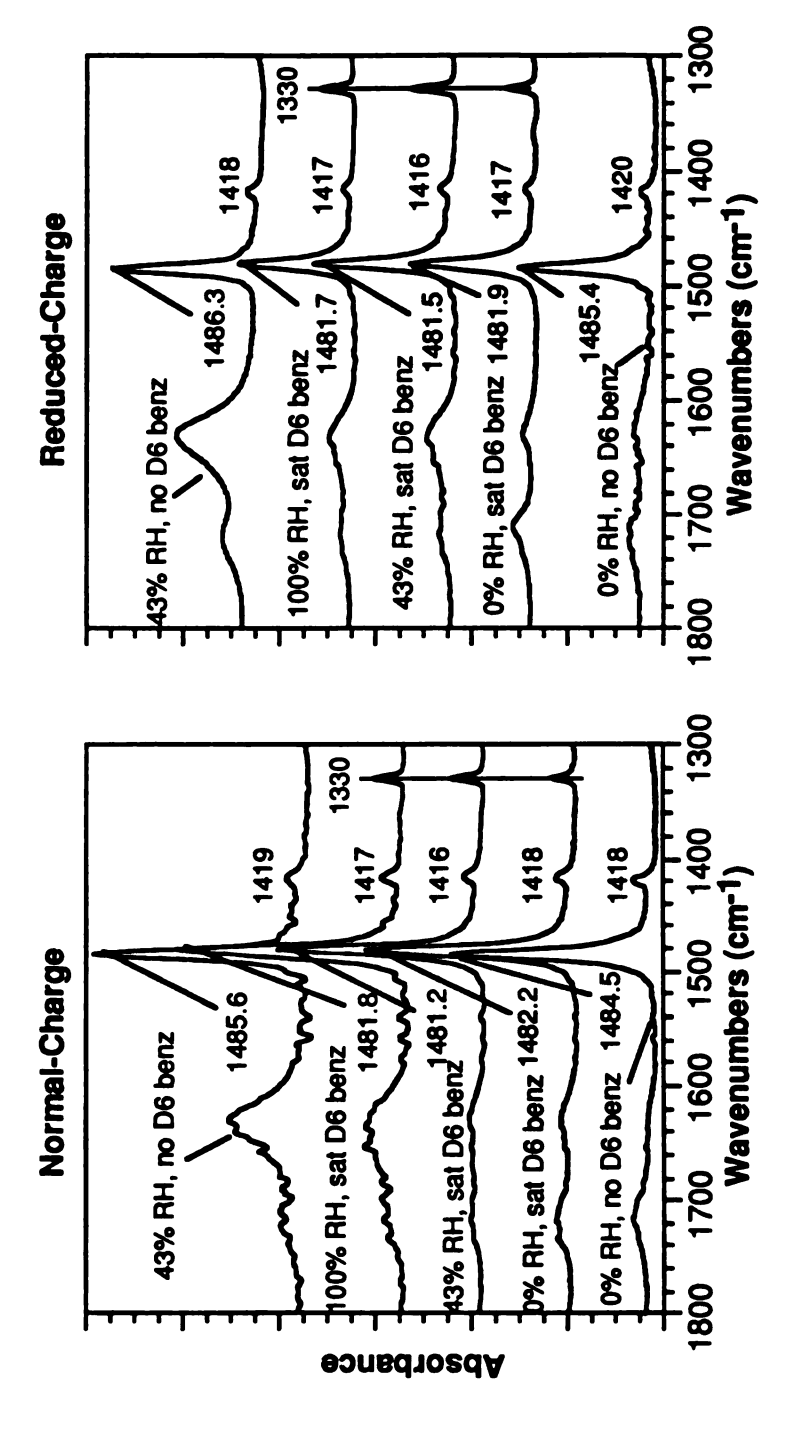
(1485.4 cm⁻¹) and reduced-charge (1484.5 cm⁻¹) clay, but if the resulting peaks at 1480 cm⁻¹ on normal-charge clay and 1479 cm⁻¹ on reduced-charge clay were due more to the methyl asymmetric deformation vibration of TMA than sorbed benzene, then benzene sorption caused the methyl asymmetric deformation vibration to shift to lower frequency. The methyl symmetric deformation vibration of TMA (≈1418 cm⁻¹) sorbed on normal- and reduced-charge clay shifted to lower frequency in response to benzene sorption. These shifts to lower frequency suggest that benzene interacts with TMA cations.

Benzene-d₆ sorption

Infrared spectra of benzene- d_6 sorption on TMA-montmorillonites (Figure 4-3) provided more information about possible interactions between benzene and adsorbed TMA, because the v_{19} band of deuterobenzene (Table 4-4) did not overlap with any TMA methyl vibrations. The 0% RH spectra in Figure 4-3 show the effect of benzene- d_6 sorption on the infrared spectrum of normal- and reduced-charge TMA-saturated Wyoming montmorillonite. Benzene- d_6 sorption caused the center-of-mass of the methyl asymmetric deformation vibration of TMA to shift from 1484.5 to 1482.2 cm⁻¹ on the normal-charge clay and from 1485.4 to 1481.9 cm⁻¹ on the reduced-charge clay. The methyl symmetric deformation vibration also shifted to slightly lower frequency due to benzene- d_6 sorption. These shifts in the methyl deformation vibrations of TMA on normal- and reduced-charge montmorillonite suggest that benzene- d_6 (and thus benzene) sorbs on cation sites of these clays.

Ethylbenzene sorption

The 0% RH spectra in Figure 4-4 show the effects of ethylbenzene sorption on the infrared spectrum of normal- and reduced-charge TMA-saturated clay films. The bands



charge (left) and reduced-charge (right) TMA-saturated clay. The spectra are drawn at the same scale, but stacked for comparison. Band assignments for TMA are given in Table 3 and benzene-d₆ Figure 4-3. Effect of mixed deuterobenzene-water sorption on the infrared spectrum of normalin Table 4. Peak positions were estimated from peak center-of-mass.

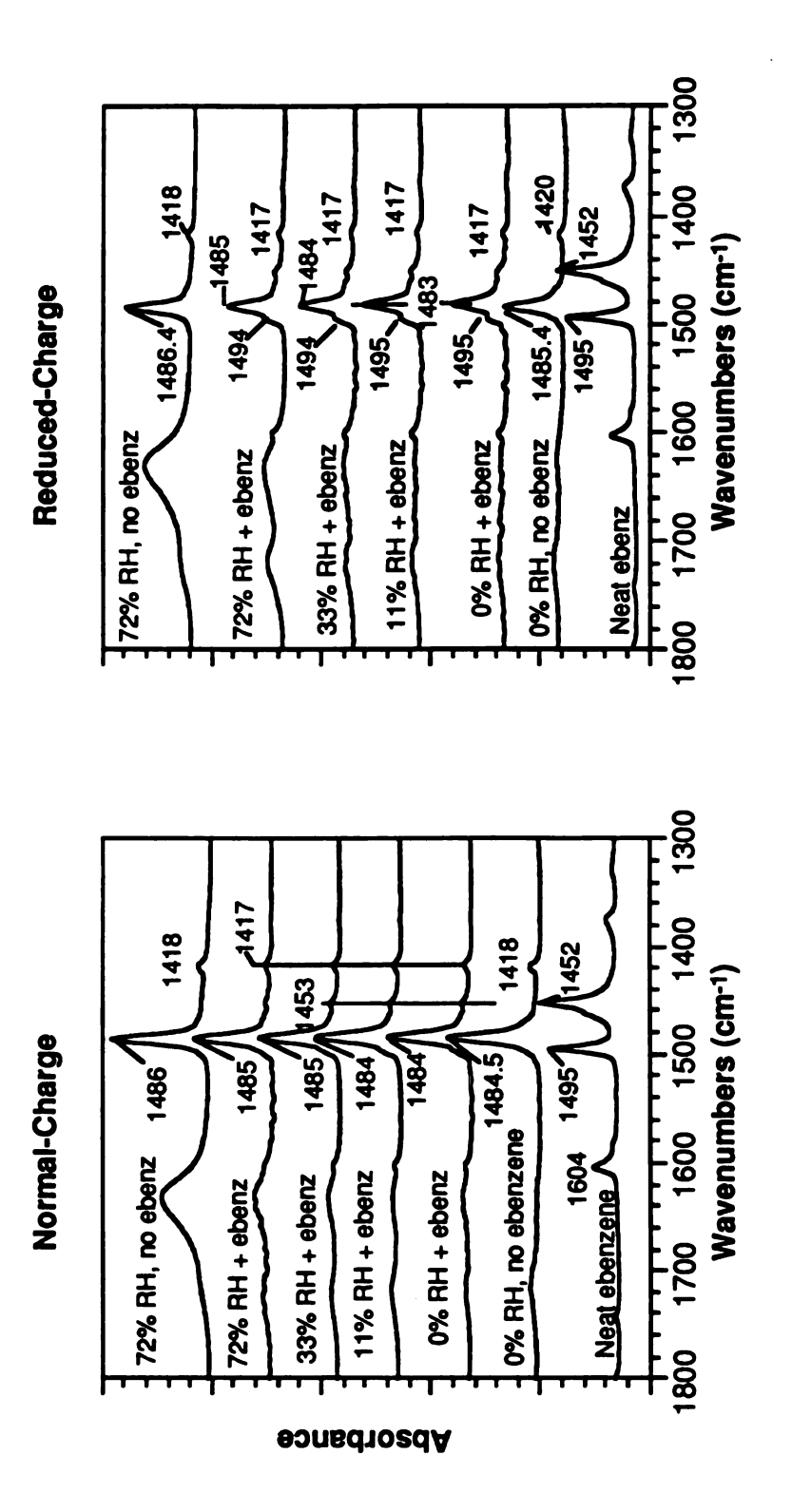


Figure 4-4. Effect of mixed ethylbenzene-water sorption on the infrared spectrum of normal-charge (left) and reduced-charge (right) TMA-saturated clay. The clay spectra are drawn at the same scale, but stacked for comparison. Band assignments for TMA are given in Table 3 and ethylbenzene in Table 4. Peak positions were estimated from peak maxima.

due to sorbed ethylbenzene (Table 4-4) at 1495 cm⁻¹ and 1452 cm⁻¹ were very small, and the TMA methyl asymmetric deformation vibration can be distinguished clearly. With ethylbenzene sorption, the peak maximum of the methyl asymmetric deformation vibration of TMA (~1485 cm⁻¹) shifted from 1484.5 to 1484 cm⁻¹ on the normal-charge clay and from 1485.4 to 1483 cm⁻¹ on the reduced-charge clay. Peak maxima were used to determine the position of the TMA methyl asymmetric deformation vibration because the ethylbenzene shoulder at ~1495 cm⁻¹ skewed the calculation of the peak center-of-mass. The TMA methyl symmetric vibration also shifted to lower frequency due to ethylbenzene sorption. The shifts in the methyl vibrations of TMA on normal- and reduced-charge montmorillonite suggest that ethylbenzene interacts with TMA adsorbed on these clays.

Summary for arene sorption on dry TMA-clay

Shifts in the methyl asymmetric and symmetric deformation vibrations of TMA-montmorillonite due to benzene-d₆ and ethylbenzene sorption strongly suggest that these arenes sorb on cation sites of dry TMA-saturated clay. Differences in the TMA peak shifts of dry TMA-saturated clays due to arene size and clay charge density will be discussed in a later section.

Arene-water competition on hydrated TMA-montmorillonite

Benzene-d₆ sorption

When benzene-d₆ vapor and water vapor competed for sorption sites at 43% and 100% RH, the TMA methyl asymmetric deformation frequencies remained nearly the same as for benzene-d₆ sorption on dry TMA-montmorillonites (Figure 4-3). At 100% RH, visual inspection of the clay films suggested that water containing benzene-d₆ had condensed on the clay, yet the TMA methyl asymmetric deformation vibration remained at 1482 cm⁻¹, characteristic of benzene-TMA interaction. In contrast, when water sorbed on

normal- and reduced-charge TMA-clay at 43% RH in the absence of benzene, the methyl asymmetric deformation vibration was at \approx 1486 cm⁻¹ (Figure 4-3). Thus, there was no evidence that water prevented benzene-TMA interaction, or that water interacted with TMA ions in the presence of benzene. The same result was obtained whether the clay was first equilibrated with water vapor only, then exposed to the benzene-d₆-water vapor commbination, or by equilibrating with benzene-d₆ first, follwed by the combination. This suggested that benzene-d₆ (and, by inference, benzene) had more affinity for TMA cation sorption sites than water did.

Ethylbenzene sorption

As RH increased from 0% to 72% in the competitive ethylbenzene-water vapor treatments, the TMA methyl asymmetric deformation increased from 1484 to 1485 cm⁻¹ on the normal-charge clay and from 1483 to 1485 cm⁻¹ on the reduced-charge clay (Figure 4-4). When water vapor sorbed on TMA-montmorillonite at 72% RH in the absence of ethylbenzene, the TMA methyl asymmetric deformation vibration was 1486 cm⁻¹. Thus, increases in the methyl asymmetric deformation frequency of adsorbed TMA with increasing relative humidity (Figure 4-4) indicated that water displaced ethylbenzene from TMA sites on both normal- and reduced-charge clays.

Though water vapor sorption apparently drove ethylbenzene from TMA cation sites, there is evidence that water and ethylbenzene also competed for sites other than cations, possibly the siloxane surface. The water O-H deformation band (1630 cm⁻¹) of the 72% RH ethylbenzene-treated clays was less intense in the presence of ethylbenzene than when ethylbenzene was absent (Figure 4-4), indicating that ethylbenzene vapor sorption suppressed water vapor sorption. In the presence of water, which displaced ethylbenzene from cation sites, ethylbenzene may be restricted to sorbing on the siloxane surface of the clay. Ethylbenzene sorbed on the siloxane surface may in turn inhibit water sorption on the siloxane surface, or it may sterically restrict the size of the hydration shell

around the TMA cations on the clay. This would cause the intensity of the O-H bending vibration of the sorbed water to be less intense when water and ethylbenzene sorb competitively.

Summary for arene sorption on hydrated TMA-clay

Water vapor, even at 100% RH, did not cause benzene-d₆ to desorb from TMA cations. In contrast, water vapor was apparently preferred over ethylbenzene on the cations of TMA-montmorillonite. Both benzene-d₆ and ethylbenzene inhibit water sorption on TMA-montmorillonite, as shown by the intensities of the water O-H deformation peak at 1630 cm⁻¹.

Effect of layer charge on arene sorption on TMA-clay

.For dry TMA-montmorillonite, arene sorption caused larger shifts in the methyl asymmetric deformation vibration of TMA on reduced-charge clay than on normal-charge clay. Benzene-d₆ sorption caused a 2.3 cm⁻¹ peak shift to lower frequency on normal-charge clay, but a 3.5 cm⁻¹ shift on reduced-charge clay. Ethylbenzene sorption on TMA-clay caused a 0.5 cm⁻¹ shift to lower frequency on normal-charge clay, but a 2.4 cm⁻¹ downward shift on reduced-charge clay. These larger shifts for the reduced-charge clay may have occurred because the TMA cations on the surface of the reduced-charge clay are further apart than are the TMA cations on normal-charge clay. Close spacing of cations on the surface of the normal-charge clay may sterically restrict the arenes from sorbing on some cation sites, whereas most or all TMA cations may be accessible to arenes on reduced-charge clay. Greater cation-arene interaction on the reduced-charge clay may have caused the larger bandshift.

Effect of size on arene sorption on TMA-clay

The methyl asymmetric deformation vibration of dry TMA-montmorillonite shifted more with benzene-d₆ sorption (Figure 4-3) than with ethylbenzene sorption (Figure 4-4).

Two possible reasons for this behavior are: 1) The ethyl group of ethylbenzene may sterically hinder ethylbenzene diffusion into interlayer regions. Consequently, benzene may sorb on a larger proportion of cation sites on TMA-montmorillonite than ethylbenzene does, causing the greater bandshift for benzene; 2)benzene and ethylbenzene may sorb equally on cation sites, but benzene-d₆ may perturb the methyl asymmetric deformation vibration of TMA more than ethylbenzene does because the two arenes may interact with TMA by different mechanisms.

Both close cation spacing (i.e., high surface charge density) and increases in relative humidity apparently inhibit sorption of ethylbenzene more than benzene-d₆. First, as mentioned in the previous section, larger frequency shifts for reduced-charge than normal-charge clay due to arene sorption suggest that arenes interact with a larger proportion of TMA cations in the reduced-charge clay. This effect was much greater for ethylbenzene than benzene-d₆ (Figures 3 and 4); the methyl asymmetric bandshift for ethylbenzene sorption on dry, reduced-charge clay was nearly five times greater than that measured on normal-charge montmorillonite. Second, water displaces ethylbenzene, but not the smaller benzene-d₆, from TMA cation sites. Thus, both higher clay charge density and water sorption decrease sorption of larger arenes on TMA cation sites more than sorption of smaller arenes.

TMPA-montmorillonite

Arene sorption on dry TMPA-clay

Benzene sorption

Infrared band assignments for TMPA are given in Table 4-5. Figure 4-5 shows the effect of benzene sorption on the infrared spectrum of TMPA-saturated normal- and reduced-charge Wyoming montmorillonite at 0% RH. Peak locations were determined from peak maxima. The methyl asymmetric deformation vibration of TMPA shifts from

Table 4-5. Infrared band assignments for the v_{19a} and v_{19b} C-C ring stretch of methyldeuterated (d₉) TMPA iodide and for the v_{19a} , v_{19b} , and methyl vibrations for TMPA-Br in 1)KBr using diffuse reflectance (DRIFT) and 2)in methanol using attenuated total reflectance (ATR).

	v19a C-C	v19b C-C	Methyl Asym	Methyl Symm	other
	ring stretch	ring stretch	deformation	deformation	Methyl
TMPA-I d ₉ ¹	1496	1459			
TMPA-Br (DRIFT)	1500	1461	1475, 1481	1416	1451
TMPA-Br (methano	1) 1498	1464	1475	1411	

¹ Chapter 2

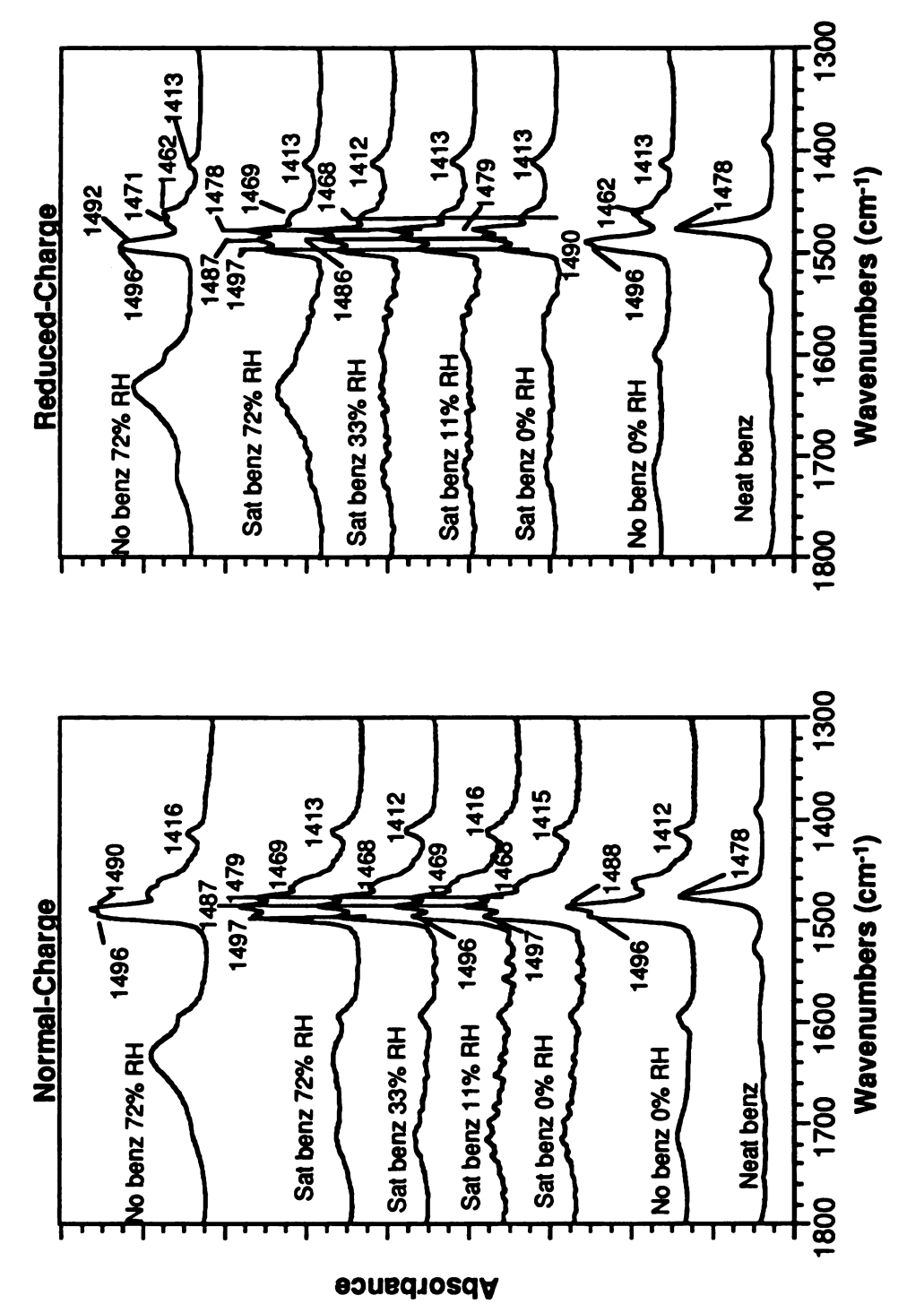
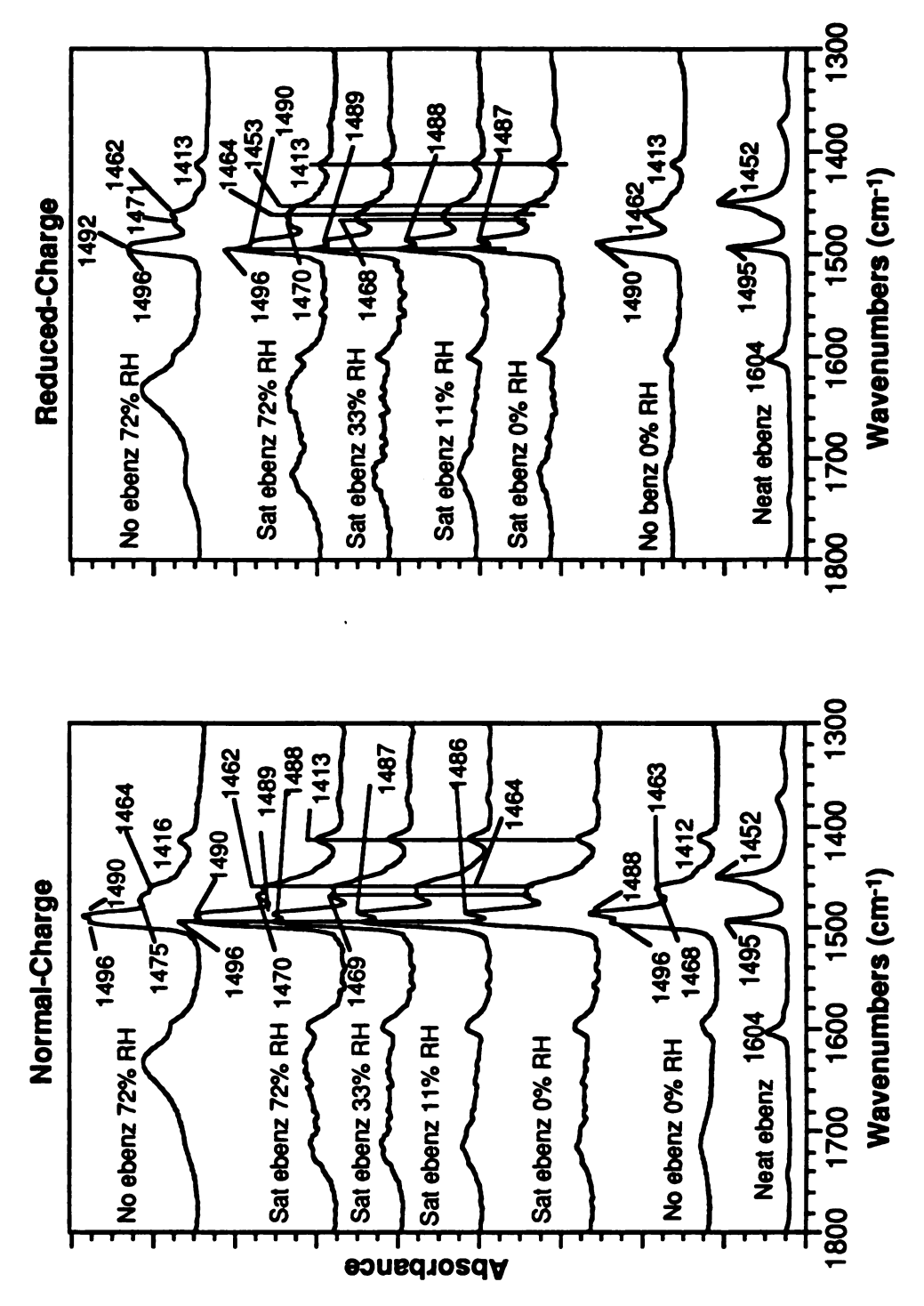


Figure 4-5. Effect of mixed benzene-water sorption on the infrared spectrum of normal-charge (left) and reduced-charge (right) TMPA-saturated clay. The clay spectra are drawn to the same scale, but stacked for comparison. Band assignments for TMPA are given in Table 4 and benzene in Table 4. Peak positions were estimated from peak maxima.

1475 cm⁻¹ for the bromide salt to \approx 1488 cm⁻¹ when sorbed on TMPA (Chapter 2). Benzene sorption caused the methyl symmetric (\approx 1412 cm⁻¹) to shift to 1415 cm⁻¹ on normal-charge clay while no shift was observed on reduced-charge clay. On normal-charge TMPA-montmorillonite, the v_{19a} ring stretch shifted 1 cm⁻¹ to higher frequency, whereas the methyl asymmetric deformation vibration decreased in frequency by 1 cm⁻¹. On reduced-charge clay, benzene sorption caused the v_{19a} to increase approximately 1 cm⁻¹, whereas the methyl asymmetric deformation vibration decreased 3 cm⁻¹. The shifts in both the v_{19a} ring stretch and the methyl asymmetric deformation vibration of TMPA saturating normal- and reduced-charge clay indicated that benzene interacted with cation sites of these clays, at both the aromatic ring and the methyl groups.

Ethylbenzene sorption

Figure 4-6 shows the effect of ethylbenzene sorption on the infrared spectrum of TMPA-saturated normal- and reduced-charge Wyoming montmorillonite at 0% RH. Ethylbenzene sorption caused the methyl symmetric deformation vibration of TMPA on normal-charge clay to shift up 1 cm-1, while no shft occurred on the reduced-charge clay. The TMPA v_{19a} ring stretch cannot be distinguished from the v_{19a} of ethylbenzene (1495 cm⁻¹), so the bandshift of the cation v_{19a} cannot be determined. Clear shifts could be observed in the methyl asymmetric deformation band of adsorbed TMPA. On normal-charge clay, the methyl asymmetric deformation shifted down 2 cm⁻¹, while on reduced-charge clay, the peak shifted down 3 cm⁻¹. The shifts in the methyl asymmetric deformation of TMPA saturating normal- and reduced-charge montmorillonite indicated that ethylbenzene interacted with cation sites of these clays at the methyl groups. Ring interactions were not observable.



and reduced-charge (right) TMPA-saturated clay. The clay spectra are drawn to the same scale, but stacked for comparison. Band assignments for ethylbenzene are given in Table 4 and TMPA in Table 5. Peak Figure 4-6. Effect of mixed ethylbenzene-water sorption on the infrared spectrum of normal-charge (left) locations estimated from peak maxima.

Summary for arene sorption on dry TMPA-clay

Shifts in the methyl asymmetric deformation band of TMPA-montmorillonite due to benzene and ethylbenzene sorption strongly suggest that these arenes interact with the methyl groups of TMPA on dry TMPA-saturated montmorillonite. Shifts in the v_{19a} of TMPA with benzene sorption suggest that ring interactions, possibly by π - π interactions are possible as well.

Arene-water competition on hydrated TMPA-montmorillonite

Benzene sorption

When benzene and water sorbed competitively on the normal-charge clay at relative humidities up to 72%, the methyl asymmetric deformation band stayed at 1487 cm⁻¹, the frequency characteristic of benzene sorption in the absence of water (*i.e.* noncompetitive benzene sorption). When benzene and water sorbed competitively on the reduced-charge clay at relative humidities up to 33%, the methyl asymmetric deformation band stayed at the frequency characteristic of noncompetitive benzene sorption (1486 cm⁻¹), but increased to 1487 cm⁻¹ as RH was increased to 72%. The 1 cm⁻¹ upward shift in the methyl asymmetric deformation of TMPA on the reduced-charge clay suggested that some competition occured between water and benzene with the higher relative humidity treatments, but not enough to cause the band to shift to the characteristic frequency of noncompetitive water sorption (1492 cm⁻¹). Therefore, water didn't displace all of the benzene that interacted with adsorbed TMPA.

The O-H bending frequencies of sorbed water at 72% RH on normal- and reduced-charge TMPA-clays (1630 cm⁻¹) were more intense in the absence of benzene than when benzene was present (Figure 4-5), which indicated that benzene sorption inhibited water

sorption. The shifts in the TMPA methyl asymmetric deformation band clearly showed that benzene inhibited water sorption on TMPA cations. In addition, benzene sorption on both the TMPA ions and on the uncharged siloxane surface of TMPA-montmorillonite may have inhibited water sorption on the siloxane surface and restricted the size of the hydration shell around those cations from which water was able to displace benzene.

Ethylbenzene sorption

When ethylbenzene and water competed for sorption sites on TMPA-montmorillonite at relative humidities up to 72%, the methyl asymmetric deformation increased from 1486 or 1487 cm⁻¹ (normal- and reduced-charge, respectively) to 1490 cm⁻¹, close to the frequency observed when water sorbed in the absence of ethylbenzene (Figure 4-6). This result suggested that water displaced ethylbenzene from TMPA sites.

The lower intensity of the sorbed water O-H deformation vibration (1630 cm⁻¹) of ethylbenzene-water treated clays compared to water-only treated clays (Figure 4-6) indicated that less water sorption occured when the two solutes competed, even at 72% RH when ethylbenzene had been driven from the cation sites. A possible mechanism for this decrease in water sorption is that ethylbenzene sorbed on siloxane surface sites inhibited water sorption on the siloxane surface and may also have restricted the size of the hydration shell around TMPA cations.

Summary for arene sorption on hydrated TMPA-clay

Water vapor was apparently preferred over ethylbenzene on the cations of TMPAmontmorillonite. Water vapor was <u>not</u> preferred over benzene on these sites, however.

Effect of layer charge on arene sorption on TMPA-clay

When arenes sorbed on dry TMPA-montmorillonite, larger shifts in the methyl asymmetric deformation vibration of TMPA were observed for reduced-charge than normal-charge TMPA-clay. Benzene sorption caused a 1 cm⁻¹ peak shift to lower

frequency on normal-charge clay, but a 3 cm⁻¹ downward shift on reduced-charge clay. Ethylbenzene sorption caused a 2 cm⁻¹ peak shift on normal-charge clay, but a 3 cm⁻¹ downward shift on reduced-charge clay. Thus, the effect of charge reduction on cationarene interaction for TMPA-montmorillonite was similar to the effect for TMA-montmorillonite, and the explanation proposed above for the greater cation-arene interaction in reduced-charge TMA-clay should be equally valid for the TMPA-montmorillonites.

Effect of solute size on arene sorption on TMPA-clay

There was no evidence that arene size affected arenes sorption on cation sites on dry TMPA-clay. Benzene (Figure 4-5) and ethylbenzene (Figure 4-6) caused identical shifts in the methyl asymmetric deformation vibration on dry, reduced-charge TMPA-montmorillonite. On normal-charge TMPA-montmorillonite, ethylbenzene caused a 1 cm⁻¹ greater band shift than did benzene. This latter result might suggest that less benzene than ethylbenzene sorbed on TMPA sites, but this does not make sense sterically. It is more likely that incomplete purging of water vapor from the spectrometer before the benzene sorption spectra at 0% RH were collected may have caused the methyl asymmetric deformation peak to apparently shift from 1486 cm⁻¹ (its position with all other arene, 0% RH TMPA-clay samples) to 1487 cm⁻¹, the position observed for benzene sorption on reduced-charge TMPA-clay.

As was discussed above for TMA-montmorillonite, increased relative humidity appeared to inhibit ethylbenzene sorption more than benzene sorption on cation sites. Shifts in the TMPA methyl asymmetric deformation showed that water drove ethylbenzene from TMPA cation sites, but not smaller benzene molecules. In contrast to the data reported for TMA-montmorillonite, however, there was no clear evidence that higher surface-charge density (*i.e.* tighter cation spacing) caused a greater decrease in cationarene interaction with ethylbenzene than with benzene.

DISCUSSION

Spectroscopic data presented here showed that arene sorption from the vapor phase occurs on cation sites on dry TMA- and TMPA-saturated clays. This conclusion appears to conflict with previous experiments (Jaynes and Boyd, 1991) showing that in the presence of water, benzene and other arenes sorb primarily on uncharged siloxane surfaces, not on cation sites of TMPA-saturated smectites. The spectroscopic data reported here, do not rule out the siloxane surface as an important site of arene sorption, particularly in the presence of water because this spectroscopic study was not designed to directly evaluate this type of sorption. Clay films prepared for this study were too thick to observe the Si-O bands of the clay, which might be perturbed by arene sorption. Furthermore, the water:arene ratio was much higher in the work reported by Jaynes and Boyd (1991) than in the present study. Since the preferred site of water sorption on these clays is on cation sites (Chapter 3), it is probable that the large excess of water during aqueous-phase arene sorption experiments (Jaynes and Boyd, 1991) caused complete arene desorption from cation sites and left the siloxane surface as the only remaining site for arene sorption.

Benzene sorption caused greater infrared peak shifts in the methyl asymmetric deformation vibration of TMA on dry normal- and reduced-charge clay than did ethylbenzene sorption, implying that more benzene than ethylbenzene interacted with TMA cations. However, another reason for this difference in peak shift could be that individual benzene molecules perturb the methyl groups of TMA more than do individual ethylbenzene molecules. On dry TMPA-saturated normal- and reduced-charge montmorillonite, benzene and ethylbenzene caused nearly identical shifts in the methyl asymmetric deformation vibration. This result suggests that the same amount of benzene as ethylbenzene may be sorbed on cation sites of dry TMPA-clay.

The band shifts observed for benzene and ethylbenzene sorption on dry, reduced-charge TMA- and TMPA-saturated clays were greater than those for normal-charge clay. This suggested that the proportion of cation sites where arene sorption occurred was greater on the reduced-charge clay than the normal-charge clay. This may be because tighter packing of cations on the surface of the normal-charge clay sterically restricted arenes from sorbing on some cation sites. On reduced-charge clay, proportionally more cation sites may be accessible for arene sorption.

Water sorption drove ethylbenzene, but not benzene from cation sorption sites on both TMA- and TMPA-clay. There are at least two explanations for this behavior. One possibility is that the competitive sorption of arene and water vapor may depend more on absolute vapor pressures (P) than their fraction of saturation vapor pressure (P/P_0). The room temperature saturation vapor pressure of benzene is 100 torr, ethylbenzene is 10 torr, and water is 24 torr (Weast, 1986). Water, with its lower absolute vapor pressure, may not be able to compete with the higher vapor pressure of saturated benzene, though it competed with the lower vapor pressure of saturated ethylbenzene. The second possibility, discussed in the results section, is that the ethyl group of ethylbenzene sterically hindered ethylbenzene from sorbing in the interlayer and interacting with cations, while smaller benzene molecules had greater access to clay interlayers. Under this second possibility, ethylbenzene may be excluded from many sorption sites at which benzene is capable of sorbing, leaving water molecules better able to compete with those ethylbenzene molecules that are able to interact with TMA or TMPA.

The combination of water sorption and high clay charge density probably inhibits cation-arene interaction more for larger arenes, like ethylbenzene, than for smaller arenes like benzene. This is because higher layer charge alone probably reduces overall sorption

regardless of arene size, and water sorption inhibits ethylbenzene sorption more than benzene sorption.

In organoclay waste treatment design applications, for sorption of the pure arene from vapor, it appears from these results that sorption of arenes may be improved by using a lower charge density parent clay, which will allow more space between cations for the arenes to diffuse through. This becomes more important when sorbing arenes with ring substituents. A larger proportion of cations on the clay perturbed by arene sorption suggests that more cation sites are accessible for arene sorption on the lower charge clay. Where more cation sites are accessible for arene sorption on the lower charge clay, it implies there are also more siloxane surface sites available for sorption. When sorbing arenes from aqueous solution, it is likely that cation sites do not function as significant sorption sites because they are hydrated (Chapter 3). Since water drove ethylbenzene from cation sites, it is possible that, with the much higher ratio of water: arene in solution, that benzene could be driven from cation sites in solution. In aqueous systems, it is more likely, the cations function as pillars, holding the clay layers open (Jaynes and Boyd, 1991; Lee et al., 1990) rather than as sorption sites.

REFERENCES

- Boyd, S. A., Jaynes, W. F. and Ross, B. S. (1991) Immobilization of organic contaminants by organo-clays: Application to soil restoration and hazardous waste containment: in *Organic substances and sediments in water*, R.S. Baker, ed., vol. 1. CRC Press, Boca Raton, FL 181-372
- Brindley, G.W and Ertem, G. (1971) Preparation and solvation properties of some variable charge montmorillonites: Clays & Clay Minerals 19, 399-404.
- Duinker, J.C., and Mills, I.M. (1968) Normal coordinates for the planar vibrations of benzene: *Spectrochim. Acta.* 24A, 417-435.
- Green, J.H.S. (1962) Vibrational spectra of benzene derivatives—III. Anisole, ethylbenzene, phenetole methyl phenyl sulphide and ethyl phenyl sulphide: *Spectrochim. Acta.* 18, 39-50.
- Greene-Kelly, R. (1953) The identification of montmorillonoids in clays: J. Soil Sci. 4, 233-237.
- Jaynes, W.J., and Bigham, J.M. (1987) Charge reduction, octahedral charge, and lithium retention in heated, Li-saturated smectites: Clays & Clay Minerals 35, 440-448.
- Jaynes, W.F., and. Boyd, S.A (1990) Trimethyphenylammonium-smectite as an effective adsorbent of water soluble aromatic hydrocarbons: *J. Air and Waste Management*. *Assoc.* 40, 1649-1653.
- Jaynes, W.J., and Boyd, S.A. (1991) Hydrophobicity of siloxane surfaces in smectites as revealed by aromatic hydrocarbon adsorption from water: *Clays & Clay Minerals* 39, 428-436.
- Lee, J.F., Mortland, M.M., Chiou, C.T., Kile, D.E. and Boyd, S.A. (1990) Adsorption of benzene, toluene, and xylene by two tetramethylammonium-smectites having different charge densities: *Clays & Clay Minerals* 38, 113-120.
- Varsányi, G. (1969) Vibrational spectra of benzene derivatives. Academic Press, New York and London. 430 pp.
- Weast, R.C. ed., (1986) CRC handbook of chemistry and physics 67th ed. CRC press, Inc. Boca Raton, Florida. D189-D212.

Appendix A

Supplementary FTIR Dichroism Data

MATERIALS AND METHODS

Clay film preparation

Methyl-deuterated TMPA-d₉ iodide was added to 10 mg of normal- or reduced-charge clay (10 times the CEC) in 10 ml of a 70% methanol-water mixture and stirred for 25 hours. The clay suspension was washed free of excess salts by centrifuging, decanting the supernatant, and re-suspending the clay in deionized water. Centrifugation and decanting was repeated three times. The TMPA-d₉-clays were resuspended in 10 ml methanol and disk-supported clay films prepared as described below below for undeuterated TMPA-clays.

Seventy mg each of normal- and reduced-charge TMPA- clay were resuspended in 10 ml of methanol by sonicating for three 10-min intervals in an ice bath using a Heat Systems sonicator with 2.5-mm microprobe and a setting of 4.5 (out of 10). After the third sonication, coarse material was allowed to settle from the suspensions and 1-ml aliquots of the suspended clay were pipetted onto 13-mm diameter DelrinTM AgCl Disks (E.I. duPont de Nemours®) and allowed to dry. It was necessary to repeat the pipetting several times to obtain a sufficiently thick film, defined as a film for which the clay O-H stretching vibration at 3650 cm⁻¹ was approximately 20% transmittance. The amount of clay on the disks was 0.8 ± 0.15 mg cm⁻². These clay films will be referred to as "disk supported films".

Spectral collection

Clay films saturated with TMPA-d₉ plated on AgCl disks were stored in a desiccator over P₂O₅ at least 24 h before infrared spectra were collected. The films were

removed from the desiccator and quickly placed in a sample holder in an N_2 -purged Nicollet IR/42 FTIR. Transmittance spectra were collected with a DTGS detector using 4-cm⁻¹ resolution, Happ-Genzel apodisation, and 100 scans. Spectra were stored on diskette as ASCII files and imported into the MS-DOS program SpectraCalc (Galactic Software Inc.), then transformed into absorbance units using the spectrum of a clean DelrinTM AgCl disk as the background. Spectra were smoothed using an 11-point Savitsky-Golay procedure. The baselines were leveled along seven selected baseline points in the spectrum, then zeroed. After collecting a spectrum of the clay films normal to the beam, a second spectrum of each treatment was collected with the clay film tilted approximately 30°. The intensities of the v_{19a} (A1 symmetry), and v_{19b} (B1 symmetry) ring-stretching vibrations and the C-H out-of-plane deformation (B2 symmetry) vibration of the phenyl group were compared between the two angles of incidence to determine whether the TMPA phenyl group is either parallel or perpendicular to the siloxane surface in the clay interlayer.

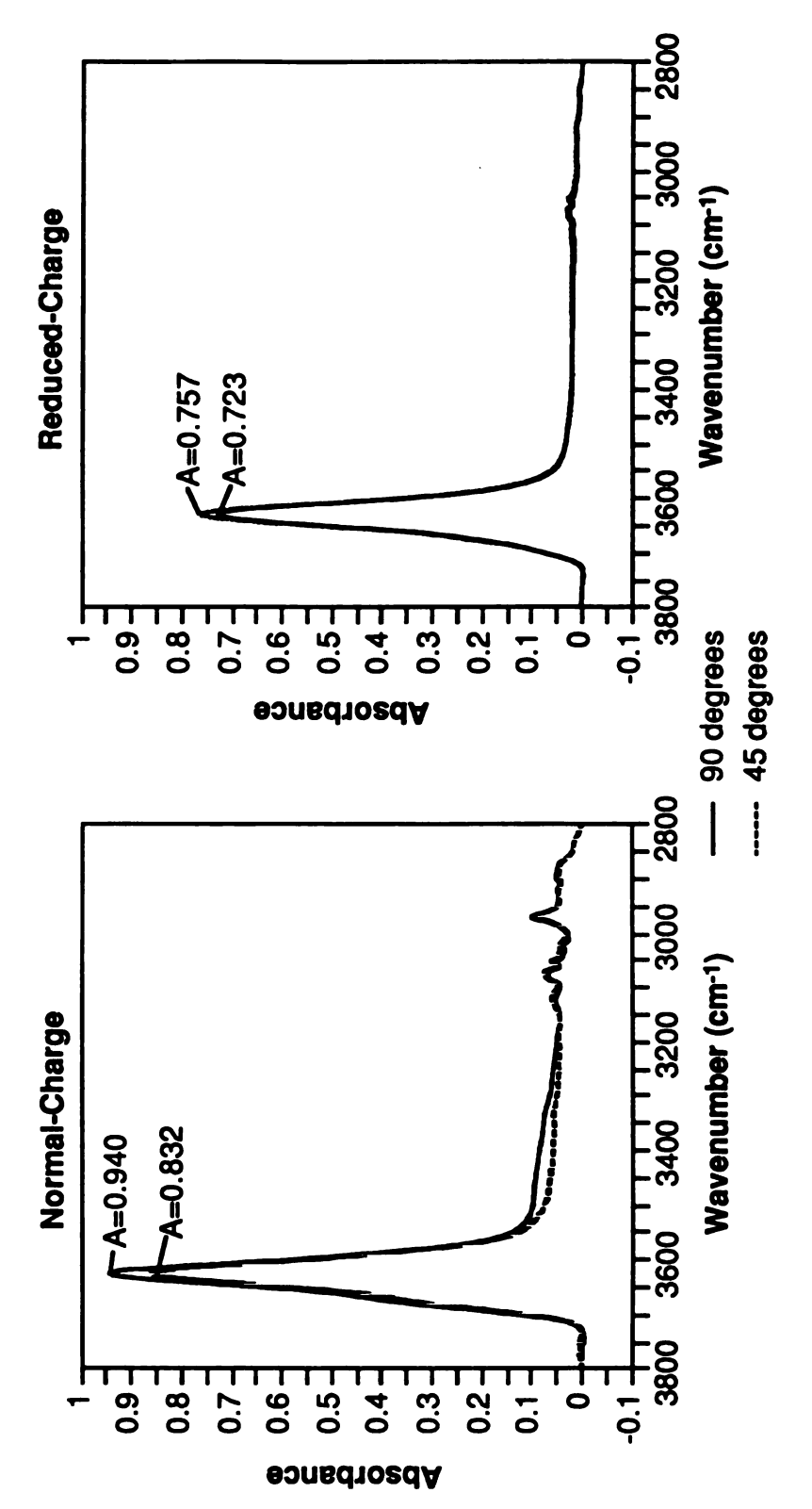
Spectra of disk-supported clay films saturated with undeuterated TMPA were collected on a Perkin-Elmer 1600 FTIR with no apodisation, 2 cm⁻¹ resolution and 50 to 75 scans with the film normal to the beam. Spectra were stored on diskette, imported into SpectraCalc® and analyzed as described above.

X-ray Diffraction

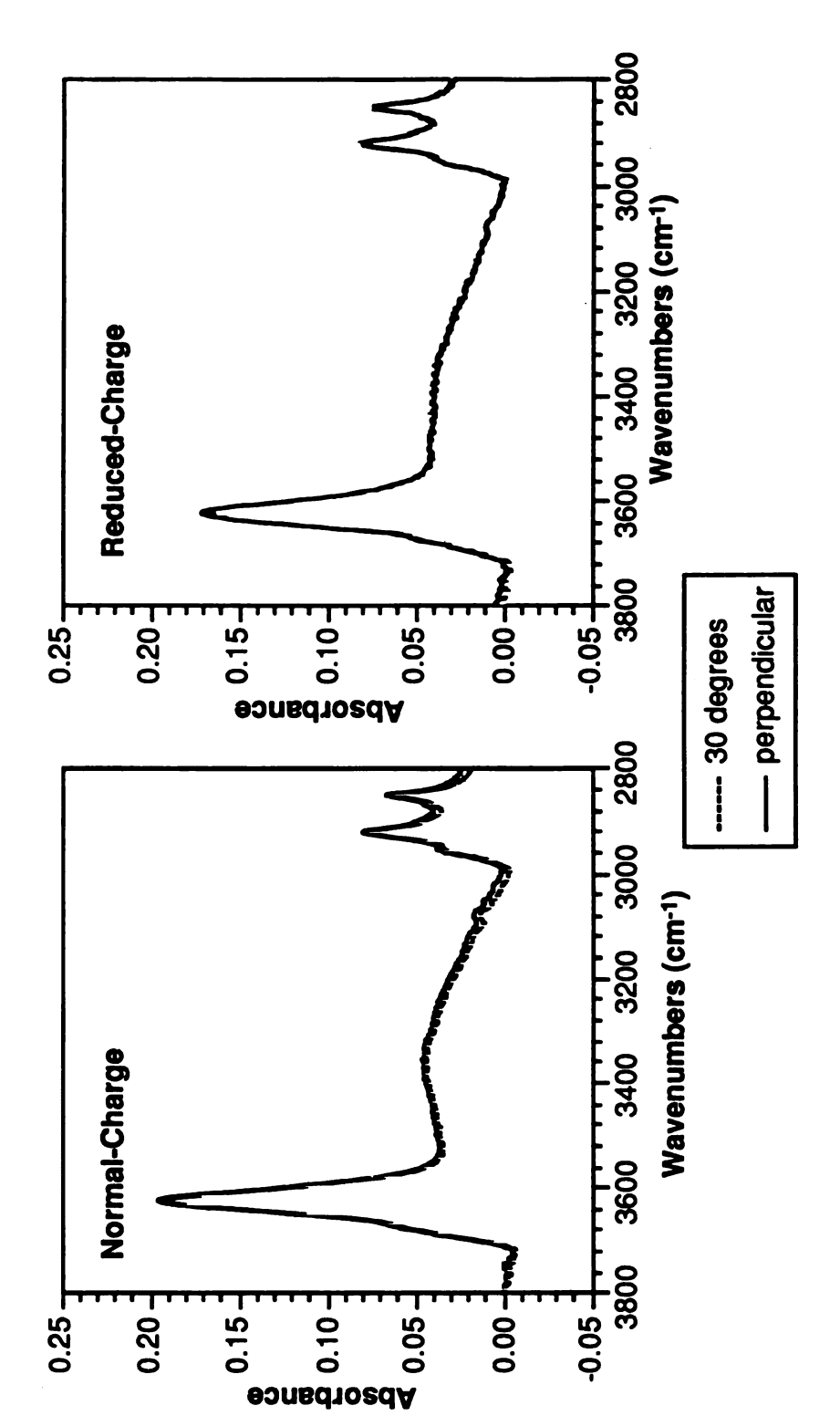
Samples were prepared for X-ray diffraction and data collected as described in Chapter 2.

Appendix A

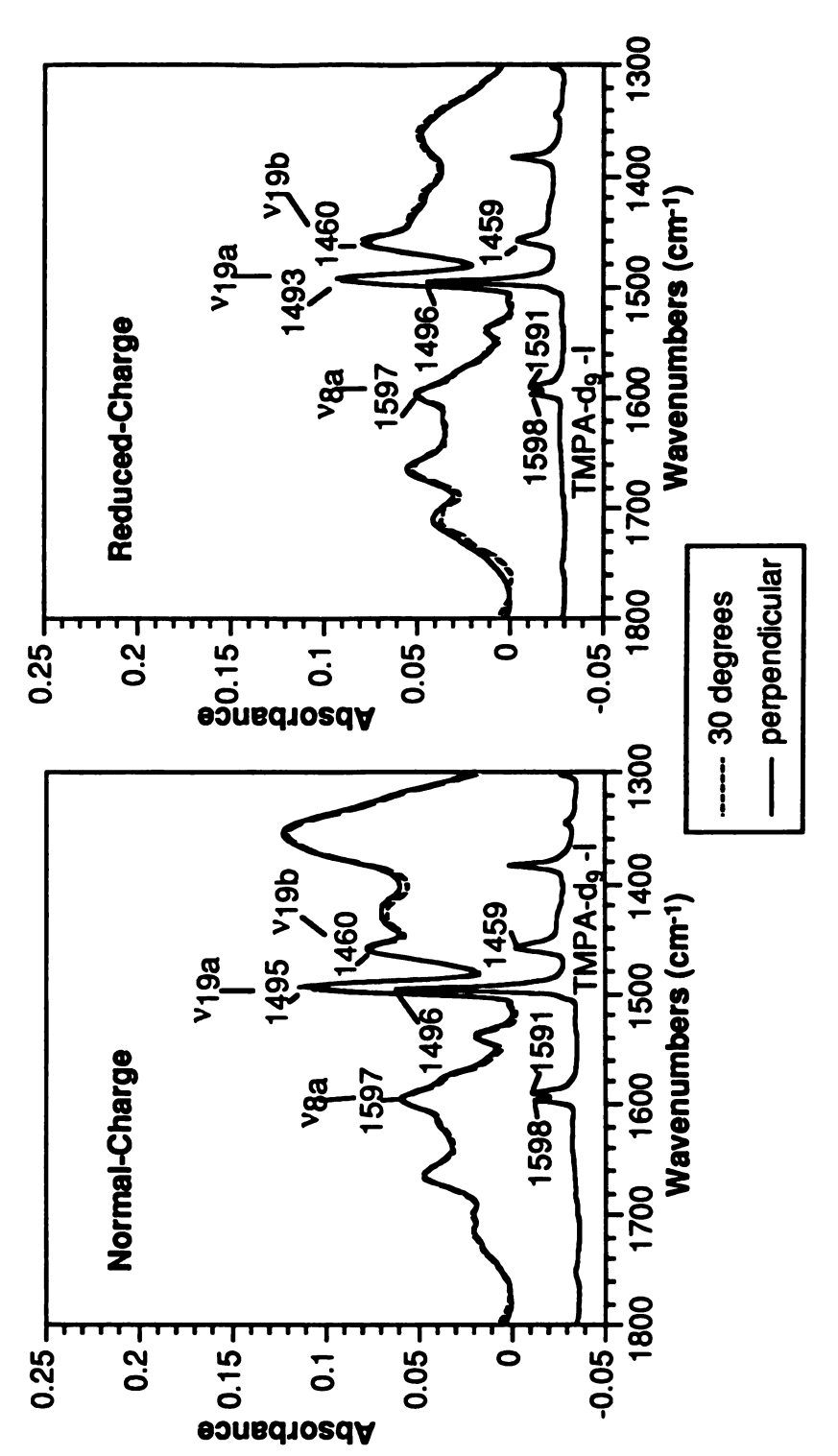
Supplementary FTIR Dichroism and X-Ray Diffraction Data



films oriented at 90° and 45° with respect to the IR beam. Normal-charge clay spectra were normalized to a clay O-H stretch absorbance of 1.000 and the reduced-charge clay spectra were normalized to a clay O-H stretch Figure A1. Clay O-H stretching region of self-supporting normal- and reduced-charge TMPA-d9-saturated clay absorbance of 0.800.



supported on AgCl disks. The overlaid spectra show the films perpendicular to the IR beam and tilted 30° from perpendicular. No normalization factor was applied. Figure A2. O-H stretching region of normal-charge and reduced-charge TMPA-d9 montmorillonite films



disks. The overlaid spectra show the film perpendicular to and tilted 30° from perp. with respect to the spectra) and normal-charge and reduced-charge TMPA-d9-montmorillonite films supported on AgCl Figure A3. C-C ring-stretching region of the TMPA-49-iodide salt in a pressed KBr pellet (bottom

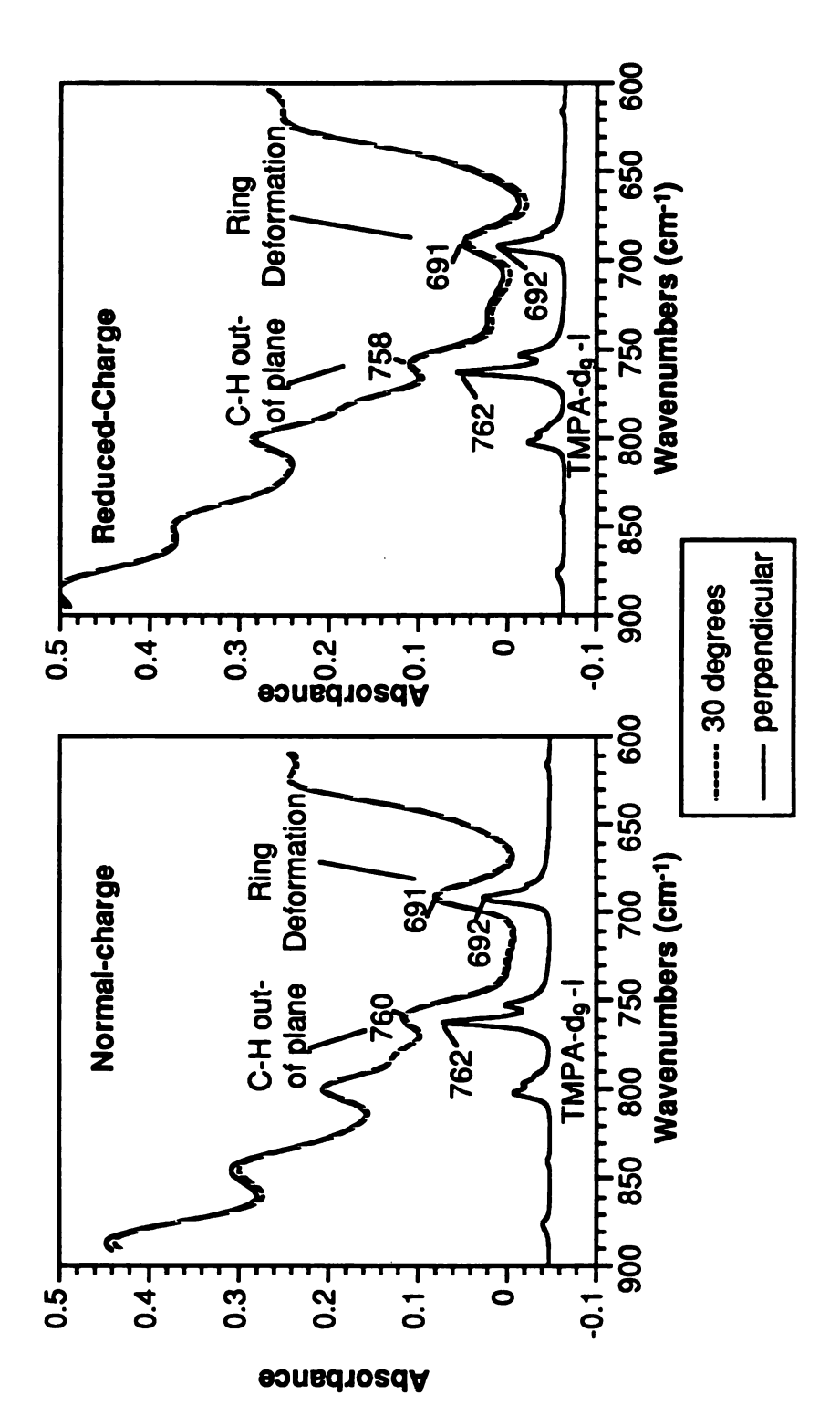


Figure A4. Ring-C-H deformation region of the TMPA-d9 iodide salt in a pressed KBr pellet (bottom spectra) and normal-charge and reduced-charge TMPA-d9-montmorillonite films supported on AgCl disks. The overlaid spectra show the film perpendicular to and tilted 30° from perpendicular. with respect to the IR beam.

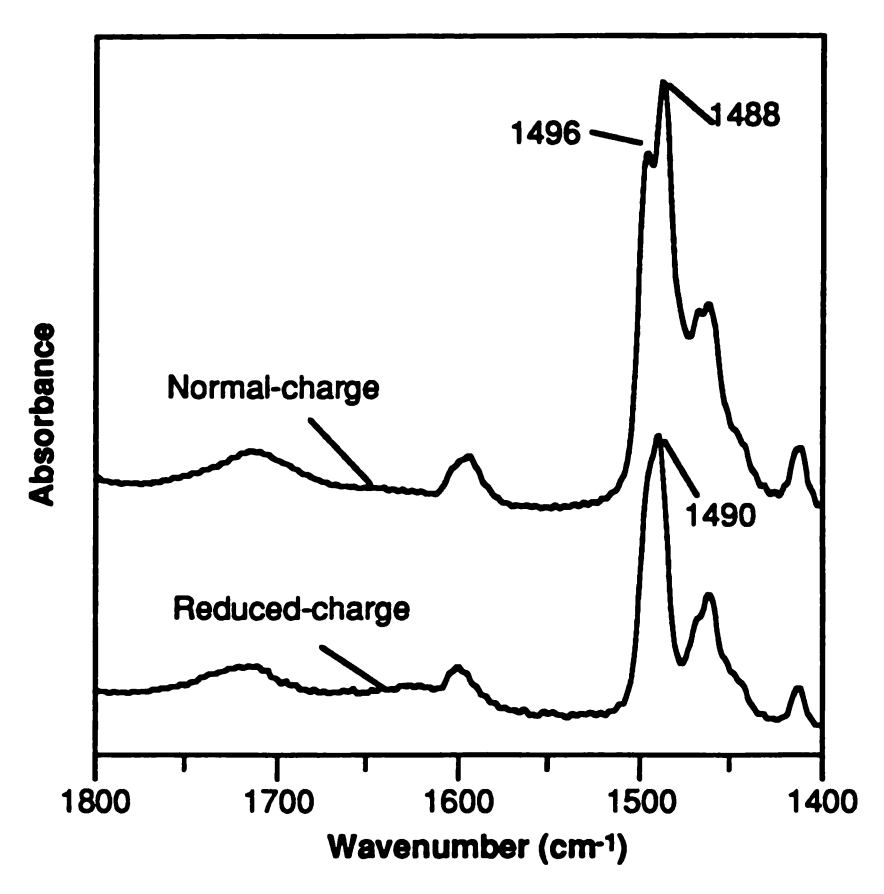


Figure A5. C-C ring stretching region of normal-charge (top) and reduced-charge (bottom) TMPA-montmorillonite films supported on AgCl disks.

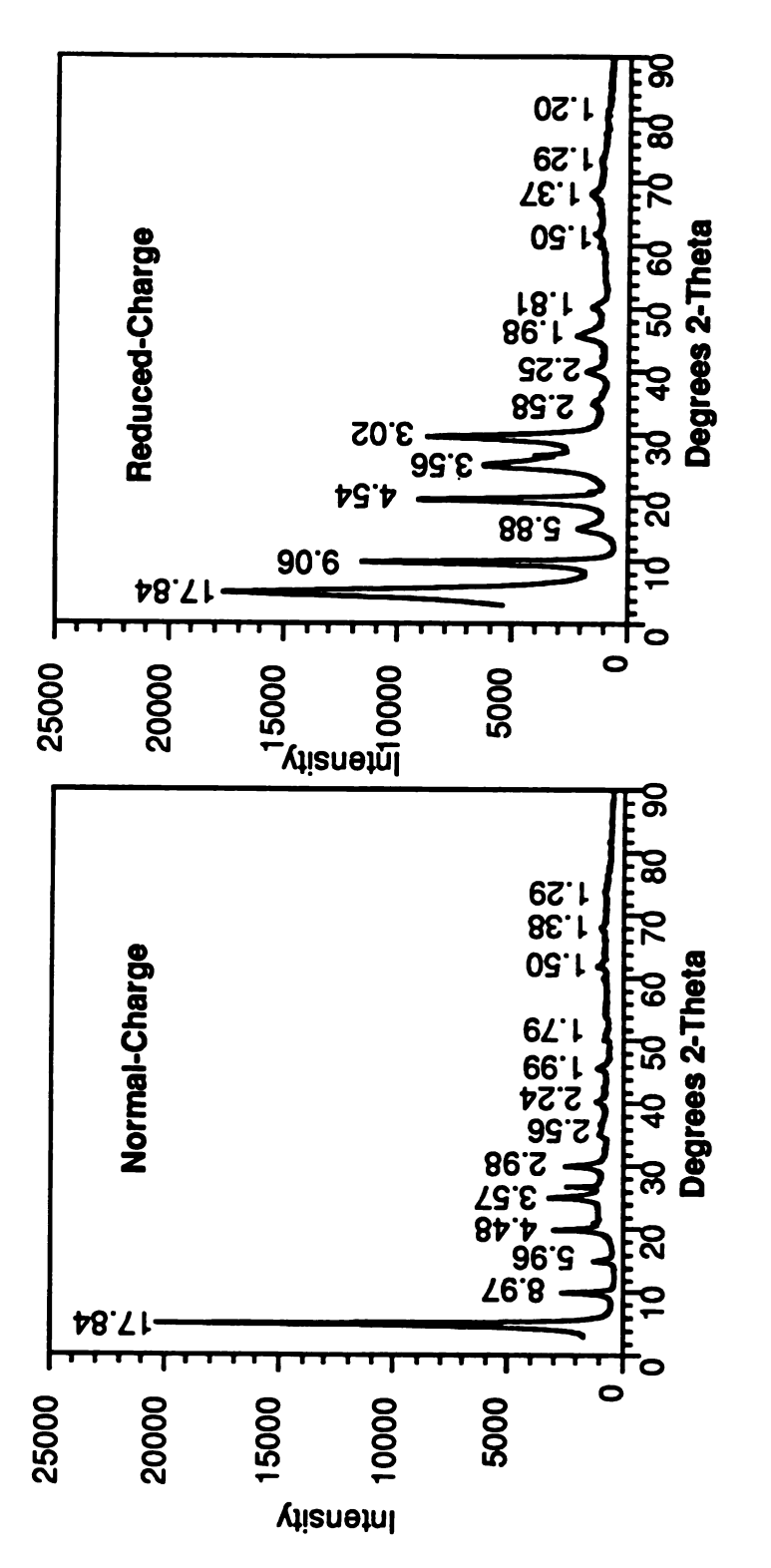


Figure A6. X-ray diffractogrms of glycerol-solvated, Na+-saturated, normal-charge (left) and reduced-charge (right) Wyoming montmorillonite. Inset numbers indicate d(001)-d(0014).

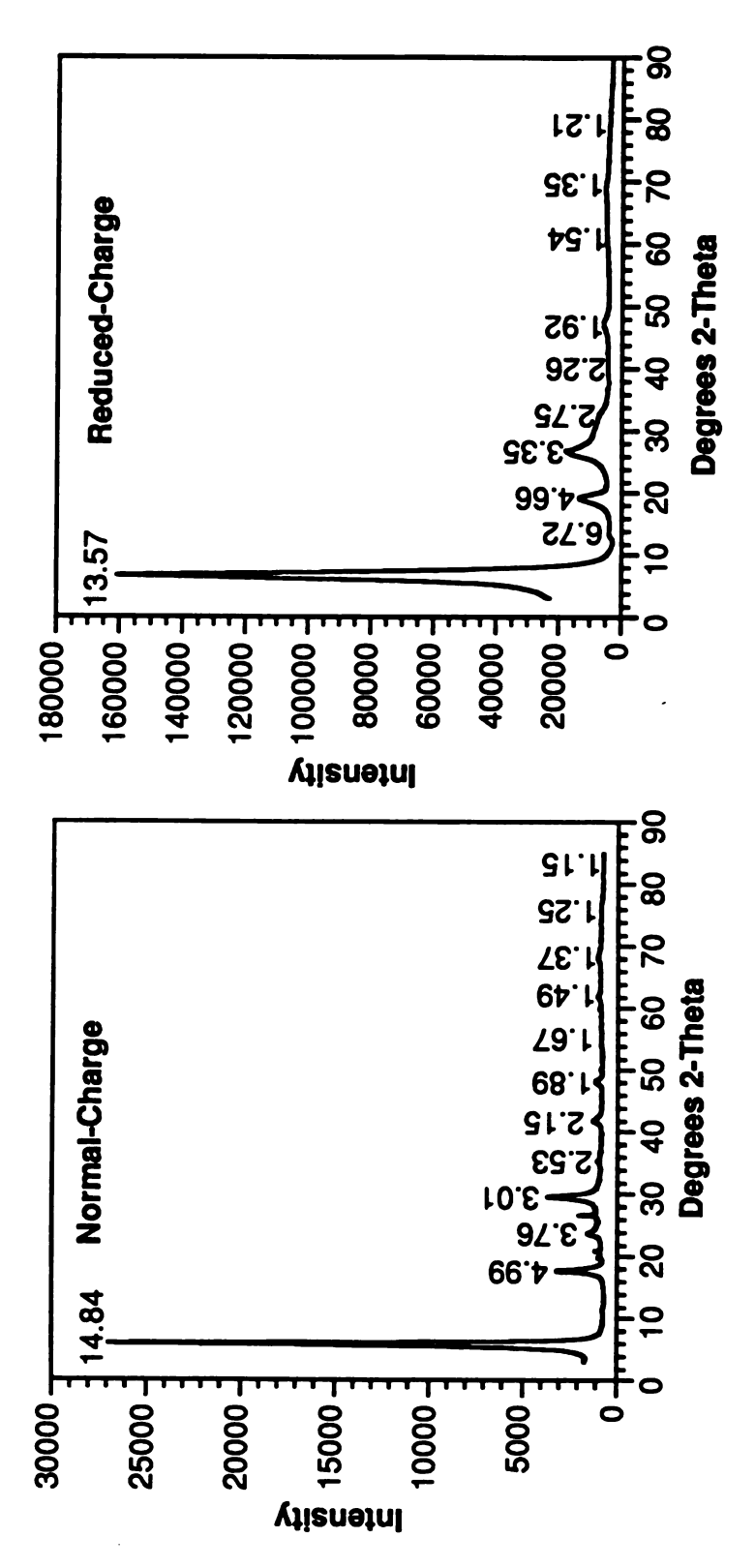


Figure A7. X-ray diffractograms of normal- (left) and reduced- (right) charge TMPA-montmorillonite.

Appendix B

Evaluation of ATR-FTIR for Determination of Benzene Sorption Mechanisms from Methanol on Clays

MATERIALS AND METHODS

Clay preparation

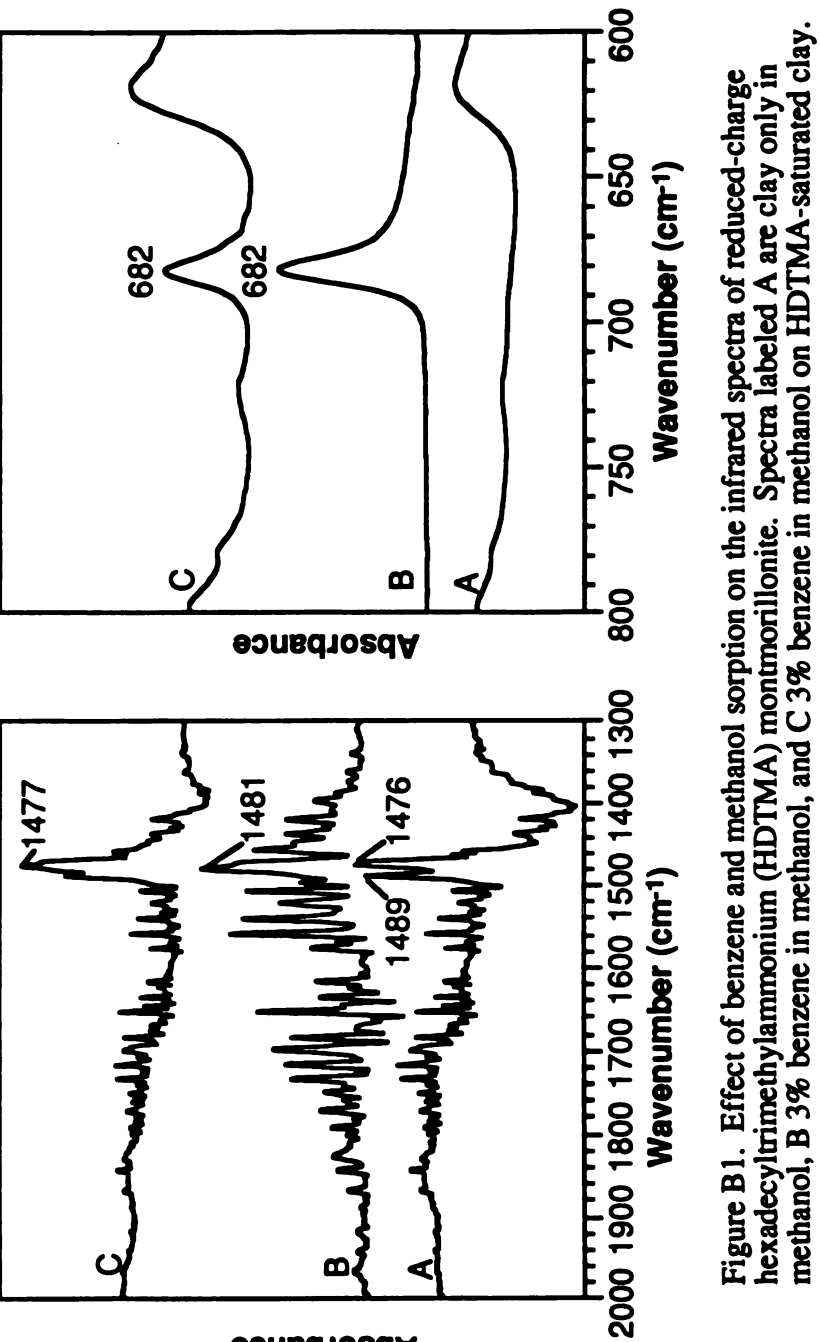
Wyoming montmorillonite (SWy-1) was obtained from the clay minerals repository at the University of Missouri - Columbia. The <2 μm fraction was separated from the coarser material by sedimentation. Half of the <2 μm clay was saturated with Na⁺ and the other half with Li⁺ by repeated saturation with the appropriate chloride salt and centrifugation. Excess salts were removed by dialysis until testing negative for Cl⁻ by the AgNO₃ test. Reduced-charge clay was prepared using a suspension composed of 50% Na⁺ saturated and 50% Li⁺ saturated clay, freeze-drying it and heating 18 hours in quartz crucibles at 250°C. The collapsed, reduced-charge clay was re-expanded by suspending the clay in a 70% methanol-water mixture (10 g l⁻¹) then sonicating 200 ml aliquots for 20 minutes (Green-Kelly, 1953; Brindley and Ertem, 1971; Jaynes and Bigham, 1987). A Heat Systems, Ultrasonic Inc. model #W-385 sonicator with a 7mm diameter probe tip on a setting of 7 (out of 10) was used. Re-expansion was verified by X-ray diffraction and cation exchange capacity measurements.

Organic cation salts were dissolved in methanol and added to the clay in 70% methanol - water suspensions and agitated for 72 hours. Four times the CEC of tetramethylammonium (TMA) chloride, ten times the CEC of trimethylphenylammonium (TMPA) bromide and 1.5 times the CEC of hexadecyltrimethylammonium (HDTMA) chloride were added to aliquots of this suspension. Separate, freeze-dried reduced - charge clay was suspended in 200-250 ml solutions of 0.5 M CsCl or MgCl₂ in 70% methanol and sonicated as above. These were centrifuged and rinsed twice with 0.1M CsCl or MgCl₂. All of the clays were dialized against deionized water until testing negative for halides using AgNO₃ then freeze-dried.

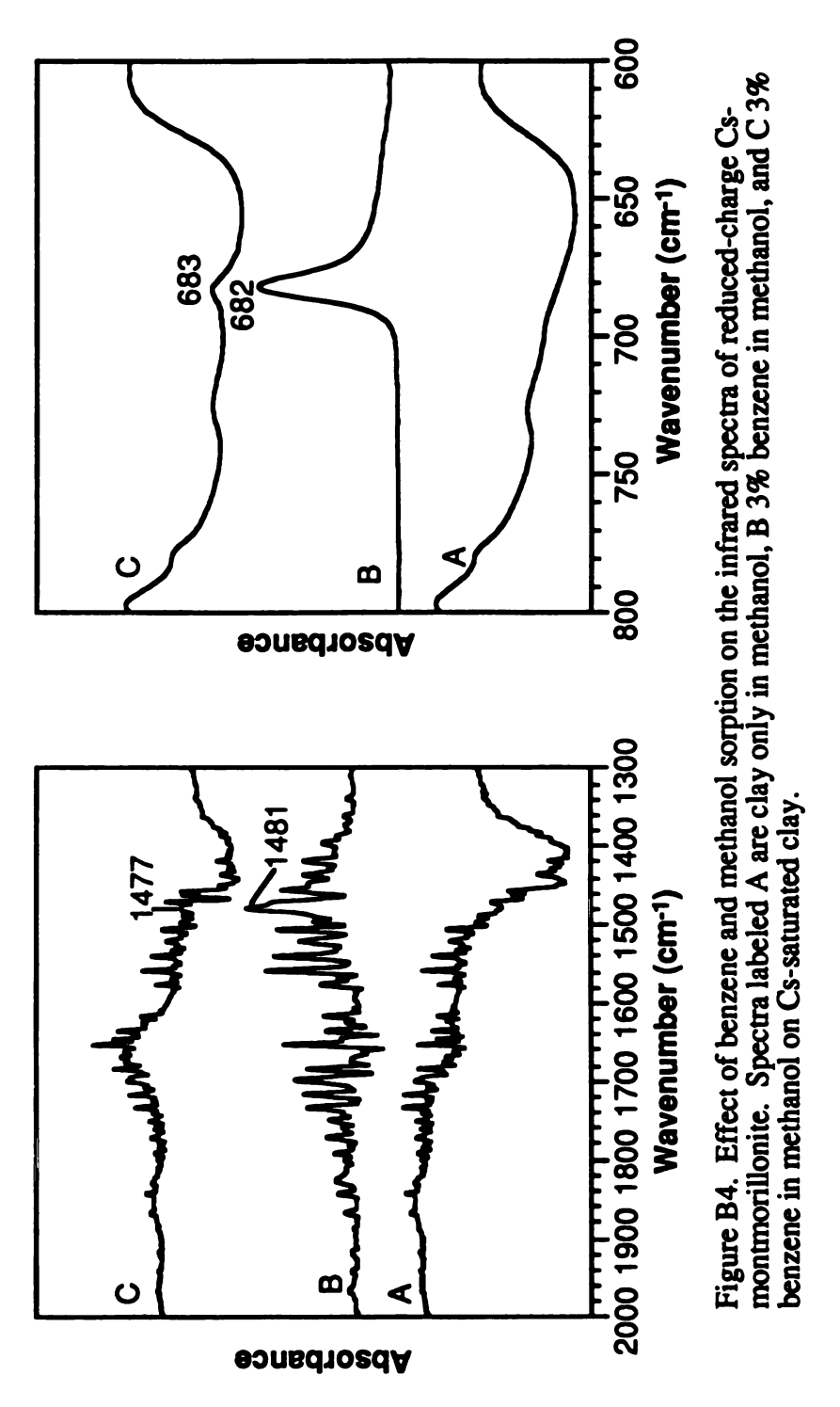
Solute equilibration and infrared spectroscopy

Approximately 50 mg of each clay was measured into 25 ml Corex tubes and shaken overnight in 25 mls of a 3% solution of benzene in methanol. After equilibration, the clay was filtered from the suspension on a 25 mm Whatmann glass fiber filter and placed on the surface of the ZnSe crystal of a Harrick single-reflection ATR cell. The sample compartment was sealed and a portion of the supernant solution was injected into the cell to maintain equilibrium of the clay with the solution. The cell and sample were placed into a Perkin-Elmer 1710 FTIR purged with dry CO₂ - free air with a DTGS detector, 2 cm⁻¹ resolution, no apodisation and 500 scans. Spectral collections were controlled by an IBM XT computer using Spectracalc[®] software and connected through the serial port to the instrument. Single-beam spectra of each solute-solvent-sorbent-complex were collected and ratioed against the single-beam spectrum of the empty cell to obtain transmittance and absorbance spectra of the complex.

The absorbance spectrum of methanol injected into the ATR cell was collected and subtracted from all clay-benzene-methanol spectra in an effort to isolate absorption bands due to the sorbent or the benzene and remove interference due to the solvent. The positions and intensities of these bands were observed and compared to literature values to determine whether interpretations of the sorption mechanism of benzene on the clays could be made.



Absorbance



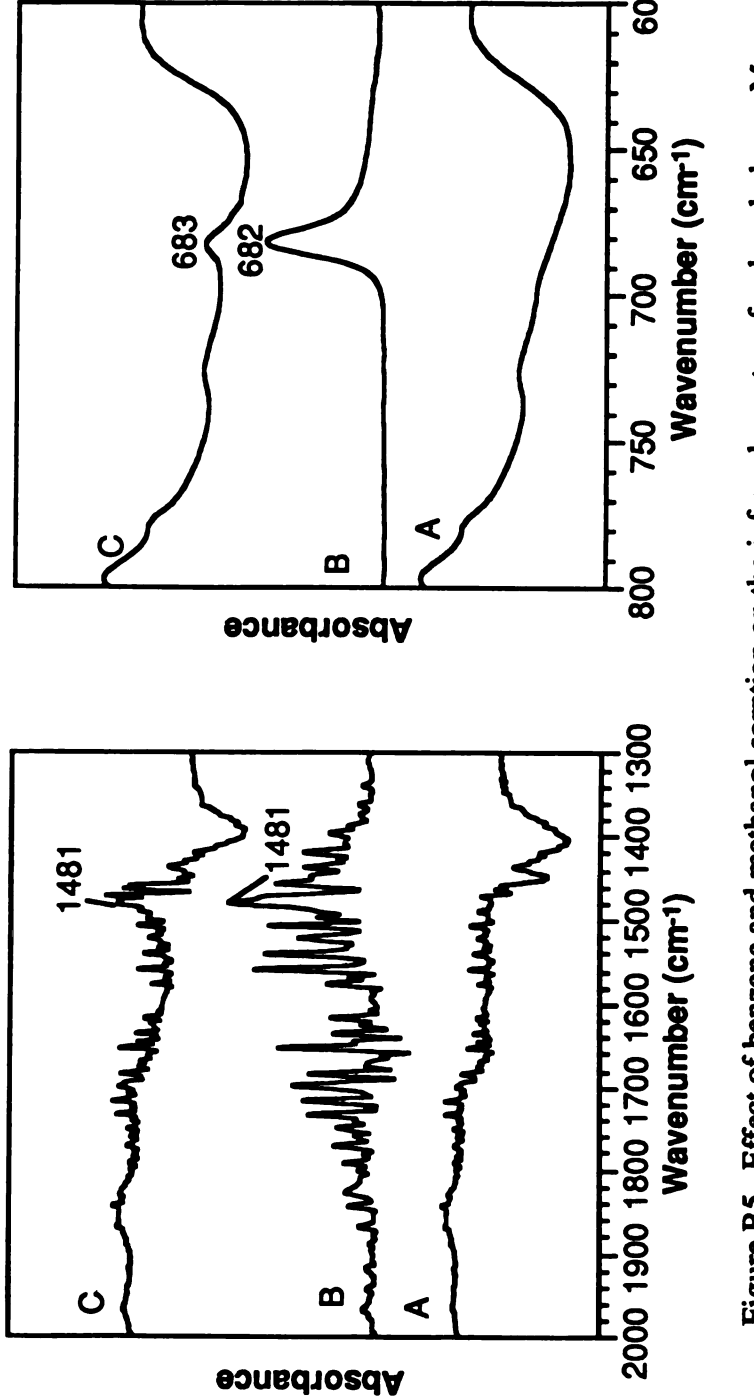
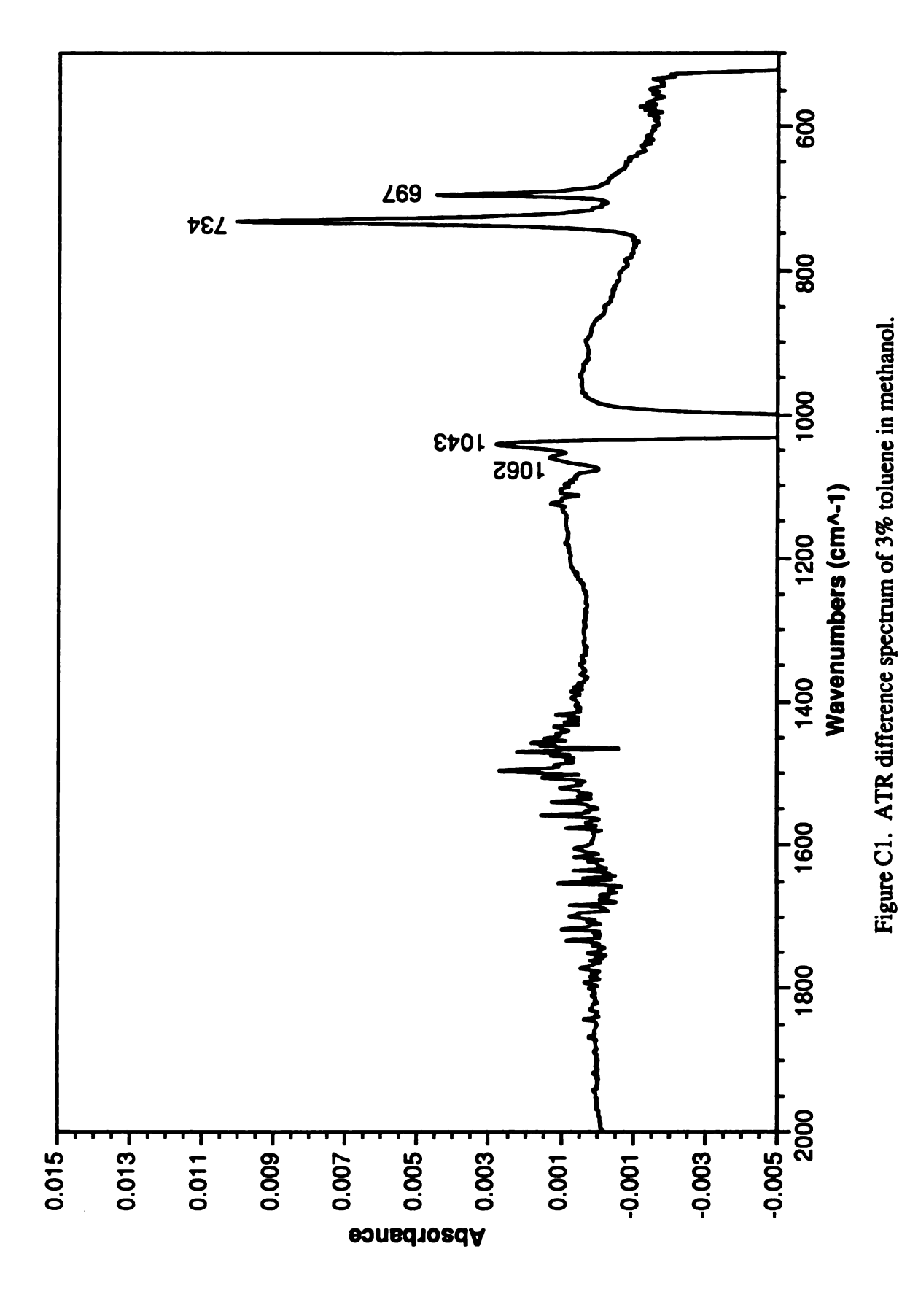
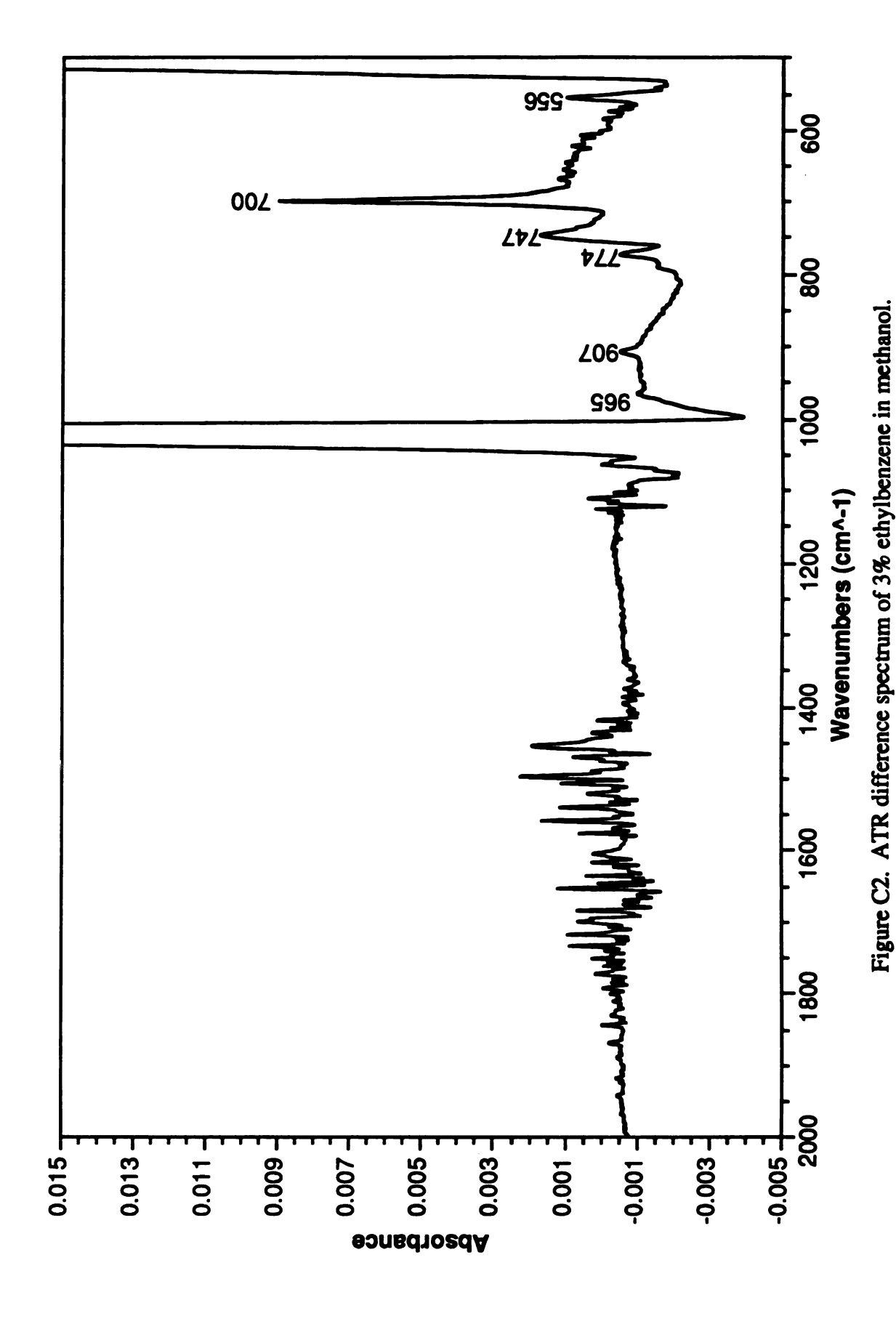


Figure B5. Effect of benzene and methanol sorption on the infrared spectra of reduced-charge Mg-montmorillonite. Spectra labeled A are clay only in methanol, B 3% benzene in methanol, and C 3% benzene in methanol on Mg-saturated clay.

Appendix C

Supplementary ATR-FTIR sorption spectra





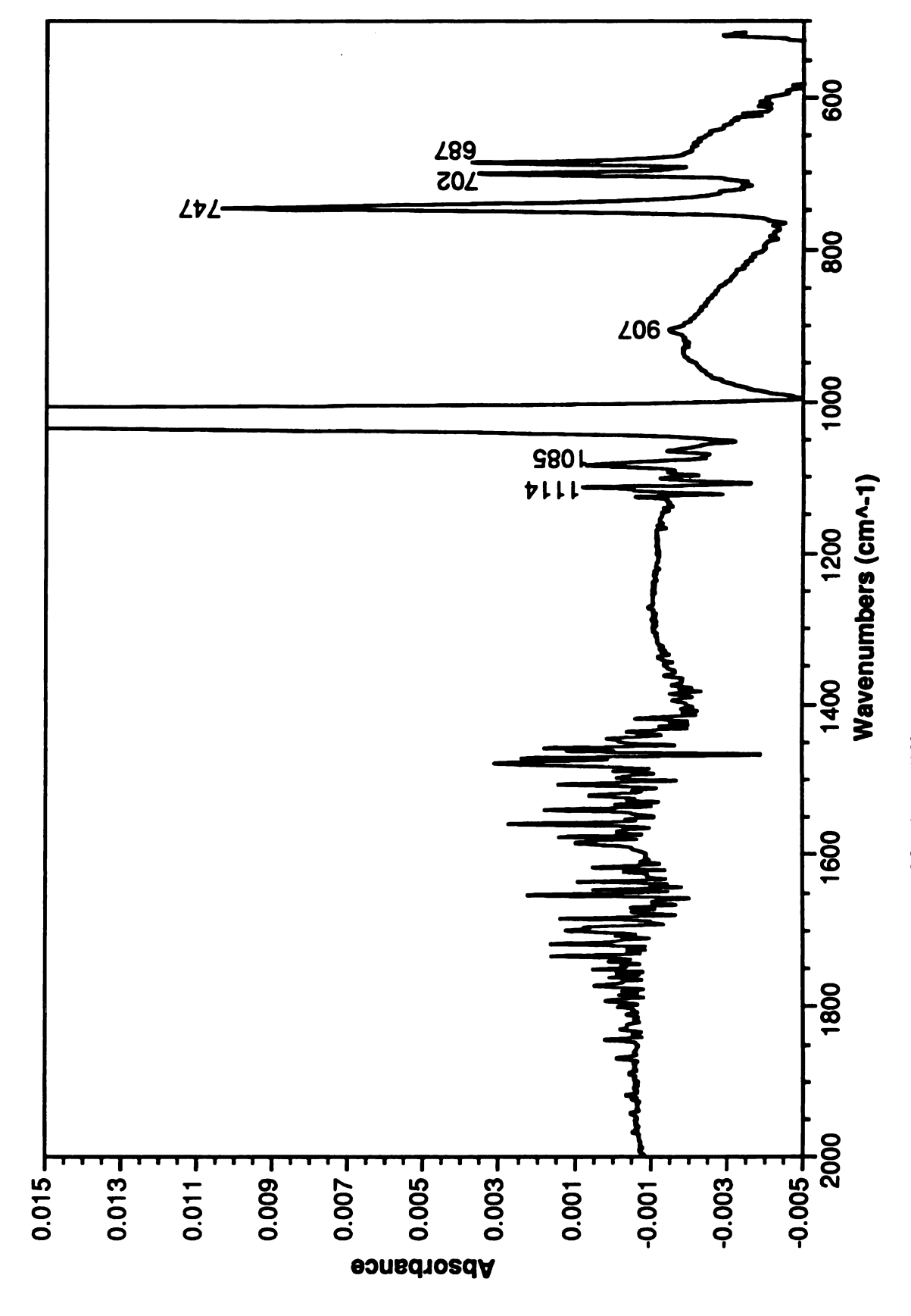
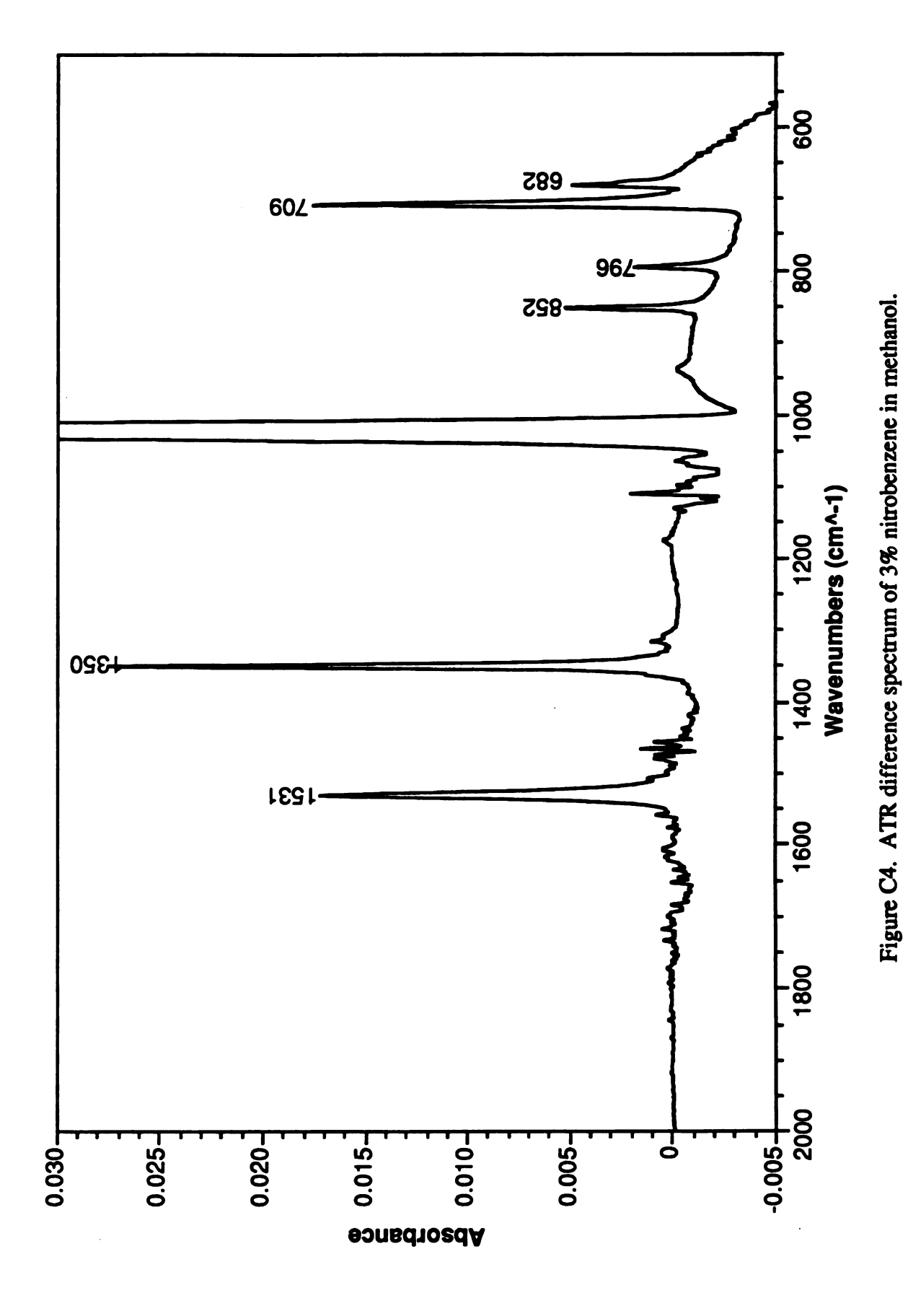
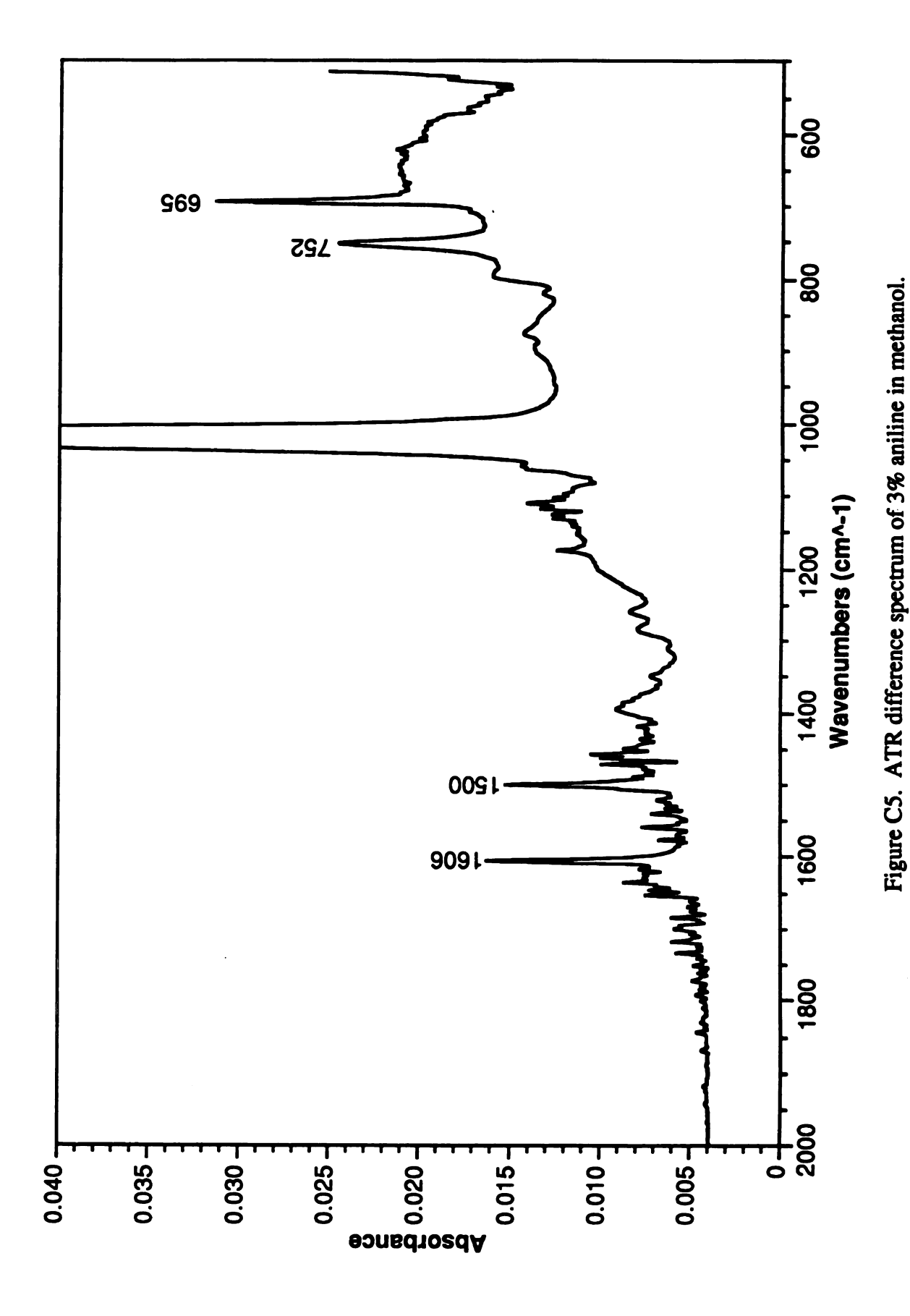
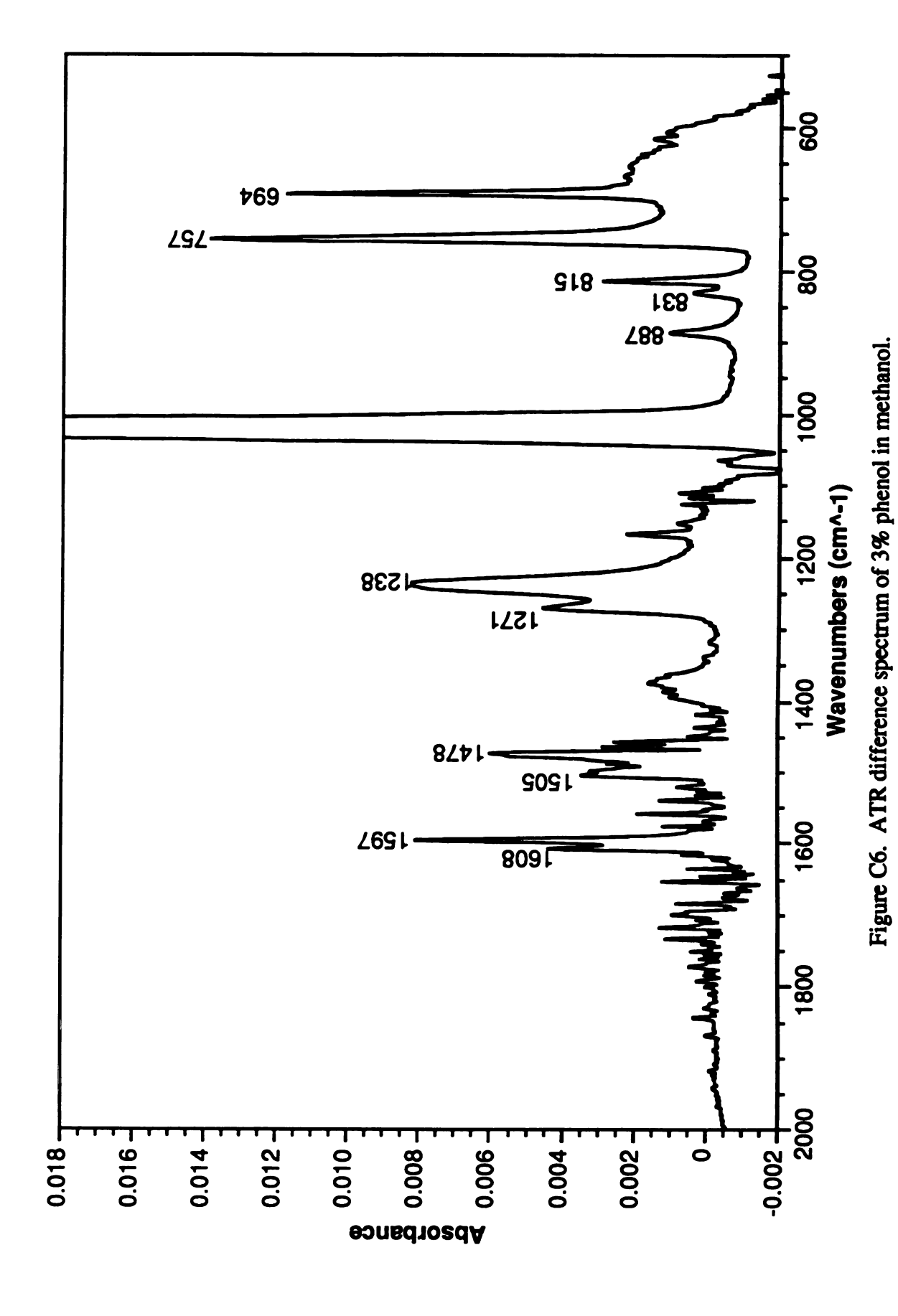


Figure C3. ATR difference spectrum of 3% chlorobenzene in methanol.







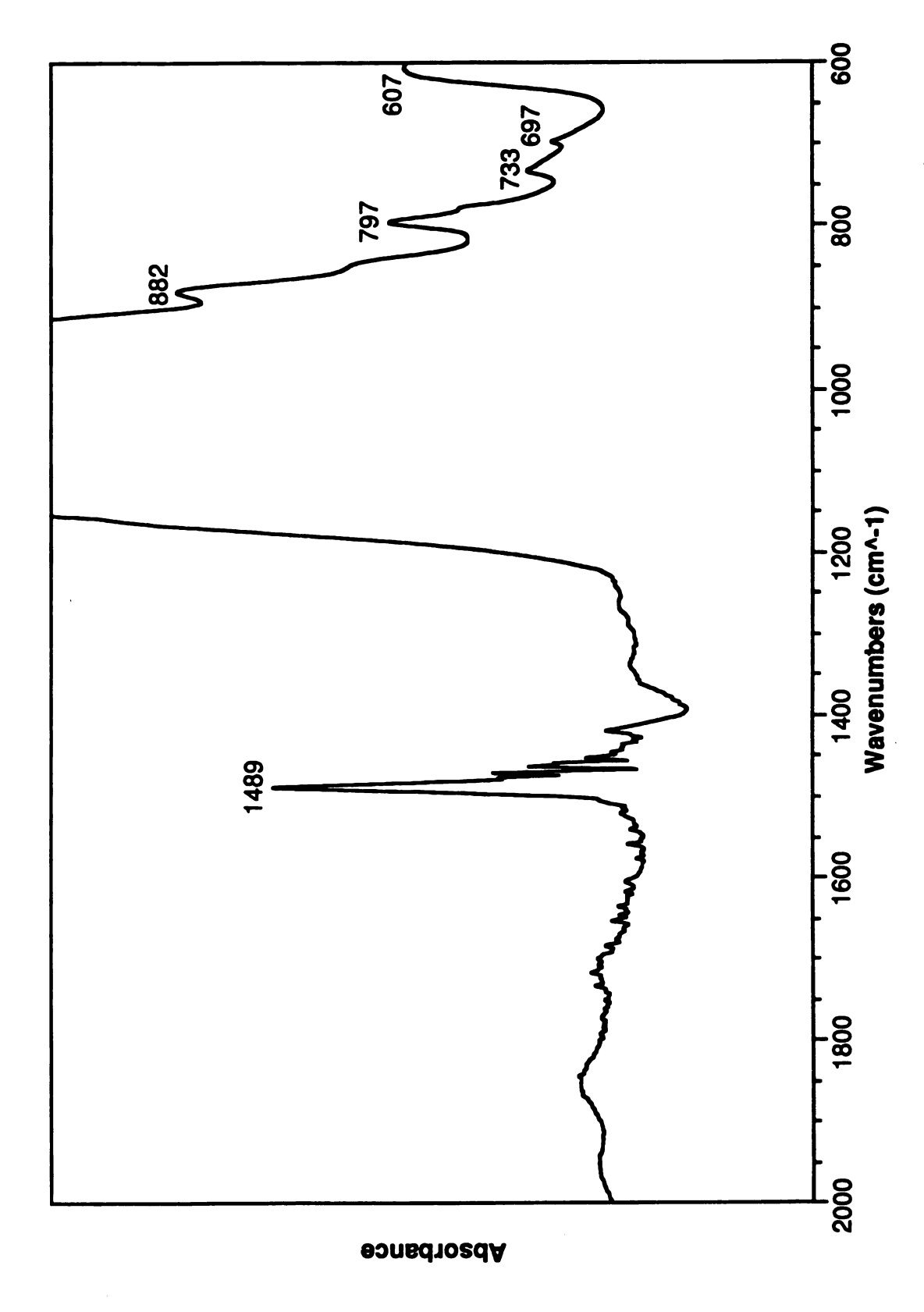


Figure C7. ATR difference spectrum (methanol subtracted) of 3% toluene in methanol on reduced-charge TMA-saturated Wyoming montmorillonite.

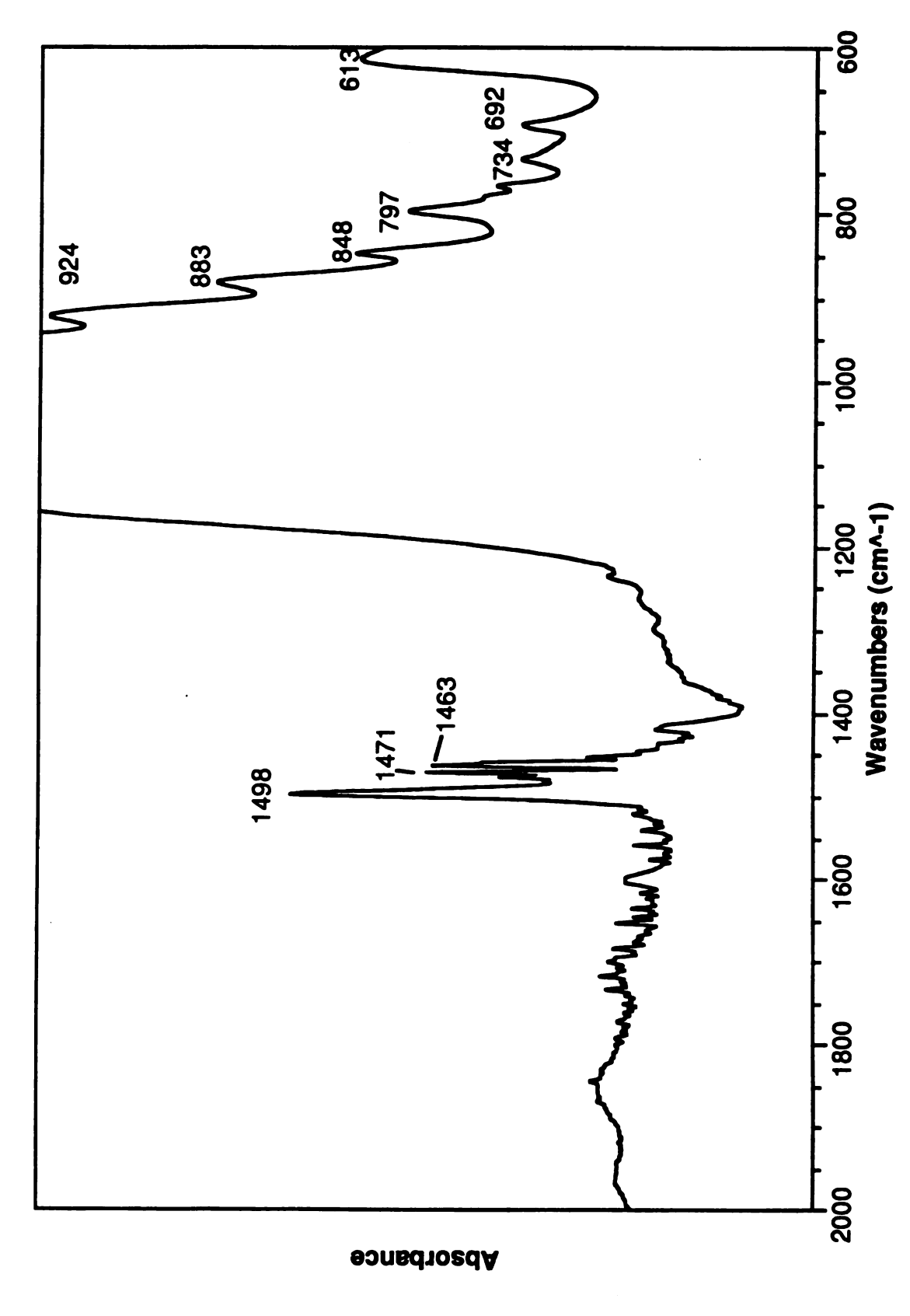


Figure C8. ATR difference spectrum (methanol subtracted) of 3% toluene in methanol on reduced-charge. TMPA-saturated Wyoming montmorillonite.

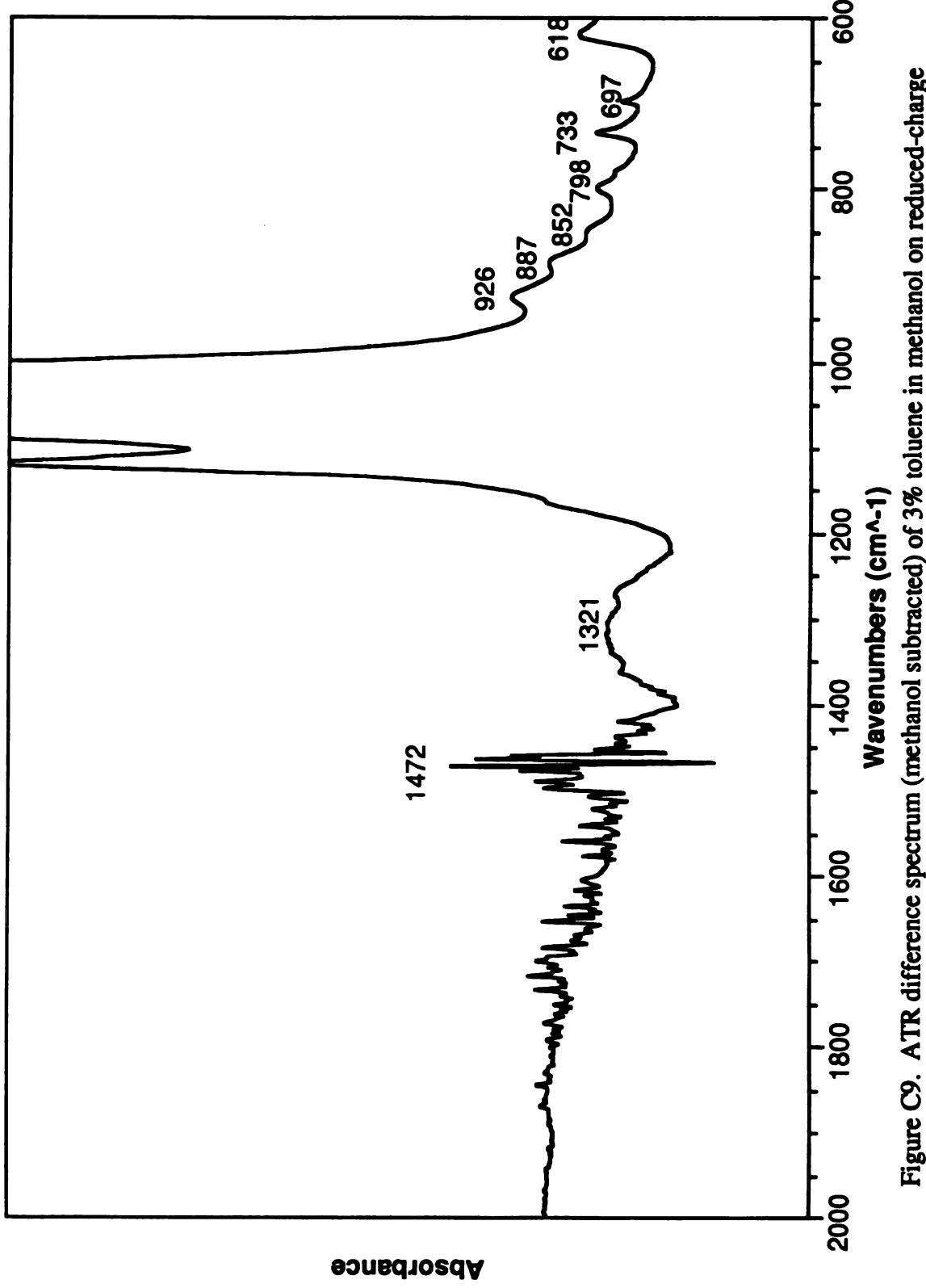


Figure C9. ATR difference spectrum (methanol subtracted) of 3% toluene in methanol on reduced-charge HDTMA-saturated Wyoming montmorillonite.

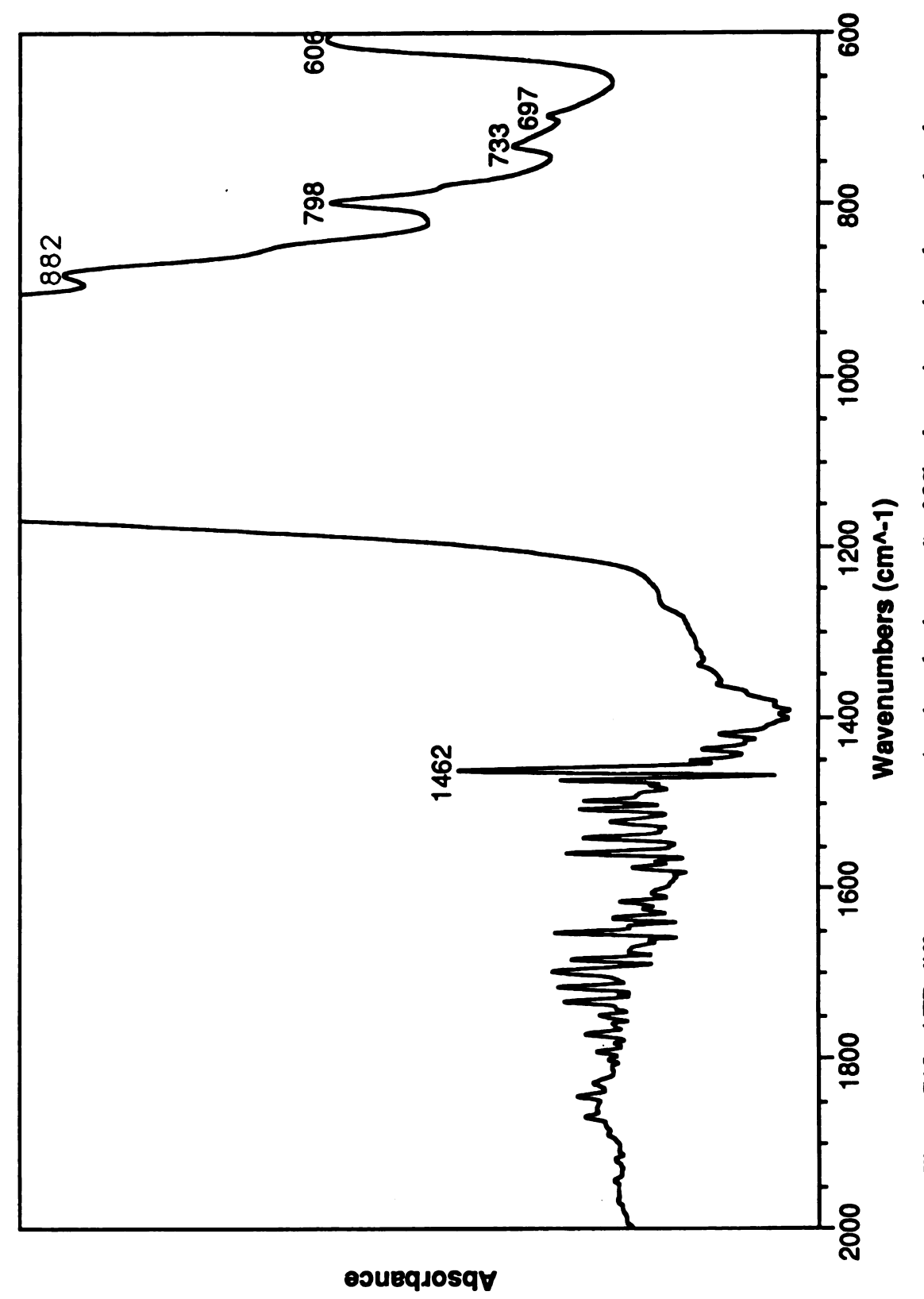


Figure C10. ATR difference spectrum (methanol subtracted) of 3% toluene in methanol on reduced-charge Cs+-saturated Wyoming montmorillonite.

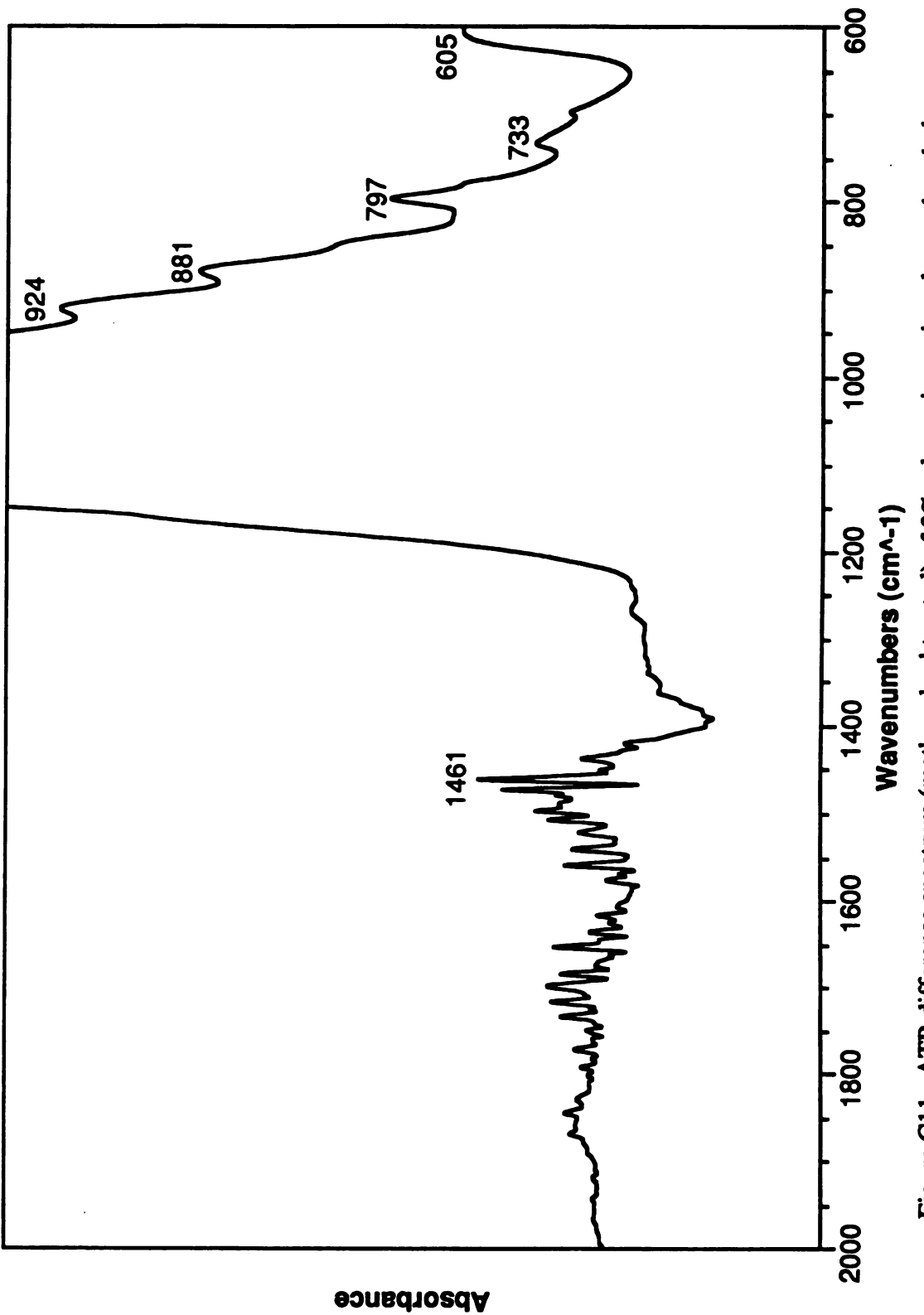


Figure C11. ATR difference spectrum (methanol subtracted) of 3% toluene in methanol on reduced-charge Mg²⁺-saturated Wyoming montmorillonite.

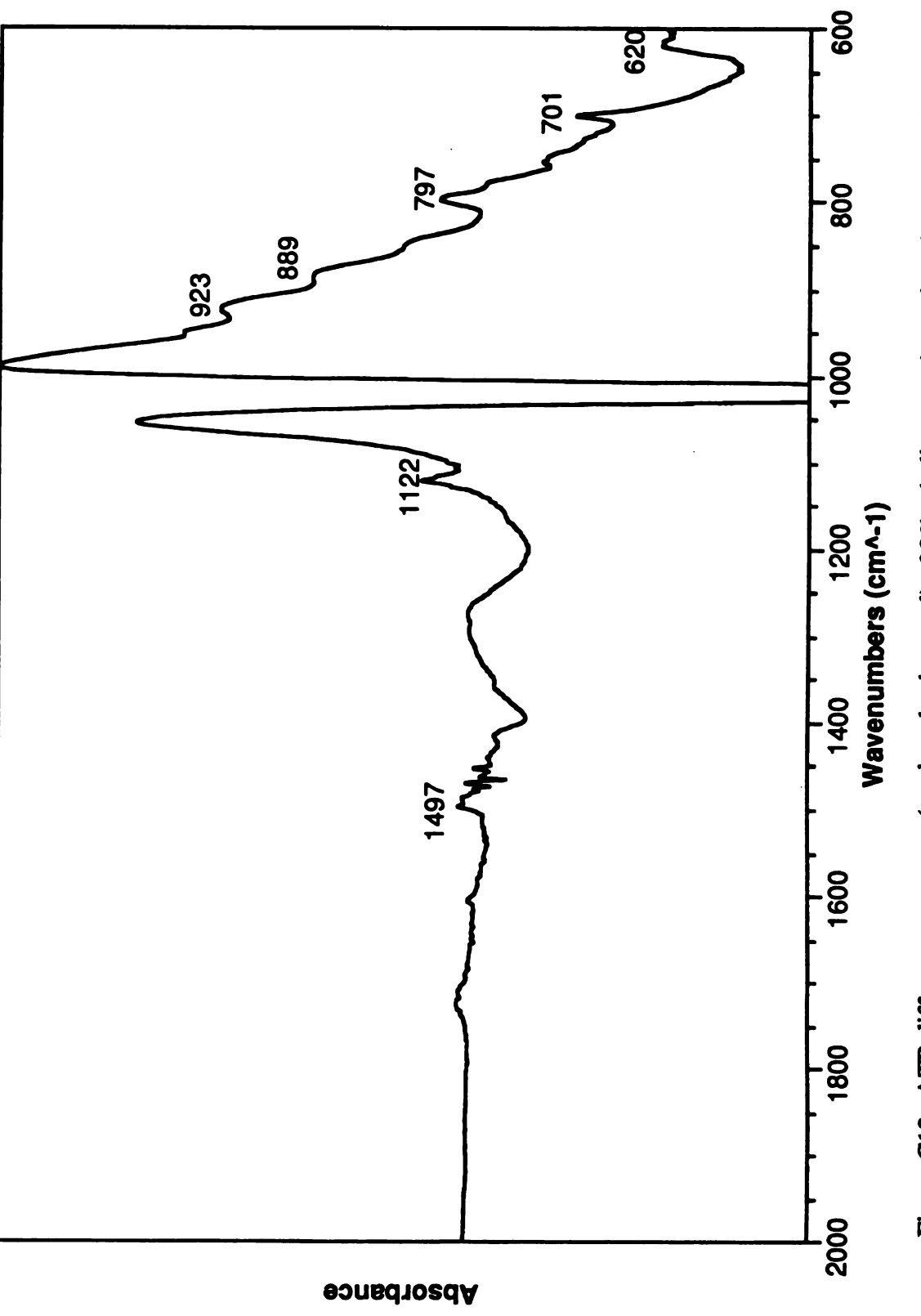


Figure C12. ATR difference spectrum (methanol subtracted) of 3% ethylbenzene in methanol on reduced-charge TMA-saturated Wyoming montmorillonite.

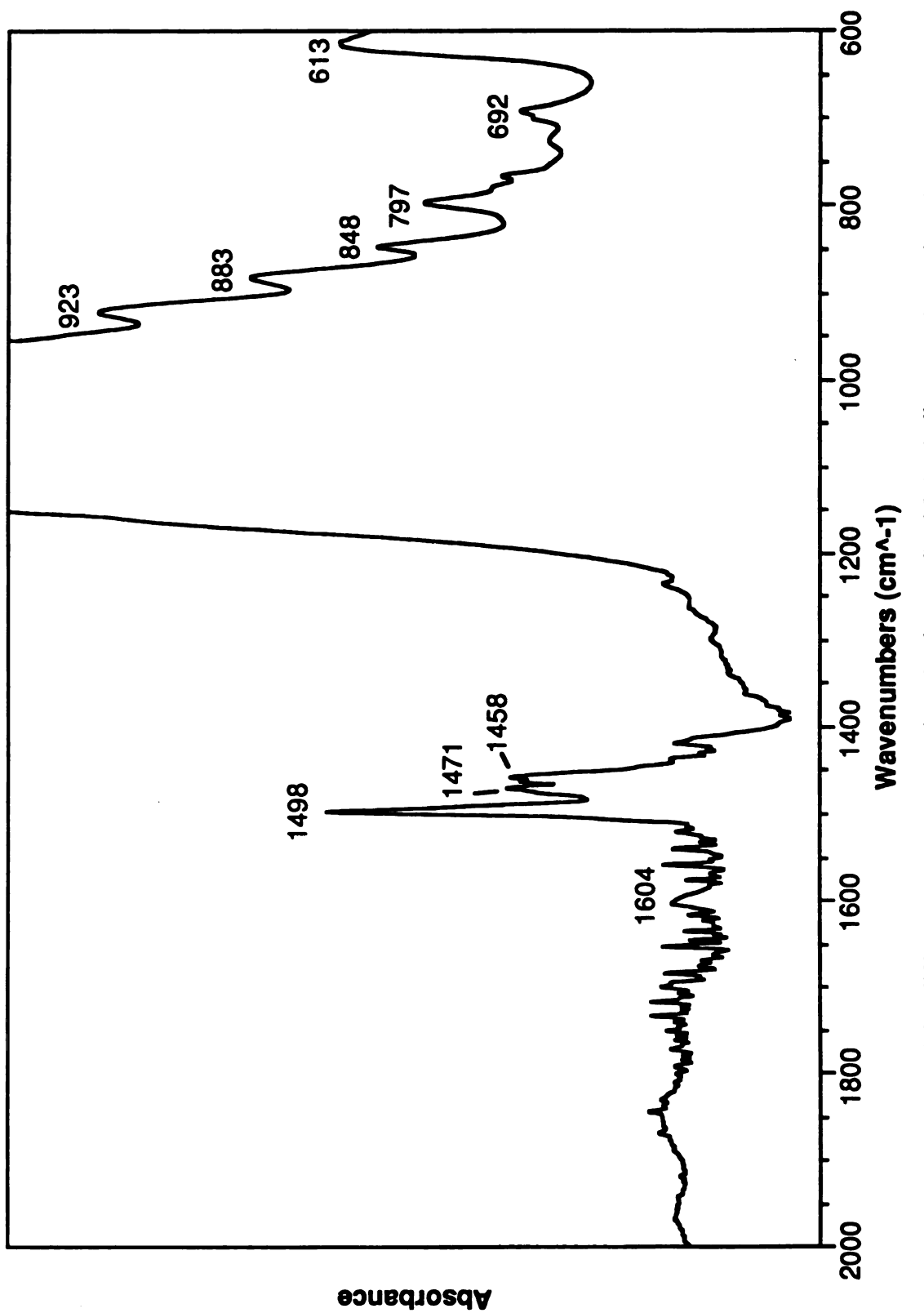


Figure C13. ATR difference spectrum (methanol subtracted) of 3% ethylbenzene in methanol on reduced-charge TMPA-saturated Wyoming montmorillonite.

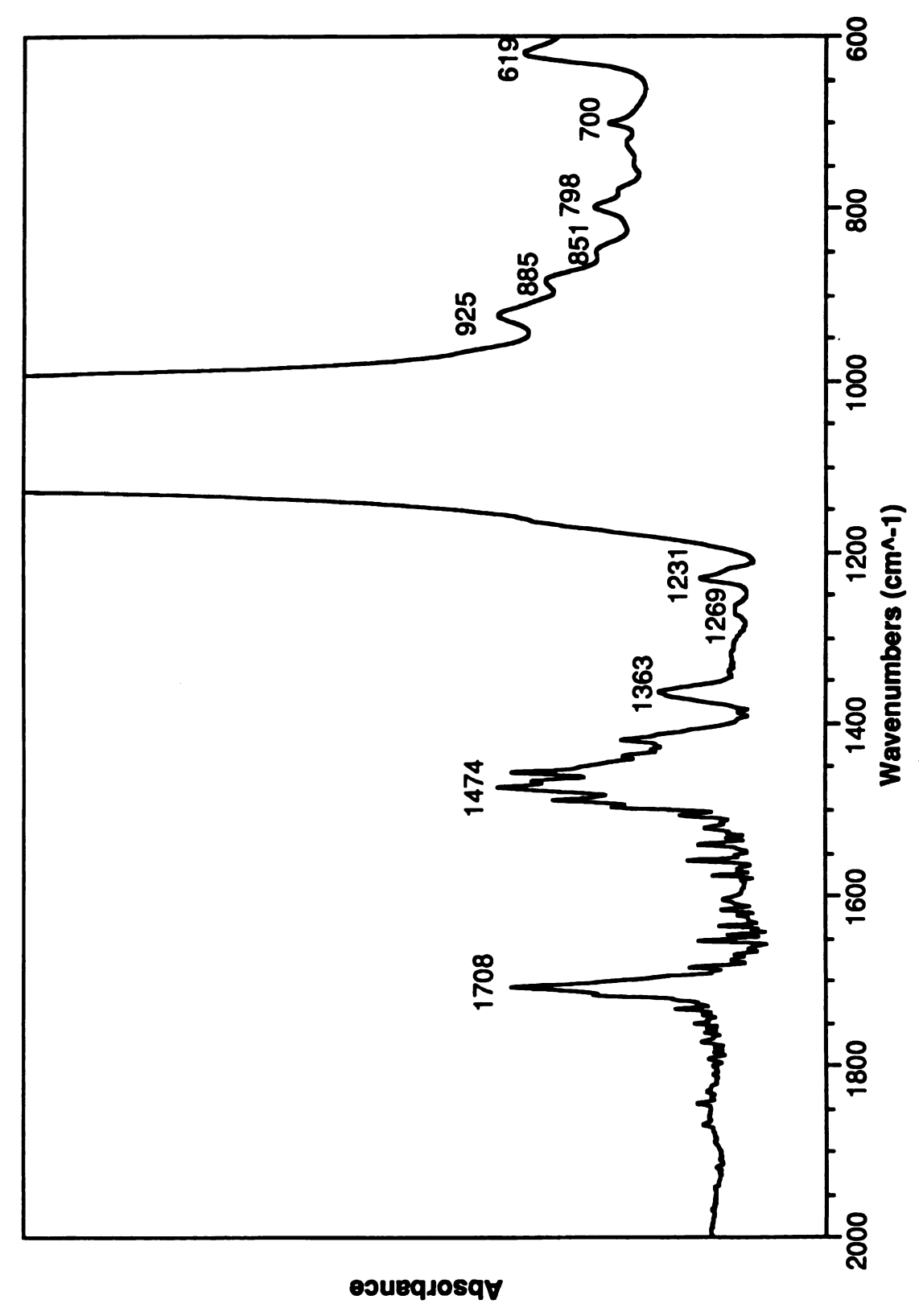


Figure C14. ATR difference spectrum (methanol subtracted) of 3% ethylbenzene in methanol on reduced-charge HDTMA-saturated Wyoming montmorillonite.

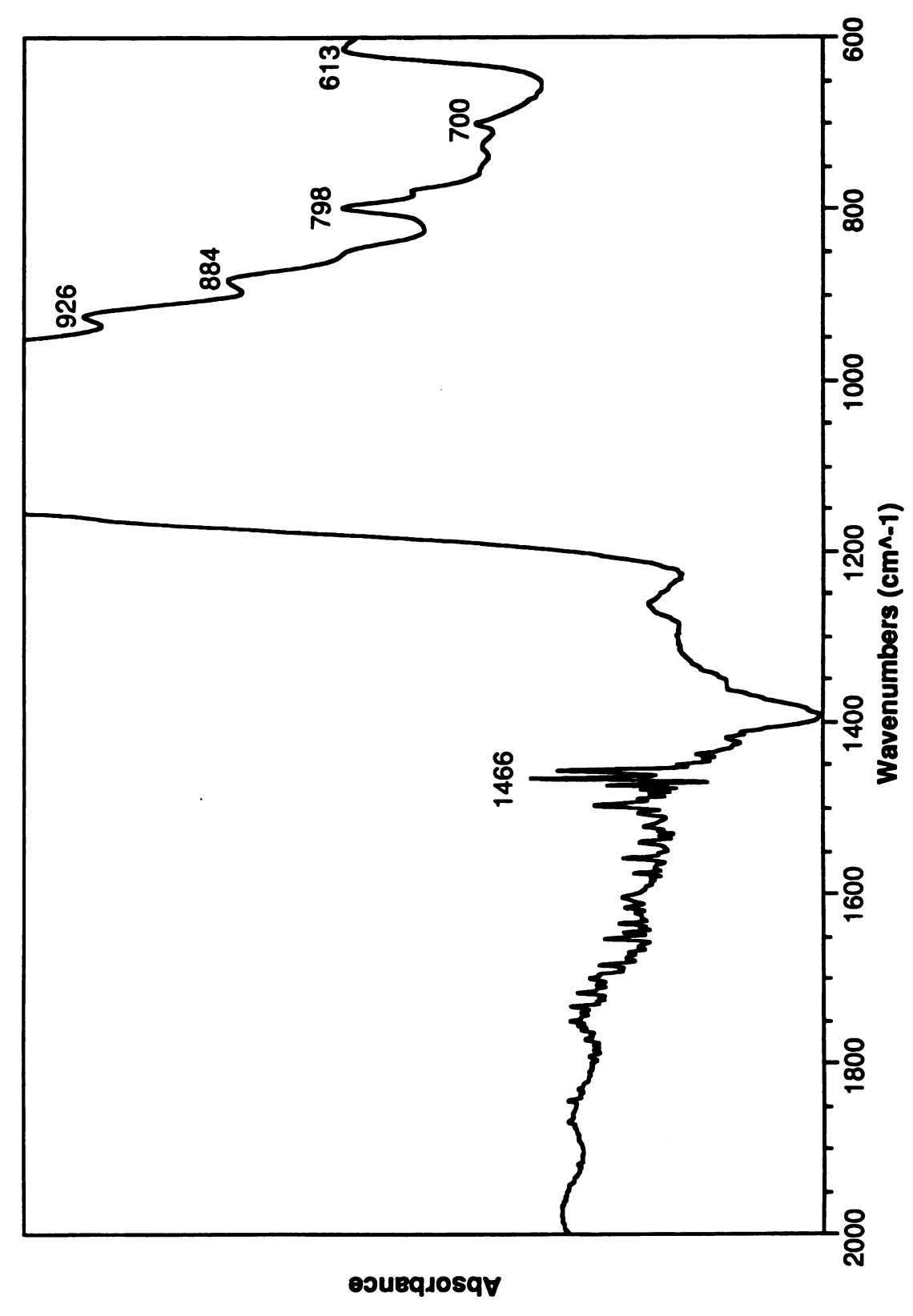
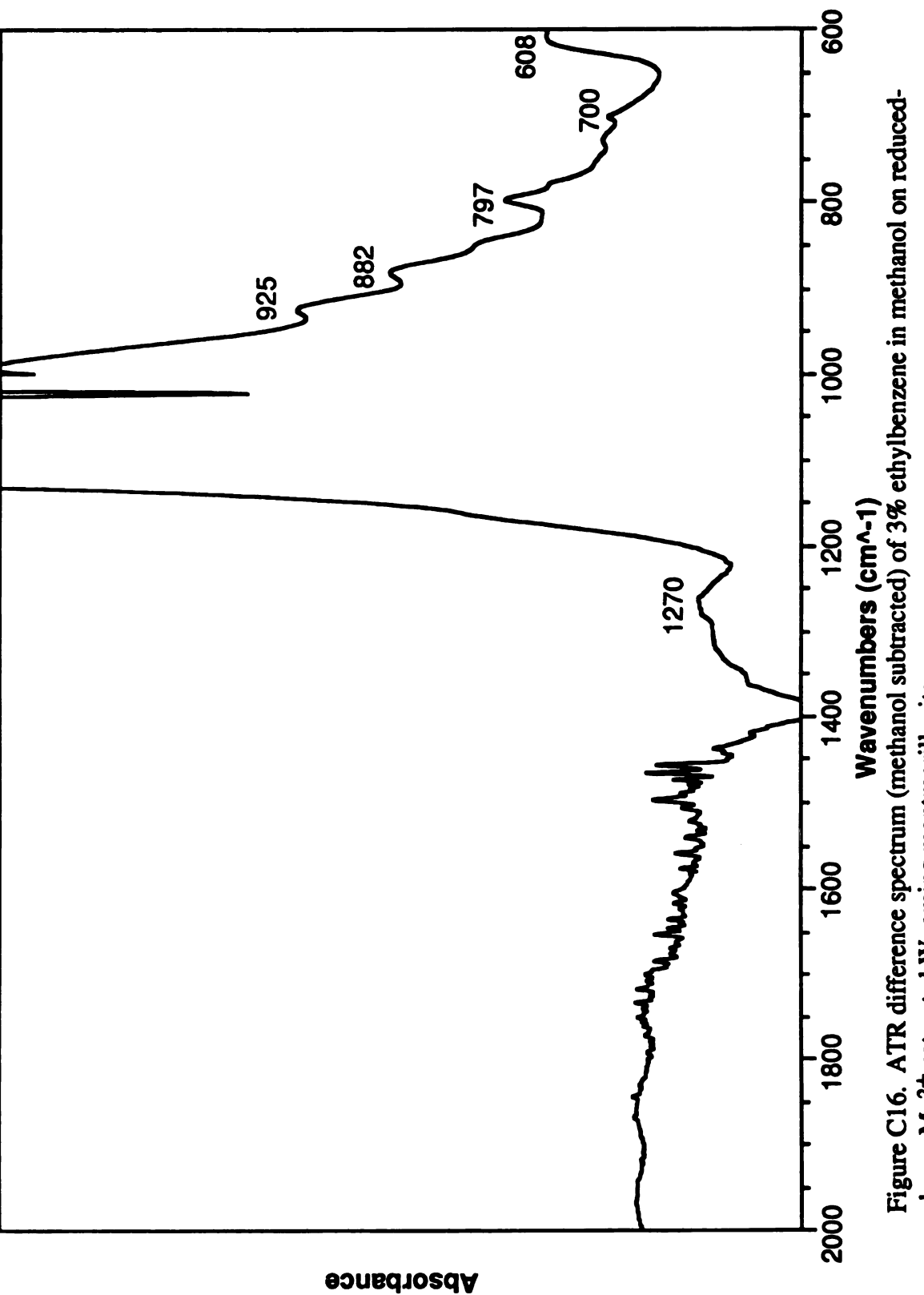


Figure C15. ATR difference spectrum (methanol subtracted) of 3% ethylbenzene in methanol on reduced-charge Cs⁺-saturated Wyoming montmorillonite.



charge Mg²⁺-saturated Wyoming montmorillonite.

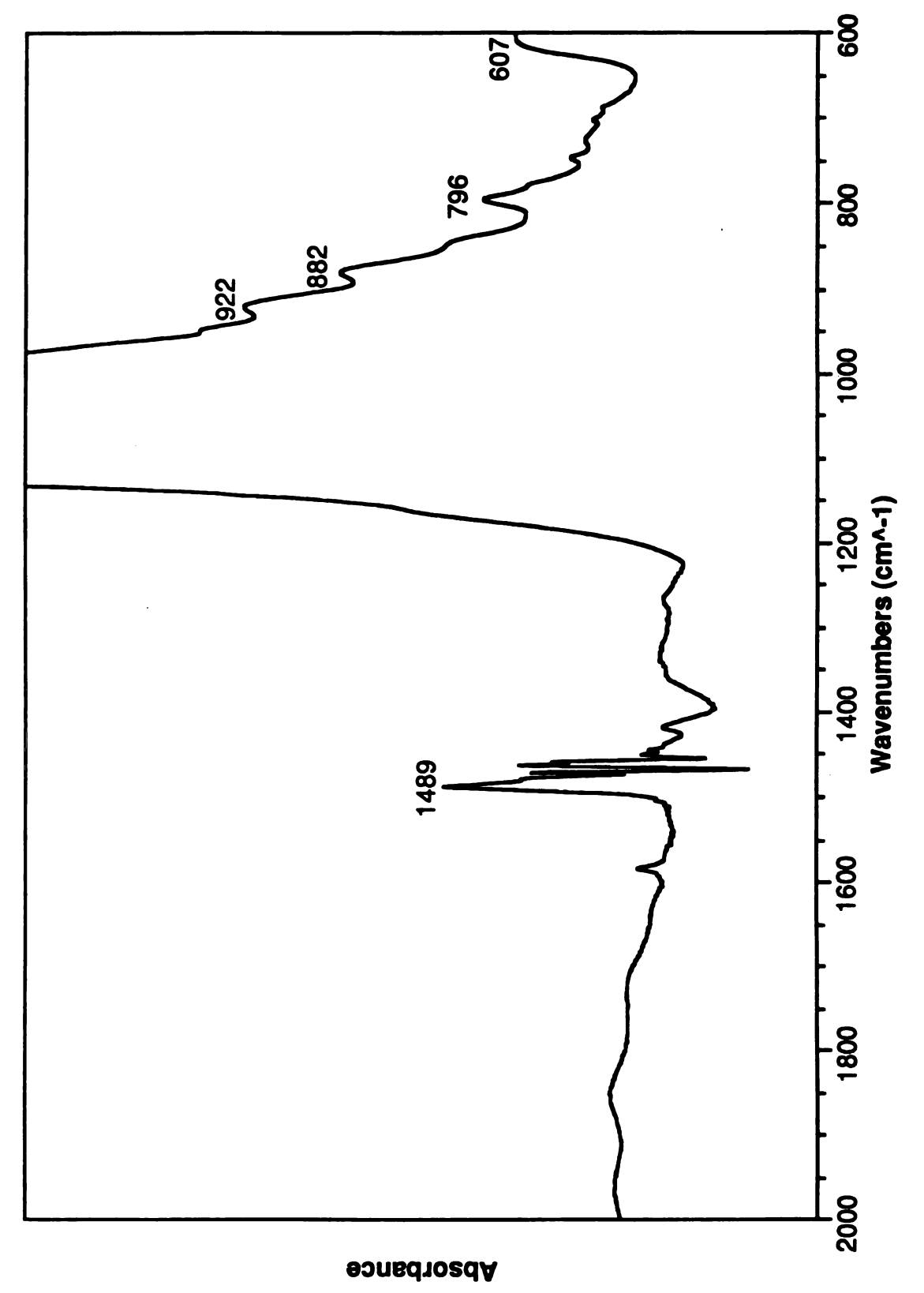


Figure C17. ATR difference spectrum (methanol subtracted) of 3% chlorobenzene in methanol on reduced-charge TMA-saturated Wyoming montmorillonite.

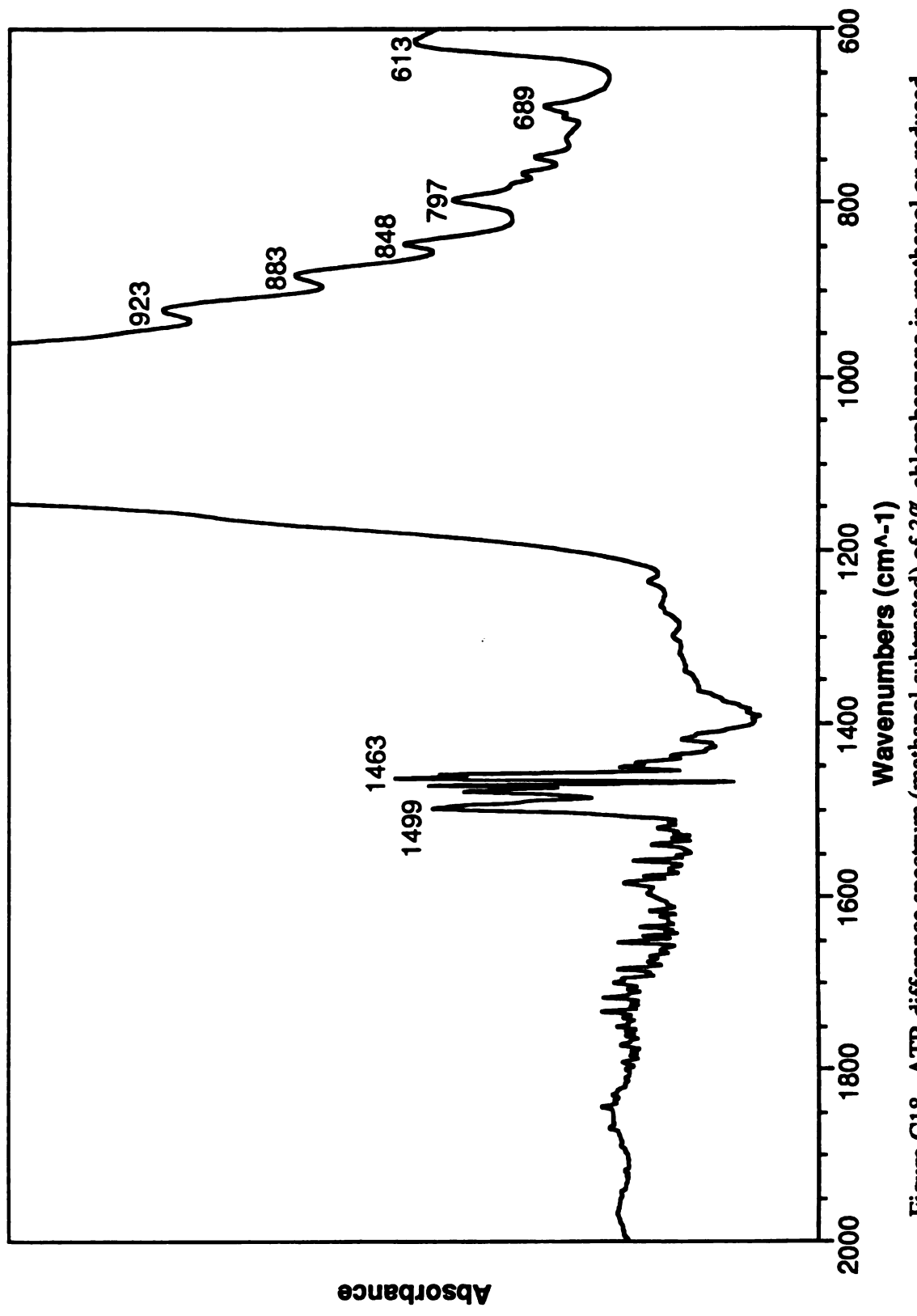


Figure C18. ATR difference spectrum (methanol subtracted) of 3% chlorobenzene in methanol on reduced-charge TMPA-saturated Wyoming montmorillonite.

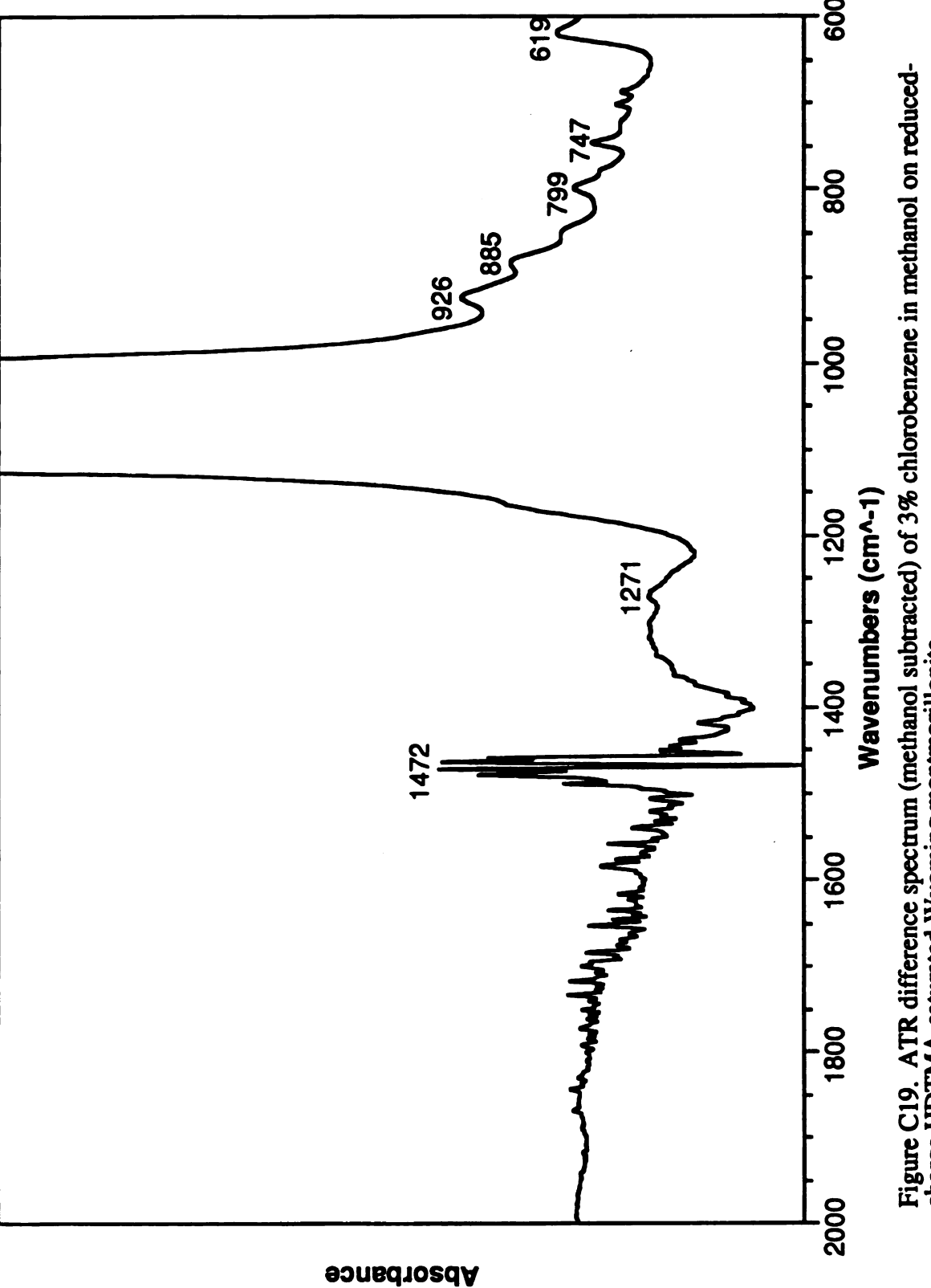


Figure C19. ATR difference spectrum (methanol subtracted) of 3% chlorobenzene in methanol on reduced-charge HDTMA-saturated Wyoming montmorillonite.

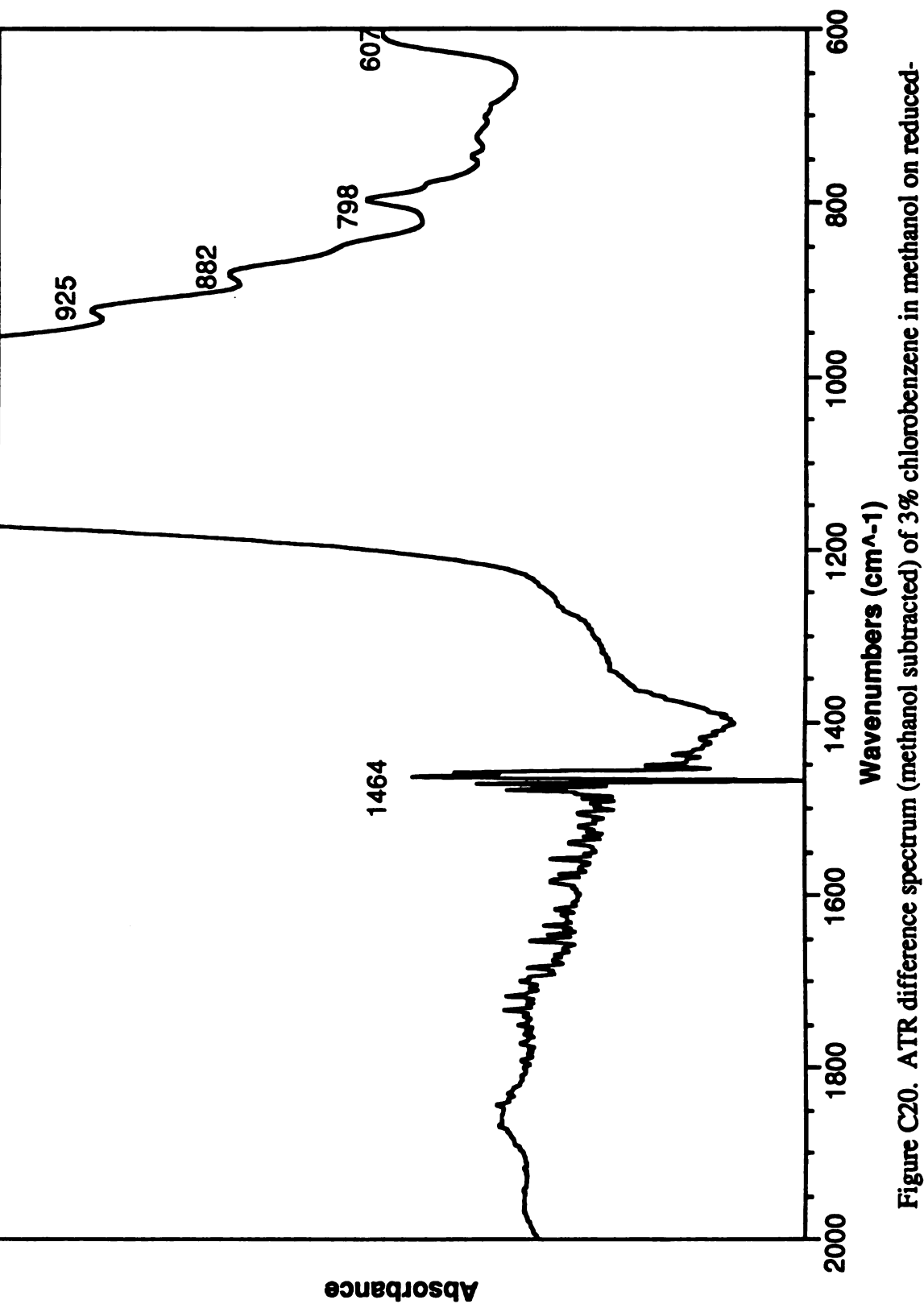


Figure C20. ATR difference spectrum (methanol subtracted) of 3% chlorobenzene in methanol on reduced-charge Cs+-saturated Wyoming montmorillonite.

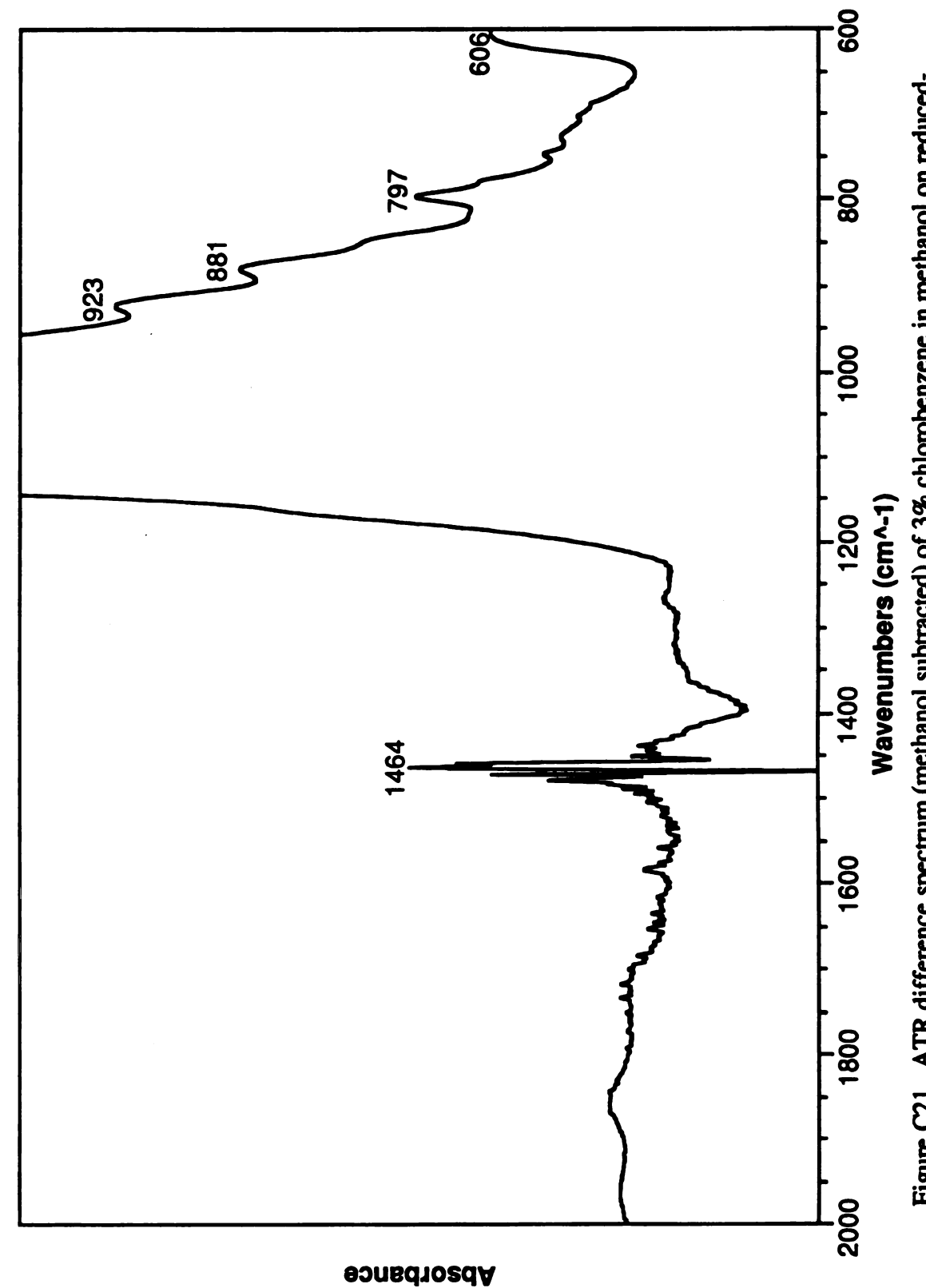


Figure C21. ATR difference spectrum (methanol subtracted) of 3% chlorobenzene in methanol on reduced-charge Mg²⁺-saturated Wyoming montmorillonite.

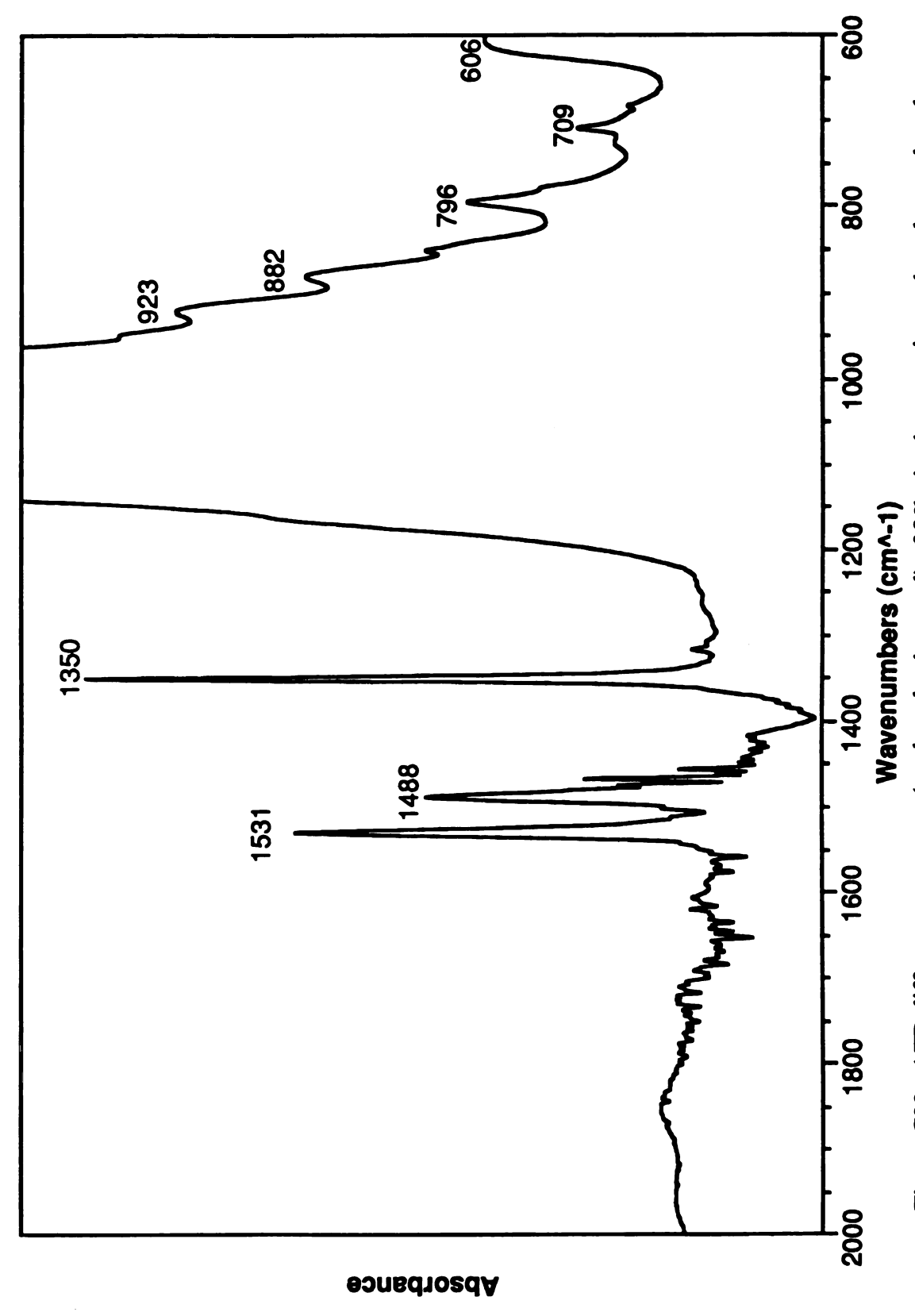


Figure C22. ATR difference spectrum (methanol subtracted) of 3% nitrobenzene in methanol on reduced-charge TMA-saturated Wyoming montmorillonite.

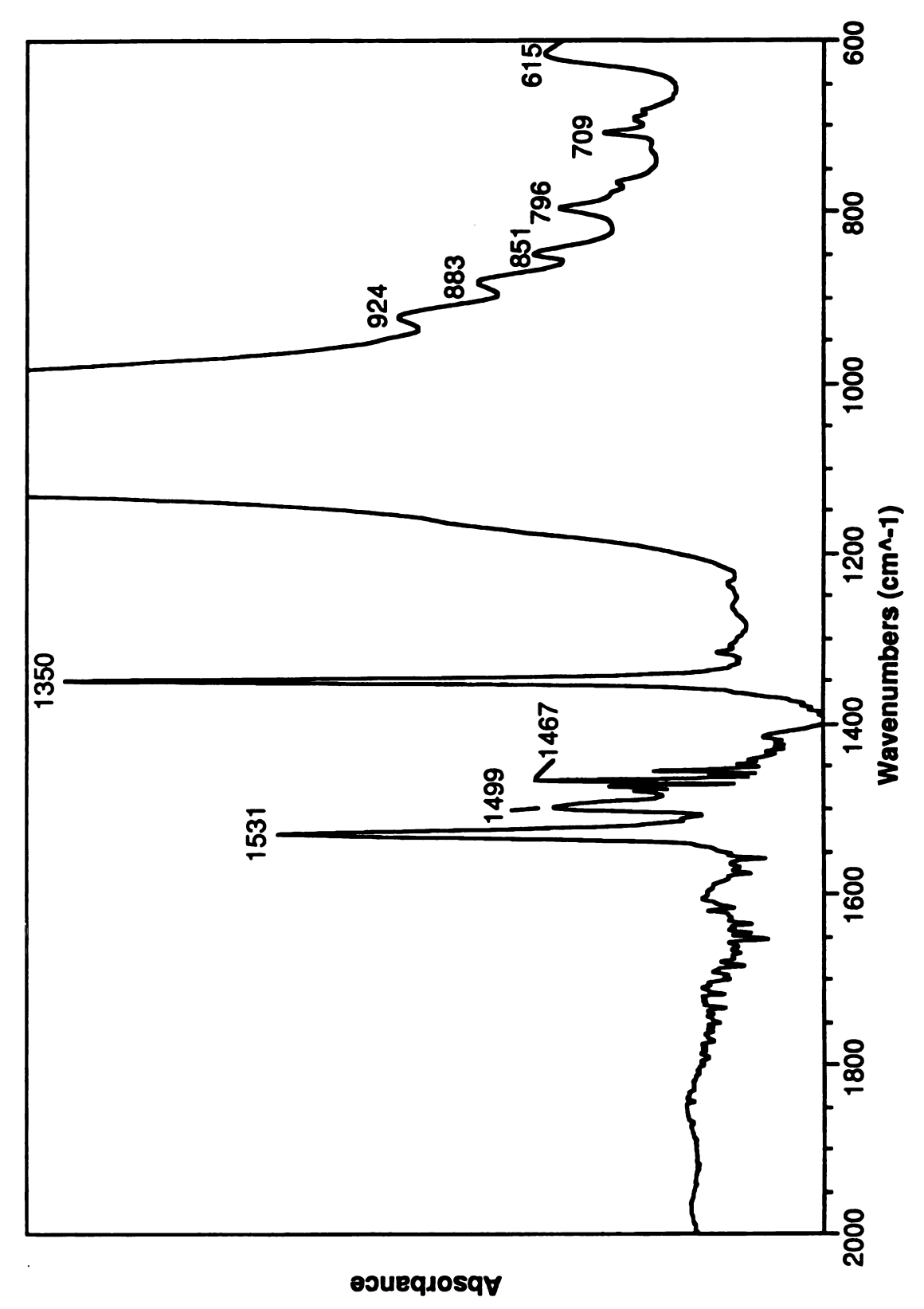
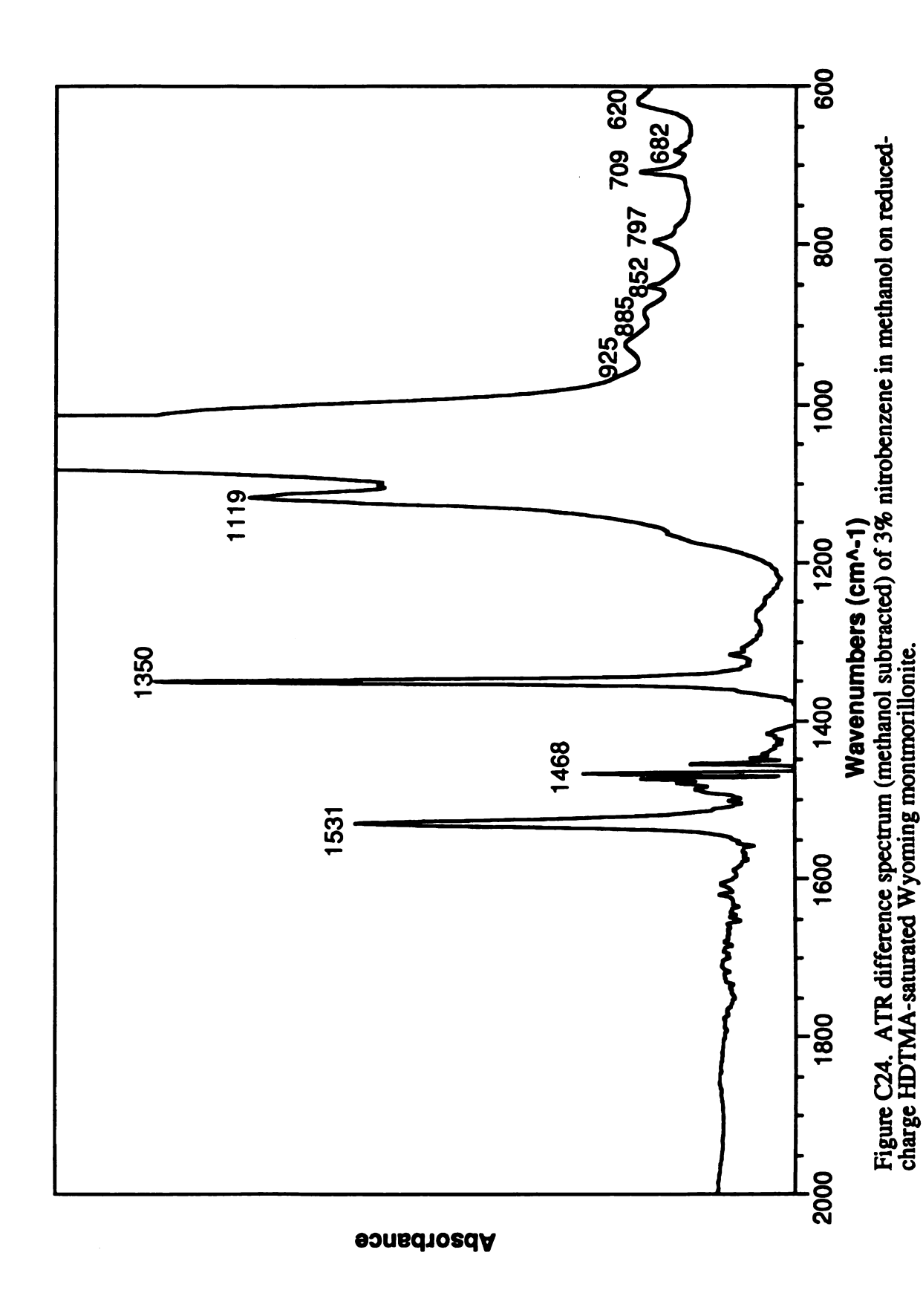


Figure C23. ATR difference spectrum (methanol subtracted) of 3% nitrobenzene in methanol on reduced-charge TMPA-saturated Wyoming montmorillonite.



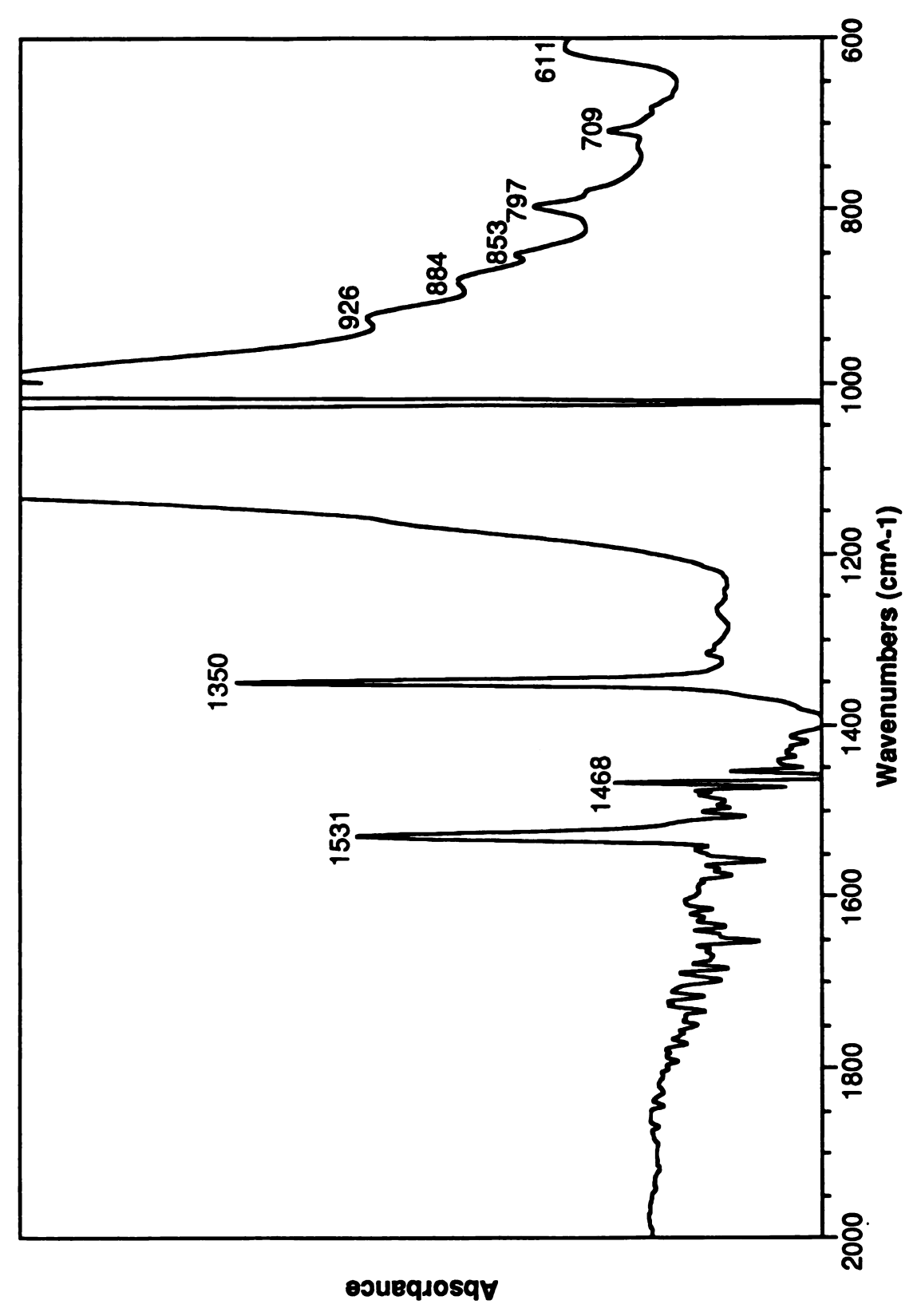
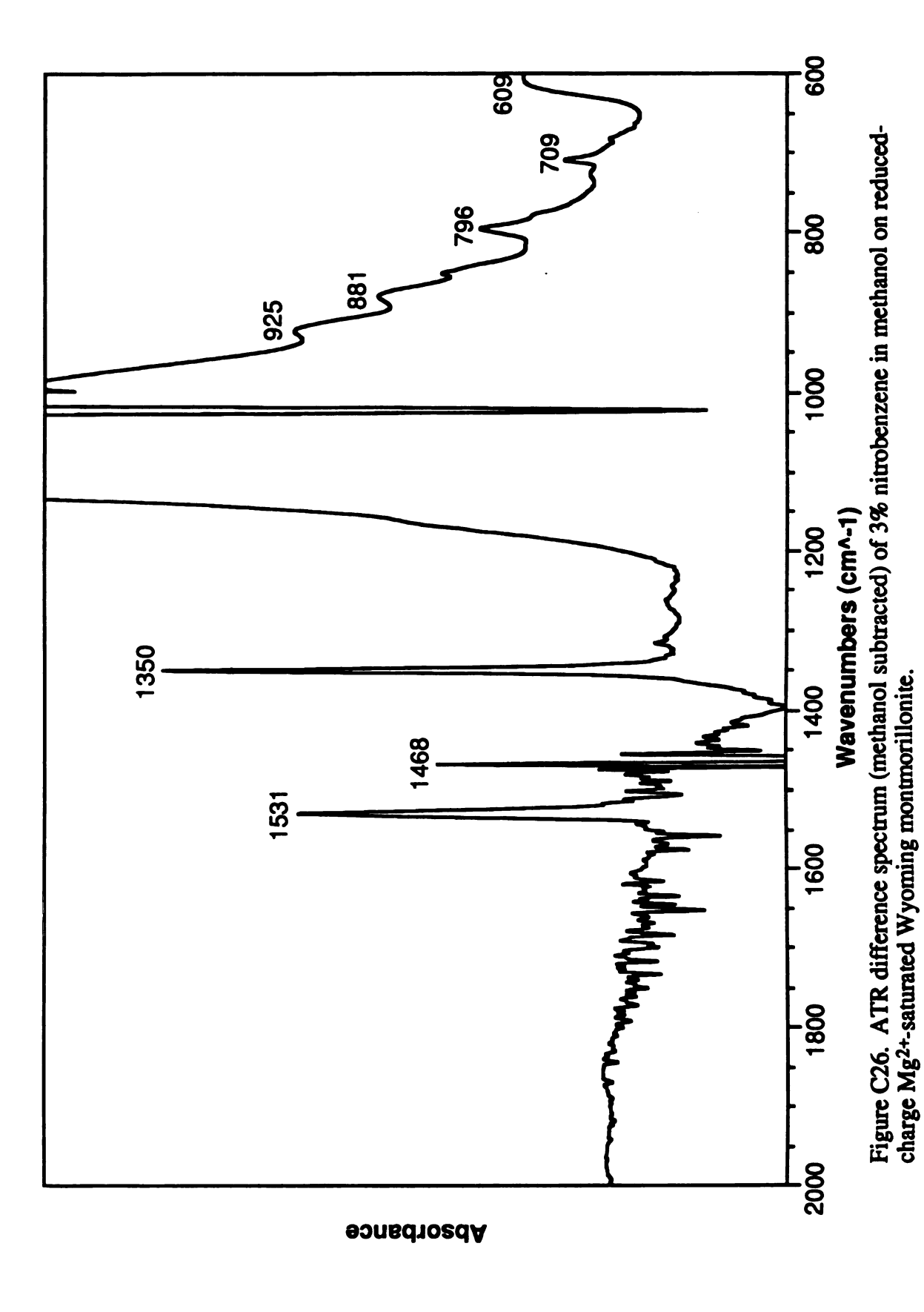


Figure C25. ATR difference spectrum (methanol subtracted) of 3% nitrobenzene in methanol on reduced-charge Cs⁺-saturated Wyoming montmorillonite.



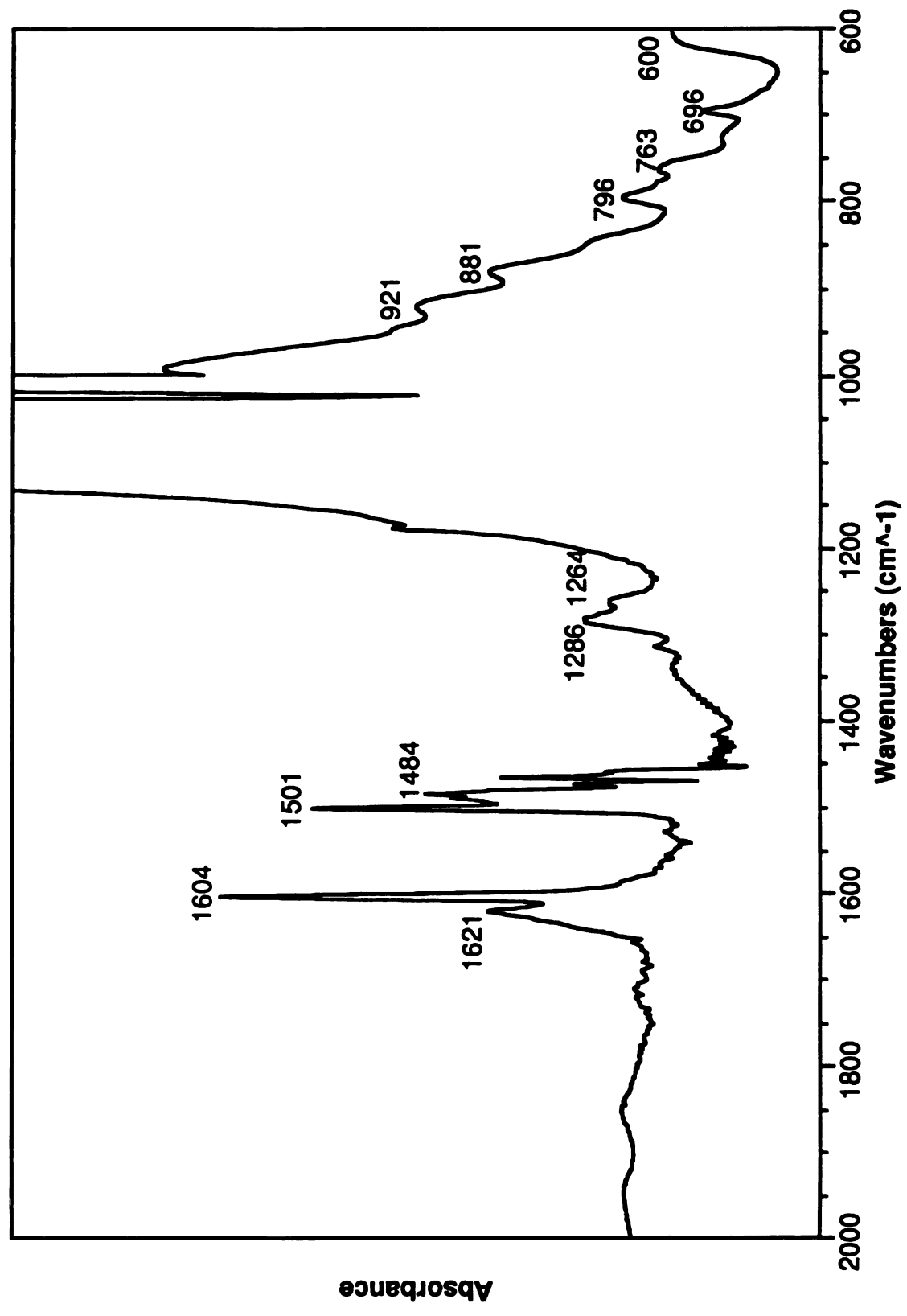


Figure C27. ATR difference spectrum (methanol subtracted) of 3% aniline in methanol on reduced-charge TMA-saturated Wyoming montmorillonite.

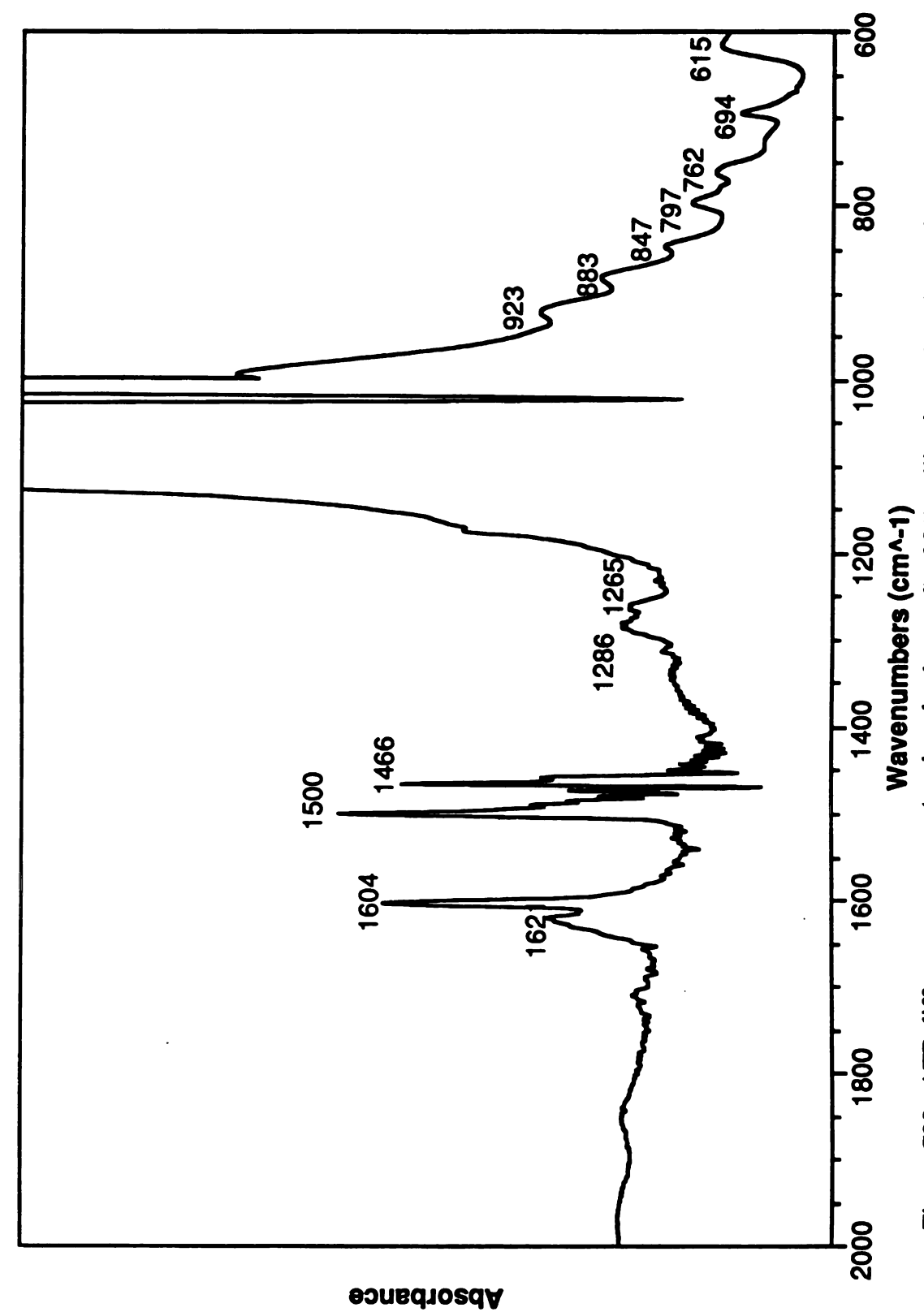


Figure C28. ATR difference spectrum (methanol subtracted) of 3% aniline in methanol on reduced-charge TMPA-saturated Wyoming montmorillonite.

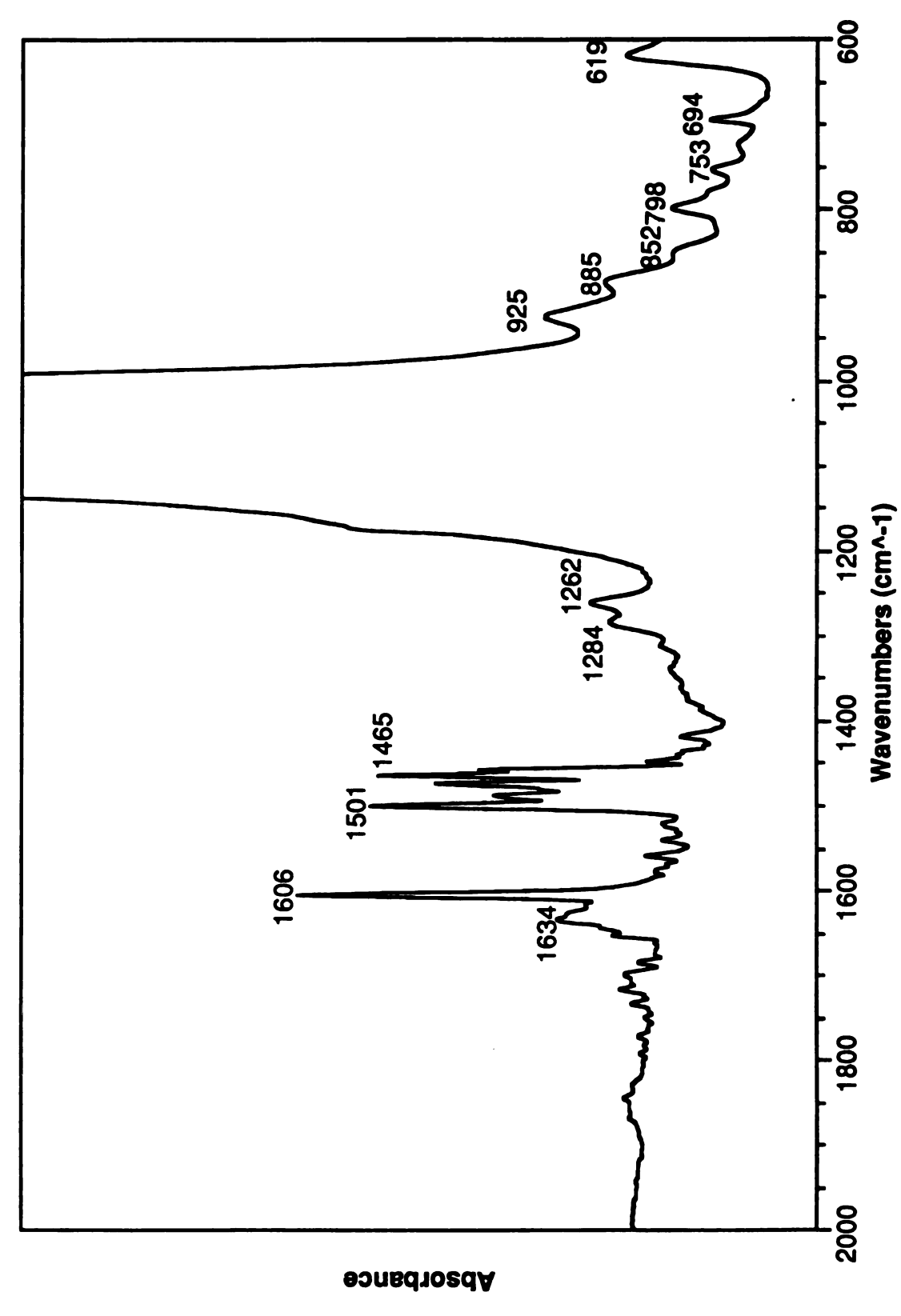
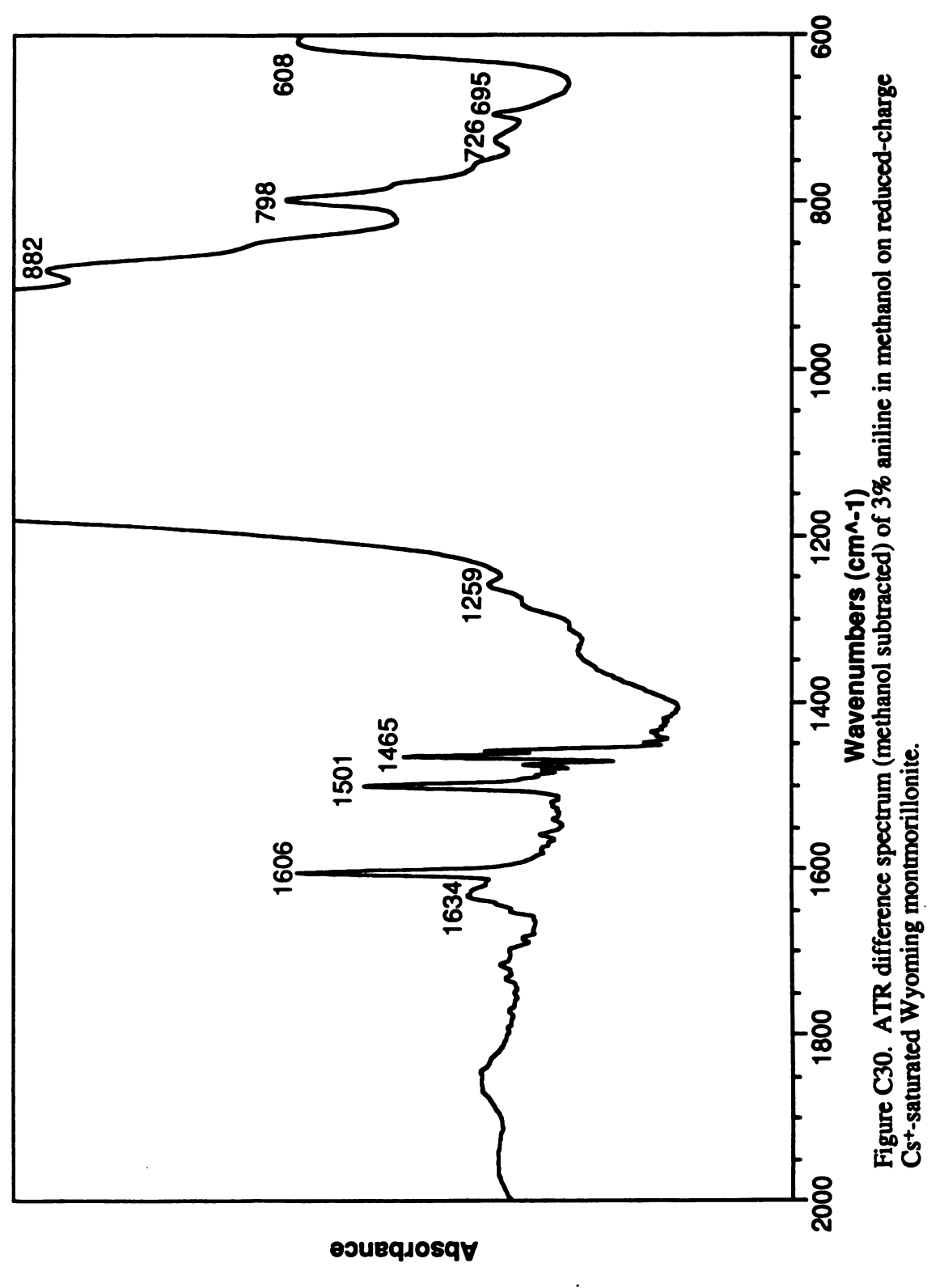
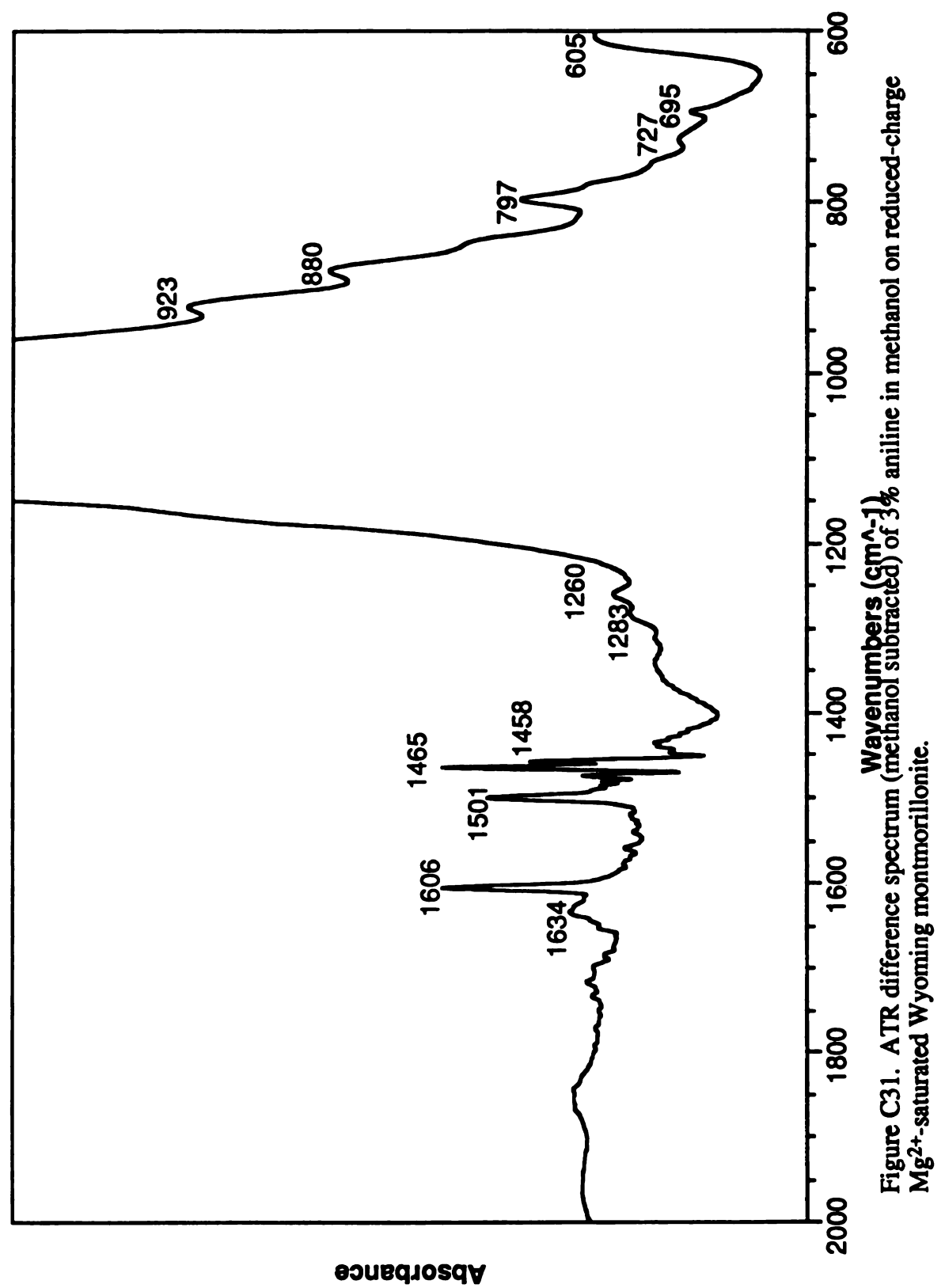
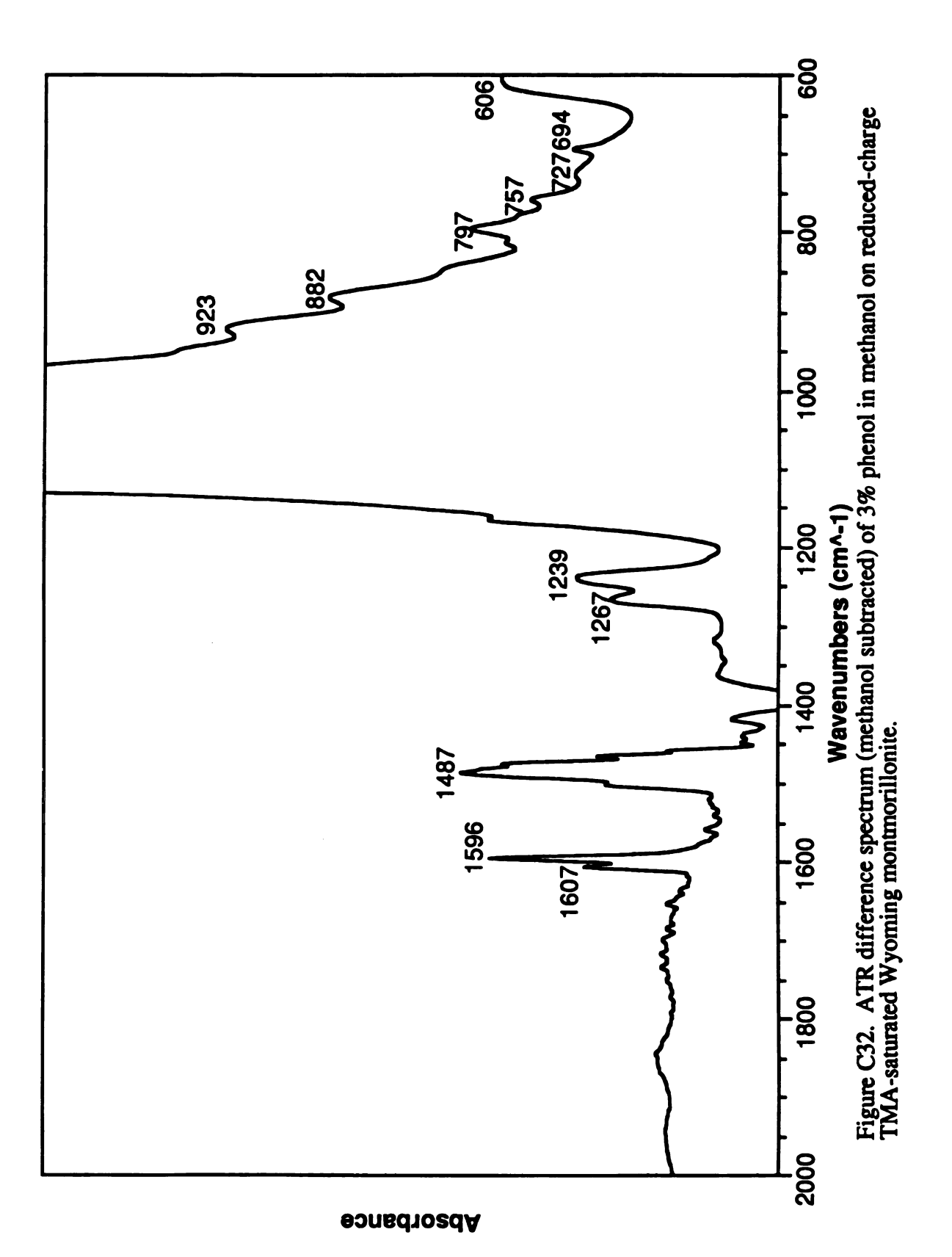


Figure C29. ATR difference spectrum (methanol subtracted) of 3% aniline in methanol on reduced-charge HDTMA-saturated Wyoming montmorillonite.







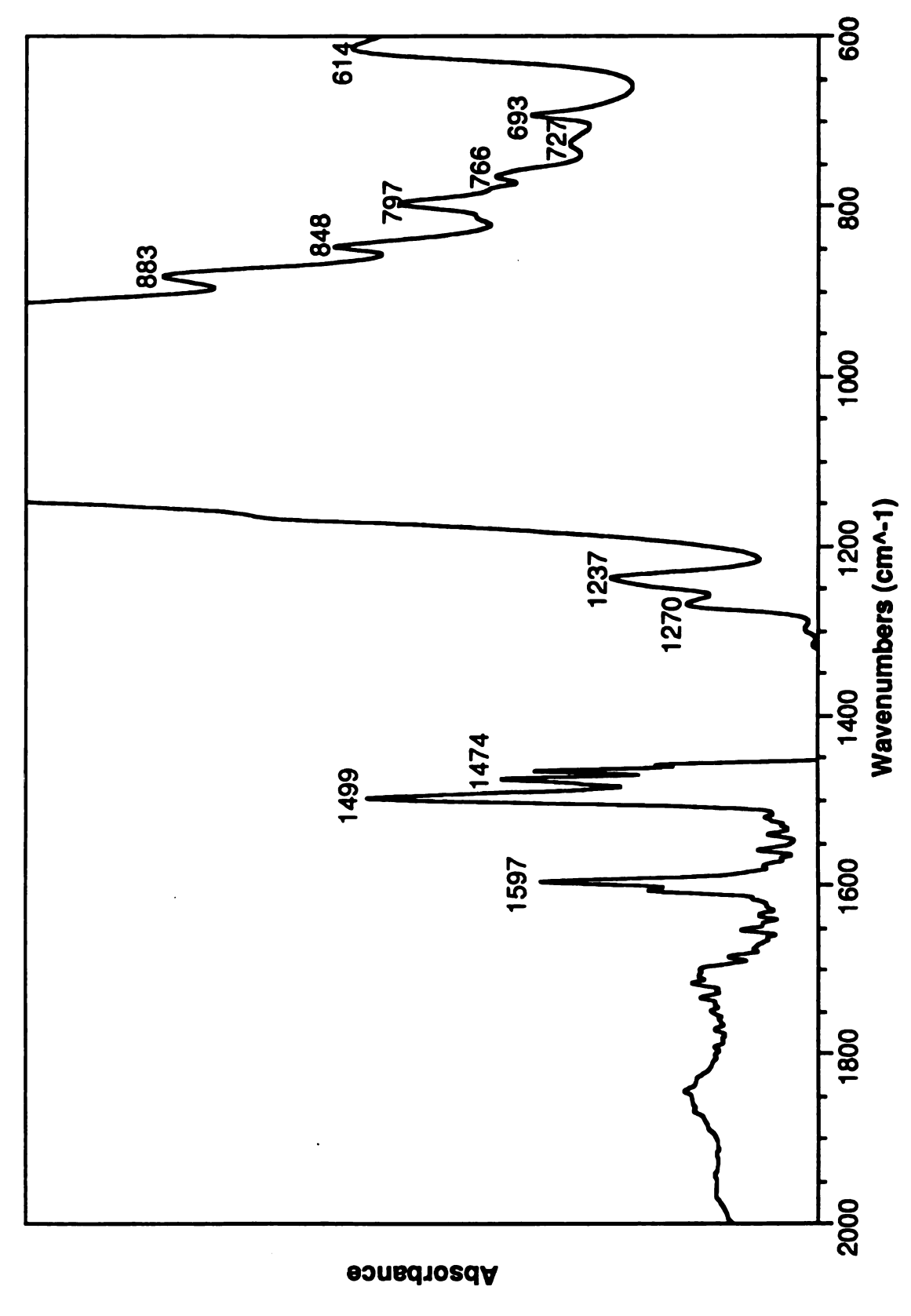


Figure C33. ATR difference spectrum (methanol subtracted) of 3% phenol in methanol on reduced-charge TMPA-saturated Wyoming montmorillonite.

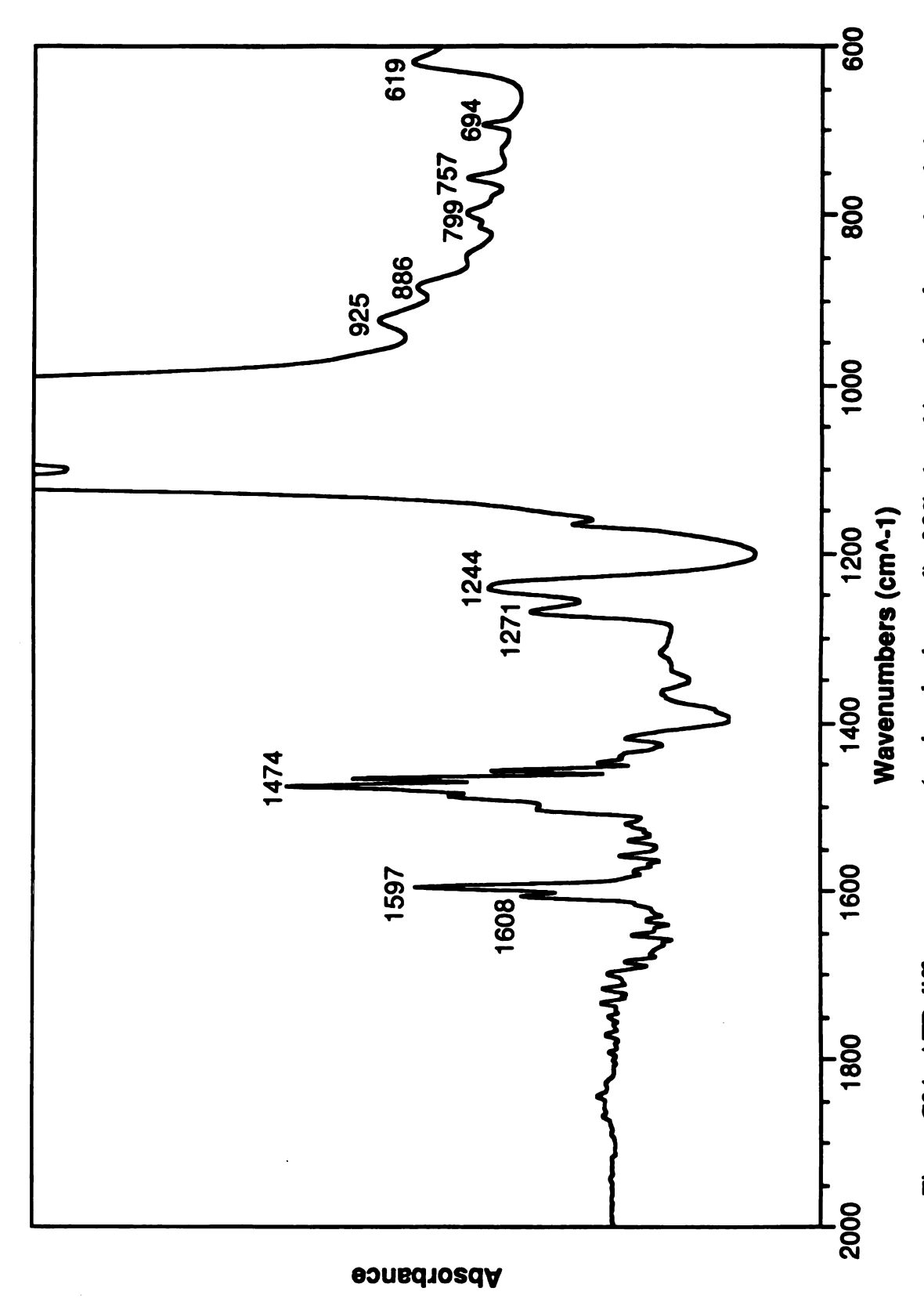


Figure C34. ATR difference spectrum (methanol subtracted) of 3% phenol in methanol on reduced-charge HDTMA-saturated Wyoming montmorillonite.

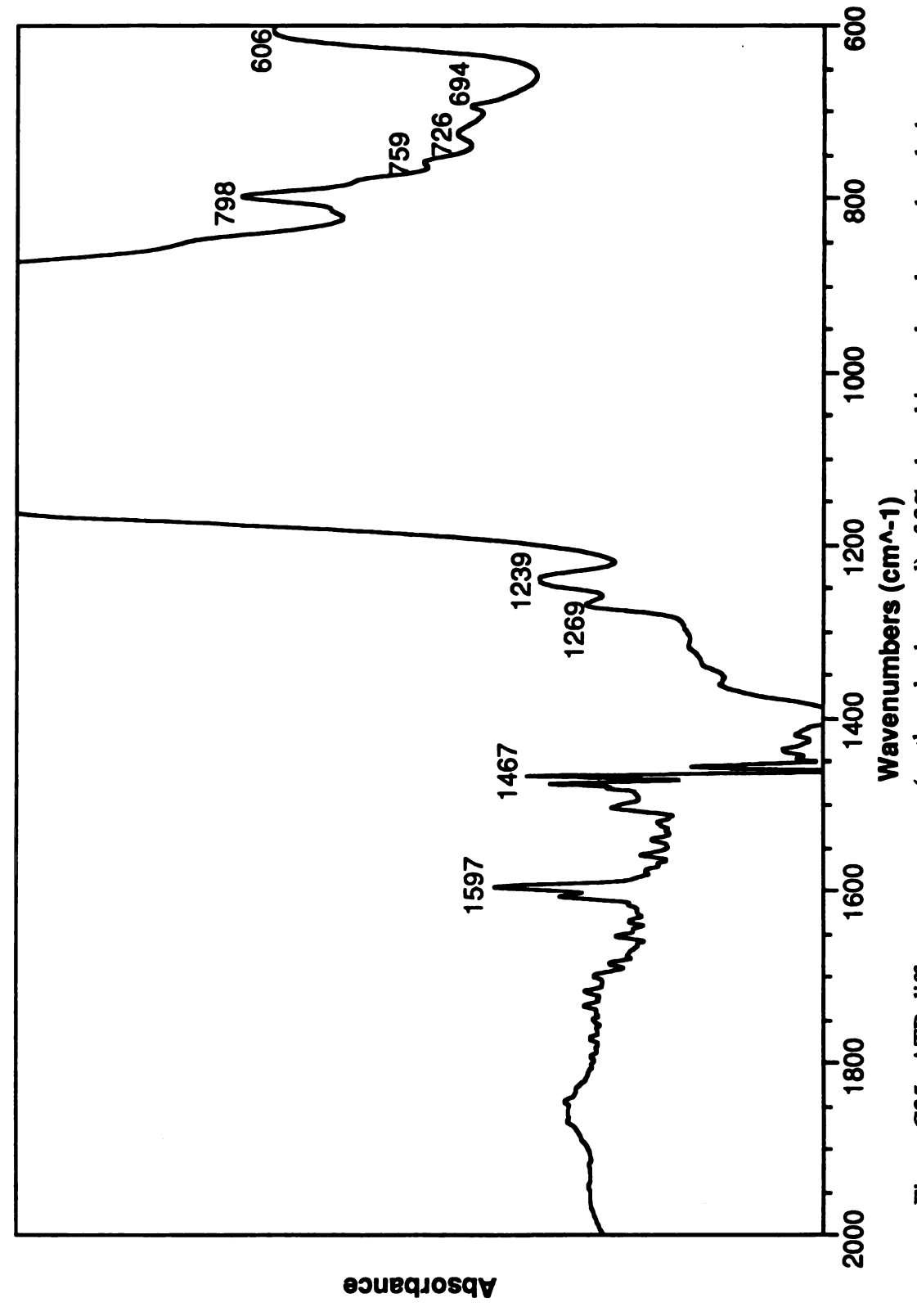


Figure C35. ATR difference spectrum (methanol subtracted) of 3% phenol in methanol on reduced-charge Cs+-saturated Wyoming montmorillonite.

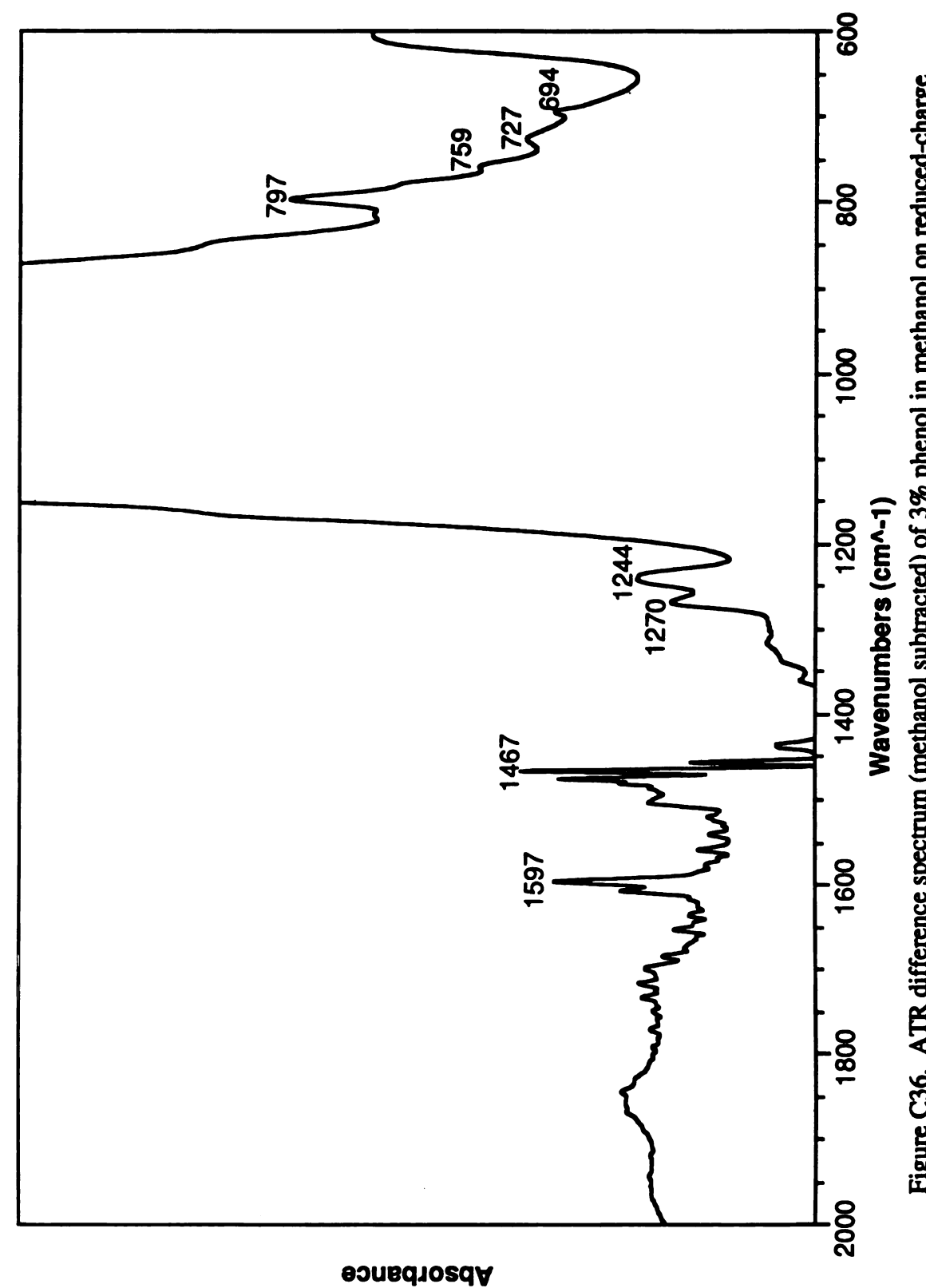


Figure C36. ATR difference spectrum (methanol subtracted) of 3% phenol in methanol on reduced-charge Mg²⁺-saturated Wyoming montmorillonite.

Appendix D

Supplementary mixed benzene-water sorption spectra

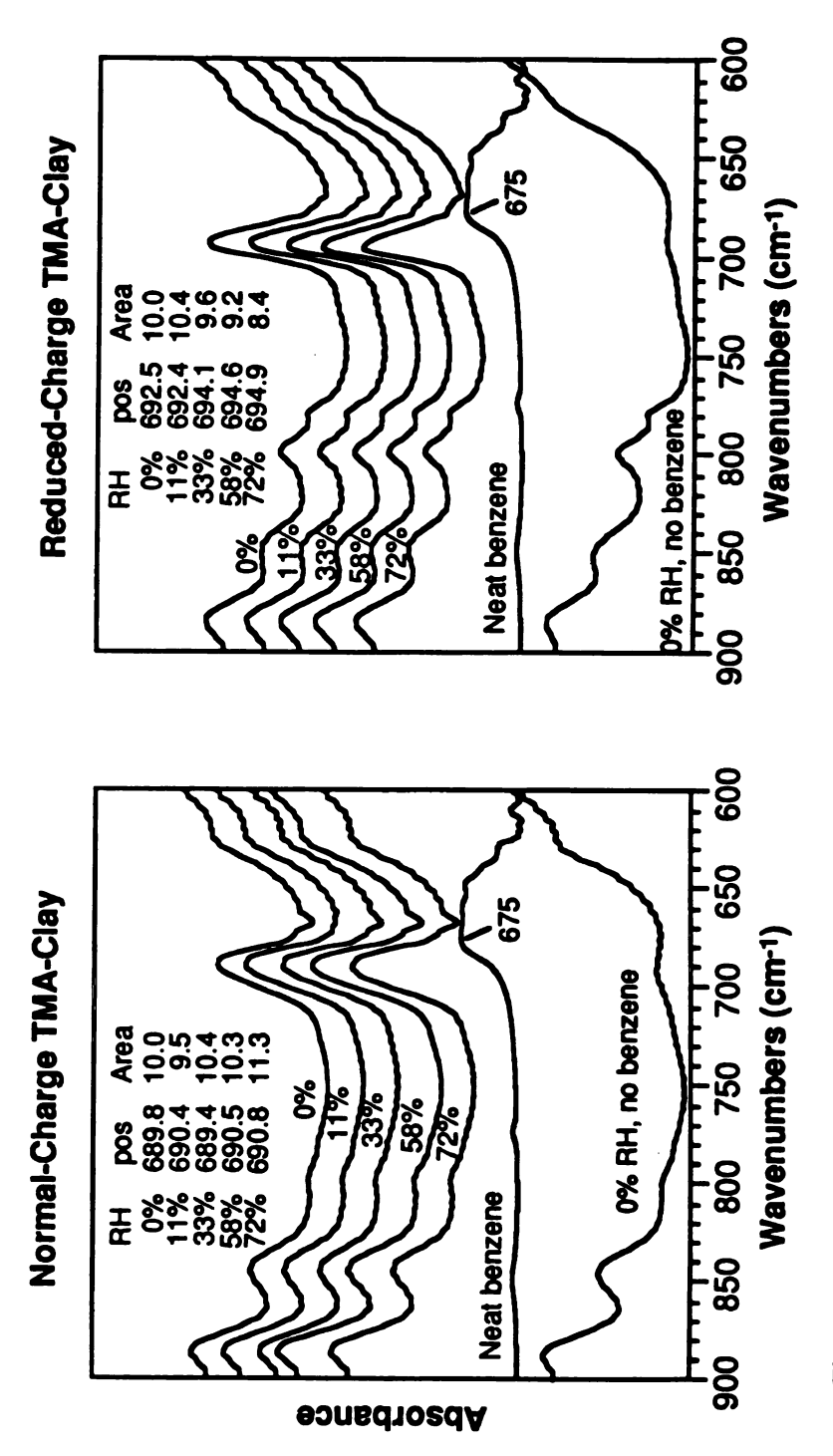


Figure D1. Effect of water sorption on the intensity and position of the C-H out-of-plane deformation vibration of sorbed benzene on normal-charge (left) and reduced-charge (right) TMA-saturated clay. Spectra are drawn to the same scale, but stacked for comparison.

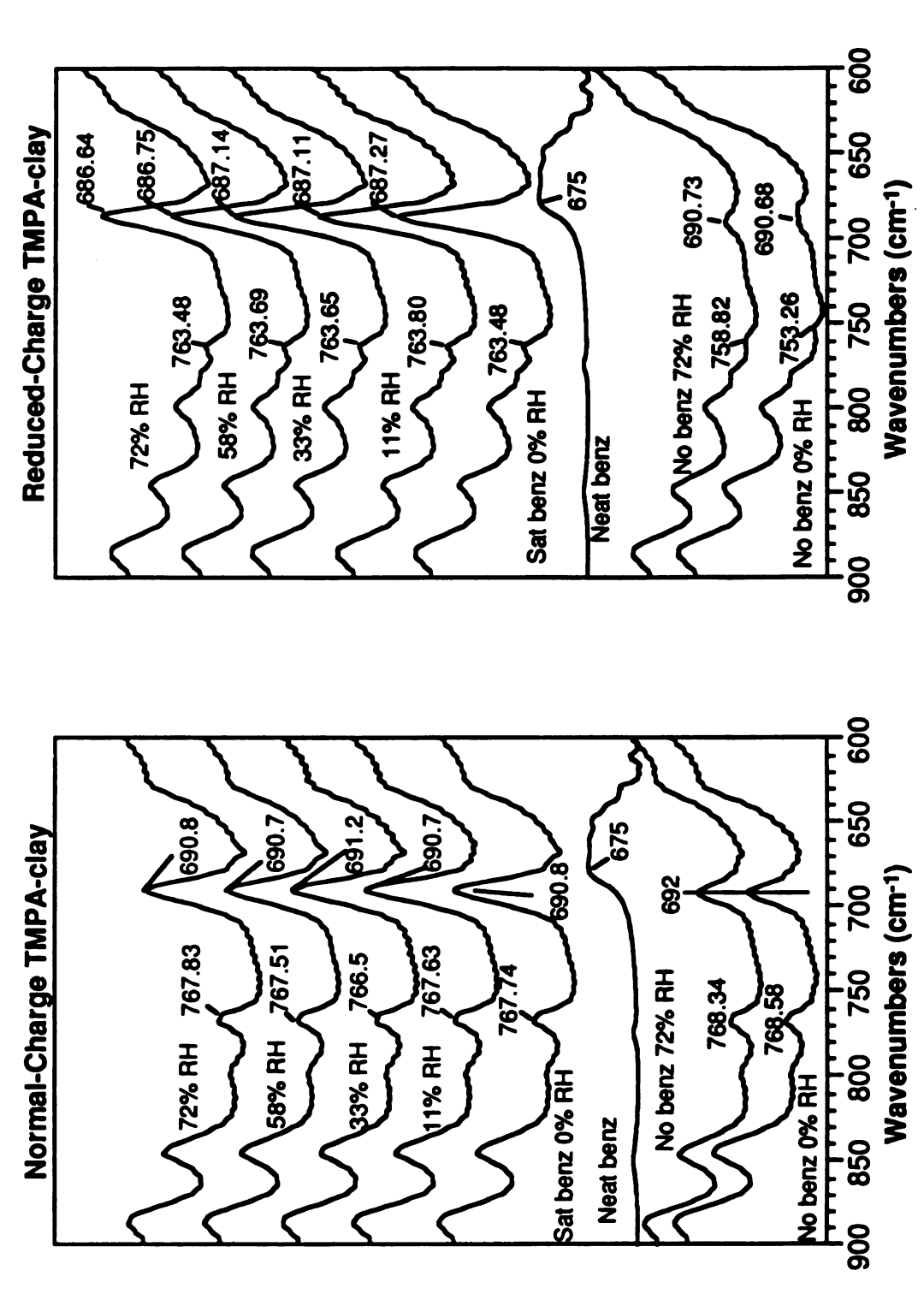


Figure D2. Effect of water sorption on the intensity and position of the C-H out-of-plane deformation vibration of sorbed benzene on normal-charge (left) and reduced-charge (right) TMPA-saturated clay. Spectra are drawn to the same scale, but stacked for comparison.

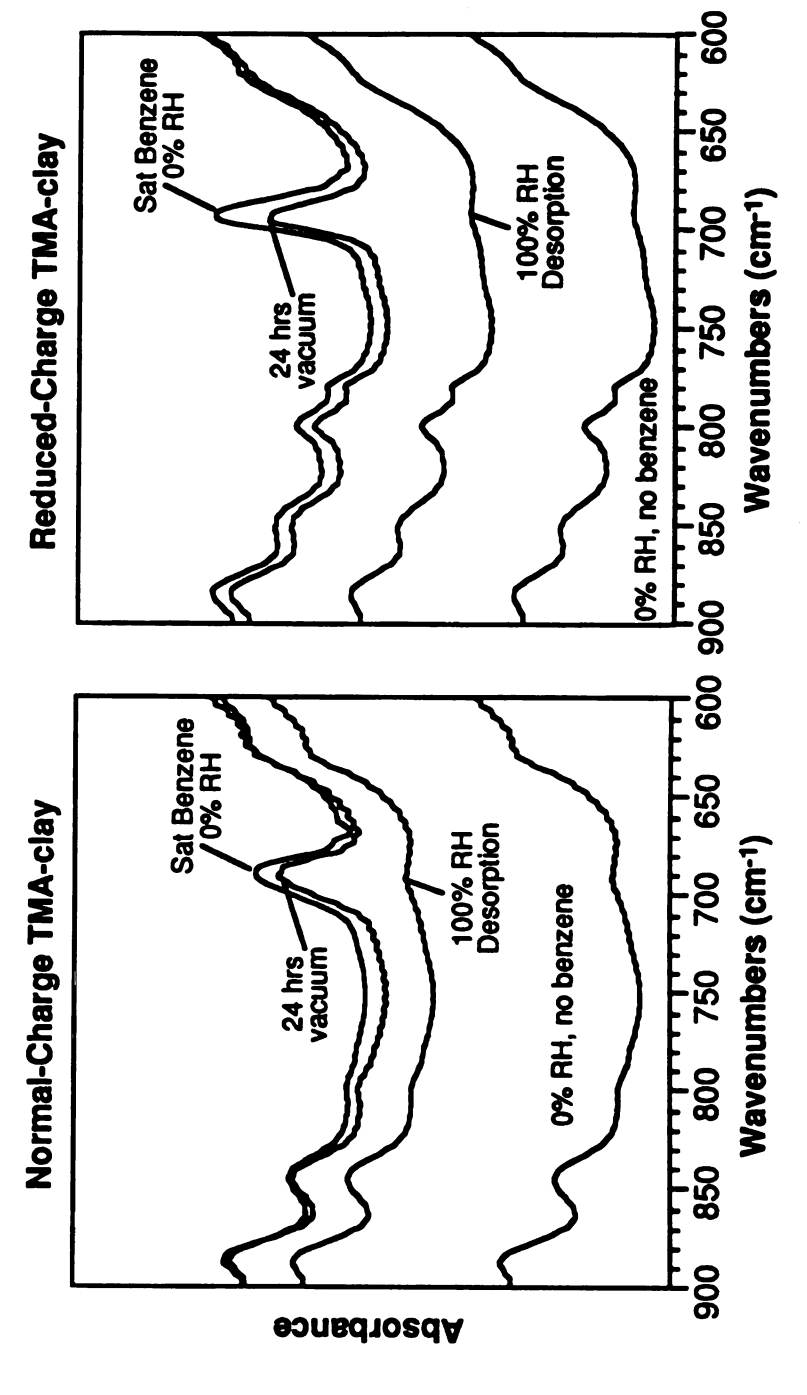


Figure D3. Effect of vacuum treatment and exposure to saturated water vapor on the intensity of the C-H out-of-plane deformation vibration of sorbed benzene on normal-charge (left) and reduced-charge (right) TMA-saturated clay. Spectra shown are drawn at same scale, but stacked for comparison.

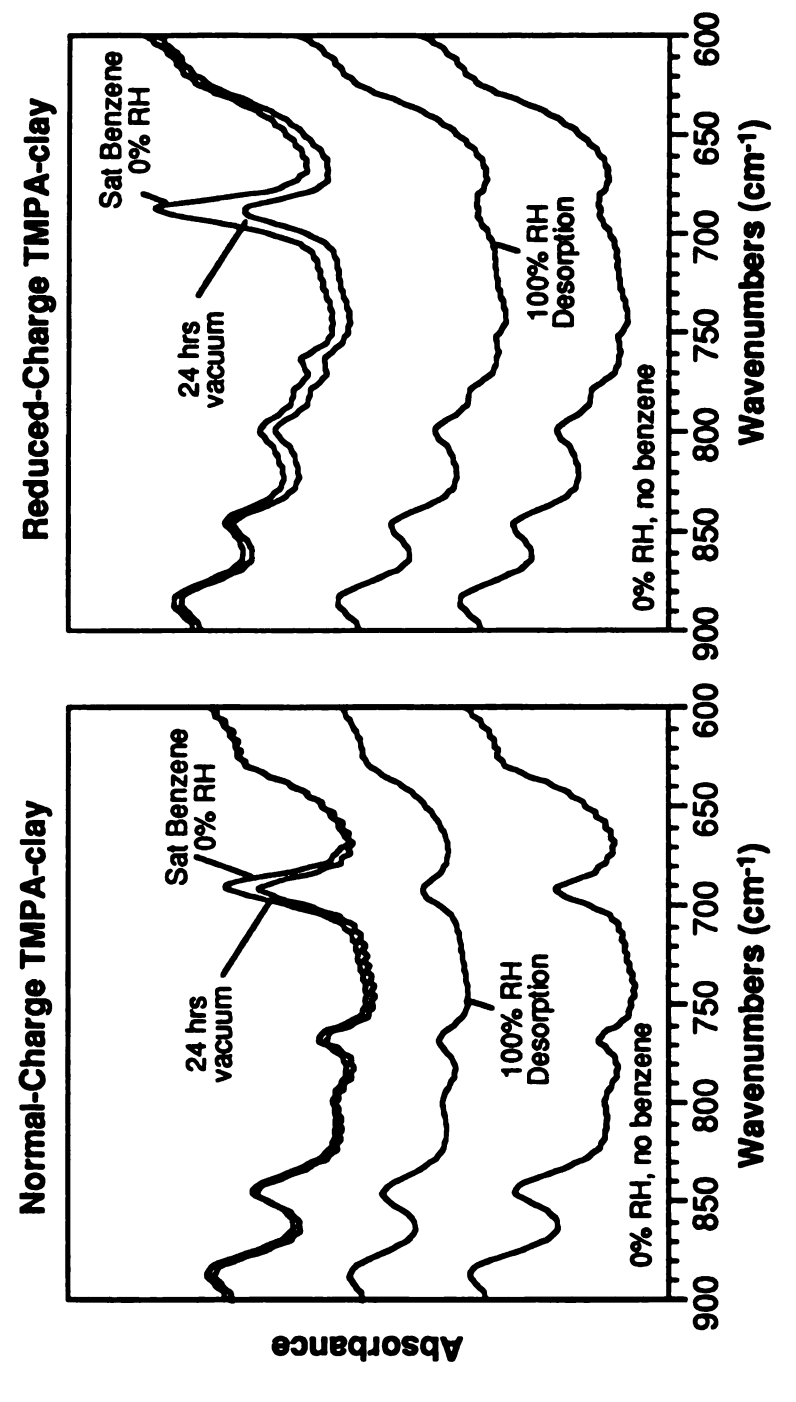


Figure D4. Effect of vacuum treatment and exposure to saturated water vapor on the intensity of the C-H out-of-plane deformation vibration of sorbed benzene on normal-charge (left) and reducedcharge (right) TMPA-saturated clay. Spectra shown are drawn at same scale, but stacked for comparison.

